

17-ELECTRON CHROMIUM NITROSYL COMPLEXES

by

WILLIAM STEPHEN MCNEIL

B.Sc., The University of British Columbia, 1991

A THESIS SUBMITTED IN PARTIAL FULFILLMENT OF
THE REQUIREMENTS FOR THE DEGREE OF
DOCTOR OF PHILOSOPHY

in

THE FACULTY OF GRADUATE STUDIES
Department of Chemistry

We accept this thesis as conforming to the required standard

THE UNIVERSITY OF BRITISH COLUMBIA

October 1995

© W. Stephen McNeil, 1995

In presenting this thesis in partial fulfilment of the requirements for an advanced degree at the University of British Columbia, I agree that the Library shall make it freely available for reference and study. I further agree that permission for extensive copying of this thesis for scholarly purposes may be granted by the head of my department or by his or her representatives. It is understood that copying or publication of this thesis for financial gain shall not be allowed without my written permission.

Department of CHEMISTRY

The University of British Columbia
Vancouver, Canada

Date DEC 18 1995

Abstract

Reaction of $[\text{CpCr}(\text{NO})\text{I}]_2$ with an excess of ammonia or allylamine yields the complex salts $[\text{CpCr}(\text{NO})\text{L}_2]^+[\text{I}]^-$ ($\text{L} = \text{NH}_3, \text{NH}_2\text{C}_3\text{H}_5$). Heating these salts results in loss of L and formation of the neutral complexes, $\text{CpCr}(\text{NO})(\text{L})\text{I}$. In contrast, reaction of $[\text{CpCr}(\text{NO})\text{I}]_2$ with the bulkier amine NH_2CMe_3 affords $\text{CpCr}(\text{NO})(\text{NH}_2\text{CMe}_3)\text{I}$ directly. Sequential reaction of $\text{CpCr}(\text{NO})(\text{NH}_2\text{CMe}_3)\text{I}$ or $\text{CpCr}(\text{NO})(\text{P}\{\text{OMe}\}_3)\text{I}$ with AgPF_6 and further L affords, respectively, the salts $[\text{CpCr}(\text{NO})(\text{L})_2]^+[\text{PF}_6]^-$ ($\text{L} = \text{NH}_2\text{CMe}_3, \text{L} = \text{P}(\text{OMe})_3$). All these species exhibit room-temperature ESR spectra and magnetic moments consistent with their possessing 17-valence-electron configurations. Abstraction of a proton from the amine ligand of $[\text{CpCr}(\text{NO})\text{L}_2]^+$ and $\text{CpCr}(\text{NO})(\text{L})\text{I}$ ($\text{L} = \text{amine}$) compounds results in the formation of amide-bridged dimers $[\text{CpCr}(\text{NO})(\text{NHR})]_2$, which exist as mixtures of various *cis*- and *trans*-isomers.

Reduction of $[\text{CpCr}(\text{NO})(\text{NH}_3)_2]^+$ to an 18-electron configuration results in loss of NH_3 , so that $\text{CpCr}(\text{NO})(\text{CO})_2$ is formed in the presence of CO. In a reverse manner, oxidation of $\text{CpCr}(\text{NO})(\text{CO})_2$ in acetonitrile produces $[\text{CpCr}(\text{NO})(\text{NCMe}_2)]^+[\text{PF}_6]^-$. These observations suggest that for $\text{CpCr}(\text{NO})\text{L}_2$ complexes, σ -basic ligands stabilize the 17-electron configurations of cations whereas π -acidic ligands stabilize the 18-electron configurations of the neutral congeners. This trend can be rationalized by the results of an Extended Hückel molecular orbital analysis of the $\text{CpCr}(\text{NO})$ fragment and the interaction of its frontier orbitals with those of various ligands, L.

Reduction of $[\text{CpCr}(\text{NO})\text{I}]_2$ in the presence of $\text{P}(\text{OMe})_3$ yields $\text{CpCr}(\text{NO})(\text{P}\{\text{OMe}\}_3)_2$, and a similar reduction with CNCMe_3 affords $\text{CpCr}(\text{NO})(\text{CNCMe}_3)_2$. Both these 18-electron species may be reversibly oxidized to their 17-electron cationic derivatives, demonstrating that ligands exhibiting intermediate σ -donor/ π -acceptor properties afford complexes that are capable of existing in both electronic configurations.

Reaction of $[\text{CpCr}(\text{NO})\text{I}]_2$ with iodide yields $[\text{CpCr}(\text{NO})\text{I}_2]^-$, a 17e anionic species. Metathesis of the halide groups affords salts of $[\text{CpCr}(\text{NO})\text{X}_2]^-$ ($\text{X} = \text{OTf}, \text{Br}$) anions, and

$[\text{CpCr}(\text{NO})\text{Cl}_2]^-$ is obtained by reaction of $[\text{CpCr}(\text{NO})\text{Cl}]_2$ with chloride. Metathesis of halide ligands in $[\text{CpCr}(\text{NO})\text{I}_2]^-$ or $[\text{CpCr}(\text{NO})\text{Cl}_2]^-$ for amide or alkoxide groups yields dimeric complexes of the form $[\text{CpCr}(\text{NO})\text{X}]_2$ ($\text{X} = \text{amide, alkoxide}$).

Treatment of $[\text{CpCr}(\text{NO})\text{Cl}_2]^-$ with one-half an equivalent of ferrocenium effects the formation of $\text{CpCr}(\text{NO})\text{Cl}_2$, which decomposes via loss of nitric oxide and a formal disproportionation reaction yielding $[\text{CpCrCl}_2]_2$ and $\text{CpCr}(\text{NO})_2\text{Cl}$. The instability of the 16e intermediate $\text{CpCr}(\text{NO})\text{Cl}_2$ is consistent with it possessing a high-spin electronic configuration, unlike its stable Mo and W analogues.

Table of Contents

Abstract	ii
Table of Contents	iv
List of Tables	xi
List of Figures	xiii
List of Schemes	xv
List of Abbreviations	xvi
Acknowledgments	xx
Quotations	xxi
Chapter 1: General Introduction.....	1
1.1 Background and Early Work.....	2
1.1.1 Organometallic Chemistry and the 18-Electron Rule.....	2
1.1.2 Metal Nitrosyl Complexes.....	4
1.1.3 Complexes Containing CpCr(NO).....	6
1.1.3.1 Dimeric Compounds of CpCr(NO).....	7
1.1.3.2 Monomeric {Cr(NO)} ⁶ Compounds.....	7
1.1.3.3 Monomeric {Cr(NO)} ⁵ Compounds.....	8
1.1.3.4 Monomeric {Cr(NO)} ⁴ Compounds.....	11
1.1.4 The Nature of [CpCr(NO)I] ₂	11
1.1.4.1 Spectroscopic Properties of [CpCr(NO)I] ₂	12
1.1.4.2 Magnetic Properties of [CpCr(NO)I] ₂	14
1.2 Scope and Format.....	17
1.3 References and Notes.....	20

Chapter 2: Reactions of [CpCr(NO)I]₂ with Amines	24
2.1 Introduction.....	25
2.2 Experimental Procedures	26
2.2.1 Methods.....	26
2.2.2 Electrochemical Measurements.....	28
2.2.3 Reagents	28
2.2.4 Preparation of [CpCr(NO)(NH ₃) ₂] ⁺ I ⁻ ([2.1] ⁺ I ⁻).....	28
2.2.5 Preparation of [CpCr(NO)(NH ₃) ₂] ⁺ [PF ₆] ⁻ ([2.1] ⁺ [PF ₆] ⁻)	29
2.2.6 Preparation of [CpCr(NO)(NH ₂ C ₃ H ₅) ₂] ⁺ I ⁻ ([2.2] ⁺ I ⁻).....	29
2.2.7 Preparation of [CpCr(NO)(NH ₂ C ₃ H ₅) ₂] ⁺ [PF ₆] ⁻ ([2.2] ⁺ [PF ₆] ⁻).....	29
2.2.8 Preparation of [CpCr(NO)(en)] ⁺ I ⁻ ([2.3] ⁺ I ⁻)	30
2.2.9 Preparation of [CpCr(NO)(en)] ⁺ [PF ₆] ⁻ ([2.3] ⁺ [PF ₆] ⁻).....	30
2.2.10 Preparation of CpCr(NO)(NH ₂ CMe ₃)I (2.4)	30
2.2.11 Preparation of [CpCr(NO)(NH ₂ CMe ₃) ₂] ⁺ [PF ₆] ⁻ ([2.5] ⁺ [PF ₆] ⁻)	30
2.2.12 Preparation of CpCr(NO)(NH ₃)I (2.6)	31
2.2.13 Preparation of CpCr(NO)(NH ₂ C ₃ H ₅)I (2.7).....	31
2.2.14 Reaction of [CpCr(NO)I] ₂ with PMe ₃	31
2.3 Characterization Data	32
2.4 Results and Discussion.....	33
2.4.1 Reactions of NH ₃ , NH ₂ C ₃ H ₅ , and ethylenediamine	33
2.4.2 Reaction with <i>tert</i> -Butylamine.....	34
2.4.3 Heating the Complex Salts: Preparation of Amine Iodide Complexes 2.6 and 2.7	36
2.4.4 ESR Monitoring of Amine Reactions.....	36
2.4.5 Solid-State Molecular Structures of [2.1] ⁺ and 2.7	38

2.4.6 Spectroscopic and Physical Properties	41
2.5 Epilogue and Future Work.....	45
2.6 References and Notes.....	47
Chapter 3: Reactivity and Redox Chemistry of the 17e Cations [CpCr(NO)(L)₂]⁺	49
3.1 Introduction.....	50
3.2 Experimental Procedures	54
3.2.1 Methods.....	54
3.2.2 Molecular Orbital Calculations	54
3.2.3 Reagents	54
3.2.4 Dissolution of Bis(ammonia) Complex [2.1] ⁺ [PF ₆] ⁻ in THF or MeCN	54
3.2.5 Exposure of Bis(ammonia) Complex [2.1] ⁺ [PF ₆] ⁻ to H ₂ O	55
3.2.6 Exposure of Bis(ammonia) Complex [2.1] ⁺ [PF ₆] ⁻ to HSn(<i>n</i> -Bu) ₃	55
3.2.7 Exposure of Bis(ammonia) Complex [2.1] ⁺ [PF ₆] ⁻ to CO	55
3.2.8 Reduction of Bis(ammonia) Complex [2.1] ⁺ [PF ₆] ⁻ under CO:	
Mg(anthracene).....	55
3.2.9 Reduction of Bis(ammonia) Complex [2.1] ⁺ [PF ₆] ⁻ under CO: Zinc.....	56
3.2.10 Reaction of CpCr(NO)(CO) ₂ with [Cp ₂ Fe] ⁺ [PF ₆] ⁻	56
3.2.11 Preparation of CpCr(NO)(P{OMe} ₃) ₂ (3.1).....	57
3.2.12 Preparation of [CpCr(NO)(P{OMe} ₃) ₂] ⁺ [PF ₆] ⁻ ([3.1] ⁺ [PF ₆] ⁻)	57
3.2.13 Preparation of <i>trans</i> - and <i>cis</i> -[CpCr(NO)(NHC ₃ H ₅) ₂] (<i>trans</i> - and <i>cis</i> -3.2).....	57
3.2.14 Reaction of <i>tert</i> -Butylamine Complex 2.4 with <i>n</i> -BuLi	58
3.2.15 Alternate Preparation of <i>trans</i> - and <i>cis</i> -[CpCr(NO)(NHCMe ₃) ₂] (<i>trans</i> - and <i>cis</i> -3.3).....	58
3.2.16 Reaction of <i>tert</i> -Butylamine Complex 2.4 with <i>t</i> -BuNHLi.....	59

3.2.17 Preparation of <i>trans</i> - and <i>cis</i> -[CpCr(NO)(NH- <i>o</i> -tol)] ₂ (<i>trans</i> - and <i>cis</i> - 3.4).....	59
3.2.18 Preparation of <i>trans</i> - and <i>cis</i> -[CpCr(NO)(NMe ₂)] ₂ (<i>trans</i> - and <i>cis</i> - 3.5).....	60
3.3 Characterization Data	61
3.4 Results and Discussion.....	63
3.4.1 Treatment of [2.1] ⁺ [PF ₆] ⁻ with Nucleophiles	63
3.4.2 Electrochemistry of [2.1] ⁺ [PF ₆] ⁻ and [2.2] ⁺ [PF ₆] ⁻	63
3.4.3 Reduction of [2.1] ⁺ [PF ₆] ⁻ under CO: Mg(anthracene).....	64
3.4.4 Reduction of [2.1] ⁺ [PF ₆] ⁻ under CO: Zinc.....	67
3.4.5 Oxidation of CpCr(NO)(CO) ₂	69
3.4.6 Synthesis of CpCr(NO)(P{OMe} ₃) ₂ and [CpCr(NO)(P{OMe} ₃) ₂] ⁺ [PF ₆] ⁻	69
3.4.7 Metal-Ligand Bonding in the CpCr(NO)(L) ₂ Systems.	72
3.4.8 Structural Comparison of Complexes 3.1 and [3.1] ⁺	75
3.4.9 Reaction of Bis(amine) Salt [2.2] ⁺ [I] ⁻ and <i>tert</i> -Butylamine Complex 2.4 with <i>n</i> -BuLi.....	78
3.5 Epilogue and Future Work.....	85
3.6 References and Notes.....	87
Chapter 4: Synthesis and Characterization of 17-Electron [CpCr(NO)X₂]⁻ Anions....	92
4.1 Introduction.....	93
4.2 Experimental Procedures	95
4.2.1 Methods.....	95
4.2.2 Reagents	95
4.2.3 Preparation of <i>n</i> -Bu ₄ N ⁺ [CpCr(NO)I ₂] ⁻ (<i>n</i> -Bu ₄ N ⁺ [4.1] ⁻).....	95
4.2.4 Preparation of <i>n</i> -Bu ₄ N ⁺ [CpCr(NO)(OTf) ₂] ⁻ (<i>n</i> -Bu ₄ N ⁺ [4.2] ⁻).....	95

4.2.5	Preparation of $n\text{-Bu}_4\text{N}^+[\text{CpCr}(\text{NO})\text{Br}_2]^-$ ($n\text{-Bu}_4\text{N}^+[\mathbf{4.3}]^-$)	96
4.2.6	Reaction of $n\text{-Bu}_4\text{N}^+[\text{CpCr}(\text{NO})(\text{OTf})_2]^-$ and KCl	96
4.2.7	Improved Preparation of $[\text{CpCr}(\text{NO})\text{Cl}]_2$	96
4.2.8	Preparation of $\text{Et}_4\text{N}^+[\text{CpCr}(\text{NO})\text{Cl}_2]^-$ ($\text{Et}_4\text{N}^+[\mathbf{4.4}]^-$)	97
4.2.9	Reaction of Diiodide Salt $n\text{-Bu}_4\text{N}^+[\mathbf{4.1}]^-$ with MeLi	97
4.2.10	Reaction of Diiodide Salt $n\text{-Bu}_4\text{N}^+[\mathbf{4.1}]^-$ with $\text{Me}_3\text{SiCH}_2\text{MgCl}$	97
4.2.11	Reaction of Diiodide Salt $n\text{-Bu}_4\text{N}^+[\mathbf{4.1}]^-$ with <i>o</i> -tolNHLi and Me_2NLi	98
4.2.12	Reaction of Dichloride Salt $\text{Et}_4\text{N}^+[\mathbf{4.4}]^-$ with <i>t</i> -BuOLi	98
4.2.13	Treatment of Diiodide Salt $n\text{-Bu}_4\text{N}^+[\mathbf{4.1}]^-$ with MeI	99
4.2.14	Treatment of Dichloride Salt $\text{Et}_4\text{N}^+[\mathbf{4.4}]^-$ with MeI	99
4.2.15	Treatment of Diiodide Salt $n\text{-Bu}_4\text{N}^+[\mathbf{4.1}]^-$ with $[\text{Me}_3\text{O}]^+[\text{BF}_4]^-$	99
4.2.16	Reaction of Dichloride Salt $\text{Et}_4\text{N}^+[\mathbf{4.4}]^-$ with $[\text{Cp}_2\text{Fe}]^+[\text{PF}_6]^-$	100
4.2.17	Reaction of Dichloride Salt $\text{Et}_4\text{N}^+[\mathbf{4.4}]^-$ with NO	100
4.2.18	Reaction of $\text{CpCr}(\text{NO})_2\text{Cl}$ with NaO- <i>i</i> -Pr	101
4.3	Characterization Data	102
4.4	Results and Discussion	103
4.4.1	Preparation of Anionic Complexes $[\text{CpCr}(\text{NO})\text{X}_2]^-$ (X = I, OTf, Br, Cl)	103
4.4.1.1	Complexes $[\mathbf{4.1}]^-$ (X = I), $[\mathbf{4.2}]^-$ (X = OTf), and $[\mathbf{4.3}]^-$ (X = Br)	103
4.4.1.2	Improved Synthesis of $[\text{CpCr}(\text{NO})\text{Cl}]_2$	106
4.4.1.3	$[\text{CpCr}(\text{NO})\text{Cl}_2]^-$ $[\mathbf{4.4}]^-$	108
4.4.2	Physical and Spectroscopic Properties of Anions $[\mathbf{4.1}]^-$ to $[\mathbf{4.4}]^-$	108
4.4.3	Reactivity of Dihalide Anions $[\mathbf{4.1}]^-$ and $[\mathbf{4.4}]^-$	112
4.4.3.1	Reaction with Nucleophiles	112
4.4.3.2	Reaction with Electrophiles	114
4.4.4	Redox Chemistry of Dihalide Anions	115

4.4.4.1 Cyclic Voltammetry.....	115
4.4.4.2 Chemical Oxidation of $\text{Et}_4\text{N}^+[\text{CpCr}(\text{NO})\text{Cl}_2]^-$	117
4.4.4.3 Mechanistic Rationale.....	120
4.4.4.4 Summary: $\text{CpM}(\text{NO})(\text{CO})_2$ plus Halide Reagents	122
4.4.5 Reaction of $\text{CpCr}(\text{NO})_2\text{Cl}$ with $\text{NaO-}i\text{-Pr}$	123
4.5 Epilogue and Future Work.....	125
4.6 References and Notes.....	128

Chapter 5: Reductive Synthesis of $\text{CpCr}(\text{NO})(\text{CNCMe}_3)_2$ and Derivative

Chemistry.....	131
5.1 Introduction.....	132
5.2 Experimental Procedures	133
5.2.1 Methods.....	133
5.2.2 Reagents	133
5.2.3 Preparation of $\text{CpCr}(\text{NO})(\text{CNCMe}_3)_2$ (5.1).....	133
5.2.4 Preparation of $[\text{CpCr}(\text{NO})(\text{CNCMe}_3)_2]^+[\text{PF}_6]^-$ ($[\text{5.1}]^+[\text{PF}_6]^-$).....	133
5.2.5 Reaction of Bis(isocyanide) 5.1 with HBF_4	134
5.2.6 Reaction of Bis(isocyanide) 5.1 with $[\text{Me}_3\text{O}]^+[\text{BF}_4]^-$	134
5.2.7 Treatment of Bis(isocyanide) 5.1 with MeLi , PhLi , and LiEt_3BH	134
5.2.8 Treatment of Bis(isocyanide) 5.1 with H_2 , CO , H_2O , MeOH , and <i>p</i> -tolNCO.....	135
5.2.9 Thermolysis of Bis(isocyanide) 5.1	135
5.2.10 Preparation of $[\text{CpCr}(\text{NO})(\text{THF})_2]^+[\text{PF}_6]^-$	135
5.2.11 Reduction of $[\text{CpCr}(\text{NO})(\text{THF})_2]^+$ in presence of diphenylacetylene or dimethylacetylenedicarboxylate.....	136
5.2.12 Reduction of $[\text{CpCr}(\text{NO})(\text{THF})_2]^+$ in presence of acetylene.....	136

5.2.13	Reduction of $[\text{CpCr}(\text{NO})(\text{THF})_2]^+$ in presence of pyridine	137
5.2.14	Reduction of $[\text{CpCr}(\text{NO})(\text{THF})_2]^+$ in presence of 2,3-dimethylbutadiene	137
5.2.15	Reduction of $[\text{CpCr}(\text{NO})(\text{THF})_2]^+$ in presence of 1,10-phenanthroline	138
5.2.16	Reduction of $[\text{CpCr}(\text{NO})\text{I}]_2$ in presence of 2,3-dimethylbutadiene	138
5.2.17	Reduction of $[\text{CpCr}(\text{NO})\text{I}]_2$ in presence of ethylene.....	138
5.2.18	Reduction of $[\text{CpCr}(\text{NO})\text{I}]_2$ in presence of 1,5-cyclooctadiene (1,5-COD).....	138
5.2.19	Reduction of $[\text{CpCr}(\text{NO})\text{I}]_2$ in presence of acetylene	139
5.2.20	Reduction of $[\text{CpCr}(\text{NO})\text{I}]_2$ in presence of diphenylacetylene	139
5.2.21	Reduction of $[\text{CpCr}(\text{NO})\text{I}]_2$ in presence of 1-phenylpropyne	140
5.3	Characterization Data	141
5.4	Results and Discussion.....	142
5.4.1	Preparation of $\text{CpCr}(\text{NO})(\text{CNCMe}_3)_2$ (5.1).....	142
5.4.2	Preparation of $[\text{CpCr}(\text{NO})(\text{CNCMe}_3)_2]^+[\text{PF}_6]^-$ ($[\text{5.1}]^+[\text{PF}_6]^-$).....	144
5.4.3	Structural Analysis of $[\text{CpCr}(\text{NO})(\text{CNCMe}_3)_2]^+$ ($[\text{5.1}]^+$)	147
5.4.4	Reaction of Bis(isocyanide) 5.1 with Electrophiles.....	149
5.4.5	Treatment of Bis(isocyanide) 5.1 with Nucleophiles and other Small Molecules.....	150
5.4.6	Thermolysis of Bis(isocyanide) 5.1	150
5.4.7	Attempted Preparation of other $\text{CpCr}(\text{NO})(\text{L})_2$ Complexes	152
5.5	Epilogue and Future Work.....	154
5.6	References and Notes.....	155
Appendix		157

List of Tables

Table 2.1. Numbering Scheme, Color, Yield and Elemental Analysis Data	32
Table 2.2. Mass Spectral, Infrared, ESR, and Magnetic Data	32
Table 2.3. Structural Parameters of {Cr(NO)} ⁵ Complexes	40
Table 3.1. Numbering Scheme, Color, Yield and Elemental Analysis Data	61
Table 3.2. Mass Spectral and Infrared Data.....	61
Table 3.3. NMR and ESR Data.....	62
Table 3.4. Predicted NMR and IR Data for Amide Complexes 3.2 and 3.3	83
Table 4.1. Numbering Scheme, Color, Yield and Elemental Analysis Data	102
Table 4.2. Mass Spectral, Infrared, and ESR Data	102
Table 5.1. Numbering Scheme, Color, Yield and Elemental Analysis Data	141
Table 5.2. Mass Spectral, Infrared, NMR, and ESR Data.....	141
Table 5.3. NMR and ESR Data.....	141
Table 5.4. Nitrosyl-stretching frequencies of CpCr(NO)(L) ₂	143
Table A1. Crystallographic Data for Complexes [2.1] ⁺ [BPh ₄] ⁻ , 2.7 , 3.1 , [3.1] ⁺ [BPh ₄] ⁻ , and [5.1] ⁺ [BPh ₄] ⁻	158
Table A2. Fractional Coordinates and Equivalent Isotropic Displacement Parameters for the Non-hydrogen Atoms of [2.1][BPh ₄]	159
Table A3. Fractional Coordinates and Isotropic Displacement Parameters for the Hydrogen Atoms of [2.1][BPh ₄].....	160
Table A4. Fractional Coordinates and Equivalent Isotropic Displacement Parameters for the Non-Hydrogen Atoms of 2.7	161
Table A5. Fractional Coordinates and Isotropic Displacement Parameters for the hydrogen atoms of 2.7	161

Table A6. Fractional Coordinates and Equivalent Isotropic Displacement Parameters for the Non-hydrogen Atoms of 3.1	162
Table A7. Fractional Coordinates and Isotropic Displacement Parameters for the Hydrogen Atoms of 3.1	163
Table A8. Fractional Coordinates and Isotropic or Equivalent Isotropic Displacement Parameters for the Non-hydrogen Atoms of [3.1][BPh ₄].....	164
Table A9. Fractional Coordinates and Isotropic Displacement Parameters for the Hydrogen Atoms of [3.1][BPh ₄].....	165
Table A10. Fractional Coordinates and B _(eq) for the Non-Hydrogen Atoms of [5.1][BPh ₄].....	166
Table A11. Fractional Coordinates and B _(eq) for the Hydrogen Atoms of [5.1][BPh ₄]	167

List of Figures

Figure 1.1. Molecular orbital energy levels of an octahedral complex	3
Figure 1.2. Interaction of metal t_{2g} orbitals with π -acceptor ligand orbitals	4
Figure 1.3. Molecular orbital diagram of nitric oxide	5
Figure 1.4. Metal-nitrosyl bonding interactions	5
Figure 1.5. Infrared Spectra of 1	13
Figure 1.6. Observed and Calculated Susceptibility of $[\text{CpCr}(\text{NO})\text{I}]_2$	15
Figure 1.7. Reactions of 1 with Lewis bases	18
Figure 2.1. ESR spectra observed when $[\text{CpCr}(\text{NO})\text{I}]_2$ in CH_2Cl_2 is treated with $\text{NH}_2\text{C}_3\text{H}_5$	37
Figure 2.2. Structure of $[\mathbf{2.1}]^+$	39
Figure 2.3. Structure of 2.7	39
Figure 2.4. ESR spectrum of $[\mathbf{2.3}]^+[\text{PF}_6]^-$	43
Figure 3.1. Interaction of a 17e Complex with Ligand L'	53
Figure 3.2. Reduction cyclic voltammogram of $[\mathbf{2.1}]^+[\text{PF}_6]^-$	64
Figure 3.3. Infrared Spectra During Reaction of $[\mathbf{2.1}]^+[\text{PF}_6]^-$ with $\text{Mg}(\text{anthracene})$	65
Figure 3.4. Cyclic voltammogram of 3.1	71
Figure 3.6. Molecular orbitals of $\text{L}_5\text{M}(\text{NO})$	72
Figure 3.5. Molecular orbital diagram for the $\text{CpCr}(\text{NO})$ fragment	73
Figure 3.7. Molecular structure of 17e complex $[\mathbf{3.1}]^+$	76
Figure 3.8. Molecular structure of 18e complex 3.1	76
Figure 3.9. Comparison of selected metrical parameters for $[\mathbf{3.1}]^+$ and 3.1	76
Figure 3.10. Isomers of $[\text{CpCr}(\text{NO})(\text{NHR})]_2$	83
Figure 4.1. FAB-MS of $n\text{-Bu}_4\text{N}^+[\mathbf{4.3}]^-$	109

Figure 4.2. ESR spectrum of $\text{Et}_4\text{N}^+[\mathbf{4.4}]^-$	111
Figure 4.3. Current for Oxidation Features of $\text{Et}_4\text{N}^+[\mathbf{4.4}]^-$	117
Figure 4.4. Frontier Orbital Population in $[\text{CpM}(\text{NO})\text{Cl}_2]^{o/-}$ Species.....	121
Figure 5.1. Cyclic voltammogram of 5.1	144
Figure 5.2. IR spectra of 5.1 and $[\mathbf{5.1}]^+[\text{PF}_6]^-$	146
Figure 5.3. Molecular structure of $[\mathbf{5.1}]^+$	147
Figure 5.4. ^1H NMR spectra of $\text{CpCr}(\text{NO})(\text{CNCMe}_3)_2$ (5.1) in C_6D_6 after heating for 0, 5, and 13 d.....	151
Figure A1. Frontier Molecular Orbitals of the $\text{CpCr}(\text{NO})$ Fragment	168
Figure A2. Frontier Molecular Orbitals of $\text{CpCr}(\text{NO})(\text{CO})_2$	169
Figure A3. Frontier Molecular Orbitals of $[\text{CpCr}(\text{NO})(\text{NH}_3)_2]^+$	170

List of Schemes

Scheme 1.1. Reactions of $\text{CpM}(\text{NO})(\text{CO})_2$ with halogen reagents.....	9
Scheme 1.2. Syntheses of 17e $\text{CpCr}(\text{NO})(\text{L})\text{X}$ Complexes.....	10
Scheme 3.1. Typical reactions of 17e complexes.....	50
Scheme 3.2. Substitution mechanisms in 18e vs. 17e complexes.....	52
Scheme 3.3. Pathways of amide dimer formation.....	80
Scheme 4.1. Reaction of $\text{CpCr}(\text{NO})(\text{CO})_2$ with chloride reagents.....	106
Scheme 4.2. Reactions of $\text{CpCr}(\text{NO})(\text{CO})_2$ with PCl_5 in CH_2Cl_2 and MeCN	107
Scheme 4.3. Comparison of reactions of $n\text{-Bu}_4\text{N}^+[\mathbf{4.1}]^-$ and $\text{CpCr}(\text{NO})(\text{PPh}_3)\text{I}$ with $\text{Me}_3\text{SiCH}_2\text{MgCl}$	113
Scheme 4.4. Proposed Electrochemical Reaction of $[\mathbf{4.4}]^-$	117
Scheme 4.5. Proposed mechanism for oxidative decomposition of $[\mathbf{4.4}]^-$	119
Scheme 4.6. Summary of reactions of $\text{CpM}(\text{NO})(\text{CO})_2$ with Halide Reagents.....	123

List of Abbreviations

The following is a list of abbreviations and symbols employed in this Thesis, most of which are in common use in the chemical literature.

<i>ne</i>	<i>n</i> valence electrons
A	coupling constant (in ESR spectroscopy)
Å	angstrom, 10^{-10} m
anal.	analysis
atm	atmosphere
A_X	coupling to atom X
br	broad
<i>n</i> -Bu	<i>n</i> -butyl, $-\text{CH}_2\text{CH}_2\text{CH}_2\text{CH}_3$
<i>t</i> -Bu	<i>tert</i> -butyl, CMe_3
^{13}C	carbon-13
$^{13}\text{C}\{\text{}^1\text{H}\}$	proton-decoupled carbon-13
$^\circ\text{C}$	degree Celsius
C_3H_5	η^1 -allyl, $-\text{CH}_2\text{CH}=\text{CH}_2$
Calcd	calculated
χ_m	molar susceptibility
χ_{TIP}	susceptibility due to temperature-independent paramagnetism
cm^{-1}	wavenumber, $1.877 \cdot 10^{-23}$ J
COD	cyclooctadiene
compd	compound
Cp'	Cp or Cp*
Cp	cyclopentadienyl, $\eta^5\text{-C}_5\text{H}_5$

Cp*	pentamethylcyclopentadienyl, $\eta^5\text{-C}_5\text{Me}_5$
CV	cyclic voltammogram, or cyclic voltammetry
δ	chemical shift
d	days, or doublet (in an NMR spectrum)
D	deuterium, ^2H
dipic	pyridine-2,6-dicarboxylate
dppe	diphenylphosphinoethane, $\text{Ph}_2\text{PCH}_2\text{CH}_2\text{PPh}_2$
E	electrochemical potential
$E_{1/2}$	potential of half-cell reaction, taken as $(E_{p,c} + E_{p,a})/2$
$E_{p,a}$	potential at peak anodic current
$E_{p,c}$	potential at peak cathodic current
EI	electron impact
en	ethylenediamine, $\text{H}_2\text{NCH}_2\text{CH}_2\text{NH}_2$
eq	equation
equiv	equivalents
ESR	electron spin resonance
Et	ethyl, $-\text{CH}_2\text{CH}_3$
ETC	electron transfer catalysis
eV	electron-volt, $1.602 \cdot 10^{-19}$ J
FAB	fast atom bombardment
G	Gauss, 10^{-4} T
^1H	proton
h	hours
HOMO	highest occupied molecular orbital
Hz	hertz, s^{-1}

I	nuclear spin value
<i>i</i> -Pr	<i>iso</i> -propyl, -CH(CH ₃) ₂
IR	infrared
J	joule, kgm ² s ⁻²
<i>J</i>	coupling constant (in NMR spectroscopy)
K	degree Kelvin
k	rate constant
L	Lewis basic, 2-electron-donor ligand; litre, 10 ⁻³ m ³
LUMO	lowest unoccupied molecular orbital
μ _B	Bohr magneton, 9.274·10 ⁻²⁴ JT ⁻¹
μ _{eff}	effective magnetic moment
M	metal (usually Group 6); molar, mole/litre
m	multiplet (in an NMR spectrum)
<i>m/z</i>	mass-to-charge ratio (in mass spectrometry)
Me	methyl, -CH ₃
Me ₆ [14]4,11-dieneN ₄	5,7,7,12,14,14-hexamethyl-1,4,8,11,tetraazacyclotetradeca-4,11-diene
min	minutes
mmol	millimole, 10 ⁻³ mole
MO	molecular orbital
mol	mole
MS	mass spectrum
ν	stretching frequency (in IR spectroscopy)
ⁿ J _{AB}	<i>n</i> -bond coupling between atoms A and B
NMR	nuclear magnetic resonance
no.	number

ORTEP	Oak Ridge Thermal Ellipsoid Program
^{31}P	phosphorus-31
$^{31}\text{P}\{^1\text{H}\}$	proton-decoupled phosphorus-31
P^+	parent molecular ion (in mass spectroscopy)
Ph	phenyl, $-\text{C}_6\text{H}_5$
ppm	parts per million
py	pyridine, $\text{C}_5\text{H}_5\text{N}$
pz	pyrazolyl, $\text{C}_3\text{H}_3\text{N}_2$
R	alkyl
s	singlet (in an NMR spectrum)
SCE	saturated calomel electrode
SOMO	singly-occupied molecular orbital
SQUID	superconducting quantum interference device
T	Tesla, $\text{kgs}^{-1}\text{C}^{-1}$
t	triplet (in an NMR spectrum)
tetraglyme	tetraethylene glycol dimethylether, $\text{CH}_3(\text{OCH}_2\text{CH}_2)_4\text{OCH}_3$
TfO	triflate, CF_3SO_3
<i>o</i> -tol	<i>ortho</i> -tolyl, $2\text{-C}_6\text{H}_4\text{CH}_3$
<i>p</i> -tol	<i>para</i> -tolyl, $4\text{-C}_6\text{H}_4\text{CH}_3$
THF	tetrahydrofuran, $\text{C}_4\text{H}_8\text{O}$
TIP	temperature-independent paramagnetism
V	volt, C/s
vs.	versus
vt	virtual triplet (in an NMR spectrum)
X	halide or other anionic 1-electron-donor ligand

Acknowledgments

There are many people who helped to make this work both a possibility and a pleasure.

First, thanks must go, as always, to Peter. His research group has always functioned with a communal sharing of both ideas and responsibilities, with guidance not from one to each, but among all. Most importantly, it functions as it does because of how Peter elects to run it: he lets the students run it for him.

It has been a pleasure to work with a long line of Legzdins students, post-docs, and assorted hangers-on, members new, old, and new again. Each of them has contributed to the real reason I was here, the "admirable camaraderie." Thanks to Penny, for secrets shared. Thanks to John, for demonstrating how to do things, and, on occasion, how not to do them. His admirable proofreading skills deserve special mention. Thanks to that strange symbiotic entity that was PennyandJohn, for morning coffee chats and laughs beyond number. Thanks to Kevin, for being more like me than I am. A mirror can be a frightening thing. Thanks to everyone else with whom I shared some time (the long-departed, the still-toiling, and the but-recently-arrived), mostly for laughing at things I said. Usually against your better judgment, I should think.

Thanks to a seeming parade of individuals whom I respect and often admire, yet who inexplicably see fit to ask me for advice on matters both chemical and personal. Mine was the greater benefit by far.

Thanks to the staff at UBC, particularly to Peter Borda and to the mass spec staff, and to Steve Rettig and Fred and Ray for solving the crystal structures.

Thanks to NSERC, which in its relationship with me since 1989 has shown either great foresight or even greater gullibility. Time will tell.

Thanks to my parents, for pride and support. The group owes a particular collective debt to WillyMom for bailing all of us out of otherwise dire computer crises.

Lastly, and above all else, thanks to Stasey, for a rock to stand on and a star to guide by, and for making this accomplishment insignificant compared to the daily act of being your husband.

You can't get a Ph.D. working 9 to 5.

Nancy Christensen

So I'm gonna try it working 10 to 4.

Penny Lundmark

I dunno. I'm making this up as I go.

Indiana Jones, *Raiders of the Lost Ark*

What is now proved was once, only imagin'd.

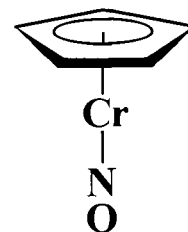
William Blake, *Proverbs of Hell*

CHAPTER 1
General Introduction

1.1 Background and Early Work.....	2
1.2 Scope and Format.....	17
1.3 References and Notes	20

1.1 Background and Early Work

The subject of this Thesis is the preparation and subsequent study of a number of new organometallic complexes that share many features. Each of the new species contains a common metal-ligand fragment, consisting of a cyclopentadienyl and a nitrosyl ligand bound to a chromium atom. The resulting fragment is depicted to the right. The compounds discussed in this Thesis are generally 17-valence-electron (17e) species with one unpaired electron, and so are paramagnetic. As such, they are somewhat unusual, in that most organometallic molecules have an even number of electrons and are diamagnetic. Therefore, the Thesis also addresses questions regarding these compounds' electronic stability: why do the complexes exist in an unusual 17e configuration, and what occurs when they are reduced or oxidized to 18e or 16e derivatives? The answers to these questions require an understanding of the molecular orbitals of these compounds, and of the orbital interactions between metal and ligands.



By way of introduction, a few general chemical topics, including some basic molecular orbital concepts as they pertain to transition-metal compounds and a large body of specific background material, will be discussed in order to ensure an understanding of relevant concepts to this work, and to place the work in its proper context.

1.1.1 Organometallic Chemistry and the 18-Electron Rule

Organometallic chemistry is generally defined as the study of compounds containing a bond between a carbon atom and a metal atom, though such a definition is more semantically correct than it is practical. The field of organometallic chemistry is generally accepted to exclude metal-cyanide compounds, which contain metal-carbon bonds, because these compounds exhibit properties more akin to those of coordination complexes. At the same time, organometallic chemists are quite comfortable discussing compounds that have no M-C bonds at all.¹ In fact, the distinction between coordination chemistry and organometallic chemistry is becoming an

increasingly arbitrary one, and, if anything, the work presented in this Thesis serves to blur this line even further.

A fundamental concept of organometallic chemistry is the 18-valence-electron (18e) rule, which states that a metal complex will be stable if there is an 18-electron count at the metal center. Indeed, in any textbook which discusses organometallic chemistry, electron counting and the 18e rule are inevitably introductory topics to the subject.² In terms of valence bond theory, the rule is analogous to the octet rule, such that a metal complex will be stable when the central atom's valence orbitals are all filled. Since a transition metal has one s, three p, and five d valence orbitals, for a total of 9, this criterion is met by 18 electrons and an $s^2p^6d^{10}$ configuration, thus closing the valence shell and giving the metal a noble gas configuration. However, such a description is somewhat over-simplified, in that it does not take into account the precise nature of the metal-ligand bonds, and it cannot help rationalize the existence of the many stable compounds which are not 18e species.

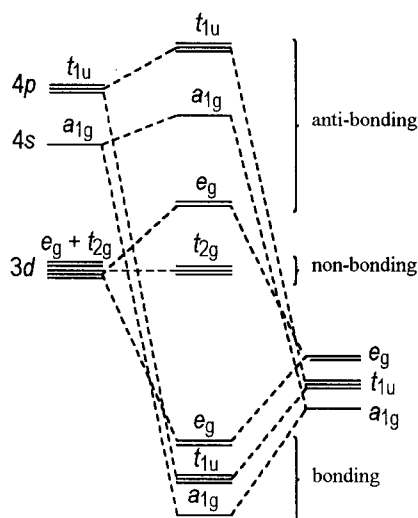


Figure 1.1. Molecular orbital energy levels of an octahedral complex. Only interactions due to M-L σ -bonds are shown.

highest-energy occupied MO (HOMO) is found in the non-bonding t_{2g} set of orbitals (d_{xz} , d_{yz} , and d_{xy}), and the lowest-energy unoccupied MO (LUMO) is found in the anti-bonding e_g orbitals (d_{z^2} , $d_{x^2-y^2}$). Thus, the HOMO-LUMO gap in the molecular orbital description is equivalent to

A more useful interpretation of metal-ligand bonding is provided by molecular orbital theory.³ In this bonding model, the metal's atomic orbitals interact with ligand-orbital combinations of appropriate symmetry to yield both bonding and antibonding molecular orbitals (MOs). This interaction of the metal's nine valence orbitals must therefore result in exactly nine MOs that are either bonding or non-bonding with respect to the ligands, and so a stable complex has these nine orbitals filled with eighteen electrons. The classic example of such an orbital scheme is that of an octahedral ML_6 complex; the corresponding MO diagram is represented in Figure 1.1. In this case, the

highest-energy occupied MO (HOMO) is found in the non-bonding t_{2g} set of orbitals (d_{xz} , d_{yz} , and d_{xy}), and the lowest-energy unoccupied MO (LUMO) is found in the anti-bonding e_g orbitals (d_{z^2} , $d_{x^2-y^2}$). Thus, the HOMO-LUMO gap in the molecular orbital description is equivalent to

the familiar Δ_0 in crystal field theory.⁴ Because organometallic chemistry generally deals with metals in a strong ligand field, this arrangement of orbitals leads to a large HOMO-LUMO gap, and a low-spin configuration of electrons.

Organometallic complexes which adhere to the 18-electron rule are generally complexes with π -acidic, strong-field ligands.

Such compounds therefore experience a large ligand field and exhibit a low-spin configuration of electrons. The large energy gap arises because the t_{2g} orbitals in Figure 1.1, non-bonding with

respect to σ -character ligands, are lowered in energy and become strongly bonding with respect to the π -acceptor ligands, so the π -interaction serves to increase both the HOMO-LUMO gap and the strength of the metal-ligand bonds (Figure 1.2). In short, strong ligand fields and π -acceptor ligands are responsible for the veracity of the 18e rule, since the rule was empirically designed to explain a class of complexes in which such π -acceptor ligands are dominant.

In complexes with a weaker ligand field, violations of the 18e rule become more common. Without a π -acceptor interaction, the t_{2g} orbitals in Figure 1.1 remain non-bonding, so if they remain unoccupied there is no net loss of M-L bonding energy. For example, it is the presence of such a non-bonding orbital that allows complexes of the type Cp_2ZrR_2 to be stable species despite a 16e count.⁵ Weaker-field complexes can also result in stable compounds with high-spin ground states in addition to low electron counts;⁶ this is something very unusual in organometallic chemistry, but not at all disturbing in the field of coordination chemistry, where the total electron count of a complex is less of a consideration.

1.1.2 Metal Nitrosyl Complexes

Nitric oxide is a thermally-stable, diatomic radical. Its electronic structure is similar to that of carbon monoxide, but with one extra electron. Thus, the orbital corresponding to the LUMO in CO, a π -symmetry antibonding orbital, is singly occupied in NO, resulting in a formal

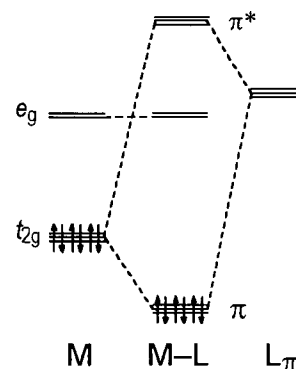


Figure 1.2. Interaction of metal t_{2g} orbitals with π -acceptor ligand orbitals.

bond order of $2\frac{1}{2}$ rather than 3, as depicted in Figure 1.3. The orbital interactions which arise when NO is bound in a linear fashion to a metal center are therefore analogous to those found for a metal carbonyl. These interactions are shown in Figure 1.4, and involve both σ - and π -bonds between metal and ligand. The latter bond is of greater import, as carbonyl and nitrosyl are both strongly π -acidic; they therefore act as net withdrawers of electron density from the metal center, and the π -bonding interaction results in a lowering in energy of the π -symmetry metal d-orbital, as depicted in Figure 1.2. NO bound in this linear fashion is usually considered to be a three-electron donor to a metal, with two electrons in the σ -bond and one electron in the π -bond.⁷ There is, of course, a second π -symmetry nitrosyl orbital orthogonal and equal in energy to the first, so that NO may be considered a $(1\sigma, 2\pi)$ ligand, in a manner analogous to carbonyl, oxo, nitrido, carbyne, or linear imido ligands.⁸

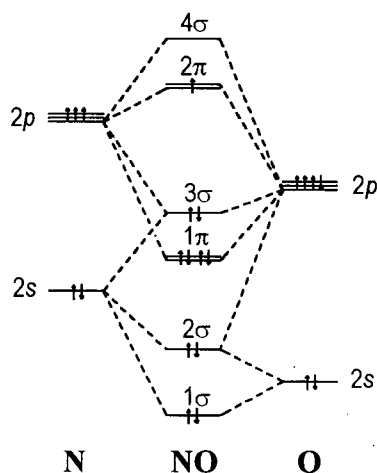


Figure 1.3. Molecular orbital diagram of nitric oxide.

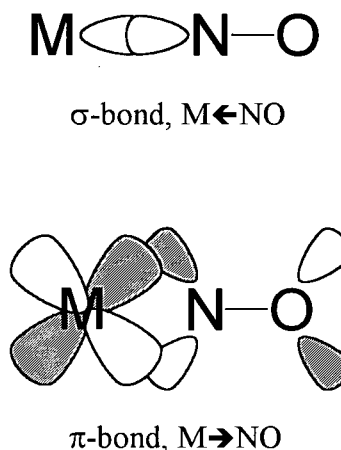


Figure 1.4. Metal-nitrosyl bonding interactions.

There are two critical differences between a carbonyl and a linear nitrosyl ligand. The first is that the nitrosyl is a much stronger π -acceptor than carbonyl, so that the nitrosyl M-N bond is considerably stronger and the N-O bond considerably weaker than the analogous bonds in a metal carbonyl system. The second, which can be inferred from the first, is that linear nitrosyl ligands are typically more difficult to displace from a metal than carbonyl ligands.⁷

There is a second potential bonding mode for nitric oxide, one in which the ligand is attached to the metal in a bent, rather than linear, fashion. When bound this way, NO is considered to be a one-electron donor, much like a halide or alkyl ligand. Because of the different binding modes of NO, because free nitric oxide carries an odd number of electrons, and because the electronic interaction between metal and nitrosyl is largely a covalent one, the assignment and determination of metal oxidation states in nitrosyl complexes has long been problematic. Historically,^{9,10} the charge division between the metal and the nitrosyl has depended upon the ligand's binding mode, so that a linear nitrosyl was thought of as NO^+ , while a bent nitrosyl was thought of as NO^- . Such an oversimplification is both imprecise and undesirable, since information which might be gained from the assignment of an integral oxidation state at the metal will generally be contradictory.¹¹

To account for the covalent nature of M-NO bonding, Enemark and Feltham¹⁰ devised a notation to describe more accurately the electronic configuration of metal centers in nitrosyl compounds. This notation treats the metal nitrosyl as a single unit with a number of valence electrons x : $\{\text{M}(\text{NO})\}^x$, where x is equal to the number of metal d electrons as determined by assigning an oxidation state to the entire M-NO unit, plus one electron in the NO π^* orbital. For example, $\text{CpCr}(\text{NO})(\text{CO})_2$ would be considered $\{\text{Cr}(\text{NO})\}^6$ using the Enemark-Feltham notation, since a Cp^- ligand leaves the metal with a d^5 electron count, plus one from the nitrosyl. The complex $\text{CpCr}(\text{NO})(\text{NH}_3)\text{I}$ would be $\{\text{Cr}(\text{NO})\}^5$: Cp^- and I^- yield a d^4 count at the metal, plus one from NO. This notation will be employed throughout this Thesis.

1.1.3 Complexes Containing $\text{CpCr}(\text{NO})$

Known complexes containing the mononitrosyl $\text{CpCr}(\text{NO})$ fragment are quite numerous, and may be divided into two major classes: dimeric and monomeric. A further division of the monomeric compounds may be employed based on the electronic configuration of the species. The history of each of these groups is outlined in the following Sections.

1.1.3.1 Dimeric Compounds of CpCr(NO)

A number of complexes of the form $[\text{CpCr}(\text{NO})\text{X}]_2$, where X is a bridging amide, alkoxide, or thiolate ligand, have been structurally characterized by Sim et al. These species include *cis*- and *trans*- $[\text{CpCr}(\text{NO})(\text{NMe}_2)]_2$,¹² *trans*- $[\text{CpCr}(\text{NO})(\text{SPh})]_2$,¹³ and *cis*- $[\text{CpCr}(\text{NO})(\text{OMe})]_2$.¹⁴ The independent synthesis and characterization of the methoxide dimer and the related $[\text{CpCr}(\text{NO})(\text{OEt})]_2$ were reported elsewhere.^{15,16} Other related dimeric species with bridging as well as terminal nitrosyl ligands include $[\text{CpCr}(\text{NO})_2]_2$ ¹⁷ and $[\text{CpCr}(\text{NO})]_2(\mu\text{-NO})(\mu\text{-NH}_2)$.¹⁸

With the exception of the methoxide dimer, all of these structurally characterized complexes have a planar Cr_2X_2 core, and are best formulated as having an 18-electron count at each metal center by virtue of a metal-metal single bond. In contrast, *cis*- $[\text{CpCr}(\text{NO})(\text{OMe})]_2$ is puckered, with an angle of 156° between the two Cr-O-Cr planes. Additionally, the Cr-X-Cr angles in this complex are greater than 90° , whereas in all the other dimers the angle is acute. This structural feature suggests the lack of a direct metal-metal interaction in this compound, though the complex is reportedly diamagnetic.

1.1.3.2 Monomeric $\{\text{Cr}(\text{NO})\}_6$ Compounds

The prototypical cyclopentadienyl chromium nitrosyl complex is $\text{CpCr}(\text{NO})(\text{CO})_2$.¹⁹ A robust, air- and thermally-stable 18e species, this bright red compound was first prepared by Fischer's group forty years ago by the reaction of nitric oxide with $[\text{CpCr}(\text{CO})_3]_2$.²⁰ Although this synthesis itself is high yielding, that of the dimeric tricarbonyl precursor is not. A more efficient synthesis of $\text{CpCr}(\text{NO})(\text{CO})_2$ involves the treatment of $[\text{CpCr}(\text{CO})_3]^-$ with Diazald.²¹

For some time, little reactivity of $\text{CpCr}(\text{NO})(\text{CO})_2$ was reported besides the Friedel-Crafts acylation of the aromatic Cp ring,²² perhaps because the substitution of the carbonyl ligands is not thermally facile. However, a CO ligand is readily displaced from the compound by photolysis, and suitable trapping agents thereby afford species of the type $\text{CpCr}(\text{NO})(\text{CO})(\text{L})$, where L = PPh_3 ,²³ MeCN, pyridine, 4-picoline, cyclooctene, or THF,²⁴ though the latter is not an isolable complex, and yields are generally low in any case. The cyclooctene ligand in $\text{CpCr}(\text{NO})(\text{CO})(\eta^2\text{-C}_8\text{H}_{14})$ is

easily displaced by a large variety of other olefins and acetylenes,²⁵ and similar reaction with CS₂ in the presence of PPh₃ yields a thiocarbonyl complex.²⁶ Treatment of photochemically generated CpCr(NO)(CO)(THF) with Ph₂CN₂ yields an alkylidene complex, CpCr(NO)(CO)(=CPh₂), which has been structurally characterized.²⁷ Again, these yields are low, and such photolytic methods generally afford only monosubstituted products, except in the case of a chelating ligand such as diphenylphosphinoethane.²⁸

A new nitrosyl carbonyl compound is also obtained by reaction of CpCr(NO)(CO)₂ with NaN(SiMe₃)₂, resulting in the complex salt Na[CpCr(NO)(CO)(CN)],²⁹ where the CN group results from the cleavage of a carbonyl C-O bond. The cyano anion may then be treated with trimethyloxonium to yield the methyl isonitrile complex, CpCr(NO)(CO)(CNMe).³⁰ Another, more predictable, reaction which modifies a carbonyl moiety is the conversion to a carbene complex. Sequential treatment of CpCr(NO)(CO)₂ with phenyllithium and trimethyloxonium affords CpCr(NO)(CO)(=C{OMe}Ph).³¹

CpCr(NO)(CO)₂ has been structurally characterized,³² as has its Cp* derivative.³³ Both these structural analyses suffer from disorder among the CO and NO ligands, a problem which is avoided in the case of (η⁵-fluorenyl)Cr(NO)(CO)₂.³²

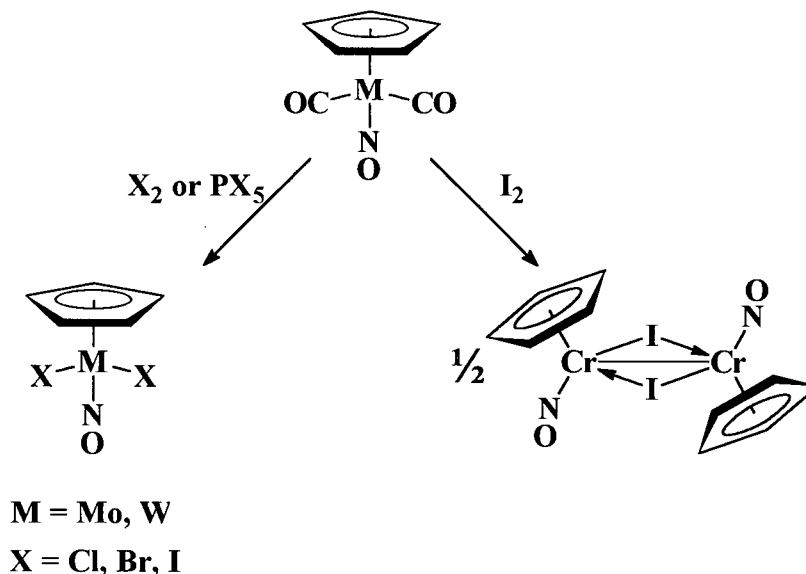
In general, then, the {Cr(NO)}⁶ class of compounds is dominated by CpCr(NO)(CO)₂, the chemistry of which primarily involves the photolytic preparation of monosubstituted products in fair-to-low yields.

1.1.3.3 Monomeric {Cr(NO)}⁵ Compounds

Just as the {Cr(NO)}⁶ complexes of CpCr(NO) are all 18e compounds, a {Cr(NO)}⁵ species containing this fragment is a 17e complex. The preparation of such species was also first reported by Fischer.³⁴ Treatment of the 18e dinitrosyl complex CpCr(NO)₂Cl with phosphines and cyclic amines surprisingly results in the displacement of nitric oxide and formation of CpCr(NO)(L)Cl species. Because a 3-electron donor nitrosyl is replaced with a 2-electron donor Lewis base, the product is a 17e compound. The products initially expected, the 18e cations [CpCr(NO)₂(L)]⁺, would result by loss of chloride rather than NO. Examples of the latter ionic

species have been prepared by Wojcicki, by the initial abstraction of the chloride ligand from $\text{CpCr(NO)}_2\text{Cl}$ with a silver salt, and the subsequent introduction of the Lewis base to the unsaturated $[\text{CpCr(NO)}_2]^+$ species.³⁵ However, when the Lewis base employed is a bidentate N-donor (phen, bipy), the result again is a 17e, $\{\text{Cr(NO)}\}^5$ species, namely the cation $[\text{CpCr(NO)}(\text{L-L})]^+$.

Additional work with this class of complexes has been performed by members of the Legzdins group since 1982. It was found that treatment of $\text{CpCr(NO)}(\text{CO})_2$ with elemental iodine results in loss of both CO ligands and formation of the dimeric species $[\text{CpCr(NO)}\text{I}]_2$ (1).¹⁵ The rapid loss of both carbonyl ligands from $\text{CpCr(NO)}(\text{CO})_2$ in this reaction contrasts with the photolytic chemistry described above. It is noteworthy that reaction of the analogous $\text{CpM(NO)}(\text{CO})_2$ ($\text{M} = \text{Mo}, \text{W}$) complexes with halide sources yields compounds with two halide ligands per metal, rather than one (Scheme 1.1).

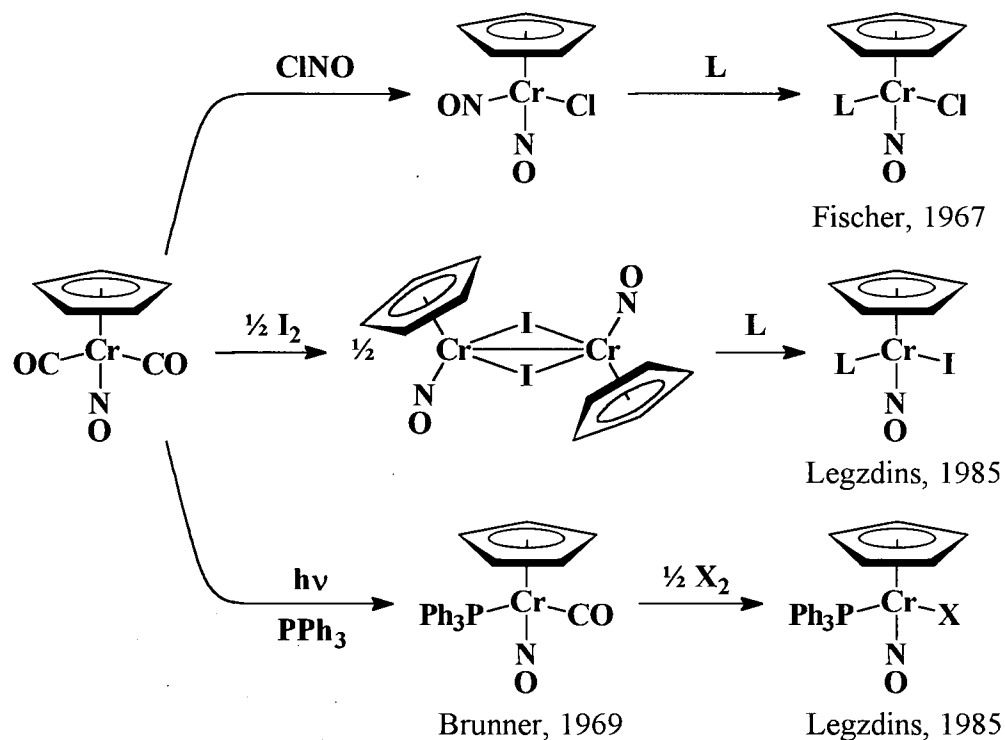


Scheme 1.1. Reactions of $\text{CpM(NO)}(\text{CO})_2$ with halogen reagents

The chromium reaction is not general, as treatment of $\text{CpCr(NO)}(\text{CO})_2$ with either Cl_2 ¹⁶ or Br_2 ¹⁵ results in $\text{CpCr(NO)}_2\text{X}$ ($\text{X} = \text{Cl}, \text{Br}$) as the only isolable nitrosyl-containing products,

rather than the halide dimers. Reaction of $[\text{CpCr}(\text{NO})\text{I}]_2$ with further I_2 also forms the analogous $\text{CpCr}(\text{NO})_2\text{I}$.

Early reactivity studies of $[\text{CpCr}(\text{NO})\text{I}]_2$, complex **1**, indicated that the dimer is easily cleaved with phosphines and phosphites to yield complexes of the sort $\text{CpCr}(\text{NO})(\text{PR}_3)\text{I}$ ($\text{R} = \text{Ph}$, OPh , OEt),¹⁵ thus affording compounds similar to those prepared by Fischer (*vide supra*). Another route to such complexes involves treatment of $\text{CpCr}(\text{NO})(\text{CO})(\text{PPh}_3)$ with X_2 ($\text{X} = \text{Cl}$, Br , I), which yields $\text{CpCr}(\text{NO})(\text{PPh}_3)\text{X}$.¹⁵ Thus, there are three routes to 17e $\text{CpCr}(\text{NO})(\text{L})(\text{X})$ species, each starting with 18e precursors but differing in the order of ligand replacement and formal oxidation, as depicted in Scheme 1.2.



Scheme 1.2. Syntheses of 17e $\text{CpCr}(\text{NO})(\text{L})\text{X}$ Complexes

In principle, the third of these routes is the most general. A wide range of $\text{CpCr}(\text{NO})(\text{CO})(\text{L})$ compounds is available by the method of Brunner,²³ as later demonstrated by Herberhold.^{24,25} As well, the subsequent halogenation reaction allows a selection of the halide

ligand, unlike the route involving $[\text{CpCr}(\text{NO})\text{I}]_2$. However, this greater versatility is offset by the lesser practicality of this route. The initial substitution requires extended photolysis and chromatographic separation of the air-sensitive monocarbonyl product from unreacted starting material, since the reaction does not proceed to completion. Also of moderate yield is the halogenation reaction to obtain the 17e product. Thus, although general, the third route is somewhat technically bothersome and is low-yielding overall.

The Fischer route also suffers from practical limitations. $\text{CpCr}(\text{NO})_2\text{Cl}$ is best prepared by reaction of $\text{CpCr}(\text{NO})(\text{CO})_2$ with nitrosyl chloride, the preparation of which is non-trivial, and the yield of the following substitution reaction is low. In contrast, both steps of the second route are very simple, quick, and high-yielding on large preparative scales. Thus, this is the route used by our group to synthesize 17e $\text{CpCr}(\text{NO})(\text{L})\text{I}$ complexes for further reactivity and study. The scope of this Thesis is the investigation of related chemistry of **1** with a wider range of Lewis bases, and is detailed in Section 1.2.

1.1.3.4 Monomeric $\{\text{Cr}(\text{NO})\}_4$ Compounds

There are two known compounds containing a $\text{Cp}'\text{Cr}(\text{NO})$ fragment where the metal is in a higher formal oxidation state than that of the above systems.³⁶ One is $\text{Cp}^*\text{Cr}(\text{NO})(\text{O-}i\text{-Pr})_2$, prepared by the reaction of $\text{Cp}^*\text{Cr}(\text{NO})_2\text{Cl}$ with excess *iso*-propoxide in *iso*-propanol.³⁸ The second is $\text{CpCr}(\text{NO})(\text{I})(\text{NPh}_2)$, isolated in unreported yield by the reaction of $\text{CpCr}(\text{NO})_2\text{Cl}$ with *in-situ*-generated LiNPh_2 , in the presence of iodomethane.³⁹ Both complexes have been structurally characterized, and both are best formulated as 18e complexes by virtue of π -donation to the metal center from the two alkoxide or the single amide ligands. Such a formulation is borne out by the preliminary reactivity studies of the bis(alkoxide) compound, which is inert toward attack by Lewis bases.

1.1.4 The Nature of $[\text{CpCr}(\text{NO})\text{I}]_2$ (**1**)

Complex **1** is isolable as a green-brown solid, soluble in solvents such as CH_2Cl_2 or THF, but much less so in Et_2O or benzene. The solid is thermally stable, and air-stable for a period of

hours, though for longer periods it is best stored under an inert atmosphere. The complex is both air- and thermally sensitive in solution, particularly in CH_2Cl_2 . Monitoring by IR spectroscopy of a CH_2Cl_2 solution of **1** kept under inert atmosphere reveals the noticeable presence of bands due to $\text{CpCr}(\text{NO})_2\text{I}$ after 6 hr, and the complete loss of features due to **1** after 2 days. Similar decomposition occurs in THF, but requires weeks instead of days.

$[\text{CpCr}(\text{NO})\text{I}]_2$ was initially assigned a dimeric structure by analogy to the structurally characterized $[\text{CpCr}(\text{NO})(\text{OMe})]_2$,¹⁴ and on the basis of its mass spectrum which displays peaks at $m/z = 548, 518, \text{ and } 488$, corresponding to P^+ , P^+-NO , and P^+-2NO for the dimeric species. However, this evidence is not entirely conclusive, as signals due to bimetallic ions are also observed in the mass spectra of $\text{Cp}^*\text{W}(\text{NO})\text{I}_2$, a complex which is monomeric in the solid state.⁴⁰ Subsequent evidence as to the nature of **1** both as solid and in solution has been accumulated by myself and others, and is summarized in the following Sections.

1.1.4.1 Spectroscopic Properties of $[\text{CpCr}(\text{NO})\text{I}]_2$ (**1**)

The spectroscopic evidence indicates that although **1** is a dimer in the solid state and maintains this dimeric structure in a solution of non- or weakly-coordinating solvents, it may be easily cleaved by donor solvents to yield solvated monomers. The dimeric species would be expected to exhibit more than one nitrosyl band, since it could exist as a mixture of *cis*- and *trans*-isomers, and the *cis*- form would have two IR active nitrosyl stretching frequencies. Thus, the IR spectrum of **1** displays three nitrosyl bands in Nujol or KBr and an asymmetric absorption indicative of multiple unresolved bands in CH_2Cl_2 . In contrast, the complex exhibits only one absorption in THF, as expected for a monomeric $\text{CpCr}(\text{NO})(\text{THF})\text{I}$ species. These IR spectra are compared in Figure 1.5.

The ESR spectra of **1** in various solvents correlates well with the IR data, and again indicates the cleavage of **1** upon dissolution in donor solvents. **1** displays no ESR signal in either CH_2Cl_2 or benzene, suggesting that the complex remains associated, but it exhibits strong ESR signals indicative of a 17e monomer as a solution in THF or NCMe. A molecular weight determination of **1** in THF yields a value consistent with the solvated monomer. A similar

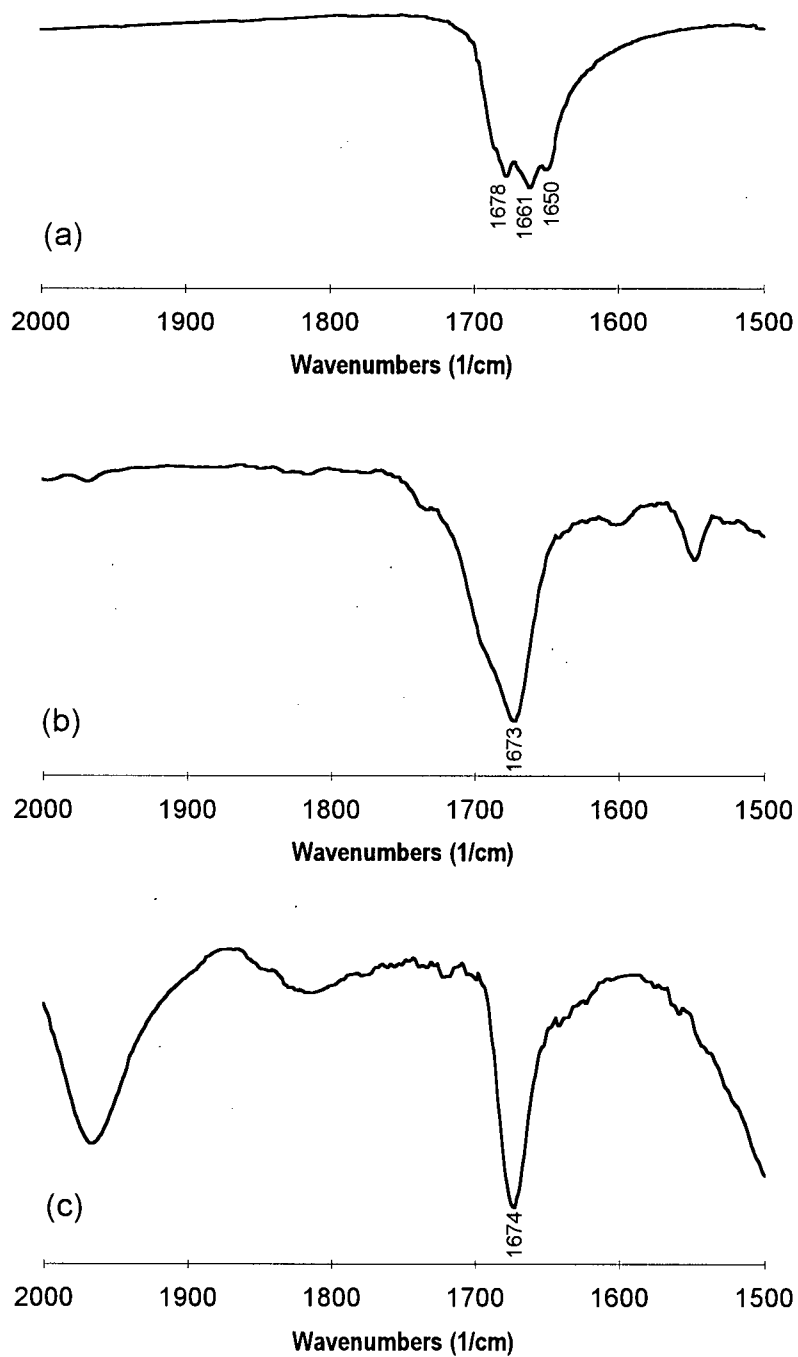


Figure 1.5. Infrared Spectra of **1** in (a) Nujol, (b) CH_2Cl_2 , and (c) THF.

determination in a poor-donor solvent to establish a dimeric structure in solution is hindered either by the low solubility or low stability of **1** in such solvents.

1.1.4.2 Magnetic Properties of [CpCr(NO)I]₂

We have traditionally depicted [CpCr(NO)I]₂ as lacking a metal-metal bond, despite the fact that the presence of such a bond would allow for an 18e count at each metal, and so would normally be an expected feature. The reasons for this are primarily indirect ones, partly due to an assumed analogy to the related [CpCr(NO)(OMe)]₂, structurally determined to lack a direct metal-metal bond,¹⁴ and partly due to the fact that **1** is not diamagnetic in the solid state. The presence of a magnetic moment suggests that the intuitively simple bonding situation, a metal-metal single bond, is not an accurate description.

An early magnetic study of **1** obtained a susceptibility of 0.165×10^{-3} cm³/mol per chromium atom in the solid state at room temperature, corresponding to a susceptibility of 0.329×10^{-3} cm³/mol and a moment of $0.90 \mu_B$ for the dimer.¹⁵ This moment is much lower than $2.45 \mu_B$, the value expected for a species containing two non-interacting $S = \frac{1}{2}$ nuclei. The low moment was attributed to strong antiferromagnetic exchange between the Cr atoms through the bridging iodide ligands.

In contrast, a susceptibility of 0.76×10^{-3} cm³/mol per chromium atom was obtained for **1** in chloroform solution, and was assigned as a corresponding moment of $1.94 \mu_B$ per dimer, much higher than that obtained from the solid-state measurement. However, this solution measurement was performed using a 8% *t*-BuOH solution of CHCl₃, and the Lewis basic alcohol would be expected to react with **1** and cleave the dimeric complex. Thus, the higher observed susceptibility is likely due to CpCr(NO)(HO-*t*-Bu)I, and not **1**.

A new series of magnetic measurements has now been carried out, including a variable-temperature solid-state study, the experimental details of which are outlined in Section 2.2.1. Evans' method solution studies⁴¹ provide further evidence that dissolution of **1** in donor solvents results in cleavage to a paramagnetic, solvated monomer. The observed room-temperature susceptibility of **1** in CDCl₃ is 0.312×10^{-3} cm³/mol per chromium atom, corresponding to a

moment of $1.22 \mu_B$ if the complex is entirely dimeric. Conversely, the observed susceptibility of **1** in CD_3CN is $0.916 \times 10^{-3} \text{ cm}^3/\text{mol}$ per chromium atom, which yields a moment of $1.48 \mu_B$ for $CpCr(NO)(NCCD_2H)I$; this value corresponds very well to that exhibited by other, related monomeric complexes (Section 2.3, Table 2.2).

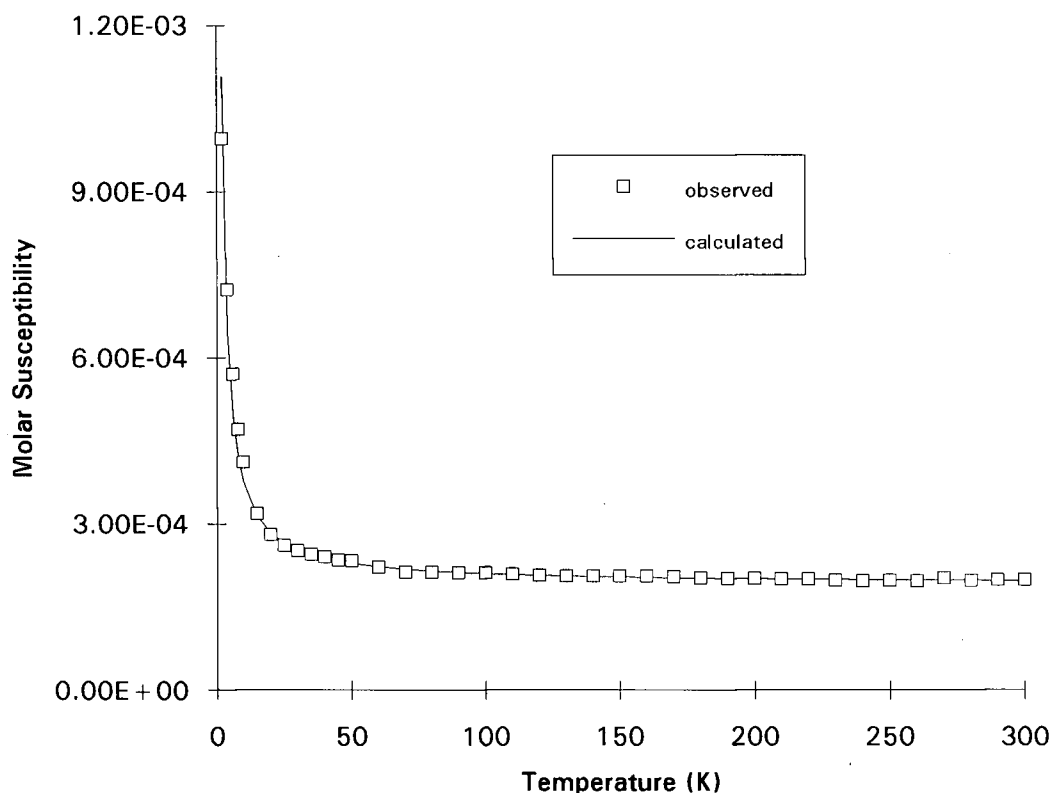


Figure 1.6. Observed and Calculated Susceptibility of $[CpCr(NO)I]_2$.
Calculation parameters: $\chi_{TIP} = 0.193 \times 10^{-3} \text{ cm}^3/\text{mol}$; %P = 0.49.

The results of the solid-state study are depicted in Figure 1.6. The observed susceptibility was best modeled by the presence of 0.49 mole percent of a paramagnetic impurity and by complex **1** exhibiting temperature-independent paramagnetism with a molar susceptibility of $\chi_m = 0.193 \times 10^{-3} \text{ cm}^3/\text{mol}$, only slightly more than half that determined from the earlier Gouy measurement. This yields for **1** a magnetic moment of $0.69 \mu_B$ at 300 K. The discrepancy between these and earlier values is somewhat understandable in light of the extremely small susceptibility exhibited by complex **1**. The corrected susceptibility is the same order of magnitude as the diamagnetic ligand corrections, so that the observed susceptibility is in fact near zero.

Small errors in measurement can therefore lead to much larger errors in the determined susceptibility and moment values.

The magnetic study clearly shows that the small magnetic moment exhibited by solid **1** at room temperature is not due to strong antiferromagnetic coupling between two $S = \frac{1}{2}$ nuclei as was originally thought, but rather is due only to temperature-independent paramagnetism (TIP). Unlike other forms of paramagnetism, TIP is not due to a non-singlet ground state. Instead, it results from the mixing of the ground state with a thermally inaccessible excited state when the magnetic field is applied. This yields a change in ground-state energy, and therefore a finite susceptibility. Because the extent of this orbital mixing is invariant with temperature, the susceptibility which results is also temperature-independent. A value on the order of 10^{-4} cm³/mol, as observed in this case, is typical.⁴²

Without this orbital mixing, complex **1** would have no magnetic moment, as the ground state of the complex is, in fact, a diamagnetic one. Thus, the dimer is best formulated as possessing a formal metal-metal bond and an 18-electron count at each metal center. Complex **1** is therefore depicted as such throughout this Thesis.

The definitive supporting evidence would, of course, be a structural analysis of **1**. This would confirm whether the inter-metal distance in the solid is consistent with a single Cr-Cr bond, and might lend insight as to the significance of the geometry of the Cr₂X₂ core in this and related complexes (*vide supra*). A structural analysis would also allow for the theoretical analysis of **1**, and possible identification of the orbital(s) responsible for the observed temperature-independent paramagnetism. Unfortunately, attempts to obtain suitable single crystals of complex **1** have to date proved unsuccessful.

1.2 Scope and Format

The nature of complex **1** has been discussed in this introductory Chapter because every other compound in this Thesis ultimately results from a reaction with this species. At the time this work was begun, little such investigation had taken place beyond the initial few reactions with phosphorus donors (Scheme 1.2).¹⁵ Although investigations into the alkylation of compounds such as $\text{CpCr}(\text{NO})(\text{PPh}_3)\text{I}$ and related halide compounds were also underway,^{43,44} there was no investigation as to the general scope of Lewis bases which could effect the cleavage of dimeric complex **1**.

The primary objective of this work was to expand this reactivity. The derivatives of complex **1** constitute an unusual class of well-defined 17e organometallic complexes, and comprehensive investigations of such compounds remain somewhat rare. It was hoped that such an extensive survey of the compounds formed from **1** might yield greater insight into the properties and reactivities of 17e complexes in general, and of these chromium nitrosyls in particular, specifically with regard to a comparison with the known 16e molybdenum and tungsten complexes. Since the reason for the disparate metal-dependent reactivities shown in Scheme 1.1 was unclear, further exploration of the chemistry of the 17e Cr compounds might offer a rationale as to why chromium prefers the 17e paramagnetic configuration, rather than the 16e diamagnetic form of molybdenum and tungsten species.

The general reactivity exhibited by **1** and examined in this Thesis is depicted in Figure 1.7. In addition to the simple reaction with a single equivalent of Lewis base as established previously,^{15,44} **1** will react with two equivalents of sufficiently nucleophilic base, resulting in the displacement of iodide and the formation of a complex salt containing a 17e cation. This reactivity, and the conversion between cations $[\text{CpCr}(\text{NO})(\text{L})_2]^+$ and their neutral precursors $\text{CpCr}(\text{NO})(\text{L})\text{I}$ is examined in Chapter 2.

Unlike more commonly-known 17e organometallic complexes, these new 17e cationic species do not exhibit a facile substitution chemistry. In fact, these paramagnetic species are more stable than their neutral, 18e reduction products, so that reduction to an even-electron form

Throughout this Thesis, a standard legal numbering format has been employed. For Chapters 2 to 5, each chapter is divided into the same six sections. Taking X to be the Chapter number, these sections are: X.1 Introduction, X.2 Experimental Procedures, X.3 Characterization Data, X.4 Results and Discussion, X.5 Epilogue and Future Work, and X.6 References and Notes. Subsections in each of these categories will be numbered, for example, X.1.1, X.1.1.1, and so on. Tables, figures, schemes, and equations will all be numerically sequenced so that the first equation in Chapter 3 will be Equation 3.1, the first figure Figure 3.1, and so on. As well, each complex prepared will be assigned a number based on the Chapter in which that complex is first described, and this compound number will be unchanged throughout the Thesis. Thus, the conversion of a complex first detailed in Chapter 2 to one prepared in Chapter 3 might read “Complex **2.4** was reacted to yield **3.3**.” The exception is the seminal species $[\text{CpCr}(\text{NO})\text{I}]_2$, which, as a complex discussed in Chapter 1, is simply described as compound **1**.

1.3 References and Notes

- (1) See, for example: Johnson, A. R.; Wanandi, P. W.; Cummins, C. C.; Davis, W. M. *Organometallics* **1994**, *13*, 2907. The subject matter of this paper is wholly appropriate to the journal in question, yet none of the compounds discussed contains a metal-carbon linkage.
- (2) For example: (a) Huheey, J. E. *Inorganic Chemistry*, 3rd ed.; Harper and Row: New York, NY, 1983, p 589. (b) Miessler, G. L., Tarr, D. A. *Inorganic Chemistry*, Prentice-Hall: Englewood Cliffs, NJ, 1991, p 418. (c) Shriver, D. F.; Atkins, P.; Langford, C. H. *Inorganic Chemistry*, 2nd ed.; W. H. Freeman: New York, NY, 1994, p 661. (d) Collman, J. P.; Hegedus, L. S.; Norton, J. R.; Finke, R. G. *Principles and Applications of Organotransition Metal Chemistry*, University Science Books: Mill Valley, CA, 1987, p 22.
- (3) Hoffmann, R. *Science* **1981**, *211*, 995.
- (4) Reference 2c, p 259.
- (5) Albright, T. A. *Tetrahedron* **1982**, *38*, 1339.
- (6) For example, $\text{Cp}^*\text{MoCl}(\text{PMe}_3)_2$ is a 16e, $S = 1$ complex which does not readily react with excess PMe_3 to form an 18e compound: Abugideri, F.; Keogh, D. W.; Poli, R. *J. Chem. Soc., Chem. Commun.* **1994**, 2317.
- (7) Legzdins, P.; Richter-Addo, G. B. *Metal Nitrosyls*; Oxford University Press: New York, 1992.
- (8) For a thorough discussion and comparison of the metal-ligand orbital interactions for various ligands, see: Gibson, V. C. *J. Chem. Soc., Dalton Trans.* **1994**, 1607.
- (9) Sidwick, N. V.; Bailey, R. W. *Proc. Roy. Soc., London* **1934**, *A144*, 521.
- (10) Enemark, J. H.; Feltham, R. D. *Coord. Chem. Rev.* **1974**, *13*, 339, and references contained therein.

- (11) See, for example: Ardon, M.; Cohen, S. *Inorg. Chem.* **1993**, *32*, 3241. Such an assignment in the complex $[\text{Cr}(\text{H}_2\text{O})_5(\text{NO})]^{2+}$ has been a matter of controversy for thirty years. The rate of substitution, pK_a , and Cr-O bond lengths are characteristic of octahedral Cr(III) complexes, while the magnetic moment and linear nitrosyl indicate Cr(I).
- (12) (a) Bush, M. A.; Sim, G. A. *J. Chem. Soc. (A)* **1970**, 611. (b) Bush, M. A.; Sim, G. A.; Knox, G. R.; Ahmad, M.; Robertson, C. G. *J. Chem. Soc. (D)* **1969**, 74.
- (13) McPhail, A. T.; Sim, G. A. *J. Chem. Soc. (A)* **1968**, 1858.
- (14) Hardy, A. D. U.; Sim, G. A. *Acta Cryst.* **1979**, *B35*, 1463.
- (15) Legzdins, P.; Nurse, C. R. *Inorg. Chem.* **1985**, *24*, 327.
- (16) Kolthammer, B. W. S.; Legzdins, P.; Malito, J. T. *Inorg. Chem.* **1977**, *16*, 3173.
- (17) (a) Calderón, J. L.; Fontana, S.; Frauendorfer, E.; Day, V. W. *J. Organomet. Chem.* **1974**, *64*, C10. (b) Kolthammer, B. W. S.; Legzdins, P.; Malito, J. T. *Inorg. Synth.* **1979**, *19*, 208.
- (18) (a) Flitcroft, N. *J. Organomet. Chem.* **1968**, *15*, 254. (b) Chan, L. Y. Y.; Einstein, F. W. B. *Acta Crystallogr., Sect. B* **1970**, *26*, 1899.
- (19) Though no longer in common use, this complex bears the trivial name "cynichrodene," derived by analogy from the name "cymantrene" for $\text{CpMn}(\text{CO})_3$: **cyclopentadienyl nitrosyl chromium dicarbonyl**.
- (20) Fischer, E. O.; Beckert, O.; Hafner, W.; Stahl, H. O. *Z. Naturforsch., B* **1955**, *10*, 598.
- (21) Chin, T. T.; Hoyano, J. K.; Legzdins, P.; Malito, J. T. *Inorg. Synth.* **1990**, *28*, 196.
- (22) Fischer, E. O.; Plesske, K. *Chem. Ber.* **1961**, *94*, 93.
- (23) Brunner, H. *J. Organomet. Chem.* **1969**, *16*, 119.
- (24) Herberhold, M.; Alt, H. *Liebigs Ann. Chem.* **1976**, 292.
- (25) Herberhold, M.; Alt, H.; Kreiter, Cornelius, C. G. *Liebigs Ann. Chem.* **1976**, 300.
- (26) Herberhold, M.; Smith, P. D.; Alt, H. *J. Organomet. Chem.* **1980**, *191*, 79.

- (27) Herrmann, W. A.; Hubbard, J. L.; Bernal, I.; Korp, J. D.; Haymore, B. L.; Hillhouse, G. L. *Inorg. Chem.* **1984**, *23*, 2978.
- (28) Sellmann, D.; Kleinschmidt, E. *Z. Naturforsch., B* **1977**, *32*, 1010.
- (29) Brunner, H. *Chem. Ber.* **1969**, *102*, 305.
- (30) Behrens, H.; Landgraf, G.; Merbach, P.; Moll, M.; Trummer, K.-H. *J. Organomet. Chem.* **1983**, *253*, 217.
- (31) Fischer, E. O.; Beck, H.-J. *Chem. Ber.* **1971**, *104*, 3101.
- (32) Atwood, J. L.; Shakir, R.; Malito, J. T.; Herberhold, M.; Kremnitz, W.; Bernhagen, W. P. E.; Alt, H. G. *J. Organomet. Chem.* **1979**, *165*, 65.
- (33) Malito, J. T., Shakir, R.; Atwood, J. L. *J. Chem. Soc., Dalton Trans.* **1980**, 1253.
- (34) Fischer, E. O.; Strametz, H. *J. Organomet. Chem.* **1967**, *10*, 323.
- (35) Wojcicki, A.; Regina, F. J. *Inorg. Chem.* **1980**, *19*, 3803.
- (36) It may be argued that there are actually three such compounds. The preparation of the alkylidene complex $\text{CpCr}(\text{NO})(\text{CO})(=\text{CPh}_2)$ is mentioned in Section 1.1.3.1. If the alkylidene moiety is taken as a two-electron π -donor ligand, and so as a 4-electron-donor dianion, then this complex is a $\{\text{Cr}(\text{NO})\}^4$ species. Such an assignment is somewhat arbitrary, and probably not warranted in any case. The $\text{Ph}_2\text{C}=\text{M}$ group tends to be electrophilic at carbon, and therefore more closely resembles a "Fischer"-type carbene than a "Schrock"-type alkylidene.³⁷ Fischer carbene ligands are generally regarded as neutral, two-electron donor (and therefore π -acceptor) groups, so that both $\text{CpCr}(\text{NO})(\text{CO})(=\text{CPh}_2)$ and $\text{CpCr}(\text{NO})(\text{CO})(=\text{C}\{\text{OMe}\}\text{Ph})$ would be considered $\{\text{Cr}(\text{NO})\}^6$ complexes.
- (37) Reference 2d, p 126.
- (38) Hubbard, J. L.; McVicar, W. K. *Inorg. Chem.* **1992**, *31*, 910. This complex and its preparation is discussed in greater detail in Chapter 4.
- (39) Sim, G. A.; Woodhouse, D. I.; Knox, G. R. *J. Chem. Soc., Dalton Trans.* **1979**, 83.

- (40) Dryden, N. H.; Legzdins, P.; Einstein, F. W. B.; Jones, R. H. *Can. J. Chem.* **1988**, *66*, 2100.
- (41) Sur, S. K. *J. Magn. Res.* **1989**, *82*, 169.
- (42) (a) Carlin, R. L. *Magnetochemistry*; Springer-Verlag: Berlin, 1986. (b) Mabbs, F. E.; Machin, D. J. *Magnetism and Transition Metal Complexes*; Chapman and Hall: London, 1973.
- (43) (a) Herring, F. G.; Legzdins, P.; McNeil, W. S.; Shaw, M. J.; Batchelor, R. J.; Einstein, F. W. B. *J. Am. Chem. Soc.* **1991**, *113*, 7049. (b) Legzdins, P.; Shaw, M. J. *J. Am. Chem. Soc.* **1994**, *116*, 7700.
- (44) Legzdins, P.; McNeil, W. S.; Shaw, M. J. *Organometallics* **1994**, *13*, 562.

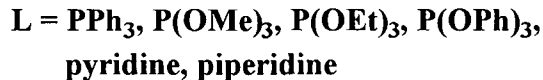
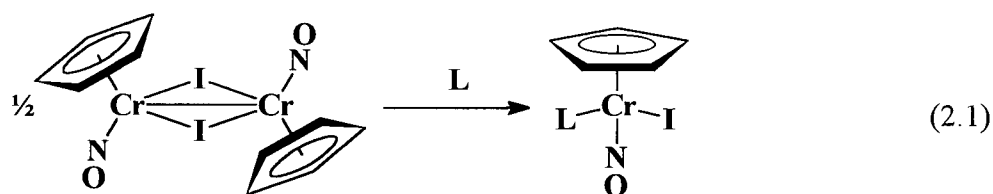
CHAPTER 2

Reactions of $[\text{CpCr}(\text{NO})\text{I}]_2$ with Amines

2.1 Introduction.....	25
2.2 Experimental Procedures.....	26
2.3 Characterization Data.....	32
2.4 Results and Discussion.....	33
2.5 Epilogue and Future Work.....	45
2.6 References and Notes.....	47

2.1 Introduction

As noted in Chapter 1, a surprisingly facile reaction of $\text{CpCr}(\text{CO})_2(\text{NO})$ is that with elemental iodine, which results in loss of both carbonyl ligands and formation of complex **1**, $[\text{CpCr}(\text{NO})\text{I}]_2$.¹ Although this reaction was initially discovered in our group nearly fifteen years ago, little chemistry of **1** had been investigated beyond that of the initial report at the time the work of this Thesis was begun. The known reactivity of complex **1** was cleavage of the dimeric structure by stoichiometric amounts of Lewis bases to yield compounds of the type $\text{CpCr}(\text{NO})(\text{L})\text{I}$, where the base is either a phosphorus donor^{1,2} or a cyclic nitrogen donor.² These transformations are depicted in eq 2.1.



The products of eq 2.1 exhibit properties consistent with their formulation as **17e**, paramagnetic monomers. Comparable spectroscopic evidence also suggests that a similar reaction occurs when **1** is dissolved in donor solvents such as THF or MeCN, though the resulting solvato complexes cannot be isolated.

By the end of 1991, the alkylation of one of these phosphine-halide compounds had been achieved, and the chemistry involved with that reaction was under investigation.³ However, the range of Lewis bases known to cleave **1** to paramagnetic monomers was still a narrow one, and the chemistry of the resulting **17e** species was almost entirely unexplored. I wished to extend this class of compounds to encompass nitrogen-donor ligands, particularly primary amines, both to generalize the reactivity depicted in eq 2.1 and also to obtain products that might exhibit further interesting reactivity.

2.2 Experimental Procedures

2.2.1 Methods

The methodologies described in this Section apply to the entire Thesis. All reactions and subsequent manipulations were performed under anaerobic and anhydrous conditions under an atmosphere of dinitrogen unless otherwise specified. Conventional glovebox and vacuum line Schlenk techniques were utilized throughout.⁴ The gloveboxes used during this work were Vacuum Atmospheres models HE-43-2 and HE-493 or an Innovative Technologies Labmaster 130 two-station glove box equipped with cold well, freezer, and rotary evaporator. Some reactions were performed in a bomb, defined here as a thick-walled glass vessel equipped with a Kontes greaseless Teflon stopcock and a side-arm for vacuum-line attachment.

Filtrations were performed through Celite 545 diatomaceous earth (Fisher), oven-dried and cooled in vacuo on a medium-porosity glass frit, unless otherwise specified. Other filtration supports such as Florosil and activity I alumina were similarly treated.

Solvents were either distilled from appropriate drying agents and purged with dinitrogen for 15 min prior to use, or were directly vacuum transferred from the drying agent.⁵ CH_2Cl_2 was doubly distilled from P_2O_5 . Et_2O was distilled from CaH_2 and then sodium/benzophenone. Hexanes were distilled from CaH_2 and then sodium/benzophenone/tetraglyme. Pentane was distilled from sodium/benzophenone/tetraglyme. THF was vacuum transferred from sodium/benzophenone at $-196\text{ }^\circ\text{C}$. CH_3CN was vacuum transferred from CaH_2 at $-196\text{ }^\circ\text{C}$. CDCl_3 was dried over P_2O_5 and filtered through a short column of neutral alumina, activity 1. Other deuterated solvents were dried on activated 4 \AA molecular sieves, thrice freeze-pump-thaw degassed, and filtered through Celite.

All IR samples were run as solutions in NaCl cells or as Nujol mulls between NaCl plates. IR spectra were recorded on an ATI Mattson Genesis Series FTIR spectrometer, interfaced to a 486DX-33 PC using WinFIRST software.

NMR spectra were obtained on either a Bruker AC-200 or a Varian Associates XL-300 spectrometer using C_6D_6 as the solvent. ^1H and $^{13}\text{C}\{^1\text{H}\}$ NMR spectra are referenced to the

residual proton or natural abundance carbon signal of C_6D_6 . $^{31}P\{^1H\}$ NMR spectra are referenced to 85% H_3PO_4 in D_2O , set to δ 0.00 ppm. Mrs. M. T. Austria, Ms. L. K. Darge, and Dr. S. O. Chan assisted in obtaining the NMR data.

Low-resolution mass spectra (EI, 70 eV) were recorded on a Kratos MS50 spectrometer using the direct-insertion method. Fast-atom bombardment (6 kV ion source, 7-8 kV xenon FAB gun) mass spectra were recorded on a AEI MS9 spectrometer using either 3-nitrobenzylalcohol or thioglycerol as matrix. All mass spectra were recorded by Dr. G. K. Eigendorf and the staff of the UBC mass spectroscopy laboratory.

Ambient-temperature X-band ESR solution spectra were recorded on an ECS 106 spectrometer with the assistance of Dr. F. G. Herring. Microwave frequency was determined with an EIP 625A CW microwave counter. Evans'-method magnetic measurements were effected by measuring the difference in proton chemical shift between the residual solvent peak of a C_6D_6 , $CDCl_3$, or CD_3CN solution of the analyte and that of the pure solvent in a sealed capillary within the NMR tube. Susceptibilities were corrected for diamagnetic ligand contributions.⁶

The solid state magnetic susceptibility of complex 1 was measured over the temperature range 2-300K using a Quantum-Design (MPMS) SQUID magnetometer (field = 10000 Oe). Temperature measurement was achieved using a combination of Ge and Pt resistance thermometers. Susceptibility calibration was performed using high-purity Ni and Bi standards. The sample was packed as a powder into a specially constructed holder made from PVC. The sample holder possessed a constant cross-sectional area, thus minimizing its contribution to the SQUID signal. The analysis was performed by David Summers.

All elemental analyses were performed by Mr. P. Borda of this department.

X-ray crystallographic analyses were performed either by Drs. R. J. Batchelor and F. W. B. Einstein of Simon Fraser University, or by Dr. S. J. Rettig of this department.

2.2.2 Electrochemical Measurements

The methodologies described in this Section apply to the entire Thesis. General methodology employed during cyclic voltammetry studies in our laboratories has been described previously;^{7,8} modifications are described below. The three-electrode cell consisted of a Pt-bead working electrode (~1 mm diameter), a Pt-wire coil auxiliary electrode, and a Ag/AgCl pseudo-reference electrode. Cyclic voltammetry studies employed THF as the solvent unless otherwise noted. THF was twice distilled, first from CaH₂ and then from sodium benzophenone or sodium/potassium benzophenone, and vacuum transferred from sodium benzophenone just prior to use. The electrochemical cell was assembled and used in a Vacuum Atmospheres model HE-43-2 glovebox. All electrochemical potentials are reported versus the saturated calomel electrode (SCE) and were measured using an internal ferrocene standard, the highly reversible Cp₂Fe/Cp₂Fe⁺ couple occurring at $E_{1/2} = +0.55$ V vs. SCE in THF under these conditions.

2.2.3 Reagents

Compound 1, [CpCr(NO)I]₂, was prepared according to the published procedure.¹ For ease of calculation, all stoichiometries involving this complex are reported per mole of *monomer*, with a mass of 274.00 g/mol. Allylamine and *tert*-butylamine (Aldrich) were subjected to two freeze-pump-thaw degas cycles and were vacuum transferred from CaH₂. PMe₃ (Aldrich) was vacuum transferred from Na/benzophenone. All other reagents were purchased from commercial suppliers and used as received.

2.2.4 Preparation of [CpCr(NO)(NH₃)₂]⁺I⁻ ([2.1]⁺I⁻)

[CpCr(NO)I]₂ (274 mg, 1.00 mmol) was placed in a Schlenk tube and was dissolved in CH₂Cl₂ (20 mL). An excess of ammonia was added in the form of ~3 mL of an ammonia-saturated CH₂Cl₂ solution. The brown reaction mixture rapidly deposited a bright green precipitate that was collected on a frit, washed with CH₂Cl₂ (2 x 10 mL), and dried in vacuo to obtain analytically pure [2.1]⁺I⁻.

2.2.5 Preparation of $[\text{CpCr}(\text{NO})(\text{NH}_3)_2]^+[\text{PF}_6]^-$ ($[\mathbf{2.1}]^+[\text{PF}_6]^-$)

Solid $[\mathbf{2.1}]^+\text{I}^-$ (0.308 g, 1.00 mmol) and AgPF_6 (0.253 g, 1.00 mmol) were placed into a Schlenk tube. The solids were stirred in MeCN (10 mL), whereupon a yellow-white precipitate deposited. The mixture was filtered, and the green filtrate was taken to dryness in vacuo. The remaining residue was triturated and washed with pentane (2 x 10 mL), and the resulting green solid was recrystallized from CH_2Cl_2 /hexanes to obtain analytically pure $[\mathbf{2.1}]^+[\text{PF}_6]^-$ as green blocks.

Dissolution of equimolar amounts $[\mathbf{2.1}]^+\text{I}^-$ and NaBPh_4 in acetonitrile, followed by slow diffusion of pentane into the resulting solution, yielded X-ray quality crystals of the analogous $[\text{BPh}_4]^-$ salt as the acetonitrile solvate (i.e. $[\mathbf{2.1}]^+[\text{BPh}_4]^- \cdot \text{NCMe}$).

2.2.6 Preparation of $[\text{CpCr}(\text{NO})(\text{NH}_2\text{C}_3\text{H}_5)_2]^+\text{I}^-$ ($[\mathbf{2.2}]^+\text{I}^-$)

THF (~10 mL) and an excess of allylamine were vacuum transferred onto $[\text{CpCr}(\text{NO})\text{I}]_2$ (0.274 g, 1.00 mmol) in a Schlenk tube. The solution was warmed to room temperature and stirred for 10 min, during which time the color changed from brown to bright green. The solvent was removed in vacuo, the green residue was triturated and washed with pentane (2 x 15 mL), and the green solid was recrystallized from CH_2Cl_2 /hexanes to obtain green needles of $[\mathbf{2.2}]^+\text{I}^-$.

2.2.7 Preparation of $[\text{CpCr}(\text{NO})(\text{NH}_2\text{C}_3\text{H}_5)_2]^+[\text{PF}_6]^-$ ($[\mathbf{2.2}]^+[\text{PF}_6]^-$)

Solid $[\mathbf{2.2}]^+\text{I}^-$ (128 mg, 0.33 mmol) and AgPF_6 (84 mg, 0.33 mmol) were weighed into a Schlenk tube and stirred in CH_2Cl_2 (15 mL). A yellow-white precipitate formed immediately, and the mixture was filtered. The green filtrate was concentrated and cooled at $-30\text{ }^\circ\text{C}$ overnight to induce the deposition of green crystals of $[\mathbf{2.2}]^+[\text{PF}_6]^-$.

2.2.8 Preparation of $[\text{CpCr}(\text{NO})(\text{en})]^+\text{I}^-$ (**[2.3]** $^+\text{I}^-$)

$[\text{CpCr}(\text{NO})\text{I}]_2$ (274 mg, 1.00 mmol) was dissolved in CH_2Cl_2 (20 mL), and ethylenediamine (80 μL , 0.72 mg, 1.2 mmol) was added to the solution. The brown reaction mixture rapidly deposited a flocculent, pale green precipitate that was collected on a frit, washed with CH_2Cl_2 (2 x 10 mL), and dried in vacuo to obtain analytically pure **[2.3]** $^+\text{I}^-$.

2.2.9 Preparation of $[\text{CpCr}(\text{NO})(\text{en})]^+\text{PF}_6^-$ (**[2.3]** $^+\text{PF}_6^-$)

Solid **[2.3]** $^+\text{I}^-$ (305 mg, 0.913 mmol) and AgPF_6 (240 mg, 0.913 mmol) were dissolved and stirred in MeCN (10 mL), resulting in the immediate formation of a yellow precipitate. The mixture was filtered, and the solvent was removed from the filtrate in vacuo. The resulting green solid was washed and triturated with CH_2Cl_2 (15 mL) and dried in vacuo to obtain analytically pure **[2.3]** $^+\text{PF}_6^-$.

2.2.10 Preparation of $\text{CpCr}(\text{NO})(\text{NH}_2\text{CMe}_3)\text{I}$ (**2.4**)

THF (~10 mL) and an excess of *tert*-butylamine were vacuum transferred onto $[\text{CpCr}(\text{NO})\text{I}]_2$ (0.274 g, 1.00 mmol) in a Schlenk tube. The solution was warmed to room temperature and stirred for 10 min, during which time the color changed from brown to bright green. The solvent was removed in vacuo, the olive green residue was triturated and washed with pentane (2 x 15 mL), and the green solid was recrystallized from CH_2Cl_2 /hexanes to obtain green prisms of **2.4**.

2.2.11 Preparation of $[\text{CpCr}(\text{NO})(\text{NH}_2\text{CMe}_3)_2]^+\text{PF}_6^-$ (**[2.5]** $^+\text{PF}_6^-$)

A mixture of solid **2.4** (219 mg, 0.500 mmol) and AgPF_6 (183 mg, 0.500 mmol) was dissolved in CH_2Cl_2 (15 mL). The mixture was stirred for 5 min, resulting in a flocculent, yellow precipitate and a bright green solution. The mixture was then filtered, and the frit was washed with a minimum of CH_2Cl_2 . An excess of *tert*-butylamine was vacuum transferred into the

filtrate, and the mixture was stirred for 2 h. The solvent was removed in vacuo, and the green residue was recrystallized from CH_2Cl_2 to obtain forest green prisms of $[\mathbf{2.5}]^+[\text{PF}_6]^-$.

2.2.12 Preparation of $\text{CpCr}(\text{NO})(\text{NH}_3)\text{I}$ (**2.6**)

A sample of $[\mathbf{2.1}]^+\text{I}^-$ (154 mg, 0.500 mmol) was suspended in CH_2Cl_2 (100 mL), and the mixture was refluxed for 18 h. The resulting green solution was concentrated under reduced pressure. Hexanes were added, and the solution was further concentrated and cooled at $-30\text{ }^\circ\text{C}$ overnight in order to induce the deposition of green, crystalline **2.6**.

2.2.13 Preparation of $\text{CpCr}(\text{NO})(\text{NH}_2\text{C}_3\text{H}_5)\text{I}$ (**2.7**)

A sample of $[\mathbf{2.2}]^+\text{I}^-$ (388 mg, 1.00 mmol) was dissolved in CH_2Cl_2 (20 mL), and the solution was refluxed overnight. The solvent was removed in vacuo from the final mixture, and the green residue was triturated and extracted with Et_2O (2 x 15 mL). The extracts were filtered, leaving behind an insoluble green material (presumably unreacted $[\mathbf{2.2}]^+\text{I}^-$). The yellow-green filtrate was concentrated, hexanes were added, and the solution was cooled at $-30\text{ }^\circ\text{C}$ overnight to induce the deposition of X-ray quality prisms of **2.7**.

2.2.14 Reaction of $[\text{CpCr}(\text{NO})\text{I}]_2$ with PMe_3

THF (~10 mL) and an excess of PMe_3 (~1 mL) were vacuum transferred onto $[\text{CpCr}(\text{NO})\text{I}]_2$ (274 mg, 1.00 mmol). The reaction mixture was stirred for two hours. Spectra of the resulting solution displayed two overlapping absorptions at 1667 and 1681 cm^{-1} (IR), and two overlapping signals, likely a poorly-resolved doublet and a 1:2:1 triplet (ESR). The solvent was removed in vacuo, and the resulting brown residue was washed with Et_2O (3 x 10 mL) to obtain a yellow-green powder. This material was identified as $[\text{CpCr}(\text{NO})(\text{PMe}_3)_2]^+\text{I}^-$, though it was impure and not fully characterized. Partial characterization data: +FAB-MS (m/z): 299 (P^+). -FAB-MS (m/z): 127 (P^-). Anal. Calcd (Found) for $\text{C}_{11}\text{H}_{23}\text{NOP}_2\text{CrI}$: C, 31.00 (29.81); H, 5.44 (5.22); 3.29 (3.12).

2.3 Characterization Data

Table 2.1. Numbering Scheme, Color, Yield and Elemental Analysis Data

complex	compd no.	color (yield, %)	elemental analysis found (calcd)		
			C	H	N
[CpCr(NO)(NH ₃) ₂] ⁺ I ⁻	[2.1] ⁺ I ⁻	green (94)	19.38 (19.49)	3.65 (3.60)	13.46 (13.64)
[CpCr(NO)(NH ₃) ₂] ⁺ PF ₆ ⁻	[2.1] ⁺ PF ₆ ⁻	green (83)	18.44 (18.41)	3.30 (3.40)	12.68 (12.88)
[CpCr(NO)(NH ₂ C ₃ H ₅) ₂] ⁺ I ⁻	[2.2] ⁺ I ⁻	dark green (65)	33.92 (34.03)	4.89 (4.93)	10.58 (10.82)
[CpCr(NO)(NH ₂ C ₃ H ₅) ₂] ⁺ PF ₆ ⁻	[2.2] ⁺ PF ₆ ⁻	dark green (58)	32.71 (32.52)	4.65 (4.71)	10.14 (10.34)
[CpCr(NO)(en)] ⁺ I ⁻	[2.3] ⁺ I ⁻	pale green (92)	25.18 (25.17)	3.89 (3.92)	12.49 (12.58)
[CpCr(NO)(en)] ⁺ PF ₆ ⁻	[2.3] ⁺ PF ₆ ⁻	green (84)	23.65 (23.87)	3.68 (3.72)	11.77 (11.93)
CpCr(NO)(NH ₂ CMe ₃)I	2.4	olive (84)	31.39 (31.14)	4.63 (4.65)	8.05 (8.07)
[CpCr(NO)(NH ₂ CMe ₃) ₂] ⁺ PF ₆ ⁻	[2.5] ⁺ PF ₆ ⁻	bright green (46)	36.15 (35.62)	6.21 (6.21)	9.32 (9.59)
CpCr(NO)(NH ₃)I	2.6	green (94)	20.33 (20.64)	2.99 (2.77)	9.58 (9.63)
CpCr(NO)(NH ₂ C ₃ H ₅)I	2.7	green (32)	29.41 (29.02)	3.82 (3.65)	8.35 (8.46)

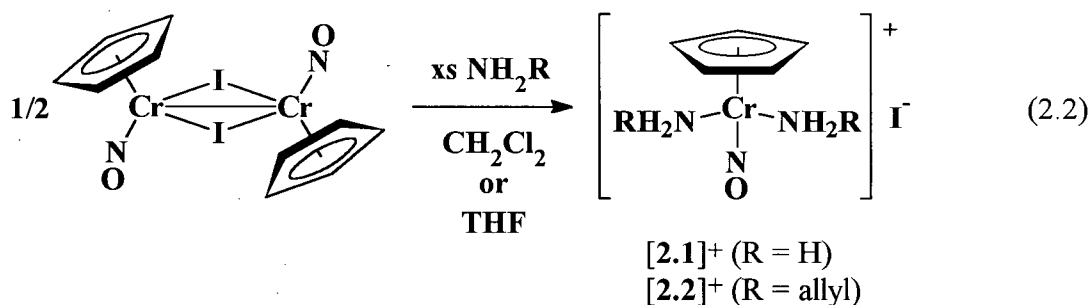
Table 2.2. Mass Spectral, Infrared, ESR, and Magnetic Data

complex	FAB-MS (<i>m/z</i>)		IR (cm ⁻¹)		ESR	μ _{eff} (μ _B)
	(+)	(-)	ν _{NO} (Nujol)	ν _{NO} (solvent)	g-value (solvent)	(solvent)
[2.1] ⁺ I ⁻	181 [P ⁺]	127 [P ⁻]	1658	-	-	-
[2.1] ⁺ PF ₆ ⁻	181 [P ⁺]	145 [P ⁻]	1667	1676 (THF)	1.986 (MeCN)	1.49 (CD ₃ CN)
[2.2] ⁺ I ⁻	261 [P ⁺]	127 [P ⁻]	1667	1672 (THF)	-	-
[2.2] ⁺ PF ₆ ⁻	261 [P ⁺]	145 [P ⁻]	1672	1683 (CH ₂ Cl ₂)	1.987 (CH ₂ Cl ₂)	1.35 (CD ₃ CN)
[2.3] ⁺ I ⁻	207 [P ⁺]	127 [P ⁻]	1680	-	-	-
[2.3] ⁺ PF ₆ ⁻	207 [P ⁺]	127 [P ⁻]	1660	1679 (MeCN)	1.989 (MeCN)	1.20 (CD ₃ CN)
2.4	347 [P ⁺]	-	1651	1667 (THF)	2.020 (CH ₂ Cl ₂)	1.26 (CDCl ₃)
[2.5] ⁺ PF ₆ ⁻	293 [P ⁺]	145 [P ⁻]	1693	1679 (CH ₂ Cl ₂)	1.986 (CH ₂ Cl ₂)	-
2.6	291 [P ⁺]	-	1658	1669 (CH ₂ Cl ₂)	2.021 (CH ₂ Cl ₂)	1.41 (CDCl ₃)
2.7	331 [P ⁺]	-	1648	1676 (Et ₂ O)	2.022 (CH ₂ Cl ₂)	1.45 (CDCl ₃)

2.4 Results and Discussion

2.4.1 Reactions of NH_3 , $\text{NH}_2\text{C}_3\text{H}_5$, and ethylenediamine

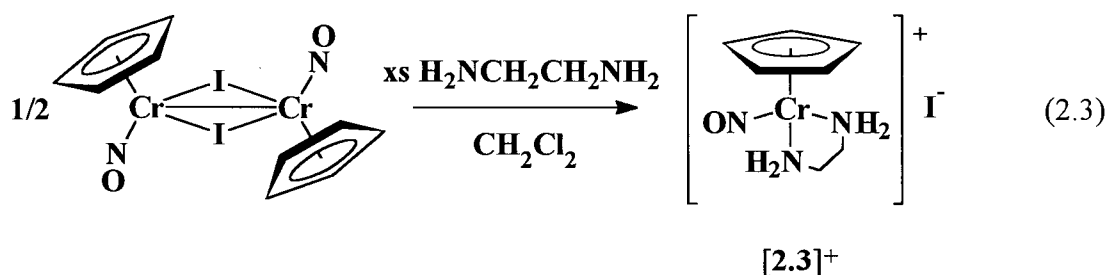
Treatment of **1** with an excess of either ammonia or allylamine in CH_2Cl_2 does not yield the $\text{CpCr}(\text{NO})(\text{L})\text{I}$ products that had been previously observed. Instead, the starting complex rapidly reacts with two equivalents of ligand per metal to afford a complex salt of the type $[\text{CpCr}(\text{NO})(\text{NH}_2\text{R})_2]^+[\text{I}]^-$, where the iodide ligand has been displaced from the metal and becomes the counterion for the 17e organometallic cation (eq 2.2). This result is partly due to the fact that unlike reagents used previously, ammonia and allylamine are highly volatile liquids and so were best added by vacuum transfer, thus delivering an excess of these species to the reaction mixture.



As salts, these compounds are relatively insoluble. They do not dissolve in Et_2O , and the bis(ammonia) complex $[\mathbf{2.1}]^+\text{I}^-$ is insoluble even in CH_2Cl_2 , precipitating from the reaction mixture as an analytically pure solid. Although both compounds dissolve in MeCN and THF, salts with greater solubility were desired, and so attempts were made to exchange the iodide counterion for other anions. The proper choice of reagent is critical for such a metathesis to be successful, since the dissolution of two ionic salts will result in a scrambling of ions if all species remain in solution, thereby rendering the desired ionic product unisolable. Thus, reaction of $[\mathbf{2.2}]^+\text{I}^-$ with NH_4PF_6 in CH_2Cl_2 yields a mixture of both the starting material and $[\mathbf{2.2}]^+\text{PF}_6^-$ (and, presumably, the associated ammonium byproducts), with no way to separate the two salts. However, treatment of either $[\mathbf{2.1}]^+\text{I}^-$ or $[\mathbf{2.2}]^+\text{I}^-$ with AgPF_6 in MeCN causes the immediate formation of insoluble AgI , which may be removed by filtration to allow isolation of the pure

hexafluorophosphate salts. As hoped, the latter complexes are both more soluble and more crystalline than are the I^- congeners.

In a similar manner, **1** reacts instantly with an excess of ethylenediamine in CH_2Cl_2 to precipitate $[CpCr(NO)(en)]^+I^-$ ($[2.3]^+[I]^-$), as shown in eq 2.3. As expected, the ethylenediamine ligand binds in a bidentate manner to the chromium center in $[2.3]^+$,⁹ and metathesis of the I^- counterion for PF_6^- using the silver salt is facile and leads to increased solubility of the resulting salt.

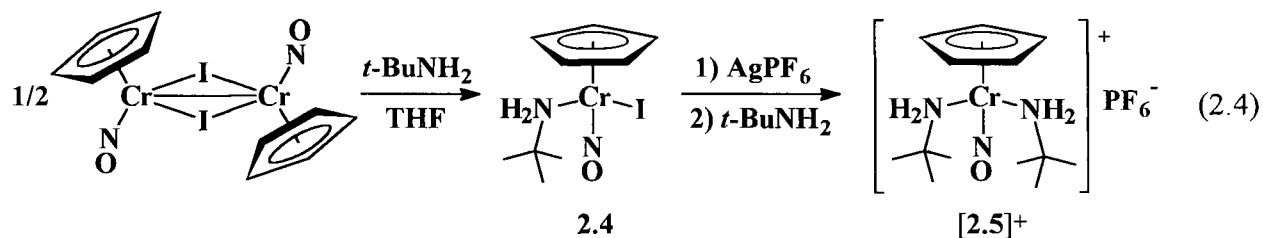


2.4.2 Reaction with *tert*-Butylamine

The formation of complex salts in these reactions differs from previously reported reactivity of $[CpCr(NO)I]_2$ with phosphorus donors to obtain neutral, monomeric products; however, the latter reagents were generally used in a stoichiometric manner, whereas the amine reagents above were used in excess. It was of interest to learn which effect determined the type of product obtained: the electronic and steric natures of the added base, or the presence of an excess of potential ligand.

Treatment of **1** with an excess of PMe_3 generates a species with two phosphine ligands, as indicated by an observed 1:2:1 triplet in the ESR spectrum. On the other hand, reaction of **1** with an excess of $P(OMe)_3$ leads only to the formation of $CpCr(NO)(P\{OMe\}_3)I$, with no evidence for the formation of bis(phosphite) species (Section 3.4.6). A similar result is obtained when the same reaction is performed with an excess of NH_2CMe_3 . Treatment of $[CpCr(NO)I]_2$ with the sterically demanding amine leads only to $CpCr(NO)(NH_2CMe_3)I$ (**2.4**) and not to the complex salt, $[CpCr(NO)(NH_2CMe_3)_2]^+[I]^-$.

However, a second NH_2CMe_3 ligand may be incorporated if the iodide is first removed from the coordination sphere. That is, abstraction of the halide from **2.4** with a silver salt, followed by the addition of further NH_2CMe_3 to the solution, results in the formation of $[\text{CpCr}(\text{NO})(\text{NH}_2\text{CMe}_3)_2]^+$ (**[2.5]⁺**). These results are depicted in eq 2.4.



The fact that amine-iodide **2.4** will not react directly with an excess of NH_2CMe_3 to produce **[2.5]⁺**, but that this latter complex is in fact stable, indicates that the substitution of amine for iodide suffers from a high kinetic barrier. The fact that the corresponding substitution does occur for ammonia and allylamine but not for the more sterically demanding *tert*-butylamine further suggests an associative mechanism for the substitution reaction.

It should be noted that the halide abstraction reaction in eq 2.4 must be performed using a sample of isolated **2.4**. Although **2.4** can easily be generated in THF solution with an excess of NH_2CMe_3 , the silver reagent cannot be reacted with **2.4** in situ while still in the presence of excess amine. The neutral complex must be isolated and the excess amine washed away, or else the halide abstraction does not take place. This is presumably due to complexation of Ag^+ by NH_2CMe_3 , which prevents the desired reactivity with the amine halide compound.

It appears that the nature of the product obtained in these reactions of **1** with Lewis bases depends on both steric and electronic factors. A clear correlation of product with the nature of Lewis base employed is not immediately apparent, since both softer phosphorus and harder nitrogen donors can lead to the presence or absence of a bis(ligand) cation in solution. In the case of nitrogen donors, this might appear to be a purely steric effect, since the smaller amines displace I^- , whereas the sterically demanding NH_2CMe_3 results only in the amine-iodide monomer **2.4**. However, reaction of **1** with excess $\text{P}(\text{OMe})_3$ generates only $\text{CpCr}(\text{NO})(\text{P}\{\text{OMe}\}_3)\text{I}$, while

reaction with excess PMe_3 affords a bis(phosphine) complex $[\text{CpCr}(\text{NO})(\text{PMe}_3)_2]^+\text{I}^-$, or at least an equilibrium mixture of bis(phosphine) and mono(phosphine) species. This difference cannot be a purely steric one, since the cone angle of $\text{P}(\text{OMe})_3$ (107°) is actually somewhat less than that of PMe_3 (118°).¹⁰ However, it can be rationalized electronically, since the electronegative OMe groups of the phosphite ligand would be expected to render it less nucleophilic than PMe_3 .

2.4.3 Heating the Complex Salts: Preparation of Amine Iodide Complexes 2.6 and 2.7

An attempt was made to obtain a crystalline sample of bis(ammonia) salt $[\mathbf{2.1}]^+\text{I}^-$ by Soxhlet extracting the complex with CH_2Cl_2 . However, instead of insoluble crystals of the salt, the result of this extraction was a homogeneous green solution, the IR and ESR spectra of which indicated the presence of a new paramagnetic nitrosyl complex. This new species was $\text{CpCr}(\text{NO})(\text{NH}_3)\text{I}$ (**2.6**), resulting from re-entrance of I^- into the coordination sphere of the metal, and loss of the volatile free ammonia. **2.6** is best prepared simply by suspending $[\mathbf{2.1}]^+\text{I}^-$ in refluxing CH_2Cl_2 , with a positive flow of inert gas above the condenser to aid the removal of NH_3 from the reaction vessel. Similar treatment of the allylamine congener $[\mathbf{2.2}]^+\text{I}^-$ affords the corresponding amine iodide complex, **2.7**. In the latter case, the reaction does not proceed to completion, and the more soluble neutral product must be preferentially extracted away from unreacted $[\mathbf{2.2}]^+\text{I}^-$. This accounts for the lower isolated yield of **2.7**, and is presumably due to the lesser volatility or greater solubility of allylamine as compared to that of ammonia.

2.4.4 ESR Monitoring of Amine Reactions

Given that reaction of **1** with an excess of NH_2CMe_3 leads to the formation only of amine-iodide **2.4**, it is reasonable to assume that the formation of bis(amine) complexes $[\mathbf{2.1}]^+\text{I}^-$ and $[\mathbf{2.2}]^+\text{I}^-$ would proceed via the intermediate formation of analogous mono(amine) iodide compounds, that is, complex **2.6** from the reaction with NH_3 , and **2.7** from the reaction with allylamine. The fact that these neutral complexes can be prepared from heating solutions of the ionic precursors suggests that the two types of complex would be in equilibrium in the presence of

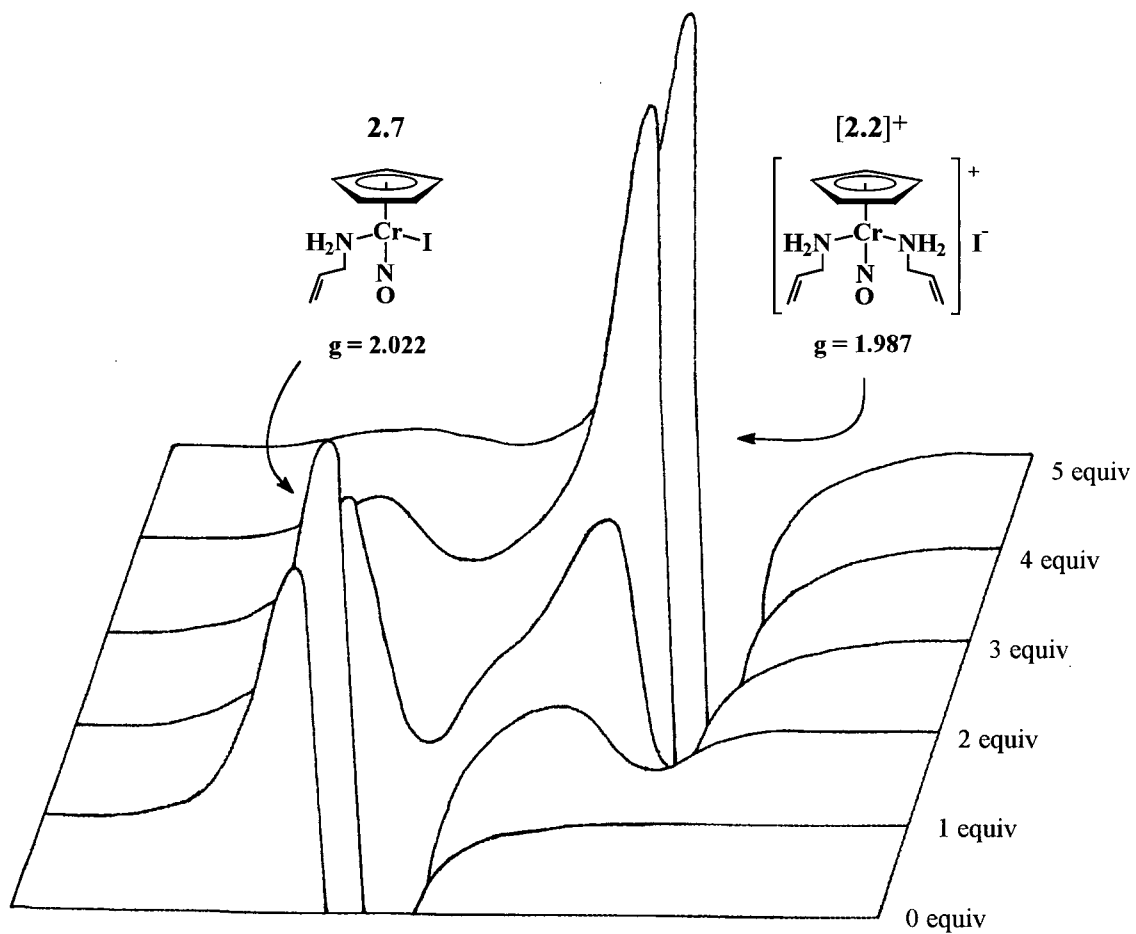


Figure 2.1. ESR spectra observed when $[\text{CpCr}(\text{NO})\text{I}]_2$ in CH_2Cl_2 is treated with sequential equivalents (per chromium atom) of $\text{NH}_2\text{C}_3\text{H}_7$.

an intermediate amount of free amine. These suppositions are borne out by spectroscopic monitoring of the reaction of **1** with amine. Single equivalents of allylamine were sequentially added to a CH_2Cl_2 solution of $[\text{CpCr}(\text{NO})\text{I}]_2$, and both ESR and IR spectra of the solution were recorded approximately 30 min after each addition. The first ESR signal to appear is that of amine iodide complex **2.7** ($g = 2.022$) (Figure 2.1). The intensity of this signal reaches a maximum with about 2 equiv of added amine, at which point a signal due to $[\mathbf{2.2}]^+\text{I}^-$ ($g = 1.987$) is observed. Further amine gradually lessens the signal of **2.7** while that of $[\mathbf{2.2}]^+\text{I}^-$ is increased, until only the latter signal is observed after the addition of 5 equiv of $\text{NH}_2\text{C}_3\text{H}_5$.¹¹ There is also a progressive color change during these additions. The solution, initially the brown color of **1**, becomes gradually green as amine iodide **2.7** reaches a maximum concentration, and this color brightens to the emerald green of bis(amine) $[\mathbf{2.2}]^+\text{I}^-$ as more $\text{NH}_2\text{C}_3\text{H}_5$ is added.

Infrared monitoring of the same solutions indicates that the final product, $[\mathbf{2.2}]^+\text{I}^-$, begins to form before **1** has been entirely consumed. In other words, **2.7** is never the lone organometallic species in solution. Thus, reaction of $[\text{CpCr}(\text{NO})\text{I}]_2$ with small amounts of NH_3 or $\text{NH}_2\text{C}_3\text{H}_5$ is not the method of choice for the preparation and isolation of the neutral complexes **2.6** or **2.7**, and they are best synthesized by the method outlined above.

2.4.5 Solid-State Molecular Structures of $[\mathbf{2.1}]^+$ and **2.7**

The bis(ammonia) complex $[\mathbf{2.1}]^+$ and allylamine iodide complex **2.7** were selected as representative examples of the cationic and neutral forms of these 17e amine compounds, respectively, and were subjected to single-crystal X-ray crystallographic analyses. X-ray quality crystals containing the cation $[\mathbf{2.1}]^+$ could be obtained only by using the bulky BPh_4^- counterion, and were isolated as the acetonitrile solvate, that is $[\text{CpCr}(\text{NO})(\text{NH}_3)_2]^+[\text{BPh}_4]^- \cdot \text{NCMe}$. Crystallographic details and tables of fractional coordinates and isotropic thermal parameters are contained in the Appendix, and ORTEP drawings of $[\mathbf{2.1}]^+$ and **2.7** are shown in Figures 2.2 and 2.3, along with selected metrical parameters of these species.

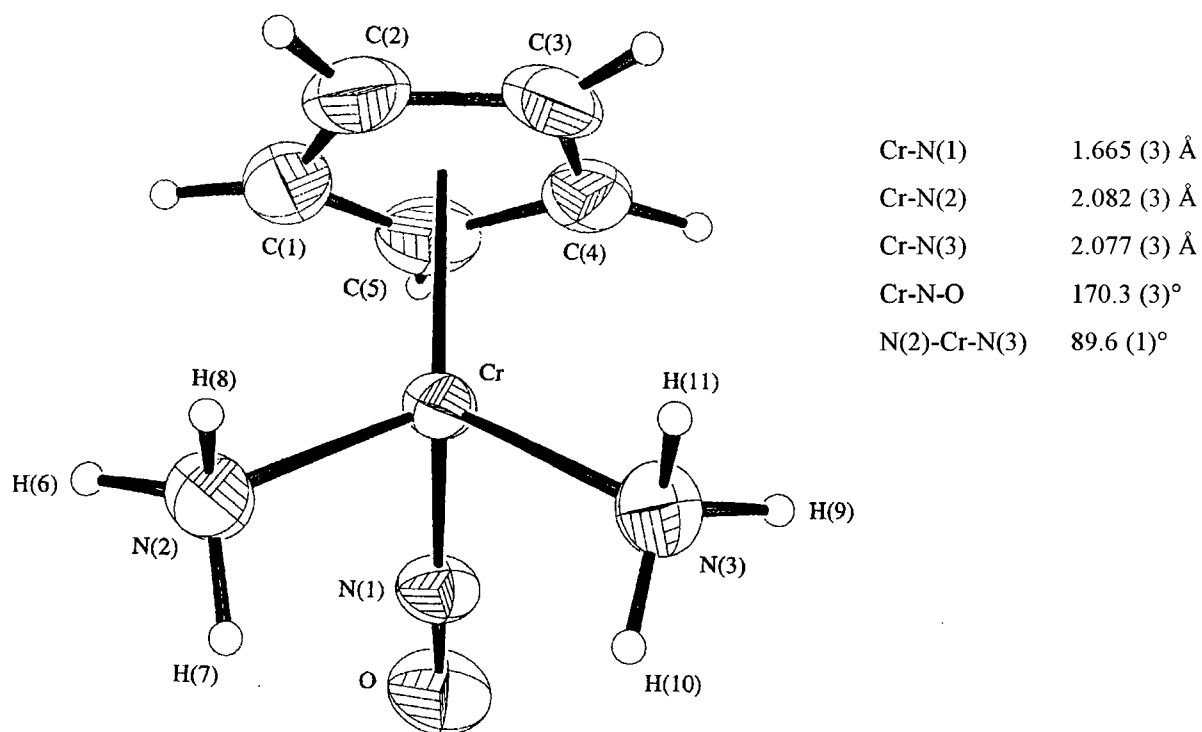


Figure 2.2. Structure of $[2.1]^+$. 50% probability ellipsoids are shown for non-hydrogen atoms. Hydrogen atoms are depicted as spheres of arbitrary radius.

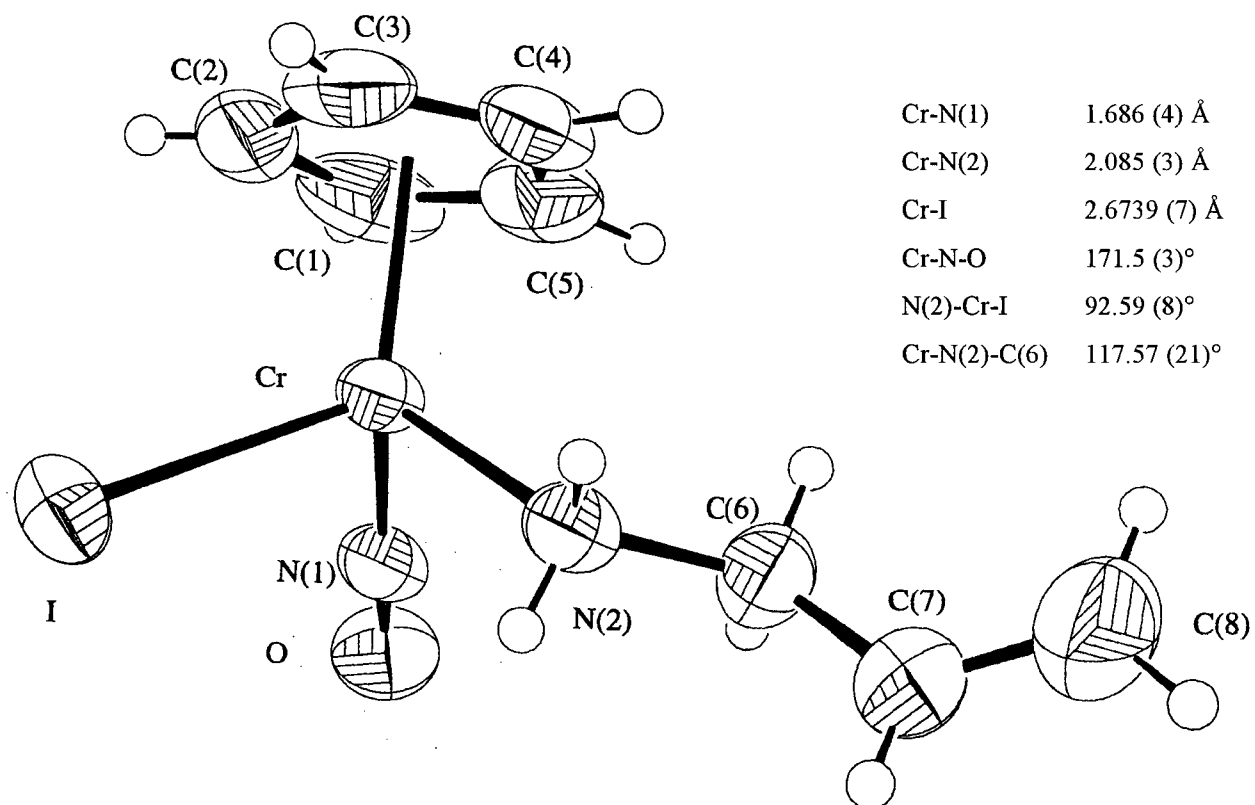


Figure 2.3. Structure of 2.7. 50% probability ellipsoids are shown for non-hydrogen atoms. Hydrogen atoms are depicted as spheres of arbitrary radius.

Immediately apparent is the monomeric nature of both compounds, despite their 17e configurations and lack of steric shielding at the metal centers. Such compounds often dimerize in the absence of sterically bulky ligands via the formation of a metal-metal single bond.¹² The nitrosyl ligands in both complexes **[2.1]**⁺ and **2.7** are essentially linear (170.3 (3)° and 171.5 (3)°), as expected for a {M(NO)}⁵ species,¹³ and both compounds exhibit the expected three-legged piano-stool arrangement of ligands. The bond lengths and bond angles in both organometallic complexes are normal, and are comparable to those exhibited by related cyclopentadienyl chromium nitrosyl species. Thus, the amine Cr-N distances of 2.077 (3) and 2.082 (3) Å in **[2.1]**⁺ and 2.085 (3) Å in **2.7** compare well to those found in other known {Cr(NO)}⁵ complexes,¹⁴ as do the nitrosyl Cr-N distances of 1.665 (3) Å and 1.686 (4) Å.^{1,14,15} These parameters are summarized for comparison in Table 2.3.

Table 2.3. Structural Parameters of {Cr(NO)}⁵ Complexes

complex	Cr-NO (Å)	Cr-N(amine) (Å)	reference
[2.1] ⁺	1.665 (3)	2.077 (3) 2.082 (3)	
2.7	1.686 (4)	2.085 (3)	
(py) ₃ (ONO)Cr(NO)	1.68 (1)	cis: 2.10 (1) trans: 2.17 (1)	14a
[(MeN(CH ₂ (3,5-Me ₂ pz)) ₂ Cr(NCMe) ₂ (NO)] ²⁺	1.648 (13)	pzN: 1.999 (11) 2.006 (12) MeN: 2.198 (11)	14b
(dipic)Cr(OH ₂) ₂ (NO)	1.699 (4)	2.012 (3)	14c
[(Me ₆ [14]4,11-dieneN ₄)Cr(NO ₂)(NO)] ⁺	1.679 (5)	2.044 (4), 2.022 (5)	14d
[CpCr(NO)(NCMe) ₂] ⁺	1.685 (6)	–	15a
CpCr(NO)(PPh ₃)(CH ₂ SiMe ₃)	1.678 (5)	–	15b
[Cr(CN) ₅ (NO)] ³⁻	1.708 (11)	–	15c
[(H ₂ O) ₅ Cr(NO)] ²⁺	1.682 (2)	–	15d

2.4.6 Spectroscopic and Physical Properties

The compounds prepared in this chapter exhibit a number of common properties. The neutral complexes are freely soluble in Et₂O or CH₂Cl₂, though some of the complex salts, particularly those with iodide anions, are soluble only in very polar solvents such as THF or MeCN. All the amine compounds are air-stable when isolated as solids, though air-sensitive as solutions. This stability is somewhat remarkable given the odd-electron configuration of these complexes.

The IR spectra of these species exhibit a strong nitrosyl-stretching frequency in the range 1645 - 1695 cm⁻¹, with the neutral compounds exhibiting bands at slightly lower frequencies than the cations, consistent with more electron-rich metal centers in the neutral complexes. These values are in an ambiguous range, and, taken by themselves, could be indicative of either linear or bent nitrosyl ligands.¹³ However, they are wholly consistent with other known {Cr(NO)}⁵ nitrosyl bands, and, as borne out by the X-ray structural analyses of [2.1]⁺ and 2.7, are due to a linear nitrosyl linkage in these cases. As well as the nitrosyl-stretching frequency, a weak IR band is consistently observed in the range 1580 - 1615 cm⁻¹, and is assigned as the amine N-H bending frequency.¹⁶ Although UV-Vis spectra of these species were not recorded, the complexes are without exception green. This is qualitatively indicative of little change in the electronic structure being effected by the range of ligands used in this Chapter.

All species prepared in this Chapter are odd-electron complexes, so a traditionally indispensable characterization technique, namely NMR, is sadly uninformative. ¹H NMR spectra of these 17e species exhibit features that are generally very broad and ill-defined. Occasional sharp signals can be discerned in the spectra of compounds where protons are physically removed from the metal center, as in the case of the *t*-BuNH₂ ligand, but even then the signals are paramagnetically shifted and not informative enough to unambiguously determine the chemical identity of a new species.

Much more useful is mass spectroscopy, particularly FAB-MS. The more usual electron-impact MS does not generally yield acceptable results for these compounds, whose spectra often

do not provide a reliable parent-ion peak. Again, this may be due to the paramagnetic nature of these complexes, or the ionic nature of the salts. However, FAB-MS consistently yields reliable parent-ion peaks for both neutral and cationic species. As well, anionic FAB identifies the mass of the counter-ion in the complex salts, and in both types of FAB spectra, peaks due to associations of ions are often observed. For instance, in the cation FAB-MS of $[2.2]^+[\text{PF}_6]^-$, in addition to expected peaks at $m/z = 261$, 204, and 174 (P^+ , P^+ -amine, and P^+ -amine-NO), there is a peak at 667, assignable to two parent cations and one PF_6^- anion. Similarly, in the anion FAB-MS of the same complex, peaks are observed at $m/z = 145$ (PF_6^-), 551 ($[\text{P}^+][\text{PF}_6^-]_2$), and 957 ($[\text{P}^+]_2[\text{PF}_6^-]_3$).

The magnetic moments of these 17e species are consistent with their possessing one unpaired electron, and therefore a low-spin $\{\text{M}(\text{NO})\}^5$ (or Cr(I) d^5) electronic configuration. Such a configuration is, of course, expected for species being only one electron short of a closed valence shell, particularly in view of the strong-field nitrosyl ligand that promotes a low-spin configuration of electrons. The room-temperature magnetic moments of these compounds are uniformly less than the expected spin-only value of $1.73 \mu_B$, occurring in a range between $1.20 \mu_B$ for ethylenediamine complex $[2.3]^+[\text{PF}_6]^-$ and $1.49 \mu_B$ for bis(ammonia) complex $[2.1]^+[\text{PF}_6]^-$. Similarly low magnetic moments have been observed for other $\{\text{Cr}(\text{NO})\}^5$ complexes of the form $[\text{Cr}(\text{NO})(\text{CNR})_5]^{2+}$, $[\text{Cr}(\text{NO})(\text{CNR})_4\text{X}]^+$, and $[\text{Cr}(\text{NO})(\text{CNR})_4(\text{PR}_3)]^{2+}$,¹⁷ so this may be a common feature to $\{\text{Cr}(\text{NO})\}^5$ species indicative of an orbital contribution to the magnetic moment which consistently reduces its value. However, it should be noted that due to the limitations of the Evans' method technique, these moment values may not be highly precise, carrying an error of approximately $\pm 0.3 \mu_B$.¹⁸

Also consistent with one unpaired electron are the ESR spectra of these complexes. The spectrum of $[2.3]^+[\text{PF}_6]^-$ is shown in Figure 2.4 as a representative example, though it was selected as the spectrum exhibiting the most discernible chromium coupling. All of the compounds in this Chapter exhibit a broad, featureless singlet in the ESR, with no resolved coupling to any ligand in the metal's coordination sphere. This suggests a lack of delocalization of the unpaired electron density away from the metal center, but due to the broadness of these

features, there may well be coupling that is simply unresolved in these spectra. In some spectra, chromium satellites are observed: the two weak features to either side of the main signal in Figure 2.4 are the outermost of four satellites due to the ^{53}Cr nucleus (9.55% abundance, $I = 3/2$), in this case representing a coupling constant of approximately 22 G.

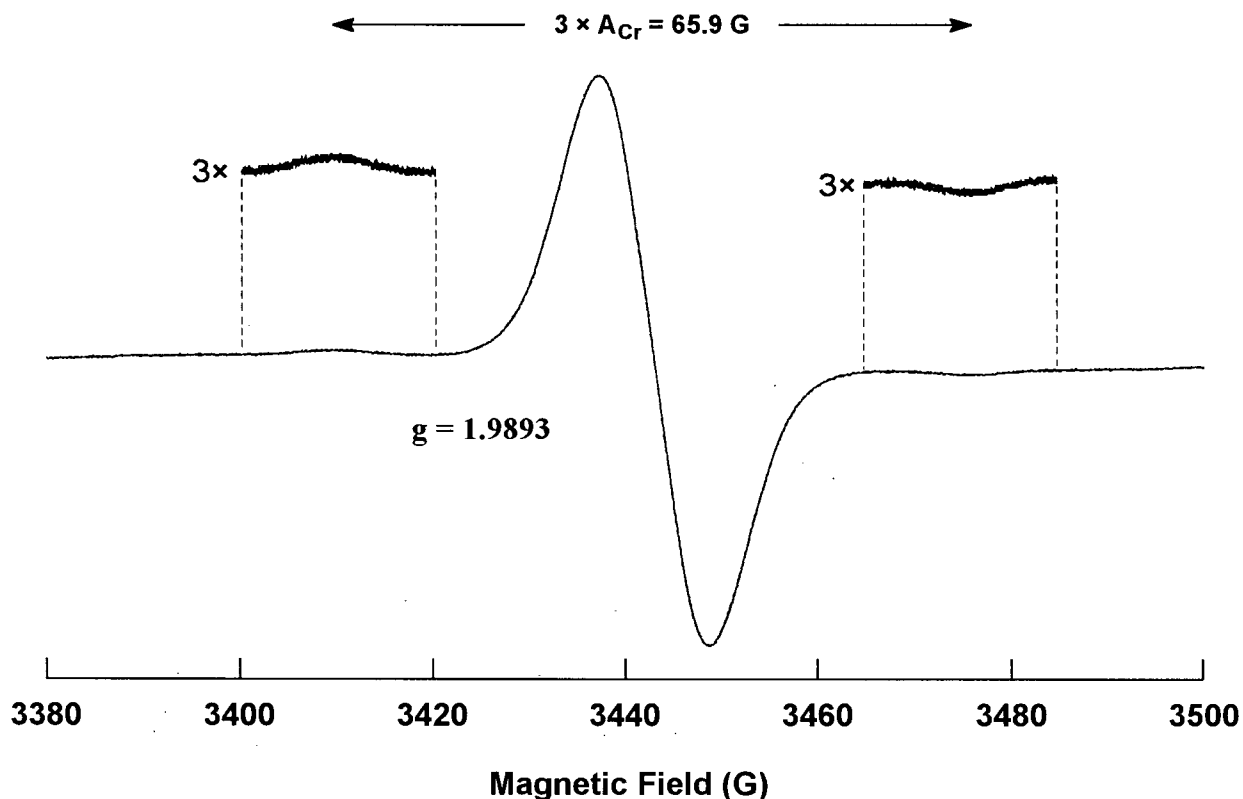


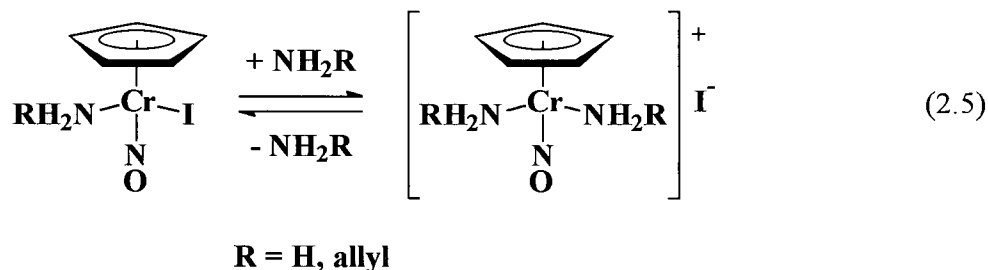
Figure 2.4. Room-Temperature ESR spectrum of $[\mathbf{2.3}]^+[\text{PF}_6]^-$ in MeCN.

An interesting trend is that all the cationic species exhibit a g -value of about 1.99, while the g -values of the neutral species are consistently higher, occurring around 2.02. These latter spectra are therefore qualitatively similar to those of other amine iodide compounds such as $\text{CpCr}(\text{NO})(\text{py})\text{I}$ and $\text{CpCr}(\text{NO})(\text{pip})\text{I}$, both in terms of observed g -value and lack of observed coupling.² The trend in g -values is likely due to the presence or absence of the iodide ligand rather than the formal charge of the 17e species, since the trend of a higher g -value exhibited by an iodide complex is observed elsewhere. For example, the series of complexes

$\text{CpCr}(\text{NO})(\text{PPh}_3)\text{X}$ ($\text{X} = \text{I}, \text{Br}, \text{Cl}$) exhibit a shift in the observed g -value as the halide ligand is changed, so that the iodide complex has a high g -value of 2.036, that of the bromide is 2.012, and that of the chloride is 1.996, similar to these bis(amine) cations.¹ A similar trend of increasing g -value as a halide ligand is changed from Cl to Br to I is also observed in Chapter 4, and is discussed there in greater detail.

2.5 Epilogue and Future Work

A variety of complexes of the form $\text{CpCr}(\text{NO})(\text{L})\text{I}$ (L = nitrogen donor) had been prepared before this work, or were prepared during its progress.² Three compounds in this Chapter, 2.4, 2.6, and 2.7, extended this class to include those with a primary amine ligand L . As well, a new group of compounds, the $[\text{CpCr}(\text{NO})\text{L}_2]^+$ (L = primary amine) cations were prepared and characterized for the first time. If L is nucleophilic enough to displace the iodide ligand from $\text{CpCr}(\text{NO})(\text{L})\text{I}$, then a reversible reaction exists between neutral mono(amine) compounds and the bis(amine) cations (eq 2.5).



These results are, at best, an introductory survey as to the range of complexes that might be prepared. Preliminary results suggest the existence of bis(phosphine) cations, a number of which should be easily preparable by the methodology described in this Chapter. Both neutral and cationic $\text{CpCr}(\text{NO})$ complexes might also be easily extended to include those with other types of Lewis-basic ligands such as alcohols or thiols. The existence of well-defined, isolable 17e organometallic species is still rare enough that such a survey of possible $\text{CpCr}(\text{NO})(\text{L})\text{X}$ and $[\text{CpCr}(\text{NO})\text{L}_2]^+$ compounds would be a valuable one.

The formation of a bis(ligand) cation appears to depend both upon the electronic and the steric nature of the donor ligand. The extent of equilibrium 2.5, that is the relative thermodynamic stabilities of the two types of complex, is not known except in the crudest sense for the case of allylamine. A detailed investigation of this equilibrium using a range of substituted anilines as ligand L would allow for quantification of the equilibrium constants and the electronic factors involved in this reaction. The kinetic mechanism of amine-for-iodide substitution is also

unknown, though common wisdom would hold that such a substitution process at a 17e metal center should proceed associatively.¹² The fact that *tert*-butylamine does not effect reaction 2.5 despite the isolable nature of bis(*tert*-butylamine) cation [2.5]⁺ suggests this to be the case.

2.6 References and Notes

- (1) Legzdins, P.; Nurse, C. R. *Inorg. Chem.* **1985**, *24*, 327.
- (2) Legzdins, P.; McNeil, W. S.; Shaw, M. J. *Organometallics* **1994**, *13*, 562.
- (3) Herring, F. G.; Legzdins, P.; McNeil, W. S.; Shaw, M. J.; Batchelor, R. J.; Einstein, F. W. B. *J. Am. Chem. Soc.* **1991**, *113*, 7049.
- (4) Shriver, D. F.; Dreznor, M. A. *The Manipulation of Air-Sensitive Compounds*, 2nd ed.; Wiley-Interscience: New York, NY, 1986.
- (5) Perrin, D. D.; Armarego, W. L. F.; Perrin, D. R. *Purification of Laboratory Chemicals*, 3rd ed.; Pergamon Press: Oxford, 1988.
- (6) (a) Sur, S. K. *J. Magn. Res.* **1989**, *82*, 169. (b) Carlin, R. L. *Magnetochemistry*; Springer-Verlag: New York, 1986.
- (7) Herring, F. G.; Legzdins, P.; Richter-Addo, G. B. *Organometallics* **1989**, *8*, 1485.
- (8) Legzdins, P.; Lundmark, P. J.; Phillips, E. C.; Rettig, S. J.; Veltheer, J. E. *Organometallics* **1992**, *11*, 2991.
- (9) Similar $[\text{CpCr}(\text{NO})(\text{L-L})]^+$ cations ($\text{L-L} = 2,2'$ -bipyridine and 1,10-phenanthroline) have been prepared by another route. Regina, F. J.; Wojcicki, A. *Inorg. Chem.* **1980**, *19*, 3803.
- (10) Tolman, C. A. *Chem. Rev.* **1977**, *77*, 313.
- (11) Qualitatively similar results are obtained when sequential equivalents of NH_3 are added to an acetonitrile solution of $\text{CpCr}(\text{NO})(\text{NCMe})\text{I}$. That is, the ESR signal of $\text{CpCr}(\text{NO})(\text{NCMe})\text{I}$ is overlapped and replaced by that of **2.6**, which in turn is gradually replaced by the signal of $[\mathbf{2.1}]^+\text{I}^-$. However, this experiment is hampered by the similar nature of the ESR signals of the two initial species ($g = 2.024$ and 2.019), and by the insolubility of $[\mathbf{2.1}]^+\text{I}^-$. It is impossible to gauge the relative intensity of the signal due to **2.6**, and as the concentration of $[\mathbf{2.1}]^+\text{I}^-$ increases, it begins to precipitate from solution. Thus, the results are unreliable in a quantitative sense.

- (12) Baird, M. C. *Chem. Rev.* **1988**, *88*, 1217.
- (13) Enemark, J. H.; Feltham, R. D. *Coord. Chem. Rev.* **1974**, *13*, 339.
- (14) It may be noted that in all these species the amine-donor nitrogen is either in an aromatic ring (such as pyridine or pyrazole), or in a chelating or macrocyclic ligand. Thus, [2.1]⁺ and 2.4 are the first structurally characterized examples of primary, monodentate amines in this class of chromium compounds. (a) Lukehart, C. M.; Troup, J. M. *Inorg. Chim. Acta* **1977**, *22*, 81. (b) Wester, D.; Edwards, R. C.; Busch, D. H. *Inorg. Chem.* **1977**, *16*, 1055. (c) Weighart, K.; Quilitzsch, U. *Inorg. Chim. Acta* **1984**, *89*, L43. (d) Shiu, K.-B.; Chou, J. L.; Wang, Y.; Lee, G.-H. *J. Chem. Soc., Dalton Trans.*, **1990**, 1989.
- (15) (a) Chin, T. T.; Legzdins, P.; Trotter, J.; Yee, V. C. *Organometallics* **1992**, *11*, 913. (b) Herring, F. G.; Legzdins, P.; McNeil, W. S.; Shaw, M. J.; Batchelor, R. J.; Einstein, F. W. B. *J. Am. Chem. Soc.* **1991**, *113*, 7049. (c) Enemark, J. H.; Quinby, M. S.; Reed, L. L.; Steuck, M. J.; Walters, K. K. *Inorg. Chem.* **1970**, *11*, 2397. (d) Ardon, M.; Cohen, S. *Inorg. Chem.* **1993**, *32*, 3241.
- (16) Nakamoto, K. *Infrared and Raman Spectra of Inorganic and Coordination Compounds*, 4th ed.; Wiley-Interscience: New York, 1986, p 191.
- (17) (a) Wigley, D. E.; Walton, R. A. *Inorg. Chem.* **1983**, *22*, 3138. (b) Wigley, D. E.; Walton, R. A. *Organometallics* **1982**, *1*, 1332.
- (18) The exact error associated with any given moment value will depend upon a number properties of the analyte complex, including its concentration in solution, its molecular weight, and its observed susceptibility. A susceptibility error on the order of $\pm 0.25 \times 10^{-3}$ cm³/mol is typical for these particular measurements, given only one unpaired electron and the relatively low solubility of some of these complexes.

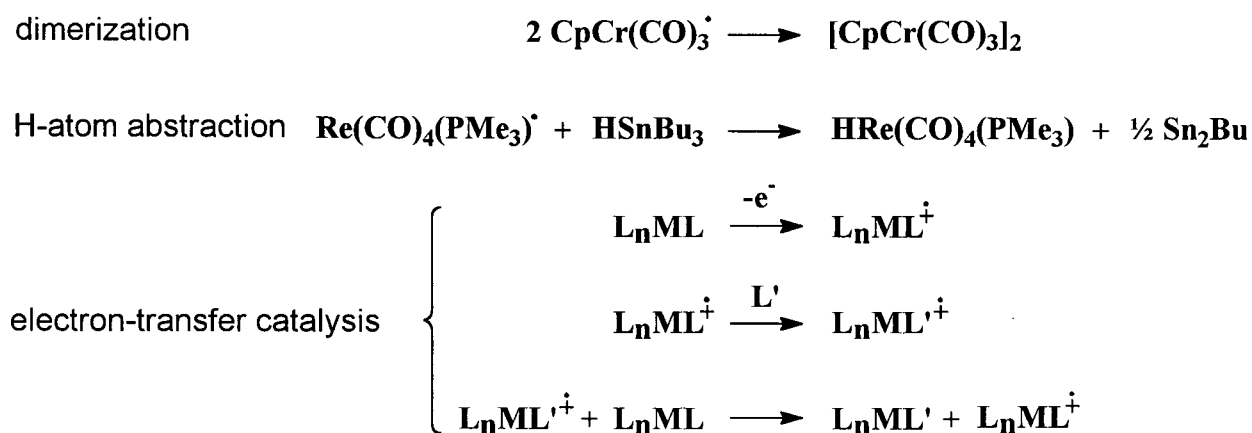
CHAPTER 3

Reactivity and Redox Chemistry of the 17e Cations $[\text{CpCr}(\text{NO})(\text{L})_2]^+$

3.1 Introduction.....	50
3.2 Experimental Procedures	54
3.3 Characterization Data	61
3.4 Results and Discussion.....	63
3.5 Epilogue and Future Work.....	85
3.6 References and Notes	87

3.1 Introduction

As stated in Chapter 1, organometallic complexes generally conform to the 18-electron rule, because eighteen valence electrons will fill all nine bonding and non-bonding orbitals derived from the metal valence orbitals and will lead to a closed valence shell.¹ It follows logically that removal of one electron, yielding a 17e compound, will generally yield a more reactive complex by virtue of its possessing both electronic unsaturation and unpaired electron density. Such 17e organotransition-metal complexes have been extensively studied, and these investigations have shown that 17e species are indeed highly reactive molecules.²⁻¹² For instance, 17e compounds can act as potent hydrogen- and halogen-atom abstraction reagents,²⁻⁴ and they are often unstable with respect to dimerization via formation of metal-metal or ligand-based carbon-carbon bonds.^{3,5,6} One-electron oxidation of 18e species is known to promote reductive elimination.⁷ Most importantly, 17e species are known to undergo ligand substitution reactions at very fast rates, often orders of magnitude faster than those of their diamagnetic, 18e analogues.³⁻¹⁰ This feature allows 17e compounds to play a pivotal role in highly efficient electron-transfer catalysis, which takes advantage of the much greater reactivity of radical species.^{11,12} Examples of some of these processes are depicted in Scheme 3.1



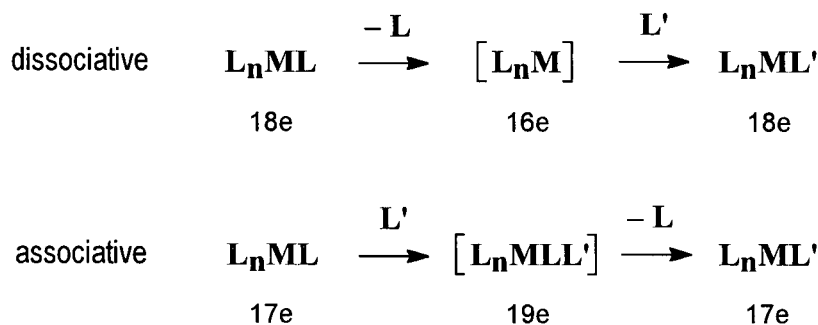
Scheme 3.1

Organometallic radicals, though highly reactive, are becoming increasingly common, both as reaction intermediates and as well-characterized, synthetically useful species in their own right. Reactions as fundamental as those of Grignard reagents have been shown to proceed via single-electron transfer pathways for both organic¹³ and organometallic¹⁴ transformations. Radical pathways have been identified in catalytic processes such as hydroformylation and hydrogenation of arenes and olefins.^{3,15,16} The role of transition-metal radicals in both catalytic¹⁷ and stoichiometric¹⁸ reactions is also steadily increasing. In fact, these complexes are common enough to render Tolman's fundamental tenet¹⁹ that "organometallic reactions, including catalytic ones, proceed by elementary steps involving only intermediates with 16 or 18 valence electrons" somewhat infamous. Nevertheless, it should be noted that these generalizations about 17e compounds are derived from exhaustive study of a relatively narrow range of transition-metal complexes, namely carbonyl compounds, in which the metal experiences a very strong ligand field due to the π -acidic natures of the CO ligands.²⁰

The various modes of reactivity of 17e organometallic complexes, and their differences as compared to those of 18e species, can be easily understood in terms of both the unpaired electron and the nature of the orbital in which it resides. If the singly-occupied orbital is primarily metal-based, then such 17e species are generally unstable with respect to dimerization.⁵ This dimerization results because the overlap of a singly-occupied orbital from each radical will result in a lower-energy bonding orbital, where the two electrons become paired, thus forming a metal-metal bond. On the other hand, if the SOMO is primarily ligand-orbital in character, the radical complex is likely to dimerize through formation of a new carbon-carbon bond, coupling through the organic ligands rather than through the metal.³ This is often the case with cationic 17e species rather than neutral complexes, due to electrostatic repulsion of the two metal centers.³ Such dimerization reactions are extremely facile, often proceeding at rates approaching diffusion control. However, such a reaction requires the overlap of the SOMO of two different molecules, so that if there is little directional character to the unpaired spin, such a dimerization may not occur. The stability of $V(CO)_6$ with respect to dimerization is attributed to this effect.²¹ The SOMO is extensively delocalized onto the ligands in this species, so that the reorganizational

energy required to make the SOMO available for bonding is prohibitive. Another factor which can prevent intermolecular SOMO overlap is steric bulk of the 17e species, so that the two metal centers simply cannot come close enough together to form a metal-metal bond. For example, $(\eta^5\text{-C}_5\text{Ph}_5)\text{Cr}(\text{CO})_3$ shows no tendency to dimerize,²² whereas $\text{CpCr}(\text{CO})_3$ dimerizes at a rate of $8.4 \times 10^5 \text{ M}^{-1}\text{s}^{-1}$ in CH_2Cl_2 at 243 K.²³

The most striking form of reactivity displayed by 17e complexes is ligand substitution. The accelerated rate of substitution exhibited by such radicals is due only in part to the weakening of metal-ligand bonds that is caused by the electronic unsaturation. The singly-occupied orbital allows substitution to proceed by a pathway entirely different from that of 18e complexes. By virtue of the coordinative and electronic saturation of such compounds, ligand substitution in 18e complexes generally proceeds via a dissociative pathway²⁴ at a first-order rate determined only by the metal complex. In contrast, substitution in 17e complexes generally exhibits second-order kinetics dependent upon both ligand and metal complex, features that are consistent with associative mechanisms. These mechanistic pathways are depicted in general form in Scheme 3.2.



Scheme 3.2

Such behavior may be rationalized in terms of the molecular-orbital diagram depicted in Figure 3.1. The overlap of a ligand orbital with the metal SOMO would result in a formally 19e intermediate with two electrons in the M-L bonding orbital and one electron in the M-L antibonding orbital. Thus, in a formal sense, the formation of half a bond would stabilize this

intermediate compared to the 17e starting complex. This stabilization of a higher-coordination intermediate makes the associative substitution pathway a facile one, and results in a fast rate of substitution.⁵

However, this reaction pathway and enhanced reactivity again requires that the complex SOMO be accessible to the incoming ligand, and it may not be observed if the half-filled orbital is sterically shielded. For instance, substitution of the CO ligand in $\text{Cp}_2\text{V}(\text{CO})$ is rapid and proceeds via an associative pathway, as would be expected for a 17e complex. However, substitution of carbonyl in $(\eta^5\text{-C}_5\text{H}_7)_2\text{V}(\text{CO})$ is on the order of 10^4 times slower and proceeds dissociatively.²⁵ This difference is attributed to the fact that in the latter case the SOMO is directed at the pentadienyl ligands and is sterically shielded from nucleophilic attack, so that an interaction of the type depicted in Figure 3.1 cannot occur.

In light of the well-studied reactivity patterns above, the generally established trend is that odd-electron species are more reactive than their even-electron analogues. A commonly employed method of inducing reactivity in unreactive even-electron species is redox, whereby electron transfer to or from the complex results in unpaired spin density and enhanced reactivity, not only toward ligand substitution but also toward reactivity such as migratory insertion^{9,26} or reductive elimination.⁷ Given this, it was expected that the 17e $[\text{CpCr}(\text{NO})\text{L}_2]^+$ and $\text{CpCr}(\text{NO})(\text{L})\text{I}$ species prepared in Chapter 2 would provide the basis for a wide range of reactivity studies. Although these studies have proved fruitful, the results were unexpected.

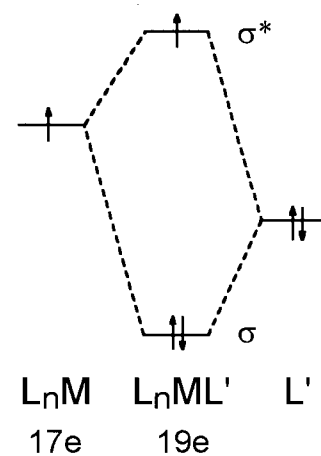


Figure 3.1. Interaction of a 17e Complex with Ligand L'

3.2 Experimental Procedures

3.2.1 Methods

The experimental methods employed throughout this Thesis are detailed in Section 2.2.1. The electrochemical methods employed are detailed in Section 2.2.2.

3.2.2 Molecular Orbital Calculations

Extended Hückel Theory calculations²⁷ were carried out with the aid of HyperChem[®] for Windows Release 3 and ChemPlus[™] extensions for HyperChem, both being commercially available software packages. In all cases, single-point calculations were performed on the structures obtained from single-crystal X-ray crystallographic analyses using an unweighted Hückel constant of 1.75.

3.2.3 Reagents

$[\text{CpCr}(\text{NO})\text{I}]_2$,²⁸ $[\text{Cp}_2\text{Fe}]^+[\text{PF}_6]^-$,²⁹ $\text{CpCr}(\text{NO})(\text{P}\{\text{OMe}\}_3)\text{I}$,³⁰ $\text{CpCr}(\text{NO})(\text{CO})_2$,³¹ and $\text{Mg}(\text{anthracene})\cdot 3\text{THF}$ ³² were all prepared by published procedures. Lithium amides were prepared by treatment of the corresponding amines with *n*-BuLi in hexanes, and aqueous solutions of the products were titrated with 0.1 M HCl to determine molarity. All other reagents were used as received from commercial suppliers.

3.2.4 Dissolution of Bis(ammonia) Complex $[\text{2.1}]^+[\text{PF}_6]^-$ in THF or MeCN

A sample of $[\text{CpCr}(\text{NO})(\text{NH}_3)_2]^+[\text{PF}_6]^-$ (65 mg, 0.20 mmol) was dissolved in either THF or MeCN (5 mL) in a Schlenk tube. In both cases, the green solution was stirred at ambient temperatures for 24 h, during which time no change was observed in either the IR or ESR spectra of either solution. The starting material was recovered from the final solution and was identified as unchanged by its characteristic IR, ESR, and mass spectra. No features attributable to the appropriate bis(solvate) complex were observed in these spectra.

3.2.5 Exposure of Bis(ammonia) Complex $[2.1]^+[\text{PF}_6]^-$ to H_2O

A sample of $[\text{CpCr}(\text{NO})(\text{NH}_3)_2]^+[\text{PF}_6]^-$ (65 mg, 0.20 mmol) was dissolved in THF (5 mL) in a Schlenk tube. Deaerated H_2O (1.0 mL, excess) was added to the solution via syringe. The reaction mixture was stirred at ambient temperatures for 24 h, during which time no change occurred in either the IR or ESR spectra of the solution.

3.2.6 Exposure of Bis(ammonia) Complex $[2.1]^+[\text{PF}_6]^-$ to $\text{HSn}(n\text{-Bu})_3$

A sample of $[\text{CpCr}(\text{NO})(\text{NH}_3)_2]^+[\text{PF}_6]^-$ (50 mg, 0.15 mmol) was dissolved in THF (10 mL) in a bomb. $\text{HSn}(n\text{-Bu})_3$ (60 μL , 82 mg, 0.23 mmol, 1.6 equiv) was added via syringe. The reaction mixture was stirred at room temperature for 24 h, during which time no change was observed in either the IR or ESR spectra of the solution. The starting material was recovered unchanged from the final solution as judged by its IR, ESR, and mass spectra.

3.2.7 Exposure of Bis(ammonia) Complex $[2.1]^+[\text{PF}_6]^-$ to CO

A sample of $[\text{CpCr}(\text{NO})(\text{NH}_3)_2]^+[\text{PF}_6]^-$ (250 mg, 0.75 mmol) was dissolved in THF (~10 mL) in a bomb. The solution was placed under an atmosphere of CO and was stirred for one week. After this time, the IR spectrum of the final green solution revealed no carbonyl bands and only one nitrosyl band, namely that due to the starting material.

3.2.8 Reduction of Bis(ammonia) Complex $[2.1]^+[\text{PF}_6]^-$ under CO: $\text{Mg}(\text{anthracene})$

THF (~10 mL) was transferred onto a mixture of $[2.1]^+[\text{PF}_6]^-$ (163 mg, 0.50 mmol) and $\text{Mg}(\text{anthracene})\cdot 3\text{THF}$ (209 mg, 0.50 mL) contained in a bomb, and 1 atm of CO was introduced into the vessel. The mixture was allowed to warm and was stirred for 1 hr, during which time the suspension of green and orange materials in an orange solution developed a red-brown color. An IR spectrum of the solution revealed two strong bands in the 1500 - 2000 cm^{-1} region at 1632 and 1894 cm^{-1} . The solvent was removed in vacuo, and the residue was extracted with Et_2O (2 x

30 mL) and filtered, resulting in a red solution exhibiting bands at 1644 and 1902 cm^{-1} . Attempts to crystallize material from this solution resulted in loss of the IR bands and deposition of an off-white solid exhibiting the mass spectrum of anthracene.

The Et_2O solution resulting from a 0.25 mmol reaction was filtered into a bomb, and this solution was transferred into a Parr reactor. The solution was stirred for 18 h at 50 $^\circ\text{C}$ under 200 psig CO. The resulting solution exhibited IR bands at 2020, 1997, and 1667 cm^{-1} , demonstrating a conversion to $\text{CpCr}(\text{NO})(\text{CO})_2$.

3.2.9 Reduction of Bis(ammonia) Complex $[\mathbf{2.1}]^+[\text{PF}_6]^-$ under CO: Zinc

THF (~10 mL) was transferred onto a mixture of $[\mathbf{2.1}]^+[\text{PF}_6]^-$ (163 mg, 0.50 mmol) and zinc powder (32 mg, 0.50 mmol) in a bomb, and 1 atm of CO was introduced into the vessel. The mixture was stirred for 5 d, after which time an IR spectrum of the solution revealed nitrosyl and carbonyl bands attributable to $\text{CpCr}(\text{NO})(\text{CO})_2$, and a weaker nitrosyl band of $[\mathbf{2.1}]^+[\text{PF}_6]^-$. The reaction mixture was transferred to a pentane column of silica gel (230-400 mesh, 3 x 10 cm), and elution with pentane afforded an orange band. The resulting eluate was taken to dryness in vacuo to obtain bright orange $\text{CpCr}(\text{NO})(\text{CO})_2$ (54 mg, 36% yield), which was identified by its characteristic IR and mass spectra.

3.2.10 Reaction of $\text{CpCr}(\text{NO})(\text{CO})_2$ with $[\text{Cp}_2\text{Fe}]^+[\text{PF}_6]^-$

$\text{CpCr}(\text{NO})(\text{CO})_2$ (0.100 g, 0.491 mmol) and $[\text{Cp}_2\text{Fe}]^+[\text{PF}_6]^-$ (0.161 g, 0.488 mmol) were weighed into a Schlenk tube and dissolved in MeCN (30 mL). The reaction mixture was stirred for 4 d at ambient temperatures. The solvent was then removed in vacuo, and the green residue was washed with Et_2O (3 x 30 mL). The resulting green solid (0.11 g, 60% yield) was identified as $[\text{CpCr}(\text{NO})(\text{NCMe})_2]^+[\text{PF}_6]^-$ by comparison of its ESR, IR, and mass spectral properties with those displayed by an authentic sample.³³

3.2.11 Preparation of $\text{CpCr}(\text{NO})(\text{P}\{\text{OMe}\}_3)_2$ (**3.1**)

The following is a modification of the previously published procedure for the synthesis of this complex.^{34a} THF (~10 mL) was vacuum transferred onto $[\text{CpCr}(\text{NO})\text{I}]_2$ (274 mg, 1.00 mmol) and Zn (0.35 g, excess, 5.4 mmol). $\text{P}(\text{OMe})_3$ (0.25 mL, 0.26 g, 2.1 mmol) was added to the frozen slurry. The mixture was stirred at room temperature for 3 h, after which time the color of the solution had changed from green to orange. The solvent was then removed in vacuo. The orange residue was extracted with Et_2O (2 x 30 mL), and the extracts were filtered through neutral alumina I. The filtrate was reduced in volume to 10 mL, and pentane (10 mL) was added. The solution was left to stand at $-30\text{ }^\circ\text{C}$ overnight, whereupon orange blocks of analytically pure **3.1** were deposited.

3.2.12 Preparation of $[\text{CpCr}(\text{NO})(\text{P}\{\text{OMe}\}_3)_2]^+[\text{PF}_6]^-$ ($[\mathbf{3.1}]^+[\text{PF}_6]^-$)

THF (~10 mL) was vacuum transferred onto $\text{CpCr}(\text{NO})(\text{P}\{\text{OMe}\}_3)\text{I}$ (100 mg, 0.25 mmol) and AgPF_6 (63 mg, 0.25 mmol), and the mixture was warmed to room temperature and stirred for 5 min, whereupon a flocculent precipitate formed. The reaction mixture was filtered, and $\text{P}(\text{OMe})_3$ (29 μL , 31 mg, 0.25 mmol) was added to the filtrate via syringe. The mixture was then stirred overnight, the solvent was removed in vacuo, and the green residue was washed with Et_2O (2 x 10 mL). The first wash had a pale lime green color, but the second was colorless. The remaining ether-insoluble, yellow-green powder was dried in vacuo to obtain analytically pure $[\mathbf{3.1}]^+[\text{PF}_6]^-$.

Bright orange X-ray quality crystals of $[\mathbf{3.1}]^+[\text{BPh}_4]^-$ were obtained by allowing Et_2O to diffuse into a CH_2Cl_2 solution of $[\mathbf{3.1}]^+[\text{PF}_6]^-$ and NaBPh_4 . The new complex exhibits an ESR spectrum identical to that of $[\mathbf{3.1}]^+[\text{PF}_6]^-$.

3.2.13 Preparation of *trans*- and *cis*- $[\text{CpCr}(\text{NO})(\text{NHC}_3\text{H}_5)]_2$ (*trans*- and *cis*-**3.2**)

$[\text{CpCr}(\text{NO})(\text{NH}_2\text{C}_3\text{H}_5)_2]^+[\text{I}]^-$, $[\mathbf{2.2}]^+[\text{I}]^-$, (388 mg, 1.00 mmol) was dissolved in THF (~15 mL) and cooled with a dry ice/acetone bath. *n*-BuLi (0.63 mL, 1.6 M solution in hexanes,

1.0 mmol) was added via syringe. The solution gradually changed from green to brown while being stirred at room temperature for 1 hr. The solvent was removed in vacuo, the residue was extracted with a minimum of CH_2Cl_2 , and the extracts were transferred to a pentane-packed column of acidic alumina I (2 x 10 cm). The column was eluted with Et_2O to afford a red band and then with CH_2Cl_2 to yield a yellow band, leaving a brown residue at the top of the column. The two eluates were collected separately, reduced in volume, diluted with hexanes, and refrigerated. Each eluate yielded an isomer of $[\text{CpCr}(\text{NO})(\text{NHC}_3\text{H}_5)]_2$ (*trans*- and *cis*-**3.2**). The red form was identified as the *trans*- species, and the orange-yellow solid as the *cis*-isomer.

3.2.14 Reaction of *tert*-Butylamine Complex 2.4 with *n*-BuLi

A sample of $\text{CpCr}(\text{NO})(\text{NH}_2\text{CMe}_3)\text{I}$ (388 mg, 1.00 mmol) was dissolved in THF (~15 mL). *n*-BuLi (0.63 mL, 1.6 M solution in hexanes, 1.0 mmol) was added via syringe. The solution changed from green to brown, and the solvent was removed in vacuo. The resulting brown residue was extracted with CH_2Cl_2 (10 mL), and the extract was transferred to an Et_2O -packed column of acidic alumina I (2 x 10 cm). The column was eluted with Et_2O to afford a red band and then with CH_2Cl_2 to yield a tan band. A bright green material remained at the top of the column. The two eluates were collected separately, the solvent was removed in vacuo, and the residues were recrystallized from Et_2O /hexanes to yield orange and brown powders, respectively. The yield of these materials was too low to allow satisfactory purification, but based on spectroscopic data, as compared with those of the same materials prepared by another route (see below), the orange and brown products were identified as impure samples of *trans*- and *cis*- $[\text{CpCr}(\text{NO})(\text{NHCMe}_3)]_2$ (*trans*- and *cis*-**3.3**).

3.2.15 Alternate Preparation of *trans*- and *cis*- $[\text{CpCr}(\text{NO})(\text{NHCMe}_3)]_2$ (*trans*- and *cis*-**3.3**)

THF (~10 mL) was transferred onto a mixture of $[\text{CpCr}(\text{NO})\text{I}]_2$ (149 mg, 0.54 mmol) and *t*-BuNHLi (43 mg, 0.54 mmol) in a Schlenk tube. The mixture was warmed to room temperature and stirred for 20 min, and then the solvent was removed in vacuo. The brown residue was

extracted with Et₂O (5 x 15 mL) and the combined extracts were filtered through acidic alumina I. The red filtrate was taken to dryness, to obtain a red-brown residue that was dissolved in a minimum of CH₂Cl₂ and transferred to the top of a pentane-packed column of acidic alumina I (2 x 10 cm). Elution of the column with Et₂O effected the development of a red band, and further elution with CH₂Cl₂ effected the development of a yellow band. Both bands were collected, and these eluates were taken to dryness to yield *trans*-[CpCr(NO)(NHCMe₃)]₂ as a red powder and *cis*-[CpCr(NO)(NHCMe₃)]₂ as a yellow powder (*trans*- and *cis*-**3.3**).

3.2.16 Reaction of *tert*-Butylamine Complex 2.4 with *t*-BuNHLi

THF was transferred onto a mixture of CpCr(NO)(NH₂CMe₃)I (175 mg, 0.50 mmol) and *t*-BuNHLi (39 mg, 0.49 mmol) in a Schlenk tube. The mixture was warmed to room temperature and stirred for 30 min, during which time the color of the solution changed from green to red-brown. The solvent was removed in vacuo, and the brown residue was extracted with Et₂O (4 x 15 mL). The combined extracts were filtered through acidic alumina I, and the resulting red solution was taken to dryness. IR, NMR, and mass spectra of the red powder indicated it to be a mixture of *trans*- and *cis*-**3.3**.

3.2.17 Preparation of *trans*- and *cis*-[CpCr(NO)(NH-*o*-tol)]₂ (*trans*- and *cis*-**3.4**)

THF (~10 mL) was transferred onto a mixture of [CpCr(NO)I]₂ (137 mg, 0.500 mmol) and *o*-tolNHLi (56 mg, 0.50 mmol) in a Schlenk tube. The mixture was warmed to room temperature and stirred for 1 h, and then the solvent was removed in vacuo. The brown residue was extracted with Et₂O (30 mL) and the extract was filtered through acidic alumina I. The red filtrate was taken to dryness, and the resulting red powder was dissolved in CH₂Cl₂ (10 mL) and transferred to the top of a pentane-packed column of acidic alumina I. Elution of this column with Et₂O developed an orange band, and further elution with CH₂Cl₂ developed a yellow band. The eluates were collected separately and taken to dryness to yield *trans*-[CpCr(NO)(NH-*o*-tol)]₂ as a red powder and *cis*-[CpCr(NO)(NH-*o*-tol)]₂ as a yellow powder (*trans*- and *cis*-**3.4**).

3.2.18 Preparation of *trans*- and *cis*-[CpCr(NO)(NMe₂)]₂ (*trans*- and *cis*-3.5)

THF (~10 mL) was transferred onto a mixture of [CpCr(NO)I]₂ (412 mg, 1.50 mmol) and Me₂NLi (79 mg, 1.5 mmol) in a Schlenk tube. The mixture was warmed to room temperature and stirred for 1 h, then the solvent was removed in vacuo. The brown residue was extracted with Et₂O (10 mL), and the extract was transferred onto a hexanes-packed column of acidic alumina I. Elution of this column with Et₂O developed an orange band, and further elution with CH₂Cl₂ developed a yellow band. These bands were collected separately and the eluates were taken to dryness to yield *trans*-[CpCr(NO)(NMe₂)]₂ as a red powder and *cis*-[CpCr(NO)(NMe₂)]₂ as an orange powder (*trans*- and *cis*-3.5).

3.3 Characterization Data

Table 3.1. Numbering Scheme, Color, Yield and Elemental Analysis Data

complex	compd no.	color (yield, %)	elemental analysis found (calcd)		
			C	H	N
CpCr(NO)(P{OMe} ₃) ₂	3.1	orange (63)	33.40 (33.43)	5.82 (5.87)	3.45 (3.54)
[CpCr(NO)(P{OMe} ₃) ₂] ⁺ PF ₆ ⁻	[3.1] ⁺ PF ₆ ⁻ -	yellow-green (54)	24.49 (24.46)	4.28 (4.29)	2.38 (2.59)
<i>trans</i> -[CpCr(NO)(NHC ₃ H ₅) ₂]	<i>trans</i> -3.2	red (12)	47.53 (47.29)	5.46 (5.46)	13.55 (13.79)
<i>cis</i> -[CpCr(NO)(NHC ₃ H ₅) ₂]	<i>cis</i> -3.2	orange-yellow (7)	47.35 (47.29)	5.40 (5.46)	13.75 (13.79)
<i>trans</i> -[CpCr(NO)(NHCMe ₃) ₂]	<i>trans</i> -3.3	red (25)	49.33 (49.31)	6.96 (6.90)	12.64 (12.78)
<i>cis</i> -[CpCr(NO)(NHCMe ₃) ₂]	<i>cis</i> -3.3	yellow (11)	-	-	-
<i>trans</i> -[CpCr(NO)(NH- <i>o</i> -tol)] ₂	<i>trans</i> -3.4	red (22)	56.77 (56.92)	5.01 (5.17)	10.86 (11.06)
<i>cis</i> -[CpCr(NO)(NH- <i>o</i> -tol)] ₂	<i>cis</i> -3.4	yellow (9)	-	-	-
<i>trans</i> -[CpCr(NO)(NMe ₂) ₂]	<i>trans</i> -3.5	red (25)	43.76 (43.98)	5.92 (5.80)	14.47 (14.65)
<i>cis</i> -[CpCr(NO)(NMe ₂) ₂]	<i>cis</i> -3.5	orange (14)	-	-	-

Table 3.2. Mass Spectral and Infrared Data

complex	EI-MS		IR (cm ⁻¹)	
	(<i>m/z</i>)	temp (°C)	ν_{NO} (Nujol)	ν_{NO} (THF)
3.1	395 [P ⁺]	120	1609	1623
[3.1] ⁺ PF ₆ ⁻	395 [P ⁺]	145 [P ⁻] ^a	1693	1705
<i>trans</i> -3.2	406 [P ⁺]	180	1603 1613 1643	-
<i>cis</i> -3.2	406 [P ⁺]	180	1591 1604 1619 1648	-
<i>trans</i> -3.3	438 [P ⁺]	120	1601	-
<i>cis</i> -3.3	438 [P ⁺]	150	1591 1609 1632 1657	-
<i>trans</i> -3.4	506 [P ⁺]	120	1605 1619 1643	-
<i>cis</i> -3.4	506 [P ⁺]	150	1606 1637	-
<i>trans</i> -3.5	382 [P ⁺]	120	1615	-
<i>cis</i> -3.5	382 [P ⁺]	120	1600 1642	-

^a These values are peaks observed in a (+) and (-) FAB-MS.

Table 3.3. NMR and ESR Data

complex	
3.1	^1H : δ 4.70 (t, 5H, $^3J_{\text{PH}} = 2.3$ Hz, Cp), 3.48 (m, 18H, 9 x Me) $^{31}\text{P}\{^1\text{H}\}$: δ 226.7
$[\mathbf{3.1}]^+\text{PF}_6^-$	ESR: $g = 2.002$ $A_{\text{P}} = 48.0$ G $A_{\text{N}} = 4.9$ G
<i>trans</i> -3.2	^1H (isomer a): δ 3.30 (dm, 1H, NHCH_aH_b), 3.53 (m, 1H, NHCH_aH_b) 4.02 (br s, 1H, NH), 5.03 (s, 5H, Cp) 5.12 (dd, 1H, $J = 2, 9$ Hz, $\text{CH}=\text{CH}_a\text{H}_b$), 5.19 (dd, 1H, $J = 2, 13$ Hz, $\text{CH}=\text{CH}_a\text{H}_b$) 5.93 (m, 1H CH) ^1H (isomer b, a:b = 5:1): δ 4.97, 5.11 (Cp); other peaks unresolved
<i>cis</i> -3.2	^1H : δ 3.56 (br s, 1H, NH) 4.15 (vt, 2H, $J = 7$ Hz, NHCH_2) 4.68 (s, 5H, Cp) 5.08 (dd, 1H, $J = 3$ Hz, 10 Hz, $\text{CH}=\text{CH}_a\text{H}_b$), 5.24 (dd, 1H, $J = 3, 17$ Hz, $\text{CH}=\text{CH}_a\text{H}_b$) 6.25 (tdd, 1H, $J = 7, 10, 17$ Hz, CH)
<i>trans</i> -3.3	^1H (two isomers, 1:1): δ 1.14, 1.20 (s, each 9H, CMe_3) 4.17, 4.69 (br s, each 1H, NH) 5.16, 5.41 (s, 5H, Cp_a) 5.31 (s, 5H, Cp_b)
<i>cis</i> -3.3	^1H (two isomers, 2:1): δ 1.28, 1.32 (s, 9H, minor CMe_3); 1.39 (s, 9H, major CMe_3) 4.71 (s, 5H, minor Cp); 4.72 (s, 5H, major Cp)
<i>trans</i> -3.4	^1H (two isomers, 2:1): δ 2.33 (s, 3H, major Me); 2.24 (s, 3H, minor Me) 4.78 (s, 5H, major Cp); 4.75, 4.98 (s, 5H, minor Cp) 6.21 (br s, 1H, major NH); 6.08 (br s, 1H, minor NH) 6.80 - 7.61 (m, aryl)
<i>cis</i> -3.4	^1H : δ 2.03, 2.20 (s, each 3H, Me) 4.80 (s, 5H, Cp) 6.6 - 7.3 (m, 4H, aryl)
<i>trans</i> -3.5	^1H : δ 2.95 (s, 6H, Me) 5.07 (s, 5H, Cp)
<i>cis</i> -3.5	^1H : δ 2.10 (s, 3H, Me) 3.53 (s, 3H, Me) 4.97 (s, 5H, Cp)

3.4 Results and Discussion

3.4.1 Treatment of $[2.1]^+[\text{PF}_6]^-$ with Nucleophiles

Given the monomeric, 17e nature of cation $[2.1]^+$, $[\text{CpCr}(\text{NO})(\text{NH}_3)_2]^+$, it would not be unreasonable to expect this species to be highly reactive. Odd-electron species are best known for exhibiting a dramatic and rapid substitution chemistry, the scope and mechanism of which has been well-established.²⁻⁹ In the case of $[2.1]^+$, the positive charge and lack of steric crowding at the metal center (Figure 2.2) could only be expected to enhance reactivity involving attack by nucleophiles. However, complex $[2.1]^+$ does not merely fail to undergo rapid substitution reactions with a variety of nucleophiles, it is, in fact, entirely unreactive toward them. Exposure of THF solutions of $[2.1]^+[\text{PF}_6]^-$ to an excess of H_2O or CO for periods up to one week results in no discernible conversion either to new 17e species (as judged by ESR spectroscopy), or new nitrosyl compounds (as judged by IR spectroscopy). When $[2.1]^+[\text{PF}_6]^-$ is stirred in THF or MeCN, the spectroscopic properties of the resulting solutions do not change, and the starting material may be easily recovered. This is particularly intriguing, since the possible products, namely $[\text{CpCr}(\text{NO})(\text{THF})_2]^+$ and $[\text{CpCr}(\text{NO})(\text{NCMe})_2]^+$, are both well-characterized and stable species.^{33,35}

Additionally, $[2.1]^+$ fails to react in another manner commonly associated with radical species, namely as a hydrogen-atom abstraction reagent. Treatment with $\text{HSn}(n\text{-Bu})_3$, a potent $\text{H}\cdot$ source, does not result in any discernible reaction of $[2.1]^+$.

3.4.2 Electrochemistry of $[2.1]^+[\text{PF}_6]^-$ and $[2.2]^+[\text{PF}_6]^-$

The one-electron reduction of cations $[2.1]^+$ and $[2.2]^+$ would result in a neutral form of these species having an 18e count and therefore a closed valence shell. These might be expected to be the more stable forms of these compounds, but this is not the case. The cyclic voltammograms of both $[2.1]^+[\text{PF}_6]^-$ and $[2.2]^+[\text{PF}_6]^-$ in THF reveal no oxidation features to the solvent limit, although both CVs do exhibit a reduction feature, and in both cases this feature is irreversible. At a scan rate of 0.4 V/s, the reduction of $[2.1]^+[\text{PF}_6]^-$ occurs at $E_{p,c} = -1.24$ V,

while that of $[2.2]^+[\text{PF}_6]^-$ occurs at $E_{p,c} = -1.28$ V. The reduction wave of $[2.1]^+$ is depicted in Figure 3.2.

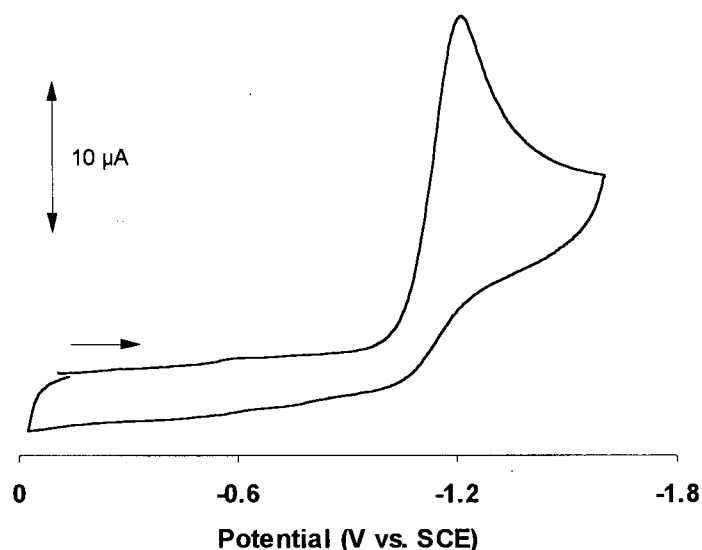


Figure 3.2. Reduction cyclic voltammogram of $[2.1]^+[\text{PF}_6]^-$ at 0.4 V/s

The irreversible electrochemical reductions of these cations are pivotal results in this work. They demonstrate that an accepted axiom of organometallic chemistry, namely that odd-electron species are generally more reactive and less stable than their even-electron analogues, does not hold for this particular class of compounds. Reduction of these 17e species to an 18e form results in very rapid decomposition of the reduced complex, such that no electrochemical return oxidation wave is observed even at scan rates exceeding 1 V/s. Thus, contrary to the usual trends, a redox process is rendering an unreactive odd-electron species more reactive in the even-electron form.

3.4.3 Reduction of $[2.1]^+[\text{PF}_6]^-$ under CO: Mg(anthracene)

After effecting a redox process electrochemically, a reasonable goal is to attempt the same process using a chemical reagent. Given that the coordination sphere of $[2.1]^+[\text{PF}_6]^-$ does not remain intact upon reduction, and given that a number of stable, 18e compounds containing the

CpCr(NO) fragment are known (Section 1.1.3.2), it may be assumed that the mechanism of reductive decomposition of $[2.1]^+$ and $[2.2]^+$ involves loss of the amine ligands. Thus, in order to generate a stable reduction product, a suitable trapping agent must be employed, namely one that can function as a ligand in the new complex. CpCr(NO)(CO)₂ is a well-known species, and CO is known to be unreactive with $[2.1]^+$ (vide supra), so the chemical reduction of $[2.1]^+[PF_6]^-$ was attempted in the presence of CO, using both magnesium anthracene and zinc powder as the reductant.

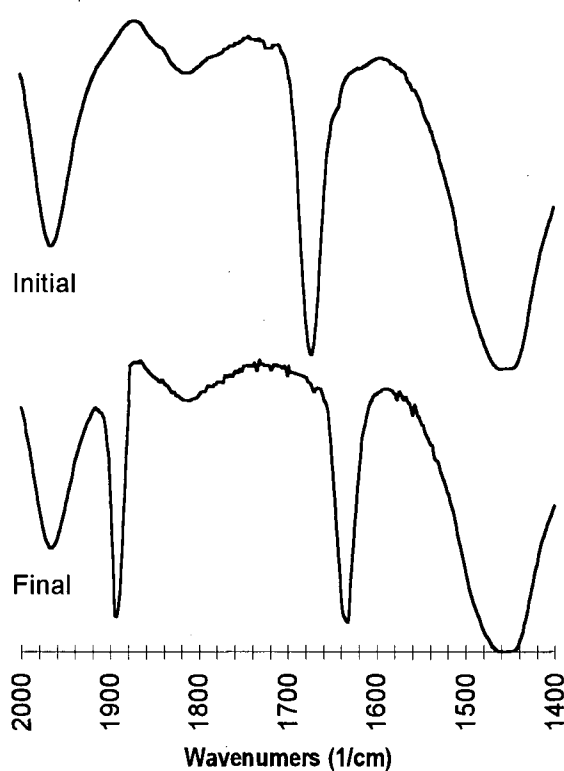


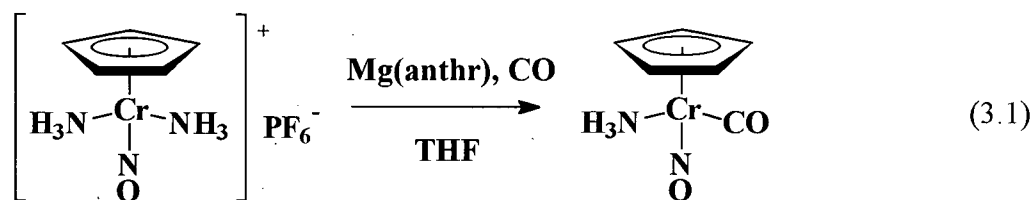
Figure 3.3. Initial and Final Infrared Spectra During Reaction of $[2.1]^+[PF_6]^-$ with Mg(anthracene) in THF.

When $[2.1]^+[PF_6]^-$ is reacted with Mg(anthracene)·3THF in THF under 1 atm of CO, the reactants are quickly consumed, resulting in a red solution that contrasts sharply with the green color of 17e compounds seen in Chapter 2. Striking evidence for the incorporation of CO into an organometallic reduction product is given by the IR spectra of this reaction mixture (Figure 3.3). The nitrosyl band of the starting material, at 1676 cm^{-1} , is replaced by a similar band at 1632

cm^{-1} , with the concomitant appearance of a second band at 1894 cm^{-1} , attributable to a carbonyl ligand. This indicates the presence of a new carbonyl nitrosyl complex. The infrared spectra of the initial and final solutions are depicted in Figure 3.3.

Unfortunately, this new carbonyl compound could not be isolated or further characterized. Solutions containing this species lose these two infrared bands upon standing, even at low temperature, thereby suggesting that the compound is not thermally stable for periods longer than a few hours. Thus, attempts to crystallize the complex were not successful. Solutions kept under an atmosphere of CO do not lose the IR bands, but the complex still cannot be isolated. Removal of the solvent in vacuo or filtration of the solution through any chromatographic support also results in loss of the IR bands. These observations suggest that the compound's thermal instability involves loss of the carbonyl ligand, a mechanism that is hindered by an excess of CO.

The fact that only one CO band is observed implies incorporation of only one carbonyl ligand. Assuming that the CpCr(NO) fragment remains intact, there are only two remaining coordination sites at chromium, and CpCr(NO)(CO)_2 is a known complex that exhibits two strong carbonyl infrared bands. Thus, only one of the two coordination sites is occupied by CO, and the other must be occupied by a different monodentate, 2e-donor ligand. The two possibilities are the THF solvent, and the original ligand, NH_3 . CpCr(NO)(CO)(THF) is a known compound, best prepared by photolysis of CpCr(NO)(CO)_2 , and it is known to exhibit IR bands in THF at 1642 and 1905 cm^{-1} ,^{34d,36} bands that are both 10 cm^{-1} higher than those observed in this case. Thus the $1632, 1894 \text{ cm}^{-1}$ species must be assigned as $\text{CpCr(NO)(NH}_3\text{)(CO)}$, as indicated in eq 3.1. Comparing $\text{CpCr(NO)(CO)(NH}_3\text{)}$ and CpCr(NO)(CO)(THF) , one would expect the ammonia species to have lower-energy CO and NO bands than the THF derivative by virtue of the greater electron-donating ability of NH_3 vs. THF, and this is indeed the observed trend.

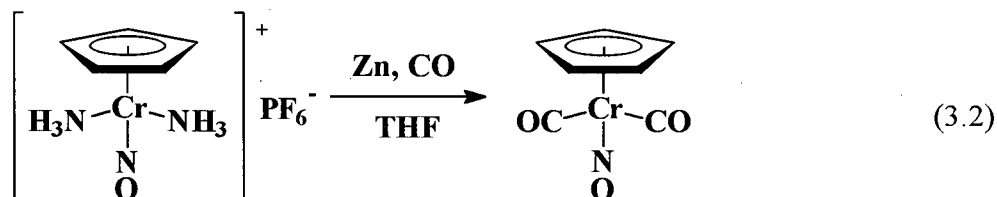


Although the ammonia carbonyl compound is only stable under an atmosphere of CO, it does not appear to react any further with CO at ambient pressure even over a period of days. In other words, 1 atm of CO is not sufficient to displace the NH₃ and form the dicarbonyl compound. However, this reaction does occur under more extreme conditions. Exposure of an Et₂O solution of the monocarbonyl intermediate to 200 psig CO at 50 °C results in the formation of CpCr(NO)(CO)₂, as indicated by the appearance of the diagnostic IR bands of this compound.

3.4.4 Reduction of [2.1]⁺[PF₆]⁻ under CO: Zinc

Interestingly, the nature of the chemical reductant employed has a dramatic effect on the outcome of the reaction of [2.1]⁺[PF₆]⁻ and CO. When the reaction is carried out using zinc powder, the reaction is considerably slower, so that whereas the 17e starting material is entirely consumed by Mg(anthracene) in less than an hour, some of the same amount of [2.1]⁺ remains unreacted after a period of days in the presence of zinc. This likely reflects both the lesser reductive potential of the zinc reagent and its heterogeneous nature of zinc powder. Mg(anthracene) effectively functions as a soluble source of Mg atoms, and so electron transfer from this reagent is kinetically much more facile than from an insoluble powder, thus resulting in a far greater reactivity.

As well, reduction by zinc leads to a different product. Instead of incorporation of only one CO ligand to form the presumed CpCr(NO)(NH₃)(CO) complex, reduction with zinc results in direct formation of CpCr(NO)(CO)₂, whereby both ammonia ligands have been lost (eq 3.2)



Indeed, not only is the monocarbonyl species not the product, it is not even an observed intermediate. The reason for this difference in reactivity is not clear, but there are two basic

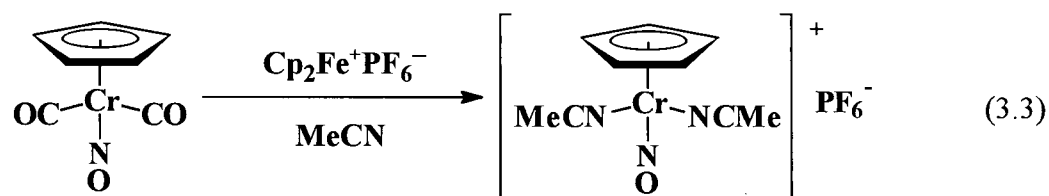
possibilities for the formation of the dicarbonyl rather than the monocarbonyl. Either the monocarbonyl species is formed transiently and reacts with further CO to yield the observed product, or the dicarbonyl compound is formed directly without proceeding via the monocarbonyl intermediate.

The observation that the monocarbonyl compound does not react with 1 atm of CO might suggest that the first pathway cannot be possible. If the presumed intermediate does not undergo the necessary reaction to form the product under the employed conditions, it simply cannot be the intermediate. However, this conclusion is not valid because the conditions under which the monocarbonyl species does not react further with 1 atm CO, that is those of eq 3.1, are not precisely those used in eq 3.2. When $\text{CpCr(NO)(CO)(NH}_3\text{)}$ is observed not to react with further CO, it is in the presence of the oxidation byproducts of the reductant, namely anthracene and Mg^{2+} ions. When the monocarbonyl species is not observed, and instead CpCr(NO)(CO)_2 is formed, the reaction mixture contains both zinc powder and zinc ions, rather than magnesium ions. It may be possible that Zn^{2+} somehow activates the monocarbonyl species toward further reactivity, perhaps via a Lewis acidic complexation of the CO or NO group.³⁷ Magnesium might be expected to behave similarly, but in this case the interaction could be prevented by binding of anthracene to the alkaline-earth ion.

Regardless of the precise mechanism, or even the exact product, the most important aspect of reactions 3.1 and 3.2 is the reduction itself. Whereas the 17-electron complex $[\mathbf{2.1}]^+$ does not react with carbon monoxide under ambient conditions, its ammonia ligands are readily substituted by CO upon reduction to an 18-electron form. This system is a rare example of an unreactive odd-electron organometallic species for which reduction to an even-electron configuration induces reactivity, a reversal of the commonly observed trend. Such a reversal has also been observed by Poli and coworkers for the $\text{CpMoI}_2(\text{PMe}_3)_2$ system for which an ETC ligand-substitution cycle exists with the 16e complexes being the catalytically active species, rather than the 17e compounds.³⁸

3.4.5 Oxidation of CpCr(NO)(CO)_2

The reduction product, CpCr(NO)(CO)_2 , is known to exhibit an irreversible electrochemical oxidation.³⁹ It might therefore be possible to effect the reverse of eq 3.2, that is to oxidize CpCr(NO)(CO)_2 , and induce substitution of CO by an amine. Unfortunately, attempts to effect such a conversion either chemically or electrochemically in order to form bis(ammonia) species $[\mathbf{2.1}]^+$ are hampered by the oxidative consumption of ammonia rather than the organometallic reactant. However, oxidation of the 18e dicarbonyl with one equivalent of $[\text{Cp}_2\text{Fe}]^+[\text{PF}_6]^-$ in acetonitrile affords the known salt, $[\text{CpCr(NO)(NCMe)}_2]^+[\text{PF}_6]^-$,³³ which contains a 17e cation similar to $[\mathbf{2.1}]^+$ (eq 3.3). Without prior oxidation, CpCr(NO)(CO)_2 is unreactive towards acetonitrile under ambient conditions.



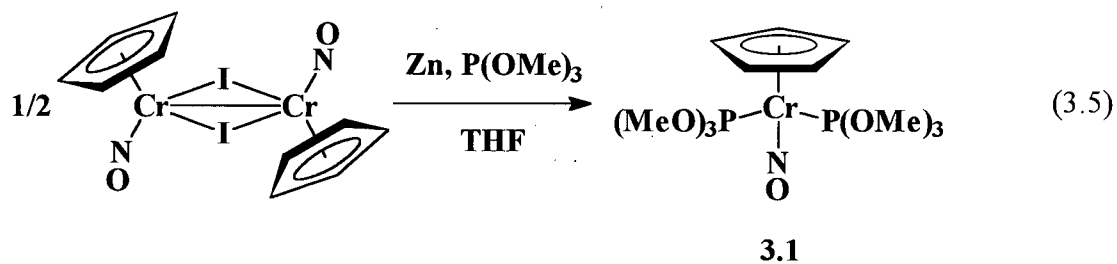
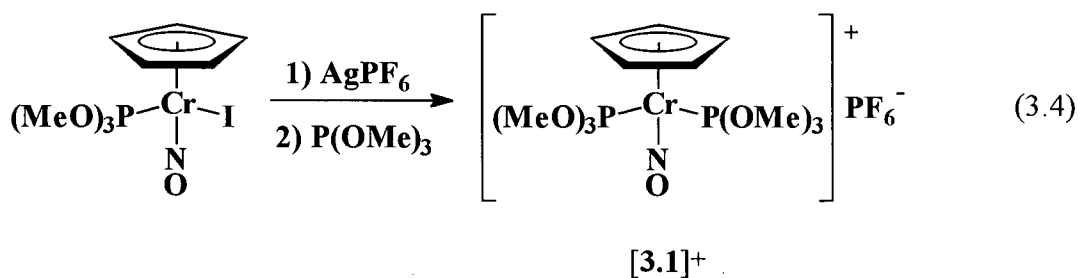
3.4.6 Synthesis of $\text{CpCr(NO)(P}\{\text{OMe}\}_3\}_2$ and $[\text{CpCr(NO)(P}\{\text{OMe}\}_3\}_2]^+[\text{PF}_6]^-$

From the outcomes of transformations 3.2 and 3.3 it appears that the preferred electronic configurations of CpCr(NO)(L)_2 molecules, i.e. the stability of the 17e paramagnetic form versus that of the 18e diamagnetic form, is determined by the nature of the ancillary ligands, L. Thus, σ -donor ligands such as NH_3 stabilize the 17e cationic compounds that decompose upon reduction to their 18e analogues. On the other hand, π -acceptor ligands such as CO evidently stabilize the 18e configuration in the neutral complexes that decompose upon oxidation to their 17e analogues. A search of the chemical literature provides further supporting evidence for this generalization. A wide range of monomeric CpCr(NO) -containing compounds are known, and those bearing σ -basic ligands are indeed 17e $\{\text{Cr(NO)}\}^5$ species,^{30,33,40,41} and those containing π -acidic ligands are 18e $\{\text{Cr(NO)}\}^6$ complexes.^{34,42} In effect, the favored electronic configuration of CpCr(NO) species is selectively determined by the bonding requirements of the ancillary ligands.

Given this conclusion, it stands to reason that a ligand possessing both σ -donor and π -acceptor properties should allow for the formation of a $\text{CpCr}(\text{NO})(\text{L})_2$ compound between the two extremes, i.e. one stable in either the 17- or 18-valence-electron form. $\text{P}(\text{OMe})_3$ is just such a ligand.

$[\text{CpCr}(\text{NO})(\text{P}\{\text{OMe}\}_3)_2]^+[\text{PF}_6]^-$ ($[\mathbf{3.1}]^+[\text{PF}_6]^-$) is prepared via the same synthetic methodology as the bis(*tert*-butylamine) complex $[\mathbf{2.5}]^+[\text{PF}_6]^-$, that is halide abstraction from $\text{CpCr}(\text{NO})(\text{P}\{\text{OMe}\}_3)\text{I}$ with a silver salt in THF and subsequent reaction of the organometallic intermediate (presumably a THF solvate) with further phosphite. As in the reaction of $[\text{CpCr}(\text{NO})\text{I}]_2$ with *tert*-butylamine (Section 2.4.2), there is no evidence for the direct formation of a $[\text{CpCr}(\text{NO})(\text{L})_2]^+$ species when $[\text{CpCr}(\text{NO})\text{I}]_2$ is treated with $\text{P}(\text{OMe})_3$, $\text{CpCr}(\text{NO})(\text{P}\{\text{OMe}\}_3)\text{I}$ being the only product observed by either IR or ESR spectroscopy. Thus, $[\mathbf{3.1}]^+[\text{PF}_6]^-$ must be prepared using isolated $\text{CpCr}(\text{NO})(\text{P}\{\text{OMe}\}_3)\text{I}$ as a precursor.

The synthesis of 18e $\text{CpCr}(\text{NO})(\text{P}\{\text{OMe}\}_3)_2$ ($\mathbf{3.1}$) takes advantage of the irreversible reduction behavior of the 17e $\text{CpCr}(\text{NO})$ system. Reaction of $\mathbf{1}$ with $\text{P}(\text{OMe})_3$ and zinc powder results in facile formation of $\mathbf{3.1}$; the organometallic species that is actually reduced by zinc is most likely $\text{CpCr}(\text{NO})(\text{P}\{\text{OMe}\}_3)\text{I}$, so in fact this phosphite halide species is the precursor to both $\mathbf{3.1}$ and $[\mathbf{3.1}]^+$. These transformations are depicted in eqs 3.4 and 3.5.



The latter reaction is an improvement over the previously known synthesis of **3.1**,^{34a} which employed Na/Hg amalgam as the reductant. Using zinc as the reductant results in a much higher yield and avoids the problems associated with the handling and disposal of an alkali amalgam.

The complexes **3.1** and **[3.1]⁺** constitute the first two such related compounds known for the CpCr(NO) system, that is an isolable 17e and 18e pair. As expected, these complexes exhibit identical cyclic voltammograms, displaying a reversible redox couple at $E_{1/2} = -0.03\text{V}$ in THF, as shown in Figure 3.4. Also as expected, the IR data indicate a large difference in electron density at the metal centers of **3.1** and **[3.1]⁺**; the nitrosyl-stretching frequency of the 18e species is more than 80 cm^{-1} lower than that of the more electron-poor 17e compound. The spectroscopic properties of **3.1** have been reported previously, but are presented in Section 3.3 for the sake of completeness.

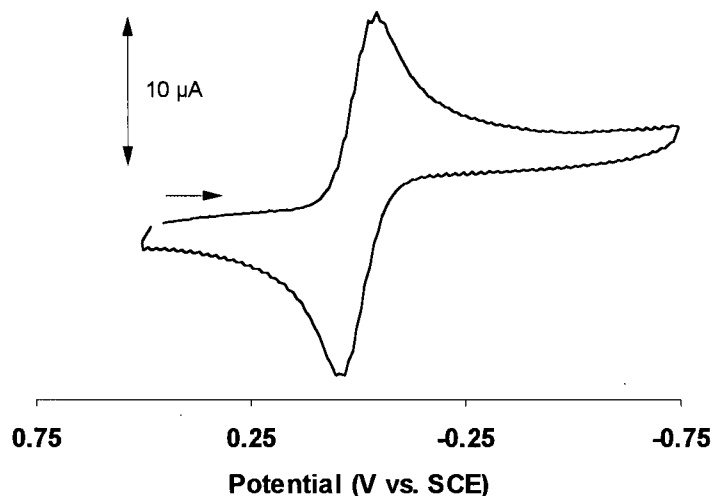


Figure 3.4. Cyclic voltammogram of **3.1** at 0.4 V/s

The spectroscopic properties of **[3.1]⁺[PF₆]⁻** are wholly consistent with the assignment of this species as a complex salt analogous to those prepared in Chapter 2. A major difference between these species and **[3.1]⁺** is the latter's ESR spectrum. The spectrum does not exhibit the broadness of those observed in Chapter 2, instead displaying a sharply resolved 1:2:1 triplet of

1:1:1 triplets, due to coupling of the unpaired spin both to the two equivalent $I = \frac{1}{2}$ ^{31}P nuclei and to the $I = 1$ ^{14}N nucleus of the nitrosyl ligand.

3.4.7 Metal-Ligand Bonding in the $\text{CpCr}(\text{NO})(\text{L})_2$ Systems.

The successful preparation of a redox pair of $[\text{CpCr}(\text{NO})(\text{L})_2]^{o/+}$ compounds, using an intermediate ligand that is neither an extreme σ -base nor an extreme π -acid, supports the idea that the electronic nature of the ligand in this system selectively determines the favored oxidation state of the complex. Clearly, the rationale for such an effect must involve the interaction of these ligands with the metal d orbitals. In order to develop such a rationale, Extended Hückel calculations of the system were performed. The results of these calculations are presented in Figure 3.5.

In the center of Figure 3.5 are shown the energies of the valence orbitals in the $\text{CpCr}(\text{NO})$ fragment as it occurs in a typical three-legged piano-stool molecule, the approximate symmetry and shape of key orbitals being as indicated. Of particular note are the natures of the three highest occupied orbitals, at -11.0 , -12.1 , and -12.3 eV. These three orbitals correspond approximately to those depicted in Figure 3.6, which shows the perturbation of the t_{2g} set of d-orbitals in an octahedral field by the two orthogonal π^* orbitals of a nitrosyl ligand. Specifically, the HOMO in the $\text{CpCr}(\text{NO})$ fragment is non-bonding and of π -symmetry, whereas the HOMO -1 and HOMO -2 orbitals represent the strongly bonding Cr-NO interaction. In the organometallic fragment these two orbitals each involve a π -interaction to the Cp ligand as well.

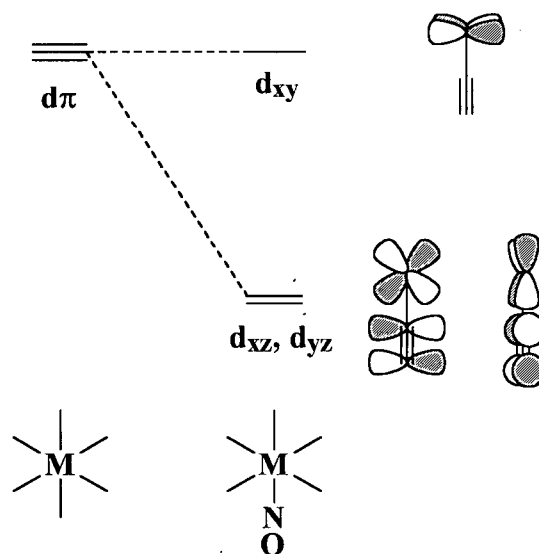


Figure 3.6

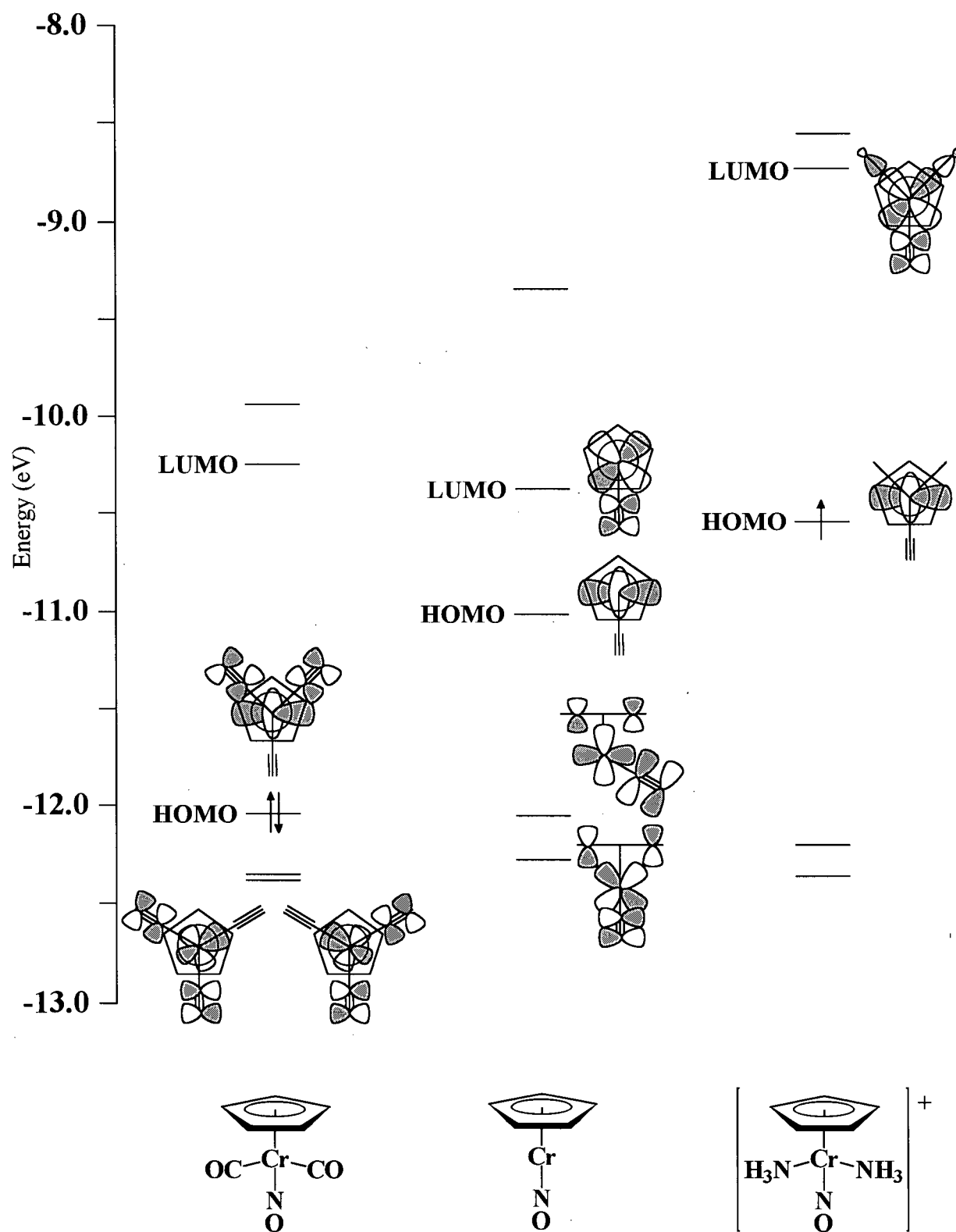


Figure 3.5. Molecular Orbital Diagram for the CpCr(NO) Fragment

The HOMO of the CpCr(NO) fragment is of proper symmetry to form a π -bond with two ligands in the available coordination sites, in that the bond axes would lie approximately in the nodal plane of this orbital. Therefore, the fragment HOMO interacts strongly with a π -acid ligand such as CO, but will not interact with a σ -base ligand such as NH₃. On the other hand, the LUMO of the CpCr(NO) fragment can form σ -bonds with respect to the ancillary ligands, since the two of the lobes of this orbital are oriented directly along the bond axes. The LUMO will therefore interact strongly with NH₃, but less so with CO. The results of these interactions can be seen on the left and right sides of Figure 3.5. In CpCr(NO)(CO)₂ (on the left), the HOMO is primarily π -bonding to the carbonyl ligands. Thus, upon oxidation, the Cr-CO bonding orbital is reduced in electron density, the Cr-CO bonds are weakened, and the complex decomposes via loss of the CO ligands.

In the case of the 17e species (on the right side of Figure 3.5), the HOMO is now a singly occupied orbital (SOMO), is essentially non-bonding, and does not interact with the σ -base ligands. This feature is consistent with the lack of coupling of the unpaired electron to the ligands that is observed in the ESR spectra of these compounds (Chapter 2). In contrast, the CpCr(NO) fragment LUMO interacts strongly with the NH₃ ligands and forms a bonding and anti-bonding pair of molecular orbitals. The bonding orbital is very low in energy (about -14.6 eV and below the scale of Figure 3.5), but the anti-bonding orbital becomes the LUMO in the 17e complex.

It is not immediately clear, therefore, why the 17e species should be unreactive toward ligand substitution. In most known cases, a reduced substitution chemistry of a 17e species is due to steric shielding of the singly occupied orbital.⁵ Clearly, steric shielding of this nature cannot be ascribed to complex [2.1]⁺, since the SOMO is not directed toward the ligands and the compound is not sterically crowded. Thus, the lack of reactivity exhibited by [2.1]⁺ is probably not kinetic in origin, but rather must be due to thermodynamically strong metal-NH₃ bonds. Reduction of [2.1]⁺ to an 18e species results in an electron-rich metal center and a weakening of the interaction with the strongly σ -basic ligands. After these ligands are lost, the complex can then be trapped by π -acidic ligands, which lower the energy of the doubly-occupied HOMO and stabilize the 18e complex. It may also be possible that the initial reduction product does not have two electrons in

the HOMO, but is a high-spin species resulting from the LUMO of the 17e compound becoming populated in the 18e derivative. Since the LUMO is antibonding with respect to σ -bases, this population would greatly facilitate the loss of NH_3 . It should be noted, however, that our calculations indicate the HOMO-LUMO gap in $[\mathbf{2.1}]^+$ to be greater than 1.8 eV, so it is unlikely that the initially reduced species will exist in its high-spin configuration.

This analysis also serves to demonstrate why $[\mathbf{2.1}]^+$ is stable with respect to dimerization. Many metal-centered 17e radicals rapidly form metal-metal bonds, but it has been observed that due to the electrostatic repulsion caused by the positive charge, this generally does not occur for 17e cationic species. Instead, such compounds tend to dimerize via the formation of ligand-ligand bonds.⁵ However, this latter process requires that some of the unpaired spin lies on the ligand, that the SOMO has enough ligand character to overlap with the corresponding orbital on another molecule, and so form the new bond. In the case of complex $[\mathbf{2.1}]^+$, the SOMO has no ligand character, and so such a dimerization cannot take place.

3.4.8 Structural Comparison of Complexes **3.1** and $[\mathbf{3.1}]^+$

Given the molecular-orbital analysis presented in the preceding section, it was of interest to us to determine what structural changes, if any, would be evident as a result of the 17e/18e redox processes in a complex that is stable in both the even- and the odd-electron configurations. Thus, the X-ray crystal structures of both trimethylphosphite complexes, **3.1** and $[\mathbf{3.1}]^+$, were determined, the latter as the $[\text{BPh}_4]^-$ salt. In an effort to obtain a high degree of accuracy so as to allow a better comparison of the two structures, they were both determined at low temperature, 205 K in the case of **3.1**, and 195 K in the case of $[\mathbf{3.1}]^+$. The ORTEP drawing of the molecular structure of $[\mathbf{3.1}]^+$ is presented Figure 3.7, and the metrical parameters associated with the phosphite and nitrosyl ligands are depicted in Figure 3.9a. The structural analysis of **3.1** revealed two crystallographically independent molecules of the complex in the unit cell; only one of these is depicted in Figure 3.8, and the metrical parameters for both are shown in Figures 3.9b and 3.9c.

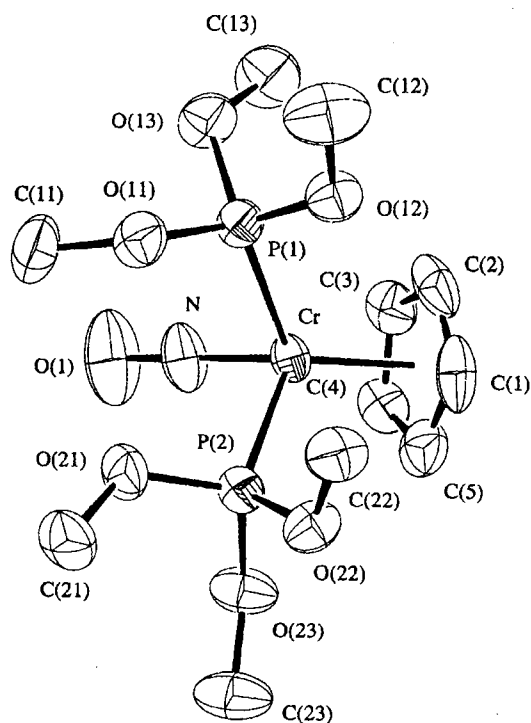


Figure 3.7. Solid-State Molecular Structure of 17e Complex $[3.1]^+$. 50% probability ellipsoids are shown for non-hydrogen atoms.

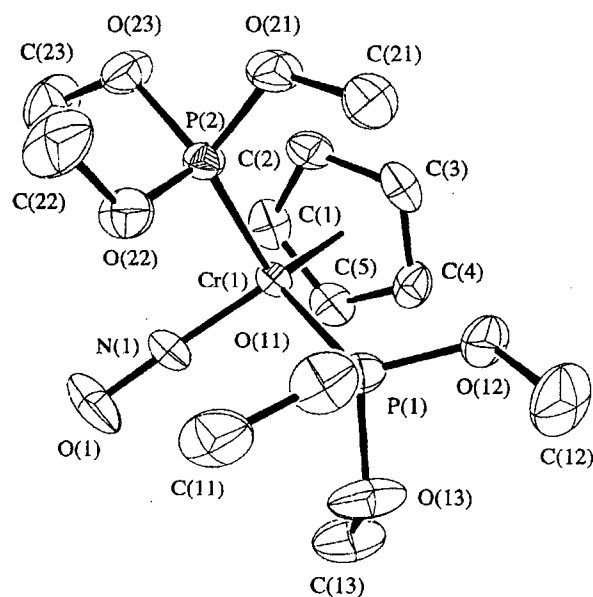


Figure 3.8. Solid-State Molecular Structure of 18e Complex **3.1**. 50% probability ellipsoids are shown for non-hydrogen atoms.

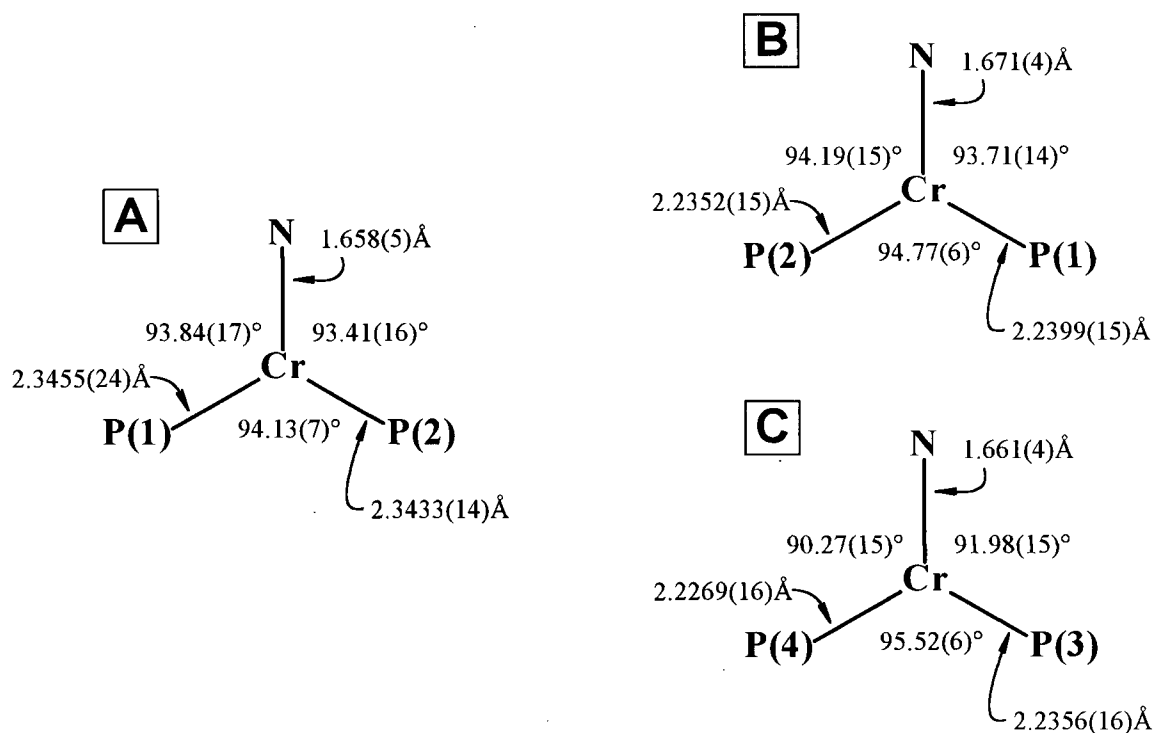


Figure 3.9. Comparison of Selected Structural Parameters of (A) Complex $[3.1]^+$, (B) Molecule #1 of Complex **3.1**, (C) Molecule #2 of Complex **3.1**

Not unexpectedly, the structures of the two molecules of the 18e complex **3.1** are similar. The bond lengths in the two compounds generally differ by less than 0.01 Å. The most dramatic difference is a slight "bending away" of the ligands with respect to the cyclopentadienyl plane in the second of the two molecules. In molecule #1, the CP-Cr-N(1) and CP-Cr-P(2) angles (taking CP as the cyclopentadienyl centroid) of 128.94° and 117.84° are somewhat less than the corresponding angles in molecule #2, at 130.63° and 120.57°. This results in a lesser angle between the nitrosyl and phosphite ligands, as shown in Figures 3.9b and 3.9c. The largest contrast is that of the N-Cr-P(2) angle in molecule #1 (94.19 (15)°) versus the corresponding N(2)-Cr-P(4) angle in molecule #2 (90.27 (15)°).

The chromium-phosphorus distances of 2.3433 (14) and 2.3455 (24) Å found in complex **[3.1]⁺** are similar to those found in other 17e chromium species such as Cp*Cr(CO)₂(PMe₃),⁴³ CpCr(CO)₂(PPh₃),⁴³ and CpCr(NO)(PPh₃)(CH₂SiMe₃).^{40b} The most striking difference between the structures of **[3.1]⁺** and **3.1** is that the Cr-P bond lengths in the 17e cation are about 0.11 Å *longer* than in either molecule of the 18e neutral form, which exhibit Cr-P bond lengths of 2.2399 (15), 2.2352 (15), 2.2356 (16), and 2.2269 (16) Å. That is, the more electron-rich, reduced metal center binds the phosphite ligands more closely. Such a feature is exactly opposite to usual trends, in that a more electron-rich ion or atom is expected to have a greater ionic radius, and so form longer metal-ligand bonds.⁴⁴ The other chromium-ligand bond lengths are essentially unchanged by the redox process.

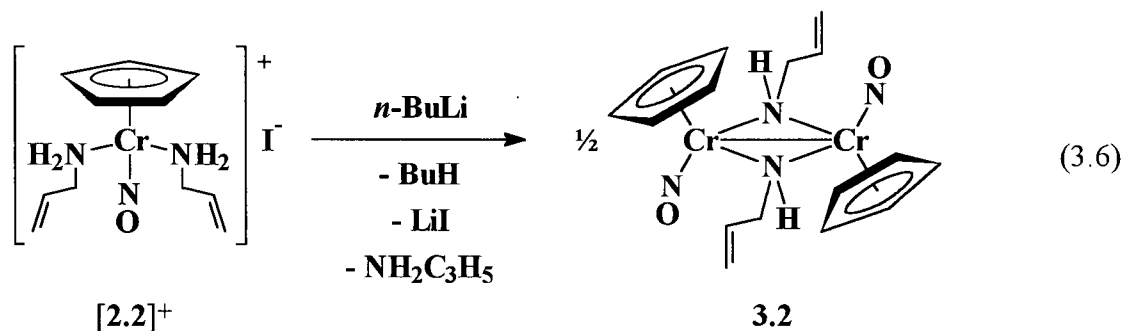
The shortening of the Cr-P distances upon reduction indicates that the HOMO of the 18e complex involves a considerable π-interaction with the phosphite ligands, a conclusion in accord with the theoretical calculations presented above, which indeed indicate the HOMO to be of π-symmetry with respect to the ligands, L. Upon effecting the transformation from **[3.1]⁺** to **3.1** via reduction, this π-bonding orbital is populated to a greater extent, thereby resulting in a greater bonding interaction, a stronger bond, and the observed shorter chromium-phosphite bond lengths. Conversely, oxidation from **3.1** to **[3.1]⁺** weakens these bonds, though not to the extent observed for the oxidation of CpCr(NO)(CO)₂, which causes the loss of the CO ligands. This is consistent with CO being a much more π-acidic ligand than P(OMe)₃.

There is another structural change in the phosphite ligands that is consistent with one-electron oxidation effecting removal of electron density from an orbital associated with π -backbonding to the phosphite. The $M(d_{\pi}) \rightarrow PX_3$ π -interaction is thought to involve the P-X σ -antibonding orbitals, rather than a d-orbital on phosphorus.⁴⁵ Thus, weakening the π -donation to the phosphorus ligand would be expected to result in a shortening of the P-X bonds, and this is the observed trend upon oxidation from **3.1** to **[3.1]⁺**. The average P-O bond lengths in the two molecules of **3.1** are 1.604 (8) Å and 1.598 (15) Å, while in the 17e cation this average distance is shortened to 1.569 (6) Å, a difference of about 0.03 Å.

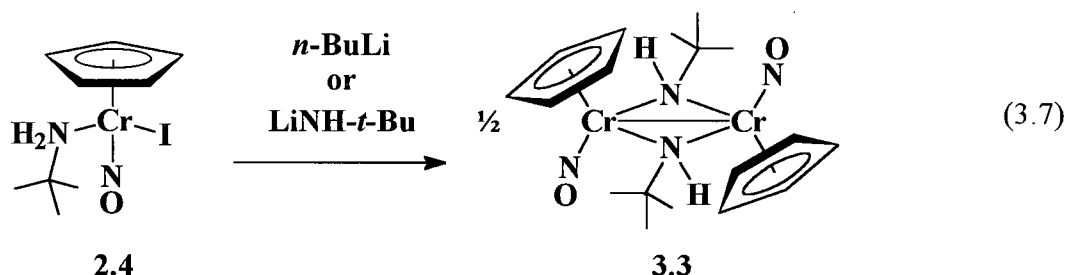
Exactly these effects have been previously observed in a variety of transition-metal phosphine and phosphite complexes.⁴⁶ In 18e complexes where the HOMO is metal-based and π -symmetry, one-electron oxidation generally results in a lengthening of M-P distances by about 0.1 Å, and a shortening of P-X distances by about 0.02 - 0.03 Å.

3.4.9 Reaction of Bis(amine) Salt **[2.2]⁺[I]⁻** and *tert*-Butylamine Complex **2.4** with *n*-BuLi

Complex **2.2⁺** contains two primary allylamine ligands. Given the positive charge of this complex, it is reasonable to expect that a good deal of this charge would be delocalized onto the amine hydrogen atoms and that these ligands should be fairly acidic in nature. An attempt was made to carry out removal of a proton from this complex, hopefully to form an amide ligand. Reaction of **[2.2]⁺[I]⁻** with *n*-BuLi does indeed result in the formation of an amide compound, but not the monomeric amine-amide that might have been expected. Instead, the result is a mixture of isomers of a bridging amide dimer of the form $[CpCr(NO)(NHC_3H_5)]_2$ (eq 3.6).

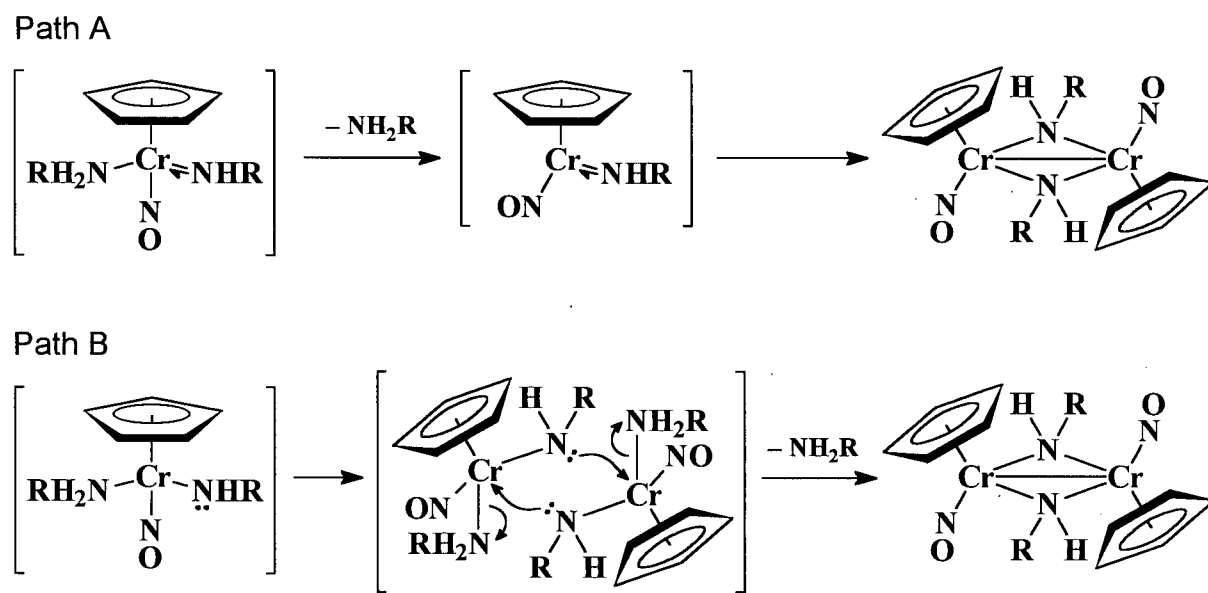


Products **3.2** presumably result from the removal of a proton from one amine ligand and complete loss of the second labile amine. The products are diamagnetic, 18e species by virtue of the metal-metal bond formed in the dimer. A similar reaction occurs when $\text{CpCr(NO)(NH}_2\text{CMe}_3\text{)I}$ (**2.4**) is treated with *n*-BuLi, so that the isolated products are the analogous amide-bridged dimers $[\text{CpCr(NO)(NHCMe}_3\text{)}]_2$ (**3.3**), though in this example the lost ligand is the iodide rather than a second amine (eq 3.7). The yield of **3.3** by this route is too low to allow satisfactory purification of the products, but, not surprisingly, dimers **3.3** are better prepared by direct reaction of **1** with an equivalent of *t*-BuNHLi. The same dimers are also obtained by reaction of *tert*-butylamine complex **2.4** with *t*-BuNHLi, though in this case it is unclear whether the amide group that is present in dimers **3.3** results from the amine ligand in the starting material, or from the added amide salt, or from both. The reaction could proceed via initial metathesis of the iodide for the amide group, and subsequent loss of the original amine ligand. Alternatively, and most likely, the reaction could be analogous to that of **2.4** with *n*-BuLi, with the amide salt simply acting as a Brønsted base.



These results suggest that the combination of a π -donor amide ligand and a σ -donor ligand such as an amine or iodide is not a compatible one. The hypothetical products, $\text{CpCr(NO)(NH}_2\text{R)(NHR)}$, would be 19e complexes if the lone pair from the amido nitrogen was donated to the metal via a π -donor interaction. There are a number of structural effects that might be expected to occur to maintain a 17-electron count. Both Cp and NO are known to exhibit bonding modes other than those observed in these complexes. Cyclopentadienyl can adopt

a non-aromatic, η^3 structure, becoming a three-electron donor.⁴⁷ Nitrosyl, as stated in Chapter 1, can adopt a bent geometry, becoming a 1-electron donor.⁴⁸ Alternatively, a terminal amide ligand may also be bent, adopting a pyramidal configuration about nitrogen rather than a planar one, and so becoming a 1-electron donor. Each of these possibilities would result in two “extra” electrons being removed to a ligand-based orbital, and the product, $\text{CpCr}(\text{NO})(\text{NH}_2\text{R})(\text{NHR})$, would be a new, formally 17e compound. However, none of these species is isolated or observed. It should be noted that the first two cases of ligand distortion would be the result of the extra electron density populating a π^* orbital to either the Cp or the NO, whereas Figure 3.5 indicates that the LUMO in these species is in fact antibonding to the two σ -basic ligands. Population of the LUMO is therefore consistent with the observed loss of amine or iodide in these reactions, rather than a bending of Cp or NO.

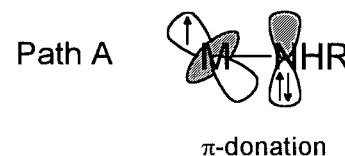


Scheme 3.3

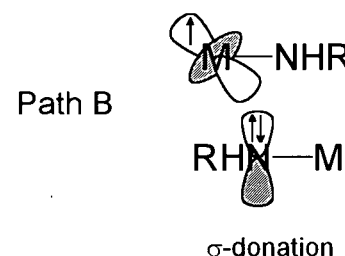
There are two possible mechanisms by which an intermediate of the type $\text{CpCr}(\text{NO})(\text{NH}_2\text{R})(\text{NHR})$ might be expected to yield the observed bridging-amide dimeric products, as indicated in Scheme 3.3. In the first instance, the formation of a π -basic amide group causes the loss of the amine ligand, and the resulting coordinatively-unsaturated fragment couples

with another such species to form a metal-metal bond in the dimeric complex (Path A). Alternatively, the amide ligand could retain the electron density in the form of a lone pair, and this ligand could serve as a nucleophile to another such species, displacing the amine ligand and forming the same dimeric product (Path B). The favored path can be thought to depend upon the extent to which the amide group functions as a π -donor.

Neglecting the potential amide π -donation, it can be assumed that a species of the type $\text{CpCr}(\text{NO})(\text{NH}_2\text{R})(\text{NHR})$ would have approximately the same orbital structure as that of the bis(amine) cations, as outlined in Figure 3.5. The singly-occupied orbital is of the correct symmetry to accept π -donation from the amide, but because the orbital is half-filled, such an interaction would force an occupied metal orbital to higher energy. Thus, a strong π -donor interaction would lead to an electron-rich metal center and the destabilization of a filled metal d-orbital, resulting in an unstable complex and loss of amine.



However, if there is little orbital overlap and the π -donation is weak, then the p-orbital on nitrogen remains strongly nucleophilic, and may attack a different metal center. In this case, the nitrogen lone-pair will act as an intermolecular σ -donor, but the acceptor orbital will be the *same* half-filled metal SOMO. Because the interaction is along a vector between the metal ligand bonds, the SOMO is now of σ -symmetry. Because the donation is to the same metal-orbital, the same destabilization will occur, and amine will again be lost.



In short, the path of dimer formation depends on the nature of the amide lone pair. It will donate this lone pair either to the metal SOMO in the form of an intramolecular π -bond (Path A), or to the SOMO of a different metal via an intermolecular σ -bond (Path B). Both interactions would result in loss of amine and formation of the same product. The current study does not provide evidence favoring either path, but given the essential similarity of the two pathways, the actual mechanism may well involve them both.

The isolation of both **3.2** and **3.3** involves filtration of the products through acidic alumina. If the products are chromatographed on the same support, separation of isomers can be effected, in both cases yielding two different colors of dimer, namely the red, *trans*-isomer and yellow, *cis*-form. The fact that the products obtained from the different eluates are isomeric is indicated by the identical mass spectra of the two forms of both **3.2** and **3.3**; the spectra of the different samples exhibit the same parent-mass peaks and the same fragmentation patterns. For example, the spectra of both the red and yellow isomers of *t*-butylamide dimer **3.3** exhibit peaks at $m/z = 438, 408, 378, \text{ and } 321$. These are assignable as the parent mass, and loss of one nitrosyl, two nitrosyls, and two nitrosyls and an amide group. Each of these peak clusters displays the isotope pattern expected for a dichromium species. Further evidence for the isomeric nature of the different products comes from the analytical data, since the separated forms of **3.2** analyze as having identical elemental compositions.

However, the NMR and IR spectral data of these species indicate that the separation of isomers is not complete, even after chromatography. This is not surprising, since there are *five* possible isomers for a complex of the form $[\text{CpCr}(\text{NO})(\text{NHR})]_2$ rather than only two. Four of these isomers and their respective point groups are depicted in Figure 3.10. The fifth isomer is another form of that depicted in the lower right, but with all the Cp and R ligands mutually *cis*-. This complex would also be of C_{2v} symmetry. However, such a compound was never observed during this study, and it is certainly the least favored form of the dimer from a steric point of view. Thus, I have elected to exclude it from discussion.

These bridging-amide complexes are presumed to contain a planar Cr_2N_2 core, in accord with the known structure of $[\text{CpCr}(\text{NO})(\text{NMe}_2)]_2$.⁴⁹ Thus, *cis*- and *trans*- isomers can result from the relative orientation of not only the Cp and NO groups, but also the amido nitrogen substituents. It is likely that the isolation of red and yellow forms represents the separation of one set of *cis*- and *trans*- isomers, either *cis*- and *trans*- with respect to Cp or *cis*- and *trans*- with respect to R, but which set is not immediately obvious. However, a close examination of the infrared and ^1H NMR spectral data reveals that for both **3.2** and **3.3** the red product is a mixture

of the two *trans*-Cp compounds, and the yellow corresponds to the *cis*-Cp form. The essential aspects of these data are summarized in Table 3.4.

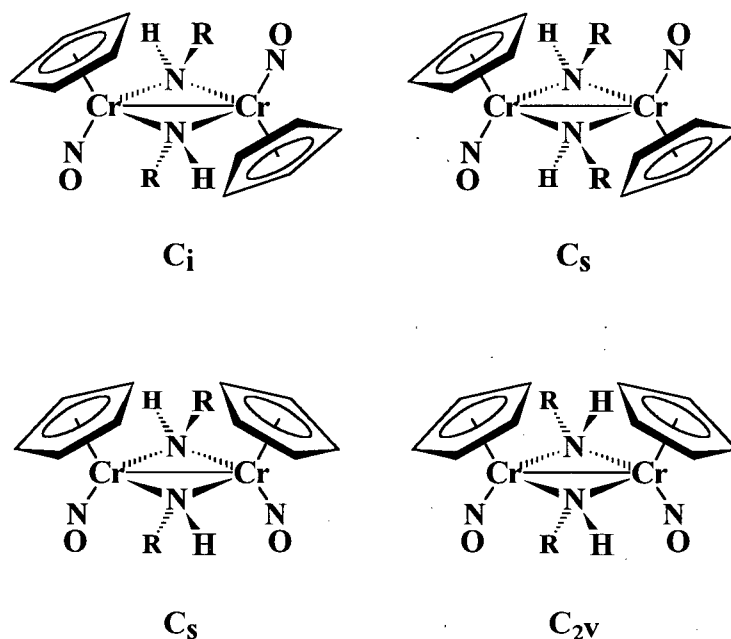


Figure 3.10. Isomers of $[\text{CpCr}(\text{NO})(\text{NHR})]_2$

Table 3.4. Predicted NMR and IR Data for Amide Complexes 3.2 and 3.3

expected signals	<i>trans</i> -Cp <i>trans</i> -R C_i	<i>trans</i> -Cp <i>cis</i> -R C_s	<i>cis</i> -Cp <i>trans</i> -R C_s	<i>cis</i> -Cp <i>cis</i> -R C_{2v}
^1H NMR	1 Cp 1 R	2 Cp 1 R	1 Cp 2 R	1 Cp 1 R
IR (ν_{NO})	1	2	2	2

A group-theoretical analysis of the isomers depicted in Figure 3.10 reveals that two IR-active nitrosyl bands would be expected for each isomer except the C_i all-*trans* form, which would exhibit only one. In the NMR spectra, the C_{2v} and C_i forms will exhibit only one set of resonances for both the Cp and the alkyl ligands, while the *trans*- C_s will exhibit two Cp resonances and one alkyl resonance, and the *cis*- C_s complex will exhibit a single Cp signal and

two due to alkyls. Comparison of these predicted results with the observed data in Tables 3.2 and 3.3 supports the assignments shown. For instance, the ^1H NMR spectra of the red forms of both **3.2** and **3.3** display Cp signals of two species, a major species with one signal and a minor species with two. This is expected for a mixture of C_1 and *trans*- C_5 isomers, and the C_1 is expected to be the more favored since it is the least sterically crowded. Thus, the red eluates contain a mixture of the C_1 and C_5 forms, with the Cp and NO ligands *trans*-, and the yellow eluates are a mixture of the C_5 and C_{2v} forms, with Cp and NO ligands *cis*-.

It is logical that a physical separation based on chromatography should proceed in this way. The polarities of two dimers differing in the orientation of alkyl groups should not be exceptionally distinct, whereas dimers differing in the orientation of Cp and nitrosyl groups should have very different polarities. Thus, the chromatographic separation distinguishes between Cp/NO isomers, but not R/H isomers.

Further support for these assignments comes from the isolation of similar red and orange isomers of $[\text{CpCr}(\text{NO})(\text{NMe})_2]_2$ (**3.5**). Since all four amide substituents are the same in this complex, isomers can only be due to orientation of the Cp and NO ligands. The same procedure that effected the separation of isomers of **3.2** and **3.3** separated *cis*- and *trans*-**3.5**, suggesting that the difference between the red and yellow isomers of the former is the same as in the latter. Again, these assignments are borne out by the IR and ^1H NMR spectral data. The red, *trans*-isomer of $[\text{CpCr}(\text{NO})(\text{NMe})_2]_2$ exhibits the single Me resonance and the single IR band expected for C_{2h} symmetry, and the yellow, *cis*-isomer exhibits two Me resonances and two nitrosyl bands consistent with the C_{2v} form. The structural assignment of these two compounds has been previously confirmed by X-ray crystallography,^{49,50} although the complexes were prepared by a different route for those reports, the synthetic details of which have never appeared in the literature. As well, the published characterization data⁵⁰ of the two dimethylamide species is both minimal and conflicting with that obtained in this work. Thus, full experimental details of the preparation and isolation of *cis*- and *trans*-**3.5**, along with more complete characterization data, are presented here.

3.5 Epilogue and Future Work

The 18e complex $\text{CpCr}(\text{NO})(\text{CO})_2$ exhibits properties that one would expect given the tenets of organometallic chemistry. Upon oxidation, the CO ligands become labile, and are easily substituted. The carbonyl ligands are lost because the HOMO of this complex is principally π -bonding to both carbonyl ligands, and so oxidation of the complex weakens the M-CO bonds. To a first approximation, this is a reasonable description of oxidatively-induced lability observed in most 18e organometallic complexes, since such species generally have very strong π -bonding interactions with the organic ligands.

However, as these π -bonding effects are reduced, the metal complex becomes more "coordination-like," and the traditional generalizations no longer hold. The 17e electron species $[\text{CpCr}(\text{NO})(\text{NH}_3)_2]^+$ exhibits none of the reactivity traditionally associated with such metal-centered radicals, and in fact may be rendered reactive by reducing it to a 18e complex, which results in amine loss. Thus, the presence of π -neutral ligands results in a reversal of expected trends in organometallic chemistry. In a way, these $[\text{CpCr}(\text{NO})(\text{L})_2]^+$ species represent a bridge between the usually strong ligand fields of organometallic compounds, caused by π -acceptor ligands, and the weaker fields of coordination chemistry resulting primarily from ligands of only σ -character. The preparation of complexes such as $\mathbf{3.1}^{+/0}$, which exist on both sides of this bridge, represents an opportunity to explore an intermediate area of chemistry by using a system in which the bonding trends now seem to be well-understood.

The theoretical analysis of bis(ammonia) complex $\mathbf{1}^+$ suggests that its lack of substitution chemistry is primarily thermodynamic in nature. It is likely that other cationic complexes would prove to be more labile. It is also likely that there are more pairs of compounds like $\mathbf{3.1}^{+/0}$, which exist as both 17 and 18e complexes. One such pair of species is presented in Chapter 5. A comparison of rates and mechanisms of reactivities of such pairs of compounds would be of interest; if substitution reactions of one species are slow, they may be faster for the other, and these compounds would allow such a comparison with exactly the same ligand field differentiated only by a single electron.

Removal of an acidic proton from an amine ligand of $\text{CpCr(NO)(NH}_2\text{R)I}$ or $[\text{CpCr(NO)(NH}_2\text{R)}_2]^+$ complexes does not result in an amide compound, as might have been expected. Instead, the result is the loss of another ligand, either halide or amine, and the dimerization of the resulting fragment to form complexes of the type $[\text{CpCr(NO)(NHR)}]_2$. The presumed amide intermediates, $[\text{CpCr(NO)(I)(NHR)}]^-$ or $\text{CpCr(NO)(NH}_2\text{R)(NHR)}$, would be either 19e complexes if no structural distortion occurred, by virtue of π -donation from the amide moiety, but 17e species if the extra electron density remained localized on the amide nitrogen atom. It may well be possible to isolate such 17e compounds by stabilizing the amide lone-pair; through either the use of an electron-withdrawing group as an amide substituent or the presence of a hydrogen-bonding solvent, both of which would serve to delocalize the amide lone-pair away from the nitrogen atom and the metal. These effects have been observed in a variety of low-valent alkoxo- and amidometal complexes.⁵¹

No reactivity studies of the bridging-amide dimers have been undertaken. It may be possible to oxidatively cleave these dimers with a halogen reagent to yield a neutral, monomeric $\{\text{Cr(NO)}\}^4$ amide-halide species of the form $\text{CpCr(NO)(X)(NR}_2)$. At least one complex of this class is known to exist.⁵² Such a compound would be formally an 18e complex, with the lower electronic configuration of the metal being stabilized by the π -donor amido group.

3.6 References and Notes

- (1) (a) Shriver, D. F.; Atkins, P.; Langford, C. H. *Inorganic Chemistry*, 2nd ed.; W. H. Freeman: New York, NY, 1994; p 661. (b) Collman, J. P.; Hegedus, L. S.; Norton, J. R.; Finke, R. G. *Principles and Applications of Organotransition Metal Chemistry*; University Science Books: Mill Valley, CA, 1987; p 22.
- (2) Brown, T. L. In *Organometallic Radical Processes*; Trogler, W. C., Ed.; Elsevier: New York, 1990; Chapter 3.
- (3) Tyler, D. R. *Prog. Inorg. Chem.* **1988**, *36*, 125.
- (4) For a recent mechanistic investigation of halide and hydrogen atom abstraction by a 17e organometallic radical, see: Huber, T. A.; Macartney, D. H.; Baird, M. C. *Organometallics* **1995**, *14*, 592.
- (5) Baird, M. C. *Chem. Rev.* **1988**, *88*, 1217.
- (6) For a recent example of dimerization of a 17e cationic complex via ligand-ligand coupling, see: Ge, Y.-W.; Ye, Y.; Sharp, P. R. *J. Am. Chem. Soc.* **1994**, *116*, 8384. For a recent kinetic study of a metal-metal dimerization process, see: Richards, T. C.; Geiger, W. E.; Baird, M. C. *Organometallics* **1994**, *13*, 4494.
- (7) (a) Pedersen, A.; Tilset, M.; Folting, K.; Caulton, K. G. *Organometallics* **1995**, *14*, 875. (b) Pedersen, A.; Tilset, M. *Organometallics* **1993**, *12*, 56.
- (8) Kowaleski, R. M.; Basolo, F.; Trogler, W. C.; Gedridge, R. W.; Newbound, T. D.; Ernst, R. D. *J. Am. Chem. Soc.* **1987**, *109*, 4860 and references contained therein.
- (9) Trogler, W. C. In *Organometallic Radical Processes*; Trogler, W. C., Ed.; Elsevier: New York, 1990; Chapter 9.
- (10) For recent examples of investigation of substitution reactions of 17e organometallic species, see: (a) Watkins, W. C.; Hensel, K.; Fortier, S.; Macartney, D. H.; Baird, M. C. *Organometallics* **1992**, *11*, 2417. (b) Shen, J. K.; Freeman, J. W.; Hallinan, N. C.; Rheingold, A. L.; Arif, A. M.; Ernst, R. D.; Basolo, F. *Organometallics* **1992**, *11*, 3215.

- (c) Scott, S. L.; Espenson, J. H.; Bakac, A. *Organometallics* **1993**, *12*, 1044. (d) Huang, Y.; Carpenter, G. B.; Sweigart, D. A.; Chung, Y. K.; Lee, B. Y. *Organometallics* **1995**, *14*, 1423.
- (11) (a) Coville, N. J. In *Organometallic Radical Processes*; Trogler, W. C., Ed.; Elsevier: New York, 1990; Chapter 4. (b) Kochi, J. K. *ibid*; Chapter 7.
- (12) Kochi, J. K. *J. Organomet. Chem.* **1986**, *300*, 139.
- (13) Ashby, E. C.; Goel, A. B. *J. Am. Chem. Soc.* **1981**, *103*, 4983.
- (14) Herring, F. G.; Legzdins, P.; Richter-Addo, G. B. *Organometallics* **1989**, *8*, 1485.
- (15) Halpern, J. *Pure Appl. Chem.* **1986**, *58*, 575 and references contained therein.
- (16) Bullock, R. M.; Samsel, E. G. *J. Am. Chem. Soc.* **1990**, *112*, 6886.
- (17) *Paramagnetic Organometallic Species in Activation/Selectivity, Catalysis*; Chanon, M., Julliard, M., Poite, J. C., Eds.; Kluwer Academic: Boston, 1989.
- (18) For some recent examples, see: (a) RajanBabu, T. V.; Nugent, W. A. *J. Am. Chem. Soc.* **1994**, *116*, 986. (b) Casty, G. L.; Stryker, J. M. *J. Am. Chem. Soc.* **1995**, *117*, 7814.
- (19) Tolman, C. A. *Chem. Soc. Rev.* **1972**, *1*, 337.
- (20) Reference 1a, pp 260, 667.
- (21) (a) Bratt, S. W.; Kassyk, A.; Perutz, R. N.; Symons, M. C. R. *J. Am. Chem. Soc.* **1982**, *104*, 490. (b) Holland, G. F.; Manning, M. C.; Ellis, D. E.; Trogler, W. C. *J. Am. Chem. Soc.* **1983**, *105*, 2308.
- (22) Hoobler, R. J.; Hutton, M. A.; Dillard, M. M.; Castellani, M. P.; Rheingold, A. L.; Rieger, A. L.; Rieger, P. H.; Richards, T. C.; Geiger, W. E. *Organometallics* **1993**, *12*, 116.
- (23) Richards, T. C.; Geiger, W. E.; Baird, M. C. *Organometallics* **1994**, *13*, 4494.
- (24) Reference 1b, p 246.
- (25) Kowaleski, R. M.; Basolo, F.; Osborne, J. H.; Trogler, W. C. *Organometallics* **1988**, *7*, 1425.
- (26) Connelly, N. G. *Chem. Soc. Rev.* **1989**, *18*, 153.

- (27) Ammeter, J. H.; Bürgi, H.-B.; Thibeault, J. C.; Hoffmann, R. *J. Am. Chem. Soc.* **1978**, *100*, 3686.
- (28) Legzdins, P.; Nurse, C. R. *Inorg. Chem.* **1985**, *24*, 327.
- (29) The hexafluorophosphate salt was prepared by addition of NaPF₆ to an aqueous [Cp₂Fe]₂[SO₄] solution. Jolly, W. L. *The Synthesis and Characterization of Inorganic Compounds*; Prentice-Hall: Englewood Cliffs, NJ, 1970; p 487.
- (30) Legzdins, P.; McNeil, W. S.; Shaw, M. J. *Organometallics* **1994**, *13*, 562.
- (31) Chin, T. T.; Hoyano, J. K.; Legzdins, P.; Malito, J. T. *Inorg. Synth.* **1990**, *28*, 196.
- (32) Freeman, P. K.; Hutchinson, L. L. *J. Org. Chem.* **1983**, *48*, 879.
- (33) Chin, T. T.; Legzdins, P.; Trotter, J.; Yee, V. C. *Organometallics* **1992**, *11*, 913.
- (34) (a) Hunter, A. D.; Legzdins, P. *Organometallics* **1986**, *5*, 1001. (b) Hermann, W. A.; Hubbard, J. L.; Bernal, I.; Korp, J. D.; Haymore, B. L.; Hillhouse, G. L. *Inorg. Chem.* **1984**, *23*, 2978. (c) Behrens, H.; Landgraf, G.; Merbach, P.; Moll, M.; Trummer, K.-H. *J. Organomet. Chem.* **1983**, *253*, 217. (d) Herberhold, M.; Alt, H. *Liebigs Ann. Chem.* **1976**, 292. (e) Herberhold, M.; Alt, H.; Kreiter, Cornelius, C. G. *Liebigs Ann. Chem.* **1976**, 300. (f) Brunner, H. *J. Organomet. Chem.* **1969**, *16*, 119. (g) Brunner, H. *Chem. Ber.* **1969**, *102*, 305.
- (35) Legzdins, P.; Shaw, M. J., unpublished observations.
- (36) Hames, B. W.; Legzdins, P.; Martin, D. T. *Inorg. Chem.* **1978**, *17*, 3644.
- (37) The tendency of Lewis acidic metal centers to bind to the oxygen atom of a coordinated CO group is well known.^{37a} Such binding to NO is less well-established, but a few such adducts have been isolated, and many have been observed.^{37b} The interaction of an electrophile with a NO^{37c} or CO^{37d,e} oxygen atom has been observed to induce reactivity or instability in otherwise unreactive compounds. (a) Horwitz, C. P.; Shriver, D. F. *Adv. Organomet. Chem.*, **1984**, *23*, 219. (b) Legzdins, P.; Richter-Addo, G. B. *Metal Nitrosyls*; Oxford University Press: New York, 1992, p 276 and references contained

- therein. (c) Legzdins, P., Shaw, M. J. *J. Am. Chem. Soc.* **1994**, *116*, 7700. (d) Ellis, J. E.; Kelsey Stein, B.; Frerichs, S. R. *J. Am. Chem. Soc.* **1993**, *115*, 4066. (e) Carnahan, E. M.; Lippard, S. J. *J. Am. Chem. Soc.* **1992**, *114*, 4166.
- (38) Poli, R.; Owens, B. E.; Linck, R. G. *J. Am. Chem. Soc.* **1992**, *114*, 1302.
- (39) Geiger, W. E.; Rieger, P. H.; Tulyathan, B.; Rausch, M. D. *J. Am. Chem. Soc.* **1984**, *106*, 7000.
- (40) (a) Legzdins, P.; Nurse, C. R. *Inorg. Chem.* **1985**, *24*, 327. (b) Herring, F. G.; Legzdins, P.; McNeil, W. S.; Shaw, M. J.; Batchelor, R. J.; Einstein, F. W. B. *J. Am. Chem. Soc.* **1991**, *113*, 7049.
- (41) (a) Regina, F. J.; Wojcicki, A. *Inorg. Chem.* **1980**, *19*, 3803. (b) Fischer, E. O.; Strametz, H. *J. Organomet. Chem.* **1967**, *10*, 323.
- (42) An apparent exception is the complex $\text{Cp}^*\text{Cr}(\text{NO})(\text{O}-i\text{-Pr})_2$: Hubbard, J. L.; McVicar, W. K. *Inorg. Chem.* **1992**, *31*, 910. This complex is formulated as an 18e compound due to π -donation of electron density from the alkoxide groups, though the metal is in a higher formal oxidation state than that in the 17e species prepared in Chapter 2. This complex may well represent a third class of $\text{Cp}'\text{Cr}(\text{NO})$ compounds, containing a formal $\{\text{Cr}(\text{NO})\}^4$ fragment and stabilized by π -basic ligands. This possibility is discussed further in Chapter 4.
- (43) Fortier, S.; Baird, M. C.; Preston, K. F.; Morton, J. R.; Ziegler, T.; Jaeger, T. J.; Watkins, W. C.; MacNeil, J. H.; Watson, K. A.; Hensel, K.; Le Page, Y.; Charland, J.-P.; Williams, A. J. *J. Am. Chem. Soc.* **1991**, *113*, 542.
- (44) Huheey, J. E. *Inorganic Chemistry*, 3rd ed.; Harper and Row: New York, NY, 1983; p 76.
- (45) (a) Marynick, D. S. *J. Am. Chem. Soc.* **1984**, *106*, 4064. (b) Xiao, S.-X.; Trogler, W. C.; Ellis, D. E.; Berkovitch-Yellin, Z. *J. Am. Chem. Soc.* **1983**, *105*, 7033.
- (46) Orpen, A. G.; Connelly, N. G. *J. Chem. Soc., Chem. Commun.* **1985**, 1311.

- (47) O'Connor, J. M.; Casey, C. P. *Chem. Rev.* **1987**, *87*, 307.
- (48) Legzdins, P.; Richter-Addo, G. B. *Metal Nitrosyls*; Oxford University Press: New York, 1992; p 18.
- (49) Bush, M. A.; Sim, G. A. *J. Chem. Soc. (A)* **1970**, 611.
- (50) Bush, M. A.; Sim, G. A.; Knox, G. R.; Ahmad, M.; Robertson, G. G. *J. Chem. Soc. (D)* **1969**, 74.
- (51) (a) Bergman, R. G. *Polyhedron* **1995**, *14*, 3227. (b) Caulton, K. G. *New. J. Chem.* **1994**, *18*, 25.
- (52) Sim, G. A.; Woodhouse, D. I.; Knox, G. R. *J. Chem. Soc., Dalton Trans.* **1979**, 83.

CHAPTER 4

Synthesis and Characterization of 17-Electron $[\text{CpCr}(\text{NO})\text{X}_2]^-$ Anions

4.1 Introduction.....	93
4.2 Experimental Procedures.....	95
4.3 Characterization Data.....	102
4.4 Results and Discussion.....	103
4.5 Epilogue and Future Work.....	125
4.6 References and Notes.....	128

4.1 Introduction

The anions prepared in this Chapter are of the form $[\text{CpCr}(\text{NO})\text{X}_2]^-$ ($\text{X} = \text{halide, triflate}$), and therefore have a $\{\text{Cr}(\text{NO})\}^5$ electronic configuration. They are the only monomeric complexes of this configuration to have known, stable molybdenum congeners, and so these 17e anions represent the first bridge between the disparate chemistries of chromium and the heavier Group 6 metals for the $\text{Cp}'\text{M}(\text{NO})$ class.¹

All six 17e molybdenum anions, $[\text{Cp}'\text{Mo}(\text{NO})\text{X}_2]^-$ ($\text{Cp}' = \text{Cp, Cp}^*$; $\text{X} = \text{Cl, Br, I}$), are easily prepared by reaction of the 16e neutral complexes with cobaltocene, and may be isolated as the cobaltocenium salts.² These reactions, as expected, are reversible, so treatment of $[\text{Cp}'\text{Mo}(\text{NO})\text{X}_2]^-$ with ferrocenium regenerates the neutral complexes. Although isolable, the molybdenum anions are considerably less stable than their neutral precursors and decompose as solids at room temperature. As well, the 17e molybdenum anions exhibit a greater substitutional lability than the oxidized 16e form, so that the alkylation of the 16e dihalide compounds by Grignard reagents actually proceeds via 17e anionic intermediates.²

The preparation of chromium analogues of these known molybdenum complexes allows the two types of compounds to be compared and contrasted, hopefully revealing some insight as to the different nature of the chromium species. Although chromium analogues to $\{\text{M}(\text{NO})\}^4$ ($\text{M} = \text{Mo, W}$) compounds are not known, these dihalide anions are electron-rich complexes that are only a one-electron oxidation away from this manifold, and so the oxidation behavior of these species should reveal information as to the stability of such chromium compounds.

As indicated in Chapter 1, there are two known $\text{Cp}'\text{Cr}(\text{NO})$ compounds of the $\{\text{Cr}(\text{NO})\}^4$ configuration, both of which contain π -basic ligands. These are $\text{Cp}^*\text{Cr}(\text{NO})(\text{O-}i\text{-Pr})_2$ ³ and $\text{CpCr}(\text{NO})(\text{I})(\text{NPh}_2)$.⁴ That the alkoxide and amide ligands in these two complexes are indeed functioning as π -donors is apparent from the relative orientation of the ligands in the crystal structures of these compounds. For instance, the simplified orbital diagram in Scheme 3.3 suggests that in a $\{\text{Cr}(\text{NO})\}^4$ complex, the non-bonding π -symmetry orbital, perpendicular to the M-NO axis, will be empty, so that donation of two electrons into this orbital via a π -bond will

result in an 18e compound. In the case of the diphenylamide complex, this π -overlap will be maximized if the Ph-N-Ph plane is parallel to the M-NO vector, and the structure of this compound shows the N-M-N-C(phenyl) dihedral angles to be less than 4.9° and 10.1° , putting one of the phenyl groups in a sterically unfavorable position with respect to the Cp ring. Thus, the orientation must be ascribed to electronic interaction, namely that of the amide group functioning as a π -donor ligand.

The existence of these two complexes suggests a continuum of three electronic configurations of CpCr(NO) compounds, each selectively stabilized by a particular ligand type. That is, $\{\text{Cr}(\text{NO})\}^6$ compounds are stabilized by π -acidic ligands, $\{\text{Cr}(\text{NO})\}^5$ compounds are favored for complexes with π -neutral ligands, and $\{\text{Cr}(\text{NO})\}^4$ species are stabilized by π -basic ligands.

This Chapter describes the preparation of a series of $[\text{CpCr}(\text{NO})\text{X}_2]^-$ anions, the reactivity of these species, and the oxidation chemistry of $[\text{CpCr}(\text{NO})\text{Cl}_2]^-$ in the context of investigating the $\{\text{Cr}(\text{NO})\}^4$ manifold.

4.2 Experimental Procedures

4.2.1 Methods

The experimental methods employed throughout this Thesis are detailed in Section 2.2.1. The electrochemical methods employed are detailed in Section 2.2.2.

4.2.2 Reagents

$[\text{CpCr}(\text{NO})\text{I}]_2$,⁵ $[\text{Cp}_2\text{Fe}]^+[\text{PF}_6]^-$,⁶ $\text{CpCr}(\text{NO})(\text{CO})_2$,⁷ $\text{CpCr}(\text{NO})_2\text{Cl}$,⁸ were all prepared by published procedures. All other reagents were used as received from commercial suppliers.

4.2.3 Preparation of $n\text{-Bu}_4\text{N}^+[\text{CpCr}(\text{NO})\text{I}_2]^-$ ($n\text{-Bu}_4\text{N}^+[\mathbf{4.1}]^-$)

$[\text{CpCr}(\text{NO})\text{I}]_2$ (548 mg, 2.00 mmol) and $n\text{-Bu}_4\text{NI}$ (739 mg, 2.00 mmol) were dissolved in CH_2Cl_2 (30 mL) and stirred for 1 hr, and the solvent was then removed in vacuo. The red-brown residue was triturated with Et_2O (25 mL), collected on a frit, and washed with further Et_2O (2 x 25 mL). The resulting red-brown powder was characterized as $n\text{-Bu}_4\text{N}^+[\text{CpCr}(\text{NO})\text{I}_2]^-$ ($n\text{-Bu}_4\text{N}^+[\mathbf{4.1}]^-$).

4.2.4 Preparation of $n\text{-Bu}_4\text{N}^+[\text{CpCr}(\text{NO})(\text{OTf})_2]^-$ ($n\text{-Bu}_4\text{N}^+[\mathbf{4.2}]^-$)

$[\text{CpCr}(\text{NO})\text{I}]_2$ (548 mg, 2.00 mmol) and $n\text{-Bu}_4\text{NI}$ (739 mg, 2.00 mmol) were dissolved in CH_2Cl_2 (20 mL) and stirred for 1 hr, after which time the solution was cannulated onto AgOTf (1.03 g, 3.99 mmol). A flocculent precipitate formed immediately. The mixture was stirred for five minutes and filtered. The brown solution was reduced to dryness in vacuo, and the residue was triturated with hexanes (2 x 15 mL) to yield $n\text{-Bu}_4\text{N}^+[\text{CpCr}(\text{NO})(\text{OTf})_2]^-$ ($n\text{-Bu}_4\text{N}^+[\mathbf{4.2}]^-$) as a brown powder.

4.2.5 Preparation of $n\text{-Bu}_4\text{N}^+[\text{CpCr}(\text{NO})\text{Br}_2]^-$ ($n\text{-Bu}_4\text{N}^+[\mathbf{4.3}]^-$)

$n\text{-Bu}_4\text{N}^+[\text{CpCr}(\text{NO})(\text{OTf})_2]^-$ (346 mg, 0.503 mmol) and KBr (120 mg, 1.01 mmol) were dissolved in CH_2Cl_2 (15 mL). The mixture was stirred for 3 d, and the resulting brown solution was filtered and taken to dryness. The brown residue was recrystallized from CH_2Cl_2 /hexanes as black prisms of $n\text{-Bu}_4\text{N}^+[\text{CpCr}(\text{NO})(\text{Br})_2]^-$ ($n\text{-Bu}_4\text{N}^+[\mathbf{4.3}]^-$).

4.2.6 Reaction of $n\text{-Bu}_4\text{N}^+[\text{CpCr}(\text{NO})(\text{OTf})_2]^-$ and KCl

$n\text{-Bu}_4\text{N}^+[\text{CpCr}(\text{NO})(\text{OTf})_2]^-$ (320 mg, 0.465 mmol) and KCl (69 mg, 0.93 mmol) were dissolved in CH_2Cl_2 (20 mL). The mixture was stirred for 1 d, and the resulting green solution was filtered and taken to dryness in vacuo. The resulting green powder was triturated with hexanes (2 x 15 mL) and recrystallized from CH_2Cl_2 /hexanes. Although a green crystalline material was obtained which exhibited spectroscopic properties consistent with its formulation as a salt of $[\text{CpCr}(\text{NO})\text{Cl}_2]^-$, the material could never be fully separated from ionic byproducts, presumably a mixture of KOTf, $n\text{-Bu}_4\text{NOTf}$ and chloride salts.

4.2.7 Improved Preparation of $[\text{CpCr}(\text{NO})\text{Cl}]_2$

$\text{CpCr}(\text{NO})(\text{CO})_2$ (812 mg, 4.00 mmol) was dissolved in MeCN (~15 mL), and the mixture was cooled to $-30\text{ }^\circ\text{C}$. PCl_5 (407 mg, 1.95 mmol) was added, and the stirred mixture was allowed to warm slowly to room temperature. The warming was accompanied by a color change to deep green and the evolution of gas. The solvent was removed in vacuo, and the green residue was washed with pentane (2 x 15 mL). The crude green powder thus isolated (674 mg) exhibited spectroscopic properties identical to those known for $[\text{CpCr}(\text{NO})\text{Cl}]_2$, though the infrared spectrum indicated the presence of a small amount of $\text{CpCr}(\text{NO})_2\text{Cl}$ in the sample. Washing the green powder with Et_2O (3 x 10 mL) followed by dissolution in, and slow evaporation, of toluene yielded green microcrystals.

Anal. Calcd (Found): C: 32.90 (33.26); H: 2.76 (3.01); N 7.67 (7.77); IR (Nujol): 823, 1652, 1665 cm^{-1} ; IR (CH_2Cl_2): 1684 cm^{-1} ; EI-MS (m/z , probe temp 180°C) 364 (P^+), 334 (P^+-NO), 304 (P^+-2NO), 182 ($\text{CpCr}(\text{NO})\text{Cl}^+$), 152 (CpCrCl^+), 117 (CpCr^+).

4.2.8 Preparation of $\text{Et}_4\text{N}^+[\text{CpCr}(\text{NO})\text{Cl}_2]^-$ ($\text{Et}_4\text{N}^+[\mathbf{4.4}]^-$)

$[\text{CpCr}(\text{NO})\text{Cl}]_2$ was prepared as described above from 4.00 mmol of $\text{CpCr}(\text{NO})(\text{CO})_2$. The resulting green powder and Et_4NCl (650 mg, 3.92 mmol) were suspended in toluene and stirred for 3 h, resulting in a color change from green to brown. The solvent was removed in vacuo, and the mixture was extracted into CH_2Cl_2 /hexanes (20 mL, 4:1 ratio) and filtered. Cooling the filtrate resulted in the crystallization of $\text{Et}_4\text{N}^+[\text{CpCr}(\text{NO})(\text{Cl})_2]^-$ ($\text{Et}_4\text{N}^+[\mathbf{4.4}]^-$) as narrow black blocks.

4.2.9 Reaction of Diiodide Salt $n\text{-Bu}_4\text{N}^+[\mathbf{4.1}]^-$ with MeLi

THF (~10 mL) was vacuum transferred onto $n\text{-Bu}_4\text{N}^+[\mathbf{4.1}]^-$ (322 mg, 0.500 mmol), and the solution temperature was controlled with an acetone/ CO_2 bath. As the solution was stirred, MeLi (0.70 mL, 1.4 M in Et_2O , 0.98 mmol) was added via syringe, and the temperature of the cooling bath was maintained below -50 °C. After 30 min, an IR spectrum of the solution revealed no net reaction of the starting material. The reaction mixture was allowed to warm slowly. After 3 h, the temperature had reached 15 °C, the color of the solution had changed from red-brown to brown, and an IR spectrum revealed the loss of the reactant's nitrosyl band (1650 cm^{-1}) and a broad, weak feature at ~1590 cm^{-1} .

4.2.10 Reaction of Diiodide Salt $n\text{-Bu}_4\text{N}^+[\mathbf{4.1}]^-$ with $\text{Me}_3\text{SiCH}_2\text{MgCl}$

THF (~10 mL) was vacuum transferred onto $n\text{-Bu}_4\text{N}^+[\mathbf{4.1}]^-$ (643 mg, 1.00 mmol), $\text{Me}_3\text{SiCH}_2\text{MgCl}$ was added by syringe (1.0 M in THF, 4.0 mL, 4.0 mmol), and the reaction solution was stirred overnight. The resulting mixture consisted of a brown solution and a grey-

white precipitate. An ESR spectrum of the solution exhibited only the characteristic eleven-line signal of $\text{CpCr}(\text{NO})(\text{THF})(\text{CH}_2\text{SiMe}_3)$.⁹

4.2.11 Reaction of Diiodide Salt $n\text{-Bu}_4\text{N}^+[\mathbf{4.1}]^-$ with $o\text{-tolNHLi}$ and Me_2NLi

THF (~10 mL) was vacuum transferred onto $n\text{-Bu}_4\text{N}^+[\mathbf{4.1}]^-$ (322 mg, 0.500 mmol) and $o\text{-tolNHLi}$ (133 mg, 1.00 mmol), and the mixture was stirred for 90 min. The solvent was removed in vacuo; the brown residue was extracted with Et_2O (2 x 15 mL), and the extracts were filtered through acidic alumina I (2 x 3 cm). The resulting brown filtrate was reduced to dryness, the residue was extracted into $\text{Et}_2\text{O}/\text{CH}_2\text{Cl}_2$ (3:1, 15 mL), and the extract loaded onto a pentane-packed column of acidic alumina I (2 x 8 cm). Elution of the column with Et_2O led to the formation and collection of an orange eluate that was stripped to dryness to yield the red (*trans*) isomers of bridging-amide dimer **3.4** (12 mg, 9.5% yield). Further elution of the column with CH_2Cl_2 led to the formation and collection of a yellow eluate, which was taken to dryness to yield the yellow (*cis*) isomers of bridging-amide dimer **3.4** (5 mg, 4% yield).

Reaction of $n\text{-Bu}_4\text{N}^+[\mathbf{4.1}]^-$ (750 mg, 1.17 mmol) and Me_2NLi (120 mg, 2.35 mmol) was performed similarly, with the following changes. The reaction mixture was stirred for 2 h, the reaction residue was extracted with 3:1 $\text{Et}_2\text{O}/\text{CH}_2\text{Cl}_2$ (3 x 20 mL), these extracts were filtered through neutral alumina I (2 x 3 cm), taken to dryness, and again extracted into Et_2O (10 mL) before chromatography. The orange and yellow eluates yielded the red (*trans*) isomers (13 mg, 12% yield) and the yellow (*cis*) isomers (6 mg, 5% yield) of bridging-amide dimer **3.5**.

4.2.12 Reaction of Dichloride Salt $\text{Et}_4\text{N}^+[\mathbf{4.4}]^-$ with $t\text{-BuOLi}$

THF (~10 mL) was vacuum transferred onto $\text{Et}_4\text{N}^+[\mathbf{4.4}]^-$ (174 mg, 0.500 mmol) and $t\text{-BuOLi}$ (80 mg, 1.0 mmol), and the suspension was stirred for 90 min, resulting in a brown-red solution. The reaction mixture was taken to dryness, the residue was extracted into Et_2O (2 x 10 mL), and the extracts were filtered. The brown filtrate was stripped to dryness, the residue was extracted into CH_2Cl_2 (2 x 10 mL), and the extracts were filtered through basic alumina I (2 x 3

cm). The resulting green-brown filtrate did not exhibit a room-temperature ESR spectrum. The solvent was removed in vacuo to yield a green brown solid, the partial characterization data of which is consistent with its formulation as $[\text{CpCr}(\text{NO})(\text{O}^t\text{Bu})]_2$: IR (Nujol) 1651, 1635 cm^{-1} ; EI-MS (probe temp. 120°C): m/z 440 (P^+), 410 (P^+-NO), 380 (P^+-2NO).

4.2.13 Treatment of Diiodide Salt $n\text{-Bu}_4\text{N}^+[\mathbf{4.1}]^-$ with MeI

THF (~10 mL) was vacuum transferred onto $n\text{-Bu}_4\text{N}^+[\mathbf{4.1}]^-$ (322 mg, 0.500 mmol) and MeI (31 μL , 0.50 mmol) was added via syringe. The IR and ESR spectra of the reaction mixture remain unchanged from that of the starting material both after 4 h and after 4 d.

4.2.14 Treatment of Dichloride Salt $\text{Et}_4\text{N}^+[\mathbf{4.4}]^-$ with MeI

THF (~10 mL) was vacuum transferred onto $\text{Et}_4\text{N}^+[\mathbf{4.4}]^-$ (174 mg, 0.500 mmol) and MeI (31 μL , 0.50 mmol) was added via syringe. The mixture was stirred for 6 hours. An ESR spectrum of the solution displayed three weak signals, two of which appeared to be those of the starting anion and of diiodide $[\mathbf{4.1}]^-$. The third was at a g -value intermediate between the two.

4.2.15 Treatment of Diiodide Salt $n\text{-Bu}_4\text{N}^+[\mathbf{4.1}]^-$ with $[\text{Me}_3\text{O}]^+[\text{BF}_4]^-$

A mixture of $n\text{-Bu}_4\text{N}^+[\mathbf{4.1}]^-$ (670 mg, 1.04 mmol) and $[\text{Me}_3\text{O}]^+[\text{BF}_4]^-$ (150 mg, 1.04 mmol) was cooled with an acetone/liquid nitrogen bath and frozen in CH_2Cl_2 (15 mL). This mixture was allowed to thaw and was stirred for 2.5 hr at -60 °C. During this time IR spectra of the solution indicated a gradual loss of the starting material's nitrosyl band (1644 cm^{-1}) and the appearance of a band at 1673 cm^{-1} . Hexanes (20 mL) were added to the solution, and the mixture was filtered. The filtrate was stripped to dryness, and the resulting brown residue was washed with Et_2O (2 x 20 mL) and recrystallized from CH_2Cl_2 /hexanes to yield complex **1**, $[\text{CpCr}(\text{NO})\text{I}]_2$ (225 mg, 79% yield).

4.2.16 Reaction of Dichloride Salt $\text{Et}_4\text{N}^+[\text{4.4}]^-$ with $[\text{Cp}_2\text{Fe}]^+[\text{PF}_6]^-$

THF (~10 mL) was vacuum transferred onto $\text{Et}_4\text{N}^+[\text{4.4}]^-$ (347 mg, 1.03 mmol) and $[\text{Cp}_2\text{Fe}]^+[\text{PF}_6]^-$ (170 mg, 0.514 mmol), and the solution was stirred for 1 hr. An IR spectrum of the green solution exhibited two strong bands at 1701 and 1807 cm^{-1} in a relative intensity indicative of a *cis*-dinitrosyl complex.¹⁰ The solvent was removed in vacuo, the residue was extracted into CH_2Cl_2 (2 x 15 mL), the combined extracts were filtered through Florisil, and the Florisil plug was washed with an additional 45 mL of CH_2Cl_2 . The filtrate was stripped to dryness, and the residue was extracted with Et_2O (2 x 15 mL), leaving an insoluble green powder that was recrystallized to yield $[\text{CpCrCl}_2]_2$ (25 mg, 13% yield).¹¹ The Et_2O extracts were combined and taken to dryness, and the resulting yellow powder was dissolved in Et_2O (15 mL) and transferred to a hexanes-packed column of Florisil (2 x 8 cm). Elution of the column with Et_2O led to the development and collection of two bands, the first orange-yellow and the second yellow-gold. The first was stripped to yield bright orange Cp_2Fe (35 mg, 37% yield). The second was stripped to yield $\text{CpCr}(\text{NO})_2\text{Cl}$ (52 mg, 25% yield).

$[\text{CpCrCl}_2]_2$: IR (Nujol): 840 cm^{-1} , no nitrosyl bands; MS (*m/z*, probe temp. 150°C): 374 376 378 (P^+), 339 341 344 (P^+-Cl)

Cp_2Fe : EI-MS (probe temp. 190°C): *m/z* 186 (P^+); ^1H NMR: δ 4.10 (s)

$\text{CpCr}(\text{NO})_2\text{Cl}$: IR (Nujol): 1706, 1814 cm^{-1} ; EI-MS (probe temp. 150°C): *m/z* 212 (P^+), 182 (P^+-NO), 152 (P^+-2NO); ^1H NMR: δ 4.70 (s)

4.2.17 Reaction of Dichloride Salt $\text{Et}_4\text{N}^+[\text{4.4}]^-$ with NO

$\text{Et}_4\text{N}^+[\text{4.4}]^-$ (174 mg, 0.500 mmol) was suspended in THF (15 mL), and nitric oxide was bubbled slowly through the solution for a total of 30 min. The dark brown-gold solution was taken to dryness, the residue was extracted with CH_2Cl_2 (2 x 20 mL), and the extracts were filtered through neutral alumina I (2 x 3 cm). The filtrate was reduced to dryness to yield 43 mg (40% yield) of a gold powder identified as $\text{CpCr}(\text{NO})_2\text{Cl}$ by its characteristic mass, infrared, and NMR spectra (*vide supra*).

4.2.18 Reaction of $\text{CpCr}(\text{NO})_2\text{Cl}$ with $\text{NaO-}i\text{-Pr}$

Sodium beads (~100 mg) were dissolved in freeze-pump-thaw-degassed isopropanol (15 mL). $\text{CpCr}(\text{NO})_2\text{Cl}$ (313 mg, 1.50 mmol) was dissolved in this solution, and the mixture was heated at 75 °C for 2 h. The brown solution was taken to dryness, the brown residue was extracted with 1:1 $\text{CH}_2\text{Cl}_2/\text{Et}_2\text{O}$ (3 x 20 mL), and the combined extracts were filtered through basic alumina I (2 x 3 cm) to yield a yellow filtrate. This solution reduced to a brown powder, which was recrystallized from hexanes to yield red-brown crystals of $[\text{CpCr}(\text{NO})(\text{O-}i\text{-Pr})]_2$ (36 mg, 12% yield).

$^1\text{H NMR}$: δ 1.71 (s, 6H, $\text{CH}(\text{CH}_3)_2$), 4.25 (br s, 1H, CHMe_2), 5.98 (br s, 5H, Cp); EI-MS (probe temp. 150°C: m/z 412 (P^+), 382 (P^+-NO), 352 (P^+-2NO); IR (Nujol): ν_{NO} 1632, 1640 cm^{-1}

4.3 Characterization Data

Table 4.1. Numbering Scheme, Color, Yield and Elemental Analysis Data

complex	compd no.	color (yield, %)	elemental analysis found (calcd)		
			C	H	N
$n\text{-Bu}_4\text{N}^+[\text{CpCr}(\text{NO})\text{I}_2]^-$	$n\text{-Bu}_4\text{N}^+[\mathbf{4.1}]^-$	red-brown (90)	39.35 (39.20)	6.47 (6.42)	4.23 (4.35)
$n\text{-Bu}_4\text{N}^+[\text{CpCr}(\text{NO})(\text{OTf})_2]^-$	$n\text{-Bu}_4\text{N}^+[\mathbf{4.2}]^-$	brown (85)	40.30 (40.17)	6.05 (6.01)	4.03 (4.07)
$n\text{-Bu}_4\text{N}^+[\text{CpCr}(\text{NO})\text{Br}_2]^-$	$n\text{-Bu}_4\text{N}^+[\mathbf{4.3}]^-$	black (62)	45.91 (45.91)	7.67 (7.52)	5.00 (5.10)
$\text{Et}_4\text{N}^+[\text{CpCr}(\text{NO})\text{Cl}_2]^-$	$\text{Et}_4\text{N}^+[\mathbf{4.4}]^-$	black (53)	44.86 (44.84)	7.33 (7.24)	8.04 (8.04)

Table 4.2. Mass Spectral, Infrared, and ESR Data

complex	FAB-MS (m/z)		IR (cm^{-1})		ESR ^c	
	(+)	(-)	ν_{NO} (Nujol)	ν_{NO} (CH_2Cl_2)	g-value	coupling (G)
$n\text{-Bu}_4\text{N}^+[\mathbf{4.1}]^-$	242 [P ⁺]	401 [P ⁻]	1637	1644	2.051	-
$n\text{-Bu}_4\text{N}^+[\mathbf{4.2}]^-$	242 [P ⁺]	445 [P ⁻]	1697	1690	1.978	$A_{\text{N}} = 5.1$ $A_{\text{Cr}} = 21.3$
$n\text{-Bu}_4\text{N}^+[\mathbf{4.3}]^-$	242 [P ⁺]	305 307 309 [P ⁻] ^a	1641	-	2.011	$A_{\text{N}} = 5.7$ $A_{\text{Cr}} = 18.6$
$\text{Et}_4\text{N}^+[\mathbf{4.4}]^-$	130 [P ⁺]	217 219 [P ⁻] ^b	1626	1641	1.986	$A_{\text{N}} = 5.4$ $A_{\text{Cr}} = 20.3$

^a This envelope of peaks is a 1:2:1 isotopic cluster as expected for a mixture of ⁷⁹Br and ⁸¹Br isotopomers, the ⁷⁹Br/⁸¹Br form being most abundant.

^b This envelope of peaks is a 3:2 isotopic cluster as expected for a mixture of ³⁵Cl and ³⁷Cl isotopomers, the ³⁵Cl/³⁵Cl form being most abundant.

^c All ESR spectra are of CH_2Cl_2 solutions.

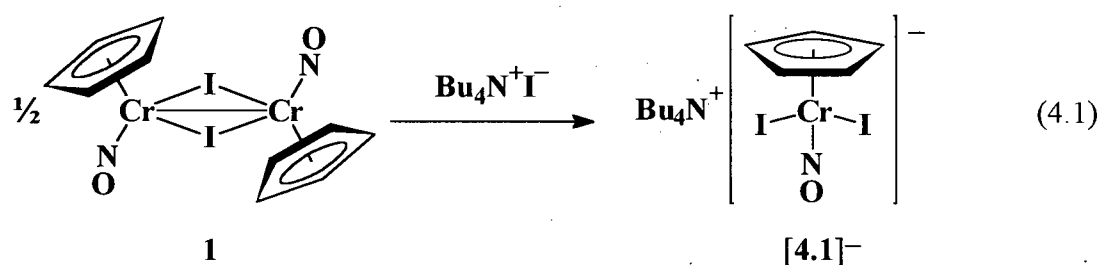
4.4 Results and Discussion

4.4.1 Preparation of Anionic Complexes $[\text{CpCr}(\text{NO})\text{X}_2]^-$ ($\text{X} = \text{I}, \text{OTf}, \text{Br}, \text{Cl}$)

4.4.1.1 Complexes $[\mathbf{4.1}]^-$ ($\text{X} = \text{I}$), $[\mathbf{4.2}]^-$ ($\text{X} = \text{OTf}$), and $[\mathbf{4.3}]^-$ ($\text{X} = \text{Br}$)

The reaction of complex **1**, $[\text{CpCr}(\text{NO})\text{I}]_2$, with an excess of elemental iodine does not result in the incorporation of a second iodide ligand into the chromium complex, which would yield the neutral 16e species $\text{CpCr}(\text{NO})\text{I}_2$. Such a reaction would be analogous that of the congeneric molybdenum and tungsten complexes (Scheme 1.1),^{12,13} and the seemingly anomalous formation of **1** represents the source of the dichotomy in this system between chromium compounds and those of the heavier metals.

Instead, the only isolable nitrosyl species from the reaction with further I_2 is $\text{CpCr}(\text{NO})_2\text{I}$, the same product as obtained by the thermal decomposition of **1**, though reaction with I_2 proceeds at a much greater rate.⁵ However, reaction of **1** with an equivalent of *iodide* effects cleavage of the dimer in a manner equivalent to that of other Lewis bases. Because iodide is an anionic Lewis base, the product is also an anion, namely $[\text{CpCr}(\text{NO})\text{I}_2]^-$ ($[\mathbf{4.1}]^-$), as shown in eq 4.1.



This reaction is extremely straightforward and high-yielding, comparable to the preparation of complex **1** itself. Treatment of **1** with stoichiometric $n\text{-Bu}_4\text{NI}$ in CH_2Cl_2 results in a color change from brown to red-brown, and a complete replacement of the starting nitrosyl band (1673 cm^{-1}) with that of the new material (1644 cm^{-1}). The shift of the nitrosyl band to lower wavenumbers suggests that the terminal iodide ligand in $[\mathbf{4.1}]^-$ is a considerably better

donor of electron density toward chromium than is the bridging iodide ligand in **1**, as would be expected.

The synthesis of anion $[4.1]^-$ suggests that a range of $[\text{CpCr}(\text{NO})\text{X}_2]^-$ complexes ($\text{X} =$ halide or pseudohalide) should also be stable species. However, attempts to metathesize the iodide ligands in $[4.1]^-$ for other halides in order to obtain directly dibromide $[4.3]^-$ and dichloride $[4.4]^-$ do not meet with success. This is due to the lability of the dihalide species, which results in a scrambling of the halide ligands. For instance, reaction of either **1** or $n\text{-Bu}_4\text{N}^+[4.1]^-$ with a source of Cl^- results in a mixture of species in solution as judged by ESR spectroscopy; such a reaction mixture exhibits an ESR spectrum with three signals, one broad singlet attributable to diiodide $[4.1]^-$, one resolved triplet attributable to dichloride $[4.3]^-$, and a third at an intermediate g -value with unresolved coupling presumably due to $[\text{CpCr}(\text{NO})(\text{I})(\text{Cl})]^-$. The isolation of any one ionic species from such a solution is problematic, and so although other anionic complexes may be generated in this manner, it is not the method of choice for their preparation and isolation.

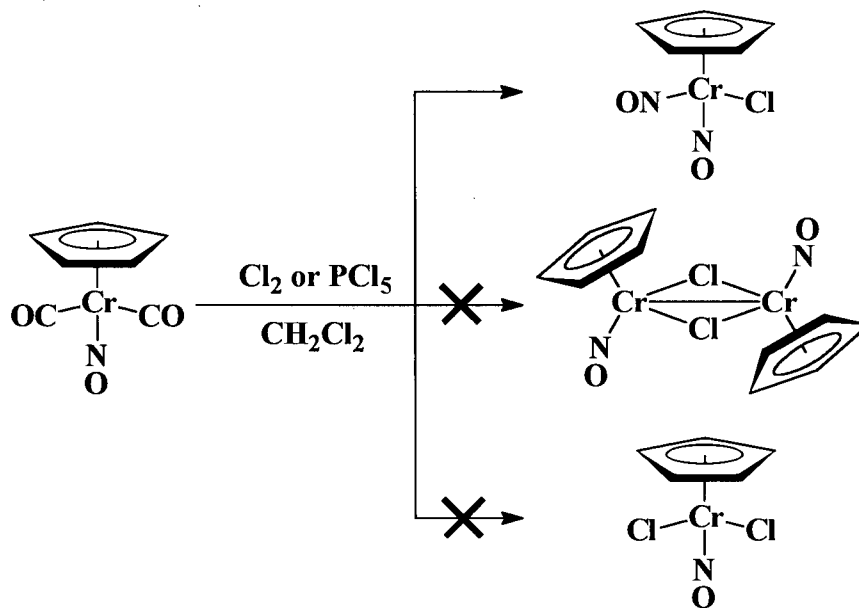
In the preparation of $n\text{-Bu}_4\text{N}^+[4.1]^-$, such ligand scrambling is not a matter for concern. The transformation of a single neutral complex to a single ionic salt ensures that one may be easily separated from the other should the reaction not proceed to completion: To isolate a complex salt when the reactants are also salts requires that the desired complex be appreciably more or less soluble than all other ionic byproducts. One solution to this problem would be to generate complexes $[4.3]^-$ and $[4.4]^-$ in a manner analogous to that of $[4.1]^-$ by using the appropriate $[\text{CpCr}(\text{NO})\text{X}]_2$ ($\text{X} = \text{Cl}, \text{Br}$) as a starting material. Unfortunately, a high-yielding route to these species did not exist at the time this work was begun since treatment of $\text{CpCr}(\text{NO})(\text{CO})_2$ with either Cl_2 ¹⁴ or Br_2 ⁵ results in $\text{CpCr}(\text{NO})_2\text{X}$ as the only isolable nitrosyl-containing complexes.

The preferred route to metathesis of the iodide ligands of $[4.1]^-$ is one which results in an insoluble ionic byproduct. Reaction of $n\text{-Bu}_4\text{N}^+[4.1]^-$ with two equivalents of AgOTf results in the immediate formation of AgI , which is completely insoluble in CH_2Cl_2 . A simple workup then affords $n\text{-Bu}_4\text{N}^+[\text{CpCr}(\text{NO})(\text{OTf})_2]^-$ ($n\text{-Bu}_4\text{N}^+[4.2]^-$) in high yield (eq 4.2).

analytically pure form. Unlike those of the dibromide salt, the solubility properties of $n\text{-Bu}_4\text{N}^+[\mathbf{4.4}]^-$ are too similar to those of the inorganic ionic byproducts, and the complete separation of these species proved to be exceedingly difficult. Thus, another route to a salt of dichloride anion $[\mathbf{4.4}]^-$ was required, and the ideal reaction would be analogous to the preparation of diiodide $n\text{-Bu}_4\text{N}^+[\mathbf{4.1}]^-$, by employing $[\text{CpCr}(\text{NO})\text{Cl}]_2$ as the starting chromium complex.

4.4.1.2 Improved Synthesis of $[\text{CpCr}(\text{NO})\text{Cl}]_2$

The reaction of $\text{CpCr}(\text{NO})(\text{CO})_2$ with either Cl_2 or an equivalent halogenating reagent such as PCl_5 may be effected in CH_2Cl_2 , by analogy to the reaction of $\text{CpCr}(\text{NO})(\text{CO})_2$ with I_2 or of $\text{CpM}(\text{NO})(\text{CO})_2$ ($\text{M} = \text{Mo}, \text{W}$) with PCl_5 . This reaction results in the rapid formation of the dinitrosyl complex $\text{CpCr}(\text{NO})_2\text{Cl}$, as shown in Scheme 4.1.¹⁴ Neither the bridging-halide dimer $[\text{CpCr}(\text{NO})\text{Cl}]_2$, the chloro analogue of $\mathbf{1}$,⁵ nor the 16e dichloride $\text{CpCr}(\text{NO})\text{Cl}_2$, the chromium congener of known molybdenum and tungsten species,¹⁵ is observed in this reaction.

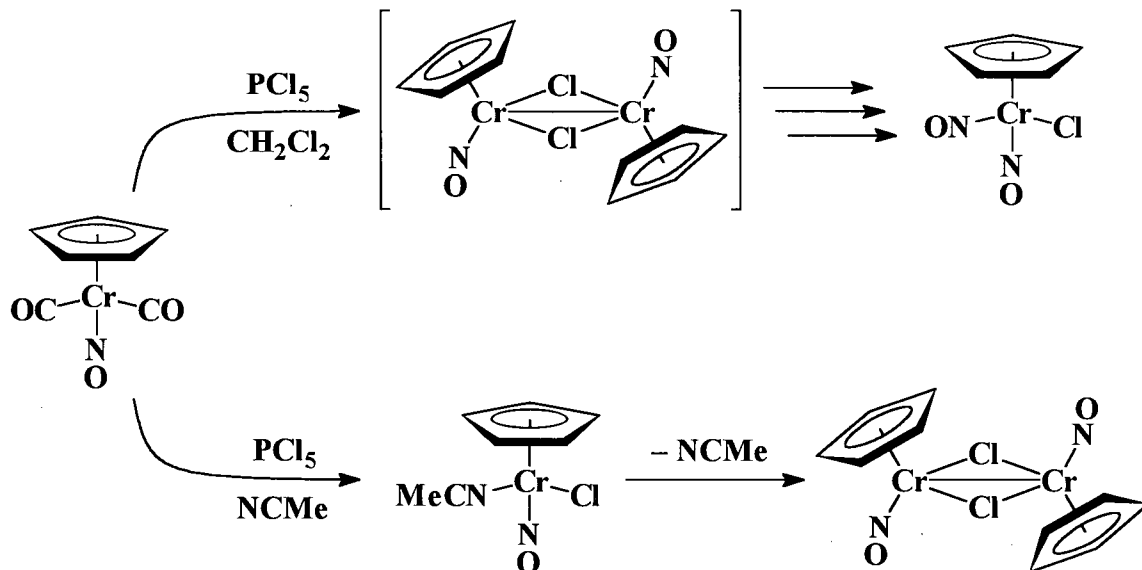


Scheme 4.1. Reaction of $\text{CpCr}(\text{NO})(\text{CO})_2$ with chloride reagents.

The formation of a dinitrosyl complex must involve the inter-metal transfer of a nitrosyl ligand; $\text{CpCr}(\text{NO})_2\text{Cl}$ can therefore represent, at best, only 50% of the chromium atoms available,

and would seem to result from a disproportionation reaction. Although the bridging-chloride dimer $[\text{CpCr}(\text{NO})\text{Cl}]_2$ is neither the product nor an observed intermediate, it is a known, stable complex.¹⁴ However, the original preparation involves reaction of HCl with $[\text{CpCr}(\text{NO})(\text{OEt})]_2$, itself prepared in low yields from $\text{CpCr}(\text{NO})_2\text{Cl}$ ¹⁴ or complex 1.⁵ This is not a viable route for further preparative chemistry.

The transformation of $\text{CpCr}(\text{NO})(\text{CO})_2$ to $\text{CpCr}(\text{NO})_2\text{Cl}$ in CH_2Cl_2 is complete within seconds at ambient temperature. Although the bridging-chloride dimer $[\text{CpCr}(\text{NO})\text{Cl}]_2$ is not the final product under these conditions, it appears to be an intermediate, and by varying the reaction conditions only slightly the chloride dimer can be sufficiently stabilized that it becomes the isolated product. For instance, performing the same reaction in acetonitrile prevents the complete decomposition of $[\text{CpCr}(\text{NO})\text{Cl}]_2$, though a small amount of the dinitrosyl product is still formed. Even this small amount of decomposition can be lessened if the reaction is performed at low temperature. The solvent dependence of this reactivity is summarized in Scheme 4.2.



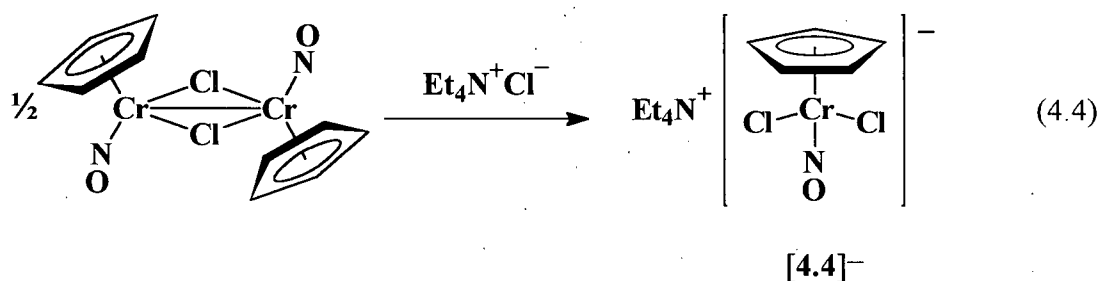
Scheme 4.2. Reactions of $\text{CpCr}(\text{NO})(\text{CO})_2$ with PCl_5 in CH_2Cl_2 and MeCN .

Though $[\text{CpCr}(\text{NO})\text{Cl}]_2$ from such a reaction mixture, isolated as a bright green powder, exhibits the expected spectroscopic properties,¹⁴ the IR spectra of these samples still indicate

contamination with a very small amount (< 2%) of $\text{CpCr}(\text{NO})_2\text{Cl}$. The dinitrosyl contaminant may be removed by washing with Et_2O and recrystallization of the $[\text{CpCr}(\text{NO})\text{Cl}]_2$ by slow evaporation of a toluene solution. However, this substantially reduces the isolated yield of the chloride-bridged dimer. If the presence of a small amount of $\text{CpCr}(\text{NO})_2\text{Cl}$ does not adversely affect a subsequent reaction or workup it is more efficient to use the crude powder. It should be noted that $[\text{CpCr}(\text{NO})\text{Cl}]_2$ is not as thermally robust as its iodide analogue, **1**.

4.4.1.3 $[\text{CpCr}(\text{NO})(\text{Cl})_2]^-$ [**4.4**]⁻

With a reliable preparative route to $[\text{CpCr}(\text{NO})\text{Cl}]_2$ in hand, the synthesis of a dichloride anion salt is trivial. Preparation of a sample of $[\text{CpCr}(\text{NO})\text{Cl}]_2$ as outlined above, followed by reaction with Et_4NCl in toluene, affords $\text{Et}_4\text{N}^+[\text{CpCr}(\text{NO})\text{Cl}_2]^-$ ($\text{Et}_4\text{N}^+[\text{4.4}]^-$) in reasonable yield (50 - 55%) from $\text{CpCr}(\text{NO})(\text{CO})_2$ (eq 4.4). As noted, it is actually more efficient to prepare a crude sample of $[\text{CpCr}(\text{NO})\text{Cl}]_2$ and carry on directly with halide addition. The facile cleavage of the bridging-chloride dimer with further chloride yields a relatively insoluble ionic salt, so recrystallization of this species to yield $\text{Et}_4\text{N}^+[\text{4.4}]^-$ is not hindered by any contaminating $\text{CpCr}(\text{NO})_2\text{Cl}$ which might be present.



4.4.2 Physical and Spectroscopic Properties of Anions [**4.1**]⁻ to [**4.4**]⁻

Like the cations prepared in Chapter 2, complexes [**4.1**]⁻ to [**4.4**]⁻ are monomeric 17e organometallic ions, each with two covalently bound halide or pseudohalide ligands. As anions, the species are isolated as complex salts containing an inorganic counterion, which are essentially insoluble in Et_2O or aliphatic solvents but soluble in CH_2Cl_2 or THF. Although the diiodide and bis(triflate) salts $n\text{-Bu}_4\text{N}^+[\text{4.1}]^-$ and $n\text{-Bu}_4\text{N}^+[\text{4.2}]^-$ were only isolated as powders, the dibromide

and dichloride salts $n\text{-Bu}_4\text{N}^+[\mathbf{4.3}]^-$ and $\text{Et}_4\text{N}^+[\mathbf{4.4}]^-$ both formed a well-defined, crystalline material.

These anions are generally more air-sensitive than are their cationic $[\text{CpCr}(\text{NO})\text{L}_2]^+$ counterparts described in Chapter 2, both as solids and in solution. The diiodide salt $n\text{-Bu}_4\text{N}^+[\mathbf{4.1}]^-$ may be handled in air as a solid for short periods of time, its robust nature being very reminiscent of the precursor dimer **1**. However, the other salts are quite air-sensitive as solids, so that bis(triflate) $n\text{-Bu}_4\text{N}^+[\mathbf{4.2}]^-$ and dibromide $n\text{-Bu}_4\text{N}^+[\mathbf{4.3}]^-$ both decompose in the atmosphere within minutes to yield viscous oils. Solutions of all these anionic species are also air-sensitive; IR spectra of air-exposed solutions show features consistent with the formation of dinitrosyl complexes. As solids, the salts may be stored at ambient temperature under an inert-atmosphere without noticeable decomposition, apparently indefinitely. This thermal stability differs from that of the molybdenum congeners, which tend to decompose under nitrogen if warmed above 0 °C.²

The mass spectra of these salts are consistent with their formulation as containing monomeric organometallic anions, and as in Chapter 2, the FAB mass spectra of these species are very useful in assigning their molecular structures. The mass spectra of each of the salts exhibit a discrete peak due to the expected parent ions, for both the cation and the anion in each salt. In the case of the anion spectra of dibromide $[\mathbf{4.3}]^-$ and dichloride $[\mathbf{4.4}]^-$ additional information may be gleaned from the isotope patterns in each cluster of peaks. For instance, in the anionic FAB spectrum of $n\text{-Bu}_4\text{N}^+[\mathbf{4.3}]^-$, the parent anion signal is actually three peaks in a 1:2:1 ratio, with the central peak at a m/z value of 307 as depicted in Figure 4.1. This value corresponds to the expected mass for a $[\text{CpCr}(\text{NO})\text{Br}_2]^-$ anion containing one ^{79}Br atom and one ^{81}Br atom, and the 1:2:1 ratio of peak intensities is exactly as expected for a complex containing two bromine atoms, given the nearly equal relative abundances of the two naturally occurring isotopes. Similarly, a species with two chlorine atoms is expected to yield a cluster of peaks in approximately a 9:6:1 ratio, each peak

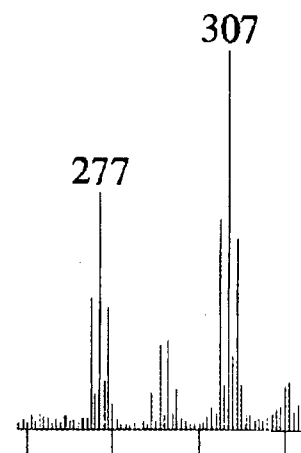


Figure 4.1. Portion of the anionic FAB-MS of $n\text{-Bu}_4\text{N}^+[\mathbf{4.3}]^-$

separated by two mass units. The anion FAB mass spectrum of the $[\text{CpCr}(\text{NO})\text{Cl}_2]^-$ displays a parent anion cluster at $m/z = 217$ and 219 in a ratio of 3:2, with the least intense peak being unresolved.

Also consistent with the assignment of anions $[\mathbf{4.1}]^-$ to $[\mathbf{4.4}]^-$ as monomeric species are the infrared spectra of these complexes. Each exhibits a single strong nitrosyl-stretching frequency in the range expected for a linear nitrosyl. In Nujol mull spectra, these nitrosyl bands are all between 1626 and 1641 cm^{-1} for the dihalide anions. These values are lower than those exhibited by complex **1** or by any of the 17e cationic or neutral species described in Chapter 2, suggesting the presence of a much greater electron density at the metal in the anions weakening the N-O bond via back-bonding to the nitrosyl. This greater electron density is entirely reasonable given the anionic nature of these complexes. Notably, the nitrosyl band of the triflate complex $n\text{-Bu}_4\text{N}^+[\mathbf{4.2}]^-$ occurs at 1697 cm^{-1} as a Nujol mull, a value higher in energy than the other anions. This is a testament to the far greater electron-withdrawing ability of the triflate ligand as compared to the halides.

In the case of $n\text{-Bu}_4\text{N}^+[\mathbf{4.2}]^-$, there is a matter of concern with regard to the nature of the triflate ligands. By analogy to the dihalide anions, the molecular structure of the anion is assigned as $[\text{CpCr}(\text{NO})(\text{OTf})_2]^-$ with two covalently bound triflate ligands. In addition to the parent mass peak at $m/z = 445$ observed in the anionic FAB-MS, the infrared spectrum gives further evidence for this assignment. The nature of a triflate group, whether ionic or covalent, has often been assigned on the basis of infrared data, though the reliability of this method is the cause for some concern.¹⁶ A general rule of thumb is that the highest-energy S-O stretching frequency of an uncoordinated CF_3SO_3^- anion will occur at approximately 1280 cm^{-1} , while that of a triflate group covalently bound to a metal center through one of the oxygen atoms will occur at a frequency up to 100 cm^{-1} higher. A more precise method relies on the distortion of symmetry which occurs when a triflate anion binds to metal. In the free triflate anion all the S-O bonds are equivalent, and the species is of approximate C_{3v} symmetry. If one oxygen atom binds to a metal, the symmetry reduces to C_s , and the number of S-O stretching modes will increase from two to three as a result. Unfortunately, the assignment of these bands is greatly complicated by the

presence of the CF_3 group, because there is usually a mixing of the C-F and S-O stretching modes. Nevertheless, the infrared spectrum of $n\text{-Bu}_4\text{N}^+[\mathbf{4.2}]^-$ in Nujol exhibits no less than nine strong bands in the region $1000 - 1350 \text{ cm}^{-1}$, indicative of the loss of symmetry associated with covalently bound triflate ligands.

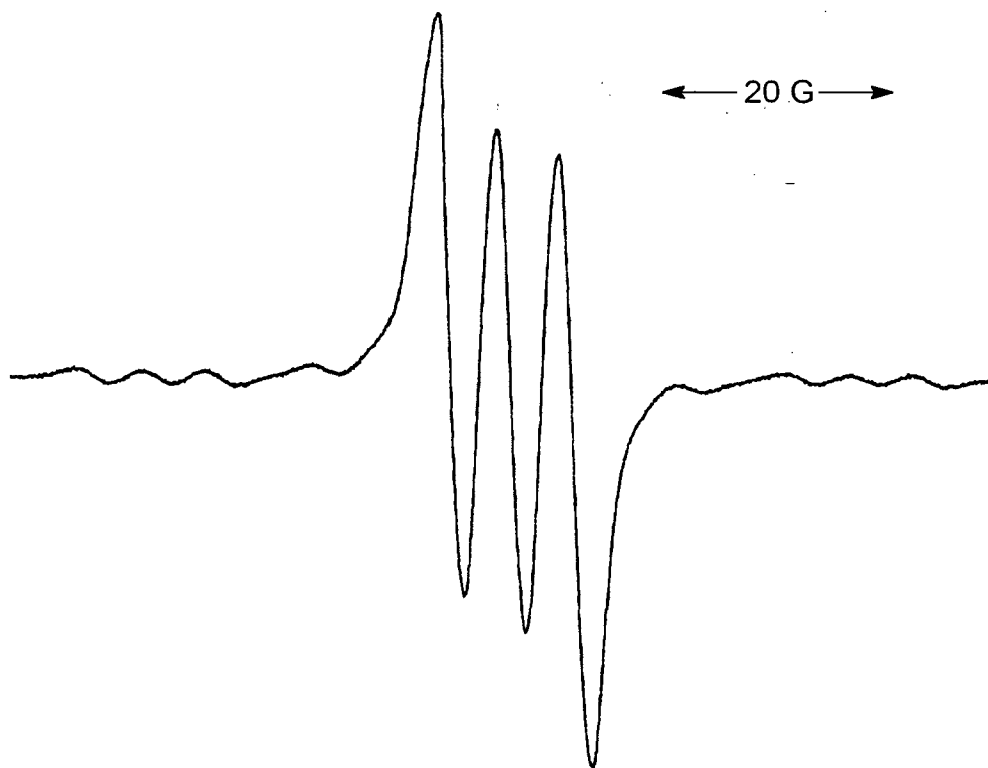


Figure 4.2. ESR spectrum of $\text{Et}_4\text{N}^+[\text{CpCr}(\text{NO})\text{Cl}_2]^-$ ($\text{Et}_4\text{N}^+[\mathbf{4.4}]^-$) in CH_2Cl_2

As expected for monomeric 17e complexes, each of the anions $[\mathbf{4.1}]^-$ to $[\mathbf{4.4}]^-$ exhibits a room-temperature ESR spectrum. These spectra are generally more revealing than those of complexes discussed in Chapter 2, in that the linewidths are much narrower and there is more resolved coupling, though the spectrum of the diiodide species is an exception in that it remains broad and featureless. The spectrum of dichloride salt $\text{Et}_4\text{N}^+[\mathbf{4.4}]^-$ in CH_2Cl_2 is typical, and is displayed in Figure 4.2. The signal is a 1:1:1 triplet due to coupling of the unpaired spin to the nitrosyl nitrogen atom, and further splitting due to coupling to the 9.55% abundant ^{53}Cr nucleus ($I = 3/2$) is apparent from the much weaker triplet patterns to either side of the main signal. The

same features are apparent in the spectra of bis(triflate) $n\text{-Bu}_4\text{N}^+[\mathbf{4.2}]^-$ and dibromide $n\text{-Bu}_4\text{N}^+[\mathbf{4.3}]^-$, with coupling constants for these three complexes being in a range of 5-6 G for the nitrogen interaction and 18-22 G for the chromium coupling.

There is a distinct increase in the g -values exhibited by the dihalide anions as the halide ligand is changed from Cl to Br to I, increasing from 1.986 to 2.011 to 2.051. This is exactly the same trend as observed for the analogous molybdenum anions, for which the g -values increase from 1.982 to 2.010 to 2.060.² The trend is also mirrored in complexes of the type $\text{CpMoX}_2(\text{PMe}_3)_2$ ¹⁷ and $\text{CpMoX}_2(\text{dppe})$ ¹⁸ ($X = \text{Cl}, \text{Br}, \text{I}$), and in the latter cases the diiodide compounds also exhibit much broader ESR signals than the other species, just as for the $[\text{CpCr}(\text{NO})\text{X}_2]^-$ complexes. These effects are likely due to a combination of a varying degree of ligand-atomic-orbital character in the SOMO, and a trend in halide-orbital contribution to the moment of the electron spin.

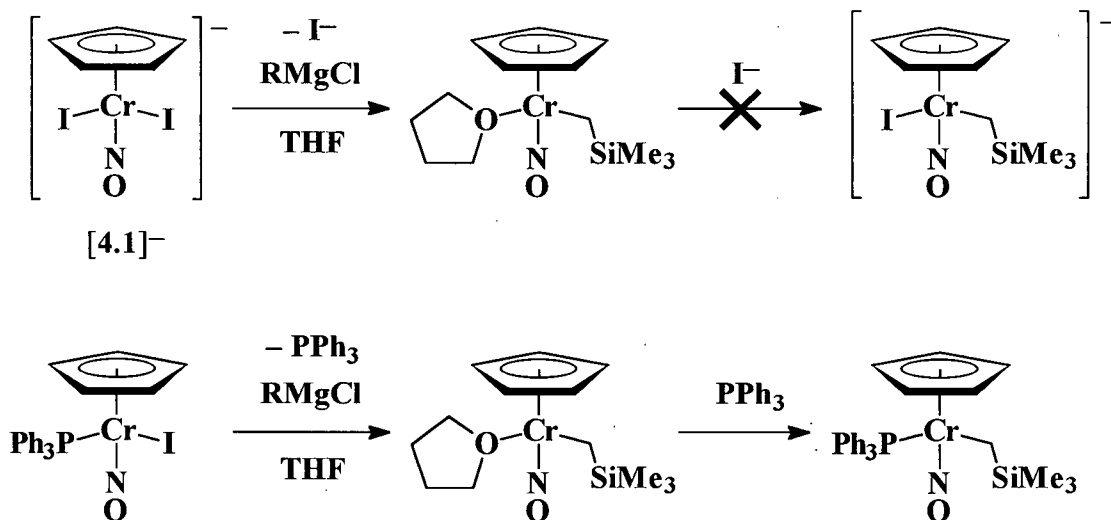
4.4.3 Reactivity of Dihalide Anions $[\mathbf{4.1}]^-$ and $[\mathbf{4.4}]^-$

It is apparent from synthetic studies that the 17e $[\text{CpCr}(\text{NO})\text{X}_2]^-$ are more substitutionally labile than 17e $[\text{CpCr}(\text{NO})\text{L}_2]^+$ cations. This is not unexpected, since the dissociation of a halide from an anionic complex should be facile. Therefore, an obvious route of investigation is to effect metathesis of these labile halide groups for other ligands, such as alkyl, amide, or alkoxide substituents. Another possible mode of reactivity is that the organometallic anion might itself be capable of acting as a nucleophile.

4.4.3.1 Reaction with Nucleophiles

Dihalide anions $[\mathbf{4.1}]^-$ and $[\mathbf{4.4}]^-$ are prone toward attack by nucleophiles. In general, replacement of one halide ligand appears to result in the loss of the second, and the formation of either a solvated monomer or a ligand-bridged dimer as the product. The second halide ligand is not metathesized even when two or more equivalents of a nucleophilic reagent are employed. Thus, reaction of $n\text{-Bu}_4\text{N}^+[\mathbf{4.1}]^-$ with an excess of $\text{Me}_3\text{SiCH}_2\text{MgCl}$ in THF generates the alkyl solvato complex $\text{CpCr}(\text{NO})(\text{THF})(\text{CH}_2\text{SiMe}_3)$. The same product is obtained from reaction of

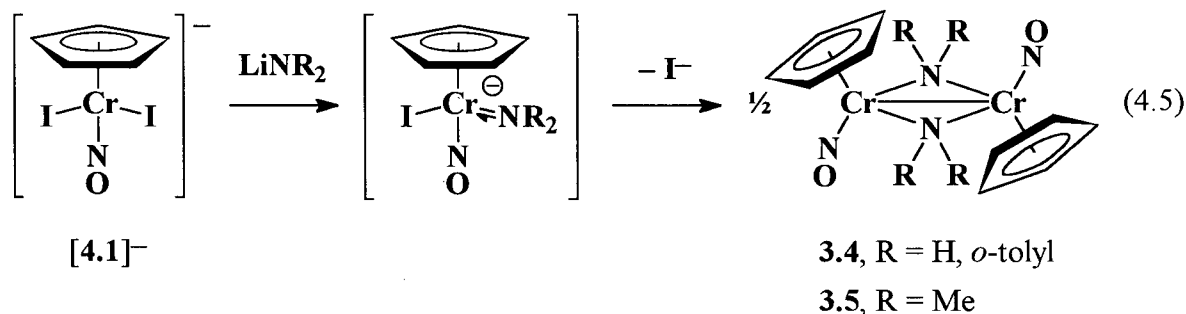
iodo dimer **1** with the Grignard reagent, and it is an intermediate in the alkylation of $\text{CpCr}(\text{NO})(\text{PPh}_3)\text{I}$.⁹ It is likely that the reaction of $n\text{-Bu}_4\text{N}^+[\mathbf{4.1}]^-$ proceeds via the same general mechanism as the latter alkylation process, in which the first step involves loss of PPh_3 as a prelude to alkyl-for-iodide metathesis. If the reaction of $[\mathbf{4.1}]^-$ follows the same path, then one I^- ligand will be replaced by THF before metathesis of the second iodide takes place, thereby generating the observed $\text{CpCr}(\text{NO})(\text{THF})(\text{CH}_2\text{SiMe}_3)$ species. The difference between the two reactions is that unlike PPh_3 , free iodide does not appear to reenter the coordination sphere of the solvated alkyl complex (Scheme 4.3).



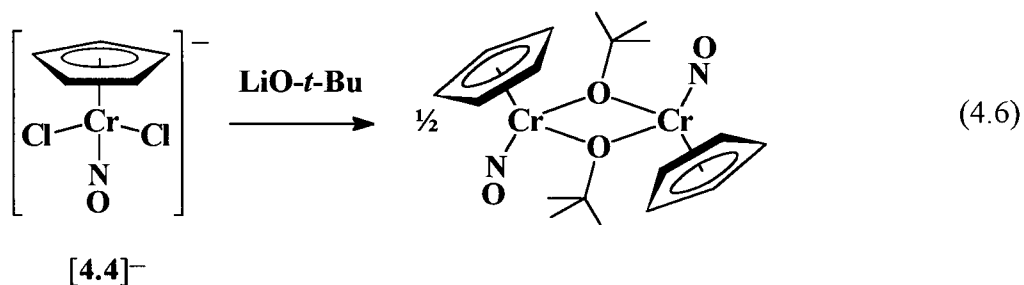
Scheme 4.3. Comparison of reactions of $n\text{-Bu}_4\text{N}^+[\mathbf{4.1}]^-$ and $\text{CpCr}(\text{NO})(\text{PPh}_3)\text{I}$ with $\text{Me}_3\text{SiCH}_2\text{MgCl}$

Reaction of $n\text{-Bu}_4\text{N}^+[\mathbf{4.1}]^-$ with amide reagents also leads to metathesis of one halide ligand and loss of the second. Thus, treatment of $n\text{-Bu}_4\text{N}^+[\mathbf{4.1}]^-$ with two equivalents of either *o*-tolNHLi or Me_2NLi causes a rapid reaction yielding the corresponding bridging-amide dimers **3.4** and **3.5** (eq 4.5). These reactions are reminiscent of that described in Scheme 3.4, where formation of an amide moiety also results in the loss of a σ -basic ligand and formation of the dimeric species. The presumed intermediate species in eq 4.5, $[\text{CpCr}(\text{NO})(\text{I})(\text{NR}_2)]^-$, would be subject to the same π -conflict as described in Section 3.4.1 by virtue of the π -donor amide group,

and the same argument as to the mechanism of dimer formation is applicable. Of the two possible pathways, intramolecular π -donation and *dissociative* loss of I^- versus intermolecular nucleophilic attack and *associative* loss of I^- , the former is more likely in this case. The negative charge on the intermediate would both favor dissociation of iodide and disfavor the bimolecular process.



Similarly, reaction of the dichloride salt $\text{Et}_4\text{N}^+[\text{4.4}]^-$ with two equivalents of $\text{LiO-}t\text{-Bu}$ effects the metathesis of one halide ligand for an alkoxide and to cause the loss of the second. In this case the isolated complex is the bridging-alkoxide dimer, analogous to the bridging-amide complexes isolated above, and presumably it is formed by a similar mechanism (eq 4.6). This species exhibits color, solubility, and spectroscopic properties similar to those of the related compounds $[\text{CpCr}(\text{NO})(\text{OMe})]_2^5$ and $[\text{CpCr}(\text{NO})(\text{OEt})]_2^{14}$



4.4.3.2 Reaction with Electrophiles

A possible reaction of an organometallic anion is to act as a metal-based nucleophile, for instance reacting with a source of Me^+ to form a new metal-carbon bond. When either diiodide salt $n\text{-Bu}_4\text{N}^+[\text{4.1}]^-$ or dichloride salt $\text{Et}_4\text{N}^+[\text{4.4}]^-$ is reacted with iodomethane, the reagent

appears to function as a source of I^- rather than Me^+ . Thus, there is no apparent net change to a solution of MeI and $n-Bu_4N^+[4.1]^-$, since a substitution of halide ligands results in the same complex. On the other hand, treatment of dichloride salt $Et_4N^+[4.4]^-$ with MeI yields a solution exhibiting the same ESR spectra as that when the diiodide anion is reacted with ionic chloride (vide supra), displaying three signals due to $[4.4]^-$, $[4.1]^-$, and the presumed mixed-halide complex $[CpCr(NO)(I)(Cl)]^-$.

Another source of Me^+ , one which cannot function as a halide source, is trimethyloxonium ion. When $n-Bu_4N^+[4.1]^-$ is reacted with $[Me_3O]^+[BF_4]^-$ in CH_2Cl_2 , a reaction occurs at low temperature which results in the loss of the nitrosyl band of the starting material from the IR spectrum of the reaction mixture and the concomitant appearance of the nitrosyl band of iodide dimer **1**, which may be isolated from the reaction mixture in reasonably high (79%) yield. Thus, it appears that Me^+ does indeed react as an electrophile toward anion $[4.1]^-$, but of attacking at the metal center, it simply abstracts an iodide ligand, leaving the unsaturated $CpCr(NO)I$ fragment to associate and form dimeric complex **1**. Thus, while nucleophilic attack at the dihalide anions results in loss of ionic halide from the metal and dimerization of the neutral unsaturated fragment, electrophilic attack results in the abstraction of the halide, and a similar dimerization. These facts are consistent with most of the negative charge in these species being delocalized onto the halide ligands, thereby rendering loss of an anionic halide from the anionic complex a facile process and the dominant reactivity of these species.

4.4.4 Redox Chemistry of Dihalide Anions

4.4.4.1 Cyclic Voltammetry

The investigation of the redox behavior of the 17e cations in Chapter 2, in particular the examination of their reduction chemistry, yielded valuable information regarding the relationship between the $\{Cr(NO)\}^5$ and $\{Cr(NO)\}^6$ electronic manifolds. It was hoped that examining the oxidation behavior of the 17e anions might establish a similar link between the $\{Cr(NO)\}^5$ and $\{Cr(NO)\}^4$ manifolds and perhaps provide some insight into the differences between these

chromium species and the known molybdenum and tungsten $\{M(NO)\}_5^5$ and $\{M(NO)\}_4^4$ dihalide complexes.

The cyclic voltammogram of diiodide salt $n\text{-Bu}_4\text{N}^+[\mathbf{4.1}]^-$ scanned at 0.4 V/s exhibits an irreversible oxidation feature in THF at $E_{p,a} = 0.53$ V. This contrasts dramatically with the electrochemical behavior of the cations considered in Chapters 2 and 3 (Section 3.4.2), since the cationic $\{\text{Cr}(\text{NO})\}_5^5$ species exhibit no oxidation features out to the solvent limit. As expected, the greater electron density present in the anionic species renders oxidation a more facile process.

The dichloride salt $\text{Et}_4\text{N}^+[\mathbf{4.4}]^-$ also displays an irreversible oxidation feature under the same conditions at a slightly higher voltage, with $E_{p,a} = 0.60$ V. If the solvent is changed to CH_2Cl_2 , which allows wider oxidation window, more features are revealed. An oxidative scan of $\text{Et}_4\text{N}^+[\mathbf{4.4}]^-$ in CH_2Cl_2 at 0.1 V/s reveals three oxidation waves at $E_{p,a} = 0.56, 1.15,$ and 1.74 V. All three oxidations are irreversible at this slow scan rate. As the speed of the scan is increased, the first feature remains completely irreversible, and the intensity of this current increases linearly with the square root of the scan rate, as expected. As the scan rate is increased, the solvent window contracts, and the second and third oxidation peaks both become less distinct, particularly the third which becomes a shoulder of the solvent oxidation feature. However, it is clear that as the scans become faster, the current maximum of the second oxidation wave does not increase to the same degree as that of the first feature does. The behaviors of the first and second oxidation waves are compared in Figure 4.3.

In a cyclic voltammogram, the strength of the current generated by a particular electrochemical process is directly proportional to the concentration of the species undergoing that process. Thus, for two similar oxidation processes undergone by two species of equal concentration, equal current will be observed. As the rate of a voltage sweep is increased the current also increases, but again, two species of equal concentration will exhibit equal current under equal conditions, and therefore the currents will change in an identical manner as the scan rate is changed. The fact that the first and second oxidation waves of the cyclic voltammogram of $\text{Et}_4\text{N}^+[\mathbf{4.4}]^-$ do not behave similarly indicates not only that the two oxidation features must be

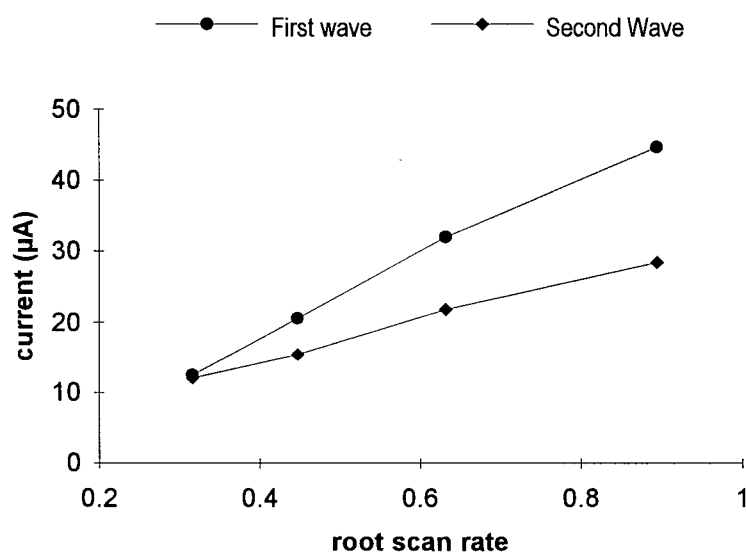
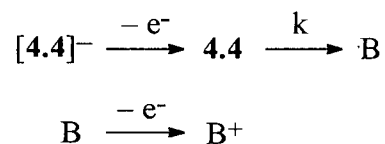


Figure 4.3. Maximal Current $I_{p,a}$ vs. for First and Second Oxidation Features of $\text{Et}_4\text{N}^+[\mathbf{4.4}]^-$ in CH_2Cl_2

due to different species, but also that the relative concentrations of the two species change as the scan rate is increased.

This observation indicates that the second oxidation feature is due to a decomposition byproduct of the first oxidation. The first oxidation wave is due to the initial analyte, $\text{Et}_4\text{N}^+[\mathbf{4.4}]^-$.



Scheme 4.4

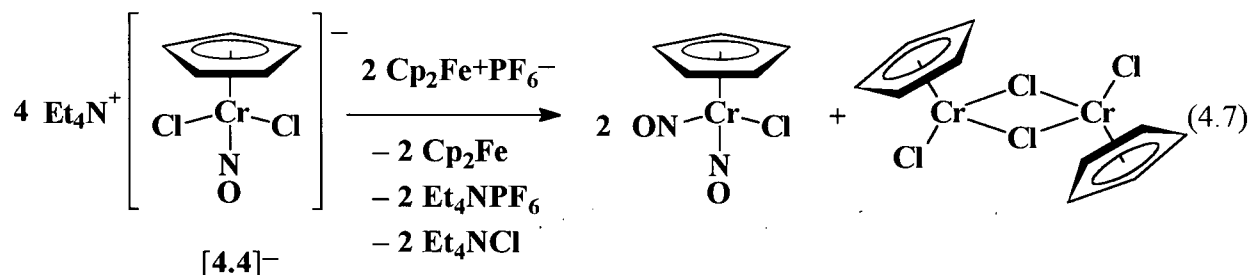
When this species is initially oxidized to its neutral 16e analogue, $\mathbf{4.4}$, the oxidation product rapidly decomposes at rate k to yield some other complex, designated as B in Scheme 4.4. The second oxidation feature is then presumably due to B . As the rate of the voltage sweep increases, the amount of time between the passage of the first and second oxidation potentials becomes shorter, and competitive with rate k . Therefore, as the scan rate increases, the reaction process has less time to generate B , and the concentration of B *decreases* relative to that of $[\mathbf{4.4}]^-$ as the scan rate *increases*.

4.4.4.2 Chemical Oxidation of $\text{Et}_4\text{N}^+[\text{CpCr}(\text{NO})\text{Cl}_2]^-$

Effecting the oxidation of $[\mathbf{4.4}]^-$ chemically demonstrates that the initial oxidation product does decompose, and allows the isolation of two organochromium products. Treatment of $\text{Et}_4\text{N}^+[\mathbf{4.4}]^-$ with $\text{Cp}_2\text{Fe}^+\text{PF}_6^-$ results in a rapid reaction and the formation of a green mixture

which contains a dinitrosyl complex as judged by the solution IR spectrum. It is noteworthy that only half an equivalent of oxidant is required to consume all the starting anion, and if a stoichiometric amount of ferrocenium ion is employed then some of it remains unreacted.

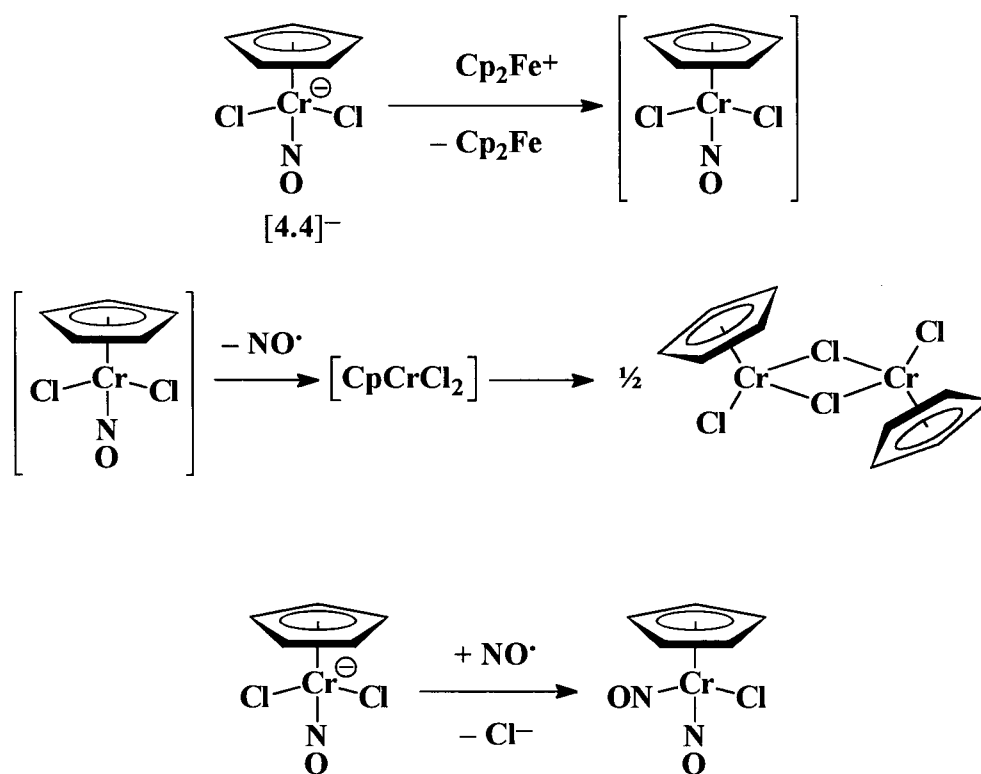
Chromatography of the reaction mixture effects the separation of three products, one being the ferrocene byproduct of the chemical oxidation, and two being derived from the decomposition of **4.4**, namely the dinitrosyl complex $\text{CpCr}(\text{NO})_2\text{Cl}$, and the Cr^{III} dimer $[\text{CpCrCl}(\mu\text{-Cl})]_2$.¹¹ A balanced reaction equation for this transformation is depicted in eq 4.7.



The reaction is not entirely straightforward. Although the reaction involves an oxidation by ferrocenium, only half the initial organochromium reagent is oxidized in this manner. As well, a mononitrosyl chromium species yields products which contain either two or zero nitrosyl ligands per metal. Nevertheless, a plausible mechanism for this transformation can be discerned by starting with the oxidation of the dichloride anion.

Removal of an electron from this complex by ferrocenium results in ferrocene and compound **4.4**, $\text{CpCr}(\text{NO})\text{Cl}_2$, a $16e \{ \text{Cr}(\text{NO}) \}^4$ complex, the molybdenum and tungsten analogues of which are thermally stable. However, **4.4** is not stable, as indicated by the irreversible electrochemical oxidation of the $17e$ anionic precursor. Loss of NO from this complex as nitric oxide radical would yield CpCrCl_2 , that is one half of the Cr^{III} dimer isolated from the reaction. Because only half an equivalent of ferrocenium is consumed, this leaves half of the starting anion unreacted. The nitric oxide liberated from the oxidized [**4.4**]⁻ may then react with the remaining anion, and substitution of chloride for NO then yields $\text{CpCr}(\text{NO})_2\text{Cl}$, the second isolated product. These steps are illustrated in Scheme 4.5.

This mechanism provides a rationale for the formation of the isolated products, for the unusual stoichiometry between the reactants, and for the transfer of a nitrosyl ligand. The loss of NO as a discrete radical allows for a formal disproportionation, so that two equivalents of $\{\text{Cr}(\text{NO})\}^5$ (or Cr^{I}) and one equivalent of oxidant yield one equivalent each of Cr^{III} and $\{\text{Cr}(\text{NO})\}^6$ (or Cr^0). As support for the overall mechanism, the last step can be shown to proceed independently. That is, treatment of $\text{Et}_4\text{N}^+[\text{4.4}]^-$ in THF with gaseous nitric oxide does indeed result in a conversion to $\text{CpCr}(\text{NO})_2\text{Cl}$.



Scheme 4.5. Proposed mechanism for oxidative decomposition of $[\text{4.4}]^-$.

The results of this oxidation answer a question about the difference in reactivities exhibited by the Group 6 $\text{CpM}(\text{NO})(\text{CO})_2$ species when they are treated with a halogenating reagent (Section 1.1.3.2, Scheme 1.1). Whereas the molybdenum and tungsten complexes yield 16e dihalide compounds, the chromium species affords compounds such as complex **1** only if the halide is iodide. Generally, such treatment with halide instead yields a dinitrosyl complex. That

this is the same product as observed via the oxidation of dichloride anion $[4.4]^-$ is therefore significant. These results suggest that when $CpM(NO)(CO)_2$ species are treated with halide, the different nitrosyl product obtained for chromium is not due to an entirely different reaction pathway, but rather that the reaction follows the same path to produce the expected 16e dihalide species (i.e. 4.4). However, this complex is simply unstable, decomposing as outlined above.

4.4.4.3 Mechanistic Rationale

It has been established that whereas the 17e anion $[4.4]^-$ is a stable species, the one-electron oxidation product $CpCr(NO)Cl_2$ is not and appears to decompose via loss of nitric oxide, ultimately forming $[CpCrCl(\mu-Cl)]_2$. Thus, this is another example of an odd-electron complex being rendered more reactive by redox to an even-electron one. There are still two questions about this particular decomposition. Firstly, why are complexes of the type $CpM(NO)X_2$ ($X =$ halide) stable for molybdenum and tungsten, but not for chromium? Secondly, why does this particular reaction involve the loss of the nitric oxide ligand, whereas the chemistry discussed elsewhere in this Thesis maintains the integrity of the $CpCr(NO)$ fragment? Both these questions may be answered in terms of the orbital structure of this fragment, which was discussed in Section 3.4.7.

The basic nature of the frontier orbitals of the fragment is that depicted in Figures 3.5 and 3.6. Two of the metal d-orbitals overlap with the orthogonal π -orbitals of the nitrosyl, while a third metal orbital of π -symmetry remains non-bonding in the $CpCr(NO)$ fragment. In the case of an 18e, $\{Cr(NO)\}^6$ complex, this latter orbital is fully occupied, and π -acidic ligands serve to lower this orbital in energy and stabilize the complex. In the case of a 17e, $\{Cr(NO)\}^5$ complex, this orbital is singly occupied, a situation that is stabilized by σ -basic ligands. The oxidation of a complex such as $[4.4]^-$ presumably effects the removal of the unpaired electron from this singly occupied orbital, thereby generating a formally 16e compound.

In the case of molybdenum compounds this is a reversible process, both chemically and electrochemically.² However, for the chromium species this is an irreversible process, and removal of the unpaired electron results in loss of the nitric oxide ligand. To explain this dramatic

difference, there must be some property which distinguishes the chromium complex from the molybdenum. A strong possibility is that the transient $\text{CpCr}(\text{NO})\text{Cl}_2$ is a high-spin complex, as illustrated in Figure 4.4.¹⁹

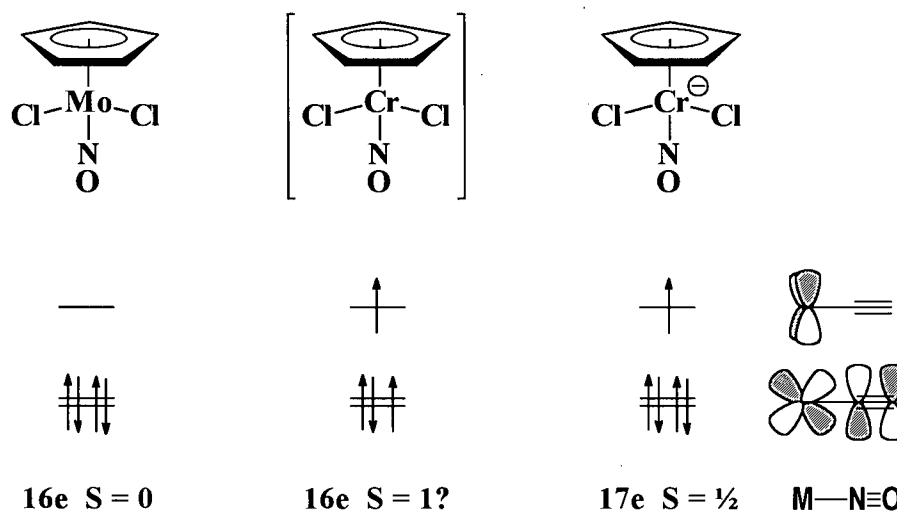


Figure 4.4. Frontier Orbital Population in $[\text{CpM}(\text{NO})\text{Cl}_2]^{0/-}$ Species

Removal of the unpaired electron from $17e$ $[\mathbf{4.4}]^-$ renders a relatively low-lying orbital vacant, and oxidizing the species will generally have the effect of contracting the orbitals and increasing the pairing energy of electrons in the complex. Whereas the HOMO-LUMO gap in the $16e$ molybdenum complex is sufficient to keep the fifteenth and sixteenth valence electrons paired in the NO-bonding orbital, moving to the smaller, first row metal again has the effect of reducing orbital size, decreasing orbital splitting, and increasing pairing energy. Thus, it is probable that whereas $\text{CpMo}(\text{NO})\text{Cl}_2$ remains a low-spin, diamagnetic complex, oxidation of $[\mathbf{4.4}]^-$ vacates an orbital of low enough energy so that the oxidized species becomes high spin.

Such a configuration leads to a situation not yet observed in this Thesis. That is, a high-spin configuration for the transient $\text{CpCr}(\text{NO})\text{Cl}_2$ means that the π -bonding orbitals to the nitrosyl are no longer completely filled, since one of the electrons in the M-NO π -orbital has been promoted to the orbital above. This would have the effect of weakening the metal-nitrogen bond, thus promoting loss of the nitrosyl ligand.

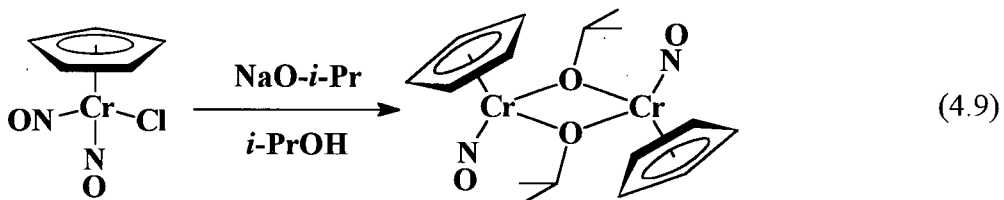
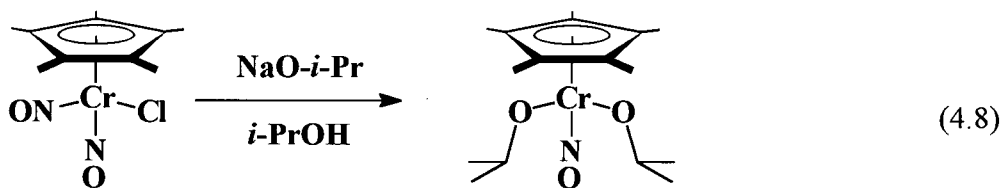
As well, this particular electronic arrangement makes dissociation of the ligand as nitric oxide radical a low-energy reaction path. Free nitric oxide has a single electron in the π -symmetry N-O antibonding orbital, and this is exactly the ligand character of the lower-energy, singly-occupied orbital in the high-spin configuration illustrated above. Such a dissociation leaves three electrons in the metal-based orbitals, so loss of nitric oxide formally oxidizes the metal to chromium (III). Thus, dissociation of nitric oxide from a complex in this electronic configuration requires little reorganizational energy and is kinetically very facile. Therefore, invoking the high-spin configuration for the intermediate CpCr(NO)Cl_2 complex explains both its instability compared to the molybdenum and tungsten congeners and its rapid release of nitric oxide as a decomposition path.

4.4.4.4 Summary: CpM(NO)(CO)_2 plus Halide Reagents

The reactivity described above allows for the first time an understanding of the diversity of products obtained in reactions of CpM(NO)(CO)_2 ($M = \text{Cr, Mo, W}$) complexes with halide sources, outlined in Scheme 4.6. Treatment of CpM(NO)(CO)_2 ($M = \text{Mo, W}$) with I_2 , Br_2 , Cl_2 or PCl_5 affords isolation of the corresponding $16e \{M(\text{NO})\}^4 \text{CpM(NO)X}_2$ species.^{20,21} In the case of chromium, an intermediate $\{M(\text{NO})\}^5$ species may be obtained in the case of iodide, namely complex **1**, $[\text{CpCr(NO)I}]_2$.⁵ The corresponding chloro dimer may also be obtained as outlined in Section 4.4.1.2, but $[\text{CpCr(NO)Cl}]_2$ is more prone to oxidation than $[\text{CpCr(NO)I}]_2$, and so reacts further to generate $\{M(\text{NO})\}^4 \text{CpCr(NO)Cl}_2$. Unlike the Mo and W analogues of this complex, the chromium dichloride is likely a high-spin compound, and decomposes via loss of nitric oxide, thereby generating $\text{CpCr(NO)}_2\text{Cl}$. Thus, whereas reaction of CpCr(NO)(CO)_2 with I_2 yields **1**, reaction with Cl_2 or Br_2 generates the dinitrosyl halide species.

When $M = \text{Cr}$ and $X = \text{I}$, the reaction affords $[\text{CpCr(NO)I}]_2$ because this complex is resistant to further oxidation to the $\{\text{Cr(NO)}\}^4$ manifold. When $M = \text{Cr}$ and $X = \text{Br}^5$ or Cl ,¹⁴ this second oxidation does take place, the result is an unstable complex, and the ultimate nitrosyl-containing product is $\text{CpCr(NO)}_2\text{X}$. When $M = \text{Mo}$ or W , the $\{M(\text{NO})\}^4$ state affords a low spin and stable configuration, so the products are the CpM(NO)X_2 species.

$[\text{CpCr}(\text{NO})(\text{O}-i\text{-Pr})]_2$, rather than a bisalkoxide monomer. These transformations are illustrated in eqs 4.8 and 4.9.



This latter reactivity is therefore similar to that of $\text{CpCr}(\text{NO})_2\text{Cl}$ with lithium amide reagents, which yields bridging-amide dimers such as those described in Chapter 3.²² Contrasting the two results, there is clearly a steric effect, and one would expect the Cp^* derivative to be less prone to form a dimeric compound. There may well be an electronic factor which distinguishes the outcome; the transformation from $\text{Cp}^*\text{Cr}(\text{NO})_2\text{Cl}$ to $\text{Cp}^*\text{Cr}(\text{NO})(\text{O}-i\text{-Pr})_2$ requires both a loss of nitric oxide, which effects an oxidation from $\{\text{Cr}(\text{NO})_2\}^6$ to $\{\text{Cr}(\text{NO})\}^5$, and a second oxidation step from $\{\text{Cr}(\text{NO})\}^5$ to $\{\text{Cr}(\text{NO})\}^4$, the nature of which is not immediately clear and which does not proceed in the case of the Cp derivative. It is possible that this second oxidation is promoted by the greater electron-donating ability of the Cp^* ligand.

4.5 Epilogue and Future Work

Although it is apparent that the organometallic anions considered in this Chapter are labile, the mechanism and quantitative extent of this lability have not been investigated. Most 17e organometallic species are known to undergo substitution reactions by following associative pathways, and in the case of 17e cationic species, an associative rate-determining step should be accelerated. However, to my knowledge, there has been no investigation as to the mechanism of substitution in organometallic *anions*. It may be possible that these 17e anions do not exhibit typical behavior in this regard, since an associated transition state for halide substitution would be destabilized by the required build-up of charge at the metal center. A kinetic investigation of halide substitution in these complexes would determine the pathways of such a reaction and yield quantitative information about the relative stability and lability of the $[\text{CpCr}(\text{NO})\text{X}_2]^-$ species.

Although it appears that $\{\text{Cr}(\text{NO})\}^4$ complexes of the type $\text{CpCr}(\text{NO})\text{X}_2$ ($\text{X} = \pi$ -basic pseudo-halide ligand, i.e. amide, alkoxide, thiolate) should be stable species, they cannot be prepared via oxidation and ligand substitution of the 17e $[\text{CpCr}(\text{NO})\text{X}_2]^-$ ($\text{X} = \text{halide}$) anions. Substitution in the latter complexes of one halide for a more electron-donating ligand results in loss of the second halide and formation of a stable, metal-metal bonded dimer. Oxidation of the dichloride species results in loss of nitric oxide. Thus, the $\{\text{Cr}(\text{NO})\}^5$ anions currently available are not viable precursors to complexes in the $\{\text{Cr}(\text{NO})\}^4$ manifold, and some other synthetic route is necessary.

A possible strategy is to begin with a complex already of the desired oxidation state. Species of the type $(\text{RO})_3\text{Cr}(\text{NO})^{23}$ and $(\text{R}_2\text{N})_3\text{Cr}(\text{NO})^{23-25}$ are known, and a reaction involving the protonation of an alkoxide or amide ligand by C_5H_6 , or a sequence of reactions that effect the same net transformation would yield the desired $\text{CpCr}(\text{NO})\text{X}_2$ ($\text{X} = \text{amide, alkoxide}$) compounds. The preparation of a series of such complexes and an investigation of their reactivity, particularly with respect to the effects of reduction back to the $\{\text{Cr}(\text{NO})\}^5$ manifold, would complete an understanding of characteristic behaviors and the relationship among the three oxidation states of the $\text{CpCr}(\text{NO})$ fragment, $\{\text{Cr}(\text{NO})\}^6$ being the favored configuration for complexes with π -acidic ligands, $\{\text{Cr}(\text{NO})\}^5$ for those with π -neutral ligands, and $\{\text{Cr}(\text{NO})\}^4$ for π -basic.

The comparison of reaction products in Scheme 4.6 summarizes the reasons that CpCr(NO)(CO)_2 does not yield a $\{\text{Cr(NO)}\}^4$ complex when treated with halide. $[\text{CpCr(NO)Cl}]_2$ is easily oxidized to a dihalide than then decomposes to a dinitrosyl complex. $[\text{CpCr(NO)I}]_2$ is somewhat resistant to this oxidation, though prolonged reaction times with further I_2 will also generate dinitrosyl species. The implication from Scheme 4.6 is that the molybdenum and tungsten reactions may proceed through similar intermediates as the chromium path, that is a $[\text{CpM(NO)X}]_2$ complex. This is by no means certain. The 18e complex $\text{Cp}^*\text{W(NO)(CO)Cl}_2$ can be isolated as a probable intermediate in the reaction of $\text{Cp}^*\text{W(NO)(CO)}_2$ with Cl_2 ,²⁶ suggesting that the reactions of Mo and W do not proceed via monohalide species. Similar CpW(NO)(CO)X_2 species are observed in reactions with I_2 ¹³ and Br_2 .²¹ In fact, the mechanism of formation of $[\text{CpCr(NO)I}]_2$ is not entirely understood. Although an intermediate complex with one nitrosyl and one carbonyl has been observed during the reaction of CpCr(NO)(CO)_2 with I_2 , it is not known whether this species is 18e CpCr(NO)(CO)I_2 or 17e CpCr(NO)(CO)I .

Oxidation of $[\text{CpCr(NO)Cl}_2]^-$ to a $\{\text{Cr(NO)}\}^4$ complex results in loss of the nitrosyl ligand as nitric oxide. Nitric oxide is now recognized as the principal regulator of human blood pressure.²⁷ It is generated *in vivo* from L-arginine by the enzyme nitric oxide synthase, which is located in the endothelial wall of the blood vessel. NO then diffuses into the muscle layer and activates another enzyme, guanylyl cyclase, triggering production of cyclic guanosine monophosphate (cGMP) and relaxation of blood vessel muscles. It has been demonstrated that efficacy of the vasodilator nitroprusside, $\text{Na}_2[\text{Fe(CN)}_5(\text{NO})]$, depends upon release of nitric oxide, thereby increasing the amount of NO delivered to guanylyl cyclase.²⁸ Nitroprusside is currently the only clinically employed metal-nitrosyl complex; release of nitric oxide from this species is triggered by a redox process, and is unfortunately accompanied by the release of two equivalents of toxic cyanide for every molecule of NO, thus requiring concomitant use of a cyanide antidote with the vasodilator.²⁹ Thus, design of new metallonitrosyl pharmaceuticals is a subject of interest, particularly with respect to determination and control of conditions under which nitric oxide is lost from the metal. The loss of NO from $[\text{CpCr(NO)Cl}_2]^-$ upon oxidation therefore represents a process worthy of much greater study, particularly in view of the fact that

oxidation-induced loss of NO from a $\{\text{Cr}(\text{NO})\}^5$ complex, or of two NO molecules from a $\{\text{Cr}(\text{NO})_2\}^6$ species, will result in an inert Cr^{III} byproduct.

4.6 References and Notes

- (1) Complexes of the type $\text{CpMo}(\text{NO})(\text{PR}_3)\text{I}$ have been cited as spectroscopically-observed intermediates in the reduction of $\text{CpMo}(\text{NO})\text{I}_2$ in the presence of phosphines and phosphites, but these species were never isolated due to thermal decomposition. Hunter, A. D.; Legzdins, P. *Organometallics* **1986**, *5*, 1001.
- (2) Herring, F. G.; Legzdins, P.; Richter-Addo, G. B. *Organometallics* **1989**, *8*, 1485.
- (3) Hubbard, J. L.; McVicar, W. K. *Inorg. Chem.* **1992**, *31*, 910.
- (4) Sim, G. A.; Woodhouse, D. I.; Knox, G. R. *J. Chem. Soc., Dalton Trans.* **1979**, 83.
- (5) Legzdins, P.; Nurse, C. R. *Inorg. Chem.* **1985**, *24*, 327.
- (6) The hexafluorophosphate salt was prepared by addition of NaPF_6 to an aqueous $[\text{Cp}_2\text{Fe}]_2\text{SO}_4$ solution. Jolly, W. L. *The Synthesis and Characterization of Inorganic Compounds*; Prentice-Hall: Englewood Cliffs, NJ, 1970; p 487.
- (7) Chin, T. T.; Hoyano, J. K.; Legzdins, P.; Malito, J. T. *Inorg. Synth.* **1990**, *28*, 196.
- (8) Hoyano, J. K.; Legzdins, P.; Malito, J. T. *Inorg. Synth.* **1978**, *18*, 126.
- (9) Legzdins, P.; Shaw, M. J. *J. Am. Chem. Soc.* **1994**, *116*, 7700.
- (10) The relative intensity of the symmetric and antisymmetric stretching vibrations for a dinitrosyl or dicarbonyl complex varies as a function of the angle 2θ between the two groups: $I_{\text{sym}}/I_{\text{antisym}} = \cotan^2\theta$. (a) Legzdins, P.; Richter-Addo, G. B. *Metal Nitrosyls*; Oxford University Press: New York, 1992; p 66. (b) Crabtree, R. H. *The Organometallic Chemistry of the Transition Metals*; Wiley-Interscience: New York, 1988; pp 233-235.
- (11) Köhler, F. H.; de Cao, R.; Ackermann, K.; Sedlmair, J. *Z. Naturforsch., B* **1983**, *38*, 1406.
- (12) For molybdenum, see: (a) King, R. B. *Inorg. Chem.* **1967**, *6*, 30; (b) James, T. A.; McCleverty, J. A. *J. Chem. Soc. (A)* **1971**, 1068.

- (13) For tungsten, see: Legzdins, P.; Martin, D. T.; Nurse, C. R. *Inorg. Chem.* **1980**, *19*, 1560.
- (14) Kolthammer, B. W. S.; Legzdins, P.; Malito, J. T. *Inorg. Chem.* **1977**, *16*, 3173.
- (15) Legzdins, P.; Veltheer, J. E. *Acc. Chem. Res.* **1993**, *26*, 41.
- (16) Lawrance, G. A. *Chem. Rev.* **1986**, *86*, 17.
- (17) Krueger, S. T.; Poli, R.; Rheingold, A. L.; Staley, D. L. *Inorg. Chem.* **1989**, *28*, 4599.
- (18) Krueger, S. T.; Owens, B. E.; Poli, R. *Inorg. Chem.* **1990**, *29*, 2001.
- (19) As a general rule, complexes of first-row transition metals are more likely to exhibit high-spin configurations than are second- or third-row metal complexes. This is because ligand field splitting is greater and electron pairing energy is smaller for 3d ions than for 4d or 5d ions. Shriver, D. F.; Atkins, P.; Langford, C. H. *Inorganic Chemistry*, 2nd ed.; W. H. Freeman: New York, NY, 1994; p 250.
- (20) CpMo(NO)X₂: Seddon, D.; Kita, W. G.; Bray, J.; McCleverty, J. A. *Inorg. Synth.* **1976**, *16*, 24. CpMo(NO)I₂: reference 12. CpMo(NO)Cl₂: (a) McCleverty, J. A.; Seddon, D. *J. Chem. Soc., Dalton Trans.* **1972**, 2527. (b) Dryden, N. H.; Legzdins, P.; Batchelor, R. J.; Einstein, F. W. B. *Organometallics* **1991**, *10*, 2077.
- (21) CpW(NO)I₂: reference 13, and Hunter, A. D.; Legzdins, P.; Martin, J. T.; Sánchez, L. *Organomet. Synth.* **1986**, *3*, 58. CpW(NO)Br₂: Martin, J. T. Ph.D. Thesis, University of British Columbia, 1987. CpW(NO)Cl₂: Dryden, N. H.; Legzdins, P.; Batchelor, R. J.; Einstein, F. W. B. *Organometallics* **1991**, *10*, 2077.
- (22) Bush, M. A.; Sim, G. A.; Knox, G. R.; Ahmad, M.; Robertson, C. G. *J. Chem. Soc. (D)*, **1969**, 74.
- (23) Bradley, D. C.; Newing, C. W.; Chisholm, M. H.; Kelly, R. L.; Haitko, D. A.; Little, D.; Cotton, F. A.; Fanwick, P. E. *Inorg. Chem.* **1980**, *19*, 3010.
- (24) Bradley, D. C.; Newing, C. W. *J. Chem. Soc., Chem. Commun.* **1970**, 219.
- (25) Odom, A. L.; Cummins, C. C.; Protasiewicz, J. D. *J. Am. Chem. Soc.* **1995**, *117*, 6613.

- (26) Gomez-Sal, P.; de Jesús, E.; Michiels, W.; Royo, P.; de Miguel, A. V. *J. Chem. Soc., Dalton Trans.* **1990**, 2445.
- (27) Snyder, S. H.; Bredt, D. S. *Sci. Am.* **1992**, 266 (5), 68.
- (28) Butler, A. R.; Glidewell, C. *Chem. Soc. Rev.* **1987**, 16, 361.
- (29) Clarke, M. J.; Gaul, J. B. In *Structure and Bonding*; Springer-Verlag: Berlin, 1993; Vol. 81, p 148.

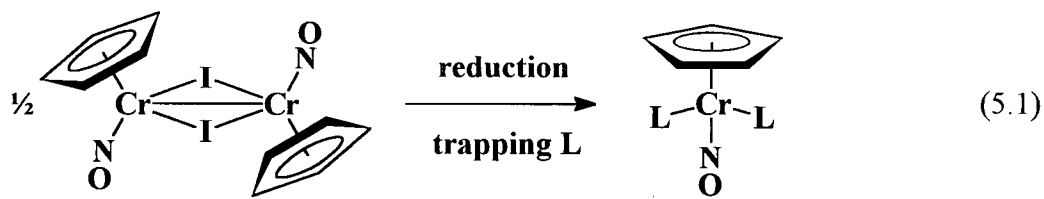
CHAPTER 5

Reductive Synthesis of $\text{CpCr}(\text{NO})(\text{CNCMe}_3)_2$ and Derivative Chemistry

5.1 Introduction.....	132
5.2 Experimental Procedures	133
5.3 Characterization Data	141
5.4 Results and Discussion.....	142
5.5 Epilogue and Future Work.....	154
5.6 References and Notes	155

5.1 Introduction

The redox investigations described in Chapter 3 demonstrated that the one-electron reduction of a 17e CpCr(NO) complex tends to result in the loss of the σ -basic ligands and that a new compound may be formed by performing this reduction in the presence of a suitable trapping ligand, namely one that will stabilize the 18e $\{\text{Cr}(\text{NO})\}^6$ configuration. For instance, reduction of bis(ammonia) cation $[\mathbf{2.1}]^+$ in the presence of carbon monoxide results in loss of NH_3 and the formation of $\text{CpCr}(\text{NO})(\text{CO})_2$. Similarly, reduction of $[\text{CpCr}(\text{NO})\text{I}]_2$ in the presence of $\text{P}(\text{OMe})_3$ yields the 18e species $\text{CpCr}(\text{NO})(\text{P}\{\text{OMe}\}_3)_2$. These reactions suggest that this reduction methodology might afford a general route to previously unknown 18e CpCr(NO) complexes (eq 5.1) obtained not by effecting ligand substitution of an 18e starting material, but rather by reduction of a 17e precursor in the presence of a trapping ligand possessing π -acidic character. As stated in Section 1.1.3.2, the substitution chemistry of $\text{CpCr}(\text{NO})(\text{CO})_2$ is generally limited to photolytic reactions resulting in fair to low yields of monosubstituted products. Thus, the chemistry of eq. 5.1 seemed to offer a facile route to a much wider range of $\{\text{Cr}(\text{NO})\}^6$ species.



**L = phosphine, phosphite, isonitrile,
olefin, acetylene, $\frac{1}{2}$ diene**

This Chapter outlines the attempts to investigate the potential of eq. 5.1 and examines some derivative chemistry of an 18e product that results, namely $\text{CpCr}(\text{NO})(\text{CNCMe}_3)_2$.

5.2 Experimental Procedures

5.2.1 Methods

The experimental methods employed throughout this Thesis are detailed in Section 2.2.1. The electrochemical methods employed are detailed in Section 2.2.2.

5.2.2 Reagents

$[\text{CpCr}(\text{NO})\text{I}]_2^1$ and $[\text{Cp}_2\text{Fe}]^+[\text{PF}_6]^-^2$ were prepared by the published procedures. H_2O and MeOH were deaerated prior to use. *p*-tolNCO was vacuum transferred from CaH_2 . Olefin reagents were dried on molecular sieves. All other reagents were used as received from commercial suppliers.

5.2.3 Preparation of $\text{CpCr}(\text{NO})(\text{CNCMe}_3)_2$ (5.1)

THF (~10 mL) was vacuum transferred onto $[\text{CpCr}(\text{NO})\text{I}]_2$ (1) (137 mg, 0.250 mmol) and Zn powder (0.16 g, excess) in a bomb. To the solution was added *tert*-butylisocyanide (250 μL , 184 mg, 2.21 mmol), and the reaction mixture was stirred for three hours, after which time the solution had changed from brown to red-orange. The solvent was removed in vacuo, and the residue was extracted with 1:1 pentane/ Et_2O (2 x 15 mL) and filtered through Florisil (2 x 3 cm). The filtrate was concentrated slowly in vacuo and refrigerated to obtain 5.1 as red blocks.

5.2.4 Preparation of $[\text{CpCr}(\text{NO})(\text{CNCMe}_3)_2]^+[\text{PF}_6]^-$ ($[\text{5.1}]^+[\text{PF}_6]^-$)

THF (~10 mL) was vacuum transferred onto 5.1 (156 mg, 0.500 mmol) and $[\text{Cp}_2\text{Fe}]^+[\text{PF}_6]^-$ (165 mg, 0.500 mmol). The mixture was warmed to room temperature and stirred for 5 min, during which time the dark color of ferrocenium was replaced by a bright yellow-orange hue; the mixture was stirred a further 40 min. The solvent was then removed in vacuo, the orange residue was dissolved in CH_2Cl_2 (5 mL), and the extract was filtered. The filtrate was stripped to dryness, triturated and washed with hexanes (2 x 15 mL), and dried in vacuo to yield $[\text{CpCr}(\text{NO})(\text{CNCMe}_3)_2]^+[\text{PF}_6]^-$ ($[\text{5.1}]^+[\text{PF}_6]^-$) as a bright yellow powder.

X-ray-quality crystals of $[5.1]^+$ could be obtained as the BPh_4^- salt ($[5.1]^+[BPh_4]^-$), by allowing slow diffusion of pentane into a CH_2Cl_2 solution of equimolar amounts of $[5.1]^+[BF_4]^-$ (vide infra) and $NaBPh_4$.

5.2.5 Reaction of Bis(isocyanide) 5.1 with HBF_4

$CpCr(NO)(CNCMe_3)_2$ (250 mg, 0.798 mmol) was dissolved in Et_2O (25 mL), and $HBF_4 \cdot Et_2O$ (1.5 mL, 1.8 M in Et_2O , 2.7 mmol) was added by syringe. A yellow precipitate quickly formed and then coagulated to a brown oil. The solvent was removed in vacuo, the residue was dissolved in CH_2Cl_2 (4 mL), and the solution was loaded onto a CH_2Cl_2 -packed column of silica gel (2 x 10 cm). Elution of the column with CH_2Cl_2 developed a red band that was collected and stripped to yield unreacted bis(isocyanide) complex 5.1. Further elution of the column with THF developed a dark gold eluate, which was reduced in volume, diluted with hexanes, and cooled overnight to yield orange crystals of $[5.1]^+[BF_4]^-$ (73 mg, 23% yield).

5.2.6 Reaction of Bis(isocyanide) 5.1 with $[Me_3O]^+[BF_4]^-$

$CpCr(NO)(CNCMe_3)_2$ (187 mg, 0.500 mmol) and $[Me_3O]^+[BF_4]^-$ (0.82 mg, 0.55 mmol) were dissolved in Et_2O (10 mL), and the mixture was stirred overnight, resulting in a red solution and a gold precipitate. The solution was cannulated off, and the gold powder was washed with Et_2O (2 x 10 mL) and dissolved in CH_2Cl_2 (10 mL). The solution was filtered and the filtrate was taken to dryness to yield $[5.1]^+[BF_4]^-$ as a gold powder (34 mg, 15 % yield)

5.2.7 Treatment of Bis(isocyanide) 5.1 with MeLi, PhLi, and $LiEt_3BH$

These experiments were performed similarly. $CpCr(NO)(CNCMe_3)_2$ (125 mg, 0.40 mmol) was dissolved in Et_2O (10 mL), and the solution was cooled with a dry-ice/acetone bath. An equimolar amount of MeLi (0.70 mL, 0.7 M in Et_2O , 0.49 mmol), PhLi (0.4 mL, 1.0 M in THF, 0.40 mmol), or $LiEt_3BH$ (0.25 mL, 1.8 M, 0.45 mmol) was added, and the solution was stirred for 90 min, after which time an IR spectrum of the solution exhibited the unchanged bands

of **5.1** ($\nu_{\text{NO}} = 1642 \text{ cm}^{-1}$) and no other nitrosyl bands. The solution was allowed to warm to room temperature and was stirred for 1 d, after which time the IR spectrum of the solution remained unchanged.

5.2.8 Treatment of Bis(isocyanide) **5.1** with H_2 , CO, H_2O , MeOH, and *p*-tolNCO

$\text{CpCr(NO)(CNCMe}_3)_2$ (25 mg, 0.080 mmol) was dissolved in C_6D_6 in an NMR tube. To the tube was added either an atmosphere of H_2 , an atmosphere of CO, H_2O (5 μL 0.28 mmol, 3.5 equiv) by syringe, MeOH (10 μL 0.25 mmol, 3.2 equiv) by syringe, or *p*-tolNCO (excess). The samples were left at ambient temperature for 1 d, after which time the ^1H NMR spectra of these mixtures revealed peaks due only to complex **5.1** and the added reagents. The samples were heated at 60 $^\circ\text{C}$ for 2 d, but the ^1H NMR spectra remained unchanged. Heating each of the samples at 100 $^\circ\text{C}$ for 3 d resulted in the appearance of the same two new singlet peaks ($\delta = 1.59, 4.72$, ratio $\sim 3.5:1$) at the expense of the signals due to **5.1** in each spectrum. Further heating at 100 $^\circ\text{C}$ increased the intensity of the new signals relative to those of **5.1**.

5.2.9 Thermolysis of Bis(isocyanide) **5.1**

$\text{CpCr(NO)(CNCMe}_3)_2$ (500 mg, 1.60 mmol) was dissolved in THF ($\sim 10 \text{ mL}$) in a bomb, and the solution was heated at 100 $^\circ\text{C}$ for 4 d. An IR spectrum of the solution exhibited strong bands at 1690 and 2143 cm^{-1} along with a much weaker band attributable to the starting material at 1634 cm^{-1} . The solvent was removed in vacuo, the residue was extracted into CH_2Cl_2 (25 mL), and the extract was filtered through neutral alumina I (2 x 3 cm). An IR spectrum of the resulting orange-brown filtrate exhibited bands at 1689 and 2144 cm^{-1} . Attempts to crystallize any material from this solution resulted only in the deposition of an insoluble tan powder.

5.2.10 Preparation of $[\text{CpCr(NO)(THF)}_2]^+[\text{PF}_6]^-$

This complex was prepared according to the original synthetic method of Michael Shaw, which is reproduced here. THF ($\sim 10 \text{ mL}$) was vacuum transferred onto a mixture of

[CpCr(NO)I]₂ (548 mg, 2.0 mmol) and AgPF₆ (480 mg, 1.90 mmol). The suspension was warmed to room temperature and stirred for 10 min, resulting in the formation of a flocculent precipitate. The solvent was removed in vacuo, and the residue was extracted into CH₂Cl₂ (2 x 25 mL). The extracts were filtered, reduced in volume to ~5 mL, and pentane (30 mL) was quickly added to induce precipitation of a green powder that was collected on a frit and dried in vacuo to yield 0.65 g (1.5 mmol, 78% yield) of [CpCr(NO)(THF)₂]⁺[PF₆]⁻.

Anal. Calcd for C₁₃H₂₁NO₃CrPF₆: C, 35.79; H, 4.85; N, 3.21. Found: C, 35.60; H, 4.71; N, 3.42. IR (THF): $\nu_{\text{NO}} = 1691 \text{ cm}^{-1}$. IR (Nujol): $\nu_{\text{NO}} = 1697 \text{ cm}^{-1}$.

5.2.11 Reduction of [CpCr(NO)(THF)₂]⁺ in presence of diphenylacetylene or dimethylacetylenedicarboxylate

THF (~10 mL) was vacuum transferred onto a mixture of [CpCr(NO)(THF)₂]⁺[PF₆]⁻ (218 mg, 0.500 mmol), diphenylacetylene (178 mg, 1.00 mmol), and Zn powder (0.16 g, 2.5 mmol). The mixture was stirred for 3 d, after which time it had turned brown. The IR spectrum of the reaction solution exhibited only bands attributable to diphenylacetylene. Removal of solvent in vacuo and filtration of an Et₂O (15 mL) extract of the brown residue yielded a pale yellow solution, the IR spectrum of which also exhibited the bands of diphenylacetylene and no other species.

A similar reaction in THF of [CpCr(NO)(THF)₂]⁺[PF₆]⁻ (110 mg, 0.250 mmol), dimethylacetylenedicarboxylate (62 μL , 72 mg, 0.50 mmol) and Zn powder (80 mg, 1.2 mmol) similarly resulted in no tractable products and no spectroscopically observable nitrosyl-containing complexes.

5.2.12 Reduction of [CpCr(NO)(THF)₂]⁺ in presence of acetylene

THF (~10 mL) was vacuum transferred onto a mixture of [CpCr(NO)(THF)₂]⁺[PF₆]⁻ (218 mg, 0.500 mmol) and Zn powder (0.16 g, 2.5 mmol). The mixture was stirred under an

atmosphere of acetylene (1 atm) for two days, resulting in a brown and extremely viscous solution.

5.2.13 Reduction of $[\text{CpCr}(\text{NO})(\text{THF})_2]^+[\text{PF}_6]^-$ in presence of pyridine

THF (~10 mL) was vacuum transferred onto a mixture of $[\text{CpCr}(\text{NO})(\text{THF})_2]^+[\text{PF}_6]^-$ (110 mg, 0.250 mmol) and Zn powder (80 mg, 1.2 mmol). Pyridine (50 μL , 49 mg, 0.62 mmol) was added by syringe, and the mixture was stirred. The initially green suspension changed to a dark green solution within minutes after the addition of pyridine. The mixture was stirred for two days, after which time the IR spectrum of the solution exhibited bands due to pyridine and a weak feature at 1686 cm^{-1} . The solvent was removed in vacuo. The green residue was extracted with CH_2Cl_2 (2 x 15 mL), and the extracts were filtered. The filtrate was stripped to dryness, and the green residue was washed and triturated with Et_2O (2 x 15 mL), yielding a green powder (39 mg). The FAB mass spectra of this material exhibited features attributable to the parent peaks of $[\text{CpCr}(\text{NO})(\text{py})_2]^+[\text{PF}_6]^-$ (+FAB: m/z 305; -FAB: m/z 145).

5.2.14 Reduction of $[\text{CpCr}(\text{NO})(\text{THF})_2]^+[\text{PF}_6]^-$ in presence of 2,3-dimethylbutadiene

THF (~10 mL) was vacuum transferred onto a mixture of $[\text{CpCr}(\text{NO})(\text{THF})_2]^+[\text{PF}_6]^-$ (218 mg, 0.500 mmol) and Zn powder (0.16 g, 2.5 mmol). 2,3-dimethylbutadiene (57 μL , 41 mg, 0.50 mmol) was added by syringe and the mixture was stirred for 4 h, after which time an IR spectrum of the solution displayed a band at 1672 cm^{-1} . The solvent was removed in vacuo, the brown residue was extracted with Et_2O (2 x 20 mL), and the combined extracts were filtered to obtain an orange solution. An IR spectra of this solution exhibited a band at 1685 cm^{-1} . Attempts to crystallize a solid from this solution failed. Reducing the solution to dryness in vacuo afforded a small amount of an intractable oily brown residue.

5.2.15 Reduction of $[\text{CpCr}(\text{NO})(\text{THF})_2]^+$ in presence of 1,10-phenanthroline

THF (~10 mL) was vacuum transferred onto a mixture of $[\text{CpCr}(\text{NO})(\text{THF})_2]^+[\text{PF}_6]^-$ (169 mg, 0.400 mmol), 1,10-phenanthroline (90 mg, 0.50 mmol), and Zn powder (0.16 g, 2.5 mmol). The mixture was stirred for 3 h, during which time the color of the solution changed from green to brown to red. The solvent was removed in vacuo, the residue was extracted with CH_2Cl_2 (2 x 15 mL), and the extracts were filtered to yield a red-orange solution. No tractable material could be isolated from this solution.

5.2.16 Reduction of $[\text{CpCr}(\text{NO})\text{I}]_2$ in presence of 2,3-dimethylbutadiene

THF (~10 mL) was vacuum transferred onto a mixture of $[\text{CpCr}(\text{NO})\text{I}]_2$ (137 mg, 0.500 mmol) and Zn powder (0.16 g, 2.5 mmol). 2,3-dimethylbutadiene (60 μL , 44 mg, 0.53 mmol) was added by syringe, and the mixture was stirred for 45 minutes, after which time the only bands evident in an IR spectrum of the reaction mixture were those of the starting reagents. After 3 d further stirring, the reaction mixture had turned black, and the only observed IR bands were those of 2,3-dimethylbutadiene.

5.2.17 Reduction of $[\text{CpCr}(\text{NO})\text{I}]_2$ in presence of ethylene

THF (~10 mL) was vacuum transferred onto a mixture of $[\text{CpCr}(\text{NO})\text{I}]_2$ (137 mg, 0.500 mmol) and Zn powder (0.16 g, 2.5 mmol). The atmosphere of the vessel was evacuated and replaced with ethylene (1 atm). The mixture was stirred for 3 d, resulting in a brown-black solution from which the solvent was removed in vacuo. The black residue was extracted with CH_2Cl_2 , and the combined extracts were filtered to obtain a pale brown solution. The solution was stripped to dryness, yielding a very small amount of an intractable brown residue.

5.2.18 Reduction of $[\text{CpCr}(\text{NO})\text{I}]_2$ in presence of 1,5-cyclooctadiene (1,5-COD)

THF (~10 mL) was vacuum transferred onto a mixture of $[\text{CpCr}(\text{NO})\text{I}]_2$ (174 mg, 0.500 mmol) and Zn powder (0.16 g, 2.5 mmol). 1,5-cyclooctadiene (1,5-COD) was added by syringe

(0.60 mL, 0.53 g, 4.9 mmol), and the mixture was stirred for 3 d. The solvent was removed in vacuo, the black residue was extracted with CH_2Cl_2 (2 x 15 mL), and the extracts were filtered to yield a brown-black solution, which was reduced to dryness in vacuo. The residue was extracted with Et_2O (3 x 15 mL), and the extracts were filtered through Florisil to yield a yellow solution that was stripped to yield a small amount of a yellow oily material. Chromatography of this material on a pentane-packed column of Florisil (2 x 8 cm) using Et_2O as eluant afforded a single yellow band that was collected and reduced to dryness, again yielding a yellow oily material. An EI mass spectrum of this substance exhibited peaks attributable to $[\text{CpCr}(\text{NO})(\text{COD})]_2$. EI-MS (Probe Temp. 120 °C): m/z 510 (P^+), 480 (P^+-NO), 430 (P^+-2NO), 343 ($\text{P}^+-2\text{NO}-\text{COD}+\text{H}$).

5.2.19 Reduction of $[\text{CpCr}(\text{NO})\text{I}]_2$ in presence of acetylene

THF (~10 mL) was vacuum transferred onto a mixture of $[\text{CpCr}(\text{NO})\text{I}]_2$ (274 mg, 1.00 mmol) and Zn powder (0.16 g, 2.5 mmol). The atmosphere was removed in vacuo and replaced with acetylene. The mixture was stirred for 1 d, after which time the solvent was removed in vacuo. An Et_2O (10 mL) extract of the residue was loaded onto a pentane-packed column of Florisil (2 x 8 cm). Elution of the column with pentane effected the elution of a pale yellow band, which was discarded. Further elution with Et_2O effected the elution of a red-orange band that was collected and stripped to yield a small amount of red residue. An EI mass spectrum (probe temp. 120 °C) of this material revealed peaks at $m/z = 306, 276, \text{ and } 250$. The ^1H NMR spectrum exhibited two singlets with a 5:2 intensity ration, at $\delta = 5.01$ and 4.84.

5.2.20 Reduction of $[\text{CpCr}(\text{NO})\text{I}]_2$ in presence of diphenylacetylene

THF (~10 mL) was vacuum transferred onto a mixture of $[\text{CpCr}(\text{NO})\text{I}]_2$ (548 mg, 2.00 mmol), Cp_2Co (378 mg, 2.00 mmol), and diphenylacetylene (1.78 g, 10 mmol). The mixture was stirred for 2 h, after which time the IR spectrum of the reaction mixture exhibited a strong band at 1637 cm^{-1} in addition to features due to free diphenylacetylene. The solvent was removed in vacuo, the residue was extracted with Et_2O (3 x 15 mL), and the extracts were filtered through

neutral alumina I (2 x 3 cm) to obtain a red solution. Removal of the solvent in vacuo resulted in the precipitation of a great deal of a white solid (presumably unreacted diphenylacetylene) contaminated with a red material. Extraction, chromatography, and recrystallization all failed to effect the complete separation of the two materials.

Attempts to repeat this reaction with lesser amounts of diphenylacetylene resulted in no Et₂O-soluble nitrosyl-containing products.

5.2.21 Reduction of [CpCr(NO)I]₂ in presence of 1-phenylpropyne

THF (~10 mL) was vacuum transferred onto a mixture of [CpCr(NO)I]₂ (548 mg, 2.00 mmol) and Cp₂Co (378 mg, 2.00 mmol). 1-phenylpropyne (1.25 mL, 1.16 g, 10.0 mmol) was added by syringe. The mixture was stirred for 90 min, and the solvent was removed in vacuo. The residue was extracted with Et₂O (5 x 10 mL), and the extracts were filtered through neutral alumina I (2 x 3 cm) to obtain an orange solution. The solvent was removed in vacuo to yield a very small amount of a red oily intractable substance.

5.3 Characterization Data

Table 5.1. Numbering Scheme, Color, Yield and Elemental Analysis Data

complex	compd no.	color (yield, %)	elemental analysis found (calcd)		
			C	H	N
CpCr(NO)(CNCMe ₃) ₂	5.1	red (72)	57.41 (57.49)	7.24 (7.40)	13.40 (13.41)
[CpCr(NO)(CNCMe ₃) ₂] ⁺ PF ₆ ⁻	[5.1] ⁺ [PF ₆] ⁻	yellow (54)	39.17 (39.31)	4.84 (5.06)	8.97 (9.17)
[CpCr(NO)(CNCMe ₃) ₂] ⁺ BF ₄ ⁻	[5.1] ⁺ [BF ₄] ⁻	yellow (23)	45.40 (45.02)	5.90 (5.79)	10.23 (10.50)

Table 5.2. Mass Spectral, Infrared, NMR, and ESR Data

complex	mass spectrum (<i>m/z</i>)			IR (cm ⁻¹)	
				$\nu_{\text{NO}}, \nu_{\text{CN}}$ (Nujol)	$\nu_{\text{NO}}, \nu_{\text{CN}}$ (THF)
5.1	EI	313 [P ⁺]	temp 150 °C	1602, 2014 (br), 2112	1635, 2100
[5.1] ⁺ PF ₆ ⁻	FAB	313 [P ⁺]	145 [P ⁻]	1698, 2224	1712, 2207
[5.1] ⁺ BF ₄ ⁻	FAB	313 [P ⁺]	87 [P ⁻]	1728, 1741, 2204	1684, 1712, 2206

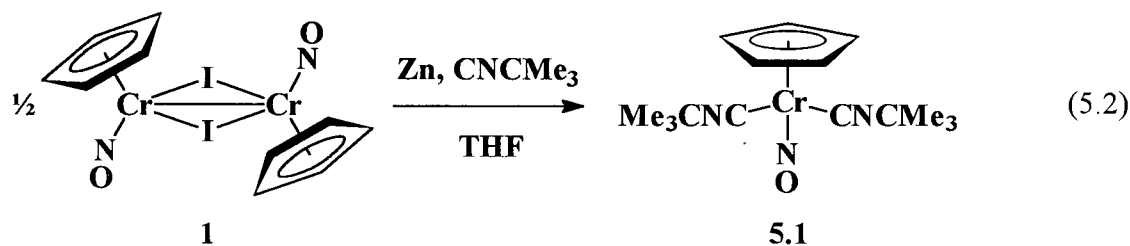
Table 5.3. NMR and ESR Data

complex	
5.1	¹ H: δ 4.89 (s, 5H, Cp), 1.05 (s, 18H, CMe ₃) ¹³ C{ ¹ H}: δ 31.1 (Me), 57.7 (CMe ₃), 89.8 (Cp), CNR not observed
[5.1] ⁺ PF ₆ ⁻	ESR: $g = 2.000$ $A_{\text{N}} = 4.2$ G $A_{\text{H}} = 0.8$ G $A_{\text{Cr}} = 16.2$ G
[5.1] ⁺ BF ₄ ⁻	ESR: $g = 2.000$ $A_{\text{N}} = 4.2$ G $A_{\text{H}} = 0.8$ G $A_{\text{Cr}} = 16.2$ G

5.4 Results and Discussion

5.4.1 Preparation of $\text{CpCr}(\text{NO})(\text{CNCMe}_3)_2$ (**5.1**)

The reduction of $[\text{CpCr}(\text{NO})\text{I}]_2$ by zinc in the presence of excess *tert*-butylisocyanide is a facile reaction and a simple experimental procedure. Monitoring of the THF reaction mixture by IR spectroscopy shows a loss of the starting nitrosyl band at 1678 cm^{-1} and the appearance of a new band at 1635 cm^{-1} , the lower nitrosyl-stretching frequency being consistent with the formation of a more electron-rich, 18e product. The high-yielding reaction effects the loss of the iodide ligand and the formation of bis(isocyanide) complex **5.1** (eq 5.2).



The spectroscopic characterization of complex **5.1** is wholly consistent with its formulation as depicted in eq 5.2. The mass spectrum exhibits the expected parent-ion peak at $m/z = 313$ as well as peaks attributable to loss of nitrosyl, butyl, and butylisocyanide fragments. The NMR spectra of the complex are also as expected, though a resonance due to the metal-bound isocyanide carbon is not observed in the ^{13}C NMR spectrum. This is common for such species, since the signal due to this carbon is expected to be of weak intensity and should be broadened by coupling to the isocyanide nitrogen nucleus.³

The preparation of **5.1** is similar to that shown in eq 3.5, i.e. the formation of the analogous 18e complex $\text{CpCr}(\text{NO})(\text{P}\{\text{OMe}\}_3)_2$ (**3.1**). For such a reaction to succeed, the trapping ligand must meet two requirements. First, it must be sufficiently nucleophilic that it can trap the $\text{CpCr}(\text{NO})$ fragment, otherwise the reduction will simply result in the decomposition of the starting material and a new $\text{CpCr}(\text{NO})(\text{L})_2$ complex will not be formed. Second, it must be sufficiently π -acidic that it can stabilize the 18e configuration. As discussed in Chapter 3, such a

ligand will withdraw electron density away from the $\{\text{Cr}(\text{NO})\}^6$ fragment and will lower the energy of the HOMO via the π -symmetry interaction. Both $\text{P}(\text{OMe})_3$ and *t*-BuNC clearly meet each of these requirements.

The *tert*-butylisocyanide ligand is isoelectronic with and formally analogous to CO, so the formation of a stable bis(isocyanide) complex is to be expected, given the known stability of the carbonyl analogue. Also as expected, the properties of **5.1** are similar to those of both $\text{CpCr}(\text{NO})(\text{CO})_2$ and the bis(phosphite) species **3.1**. For example, **5.1** is highly soluble in aliphatic hydrocarbon solvents, it is somewhat volatile, and the complex is bright red, typical of the red-to-orange colors of other known $\{\text{Cr}(\text{NO})\}^6$ $\text{CpCr}(\text{NO})$ species. Like $\text{CpCr}(\text{NO})(\text{CO})_2$, **5.1** is quite robust, and may be handled in air for short periods of time without noticeable decomposition. However, there is an important electronic difference that distinguishes $\text{CpCr}(\text{NO})(\text{CO})_2$ from both **5.1** and **3.1**.

Isocyanide ligands are generally regarded as better σ -donors but poorer π -acceptors than CO,³ and the IR data of the $\text{CpCr}(\text{NO})(\text{L})_2$ species reflect this lesser π -acceptor ability of *t*-BuNC. For example, the nitrosyl-stretching frequencies of bis(phosphite) **3.1**, bis(isocyanide) **5.1**, and $\text{CpCr}(\text{NO})(\text{CO})_2$ (Table 5.4). The nitrosyl frequency of the dicarbonyl compound is over 100 cm^{-1} higher in energy than that of either **3.1** or **5.1**, suggesting a much greater N-O bond strength in the carbonyl complex, and therefore a much more electron-poor metal center. Thus, carbonyl is a much stronger π -acid than either $\text{P}(\text{OMe})_3$ or CNCMe_3 , despite the formally analogous nature of the carbonyl and isocyanide ligands.

complex	$\nu_{\text{NO}} (\text{cm}^{-1})$
$\text{P}(\text{OMe})_3$	1609
CNCMe_3	1602
CO	1711

Table 5.4. Nitrosyl-stretching frequencies of $\text{CpCr}(\text{NO})(\text{L})_2$ in Nujol. L = $\text{P}(\text{OMe})_3$ (**3.1**), CNCMe_3 (**5.1**), and CO

Somewhat surprisingly, the IR frequencies exhibited by bis(phosphite) **3.1** and bis(isocyanide) **5.1** are nearly the same, suggesting that the two ligands have an approximately equal electronic effect on the $\text{CpCr}(\text{NO})$ fragment. In Chapter 3, $\text{P}(\text{OMe})_3$ was utilized as a ligand with intermediate π -acceptor/ σ -donor properties, i.e. one with a strong enough π -interaction to stabilize the 18e configuration of a $\text{CpCr}(\text{NO})(\text{L})_2$ fragment, but not so strong

that the ligands would be lost upon oxidation to the 17e cation, as is the case with CO in CpCr(NO)(CO)_2 . The fact that bis(isocyanide) **5.1** seems to be electronically more similar to $\text{CpCr(NO)(P(OMe)}_3)_2$ than CpCr(NO)(CO)_2 is consistent with *t*-BuNC being a better σ -base than CO and suggests that **5.1** might exhibit the same oxidative behavior as **3.1**, i.e. a reversible redox couple with the 17e cation $[\mathbf{5.1}]^+$.

5.4.2 Preparation of $[\text{CpCr(NO)(CNCMe}_3)_2]^+[\text{PF}_6]^-$ ($[\mathbf{5.1}]^+[\text{PF}_6]^-$)

Cyclic voltammetry of bis(isocyanide) **5.1** in THF reveals no observable reduction features to the solvent limit (~ -2.5 V). This markedly differentiates the complex from CpCr(NO)(CO)_2 , which exhibits a one-electron reduction at $E_{1/2} = -1.83$ V.⁴ A more important difference is the oxidation chemistry, for like bis(phosphite) **3.1**, $\text{CpCr(NO)(CNCMe}_3)_2$ exhibits a facile and reversible oxidation, the **5.1**/**5.1**⁺ couple occurring at $E_{1/2} = -0.18$ V (Figure 5.1). Thus, the isocyanide complex is even easier to oxidize than the phosphite species ($E_{1/2} = -0.03$ V), the isocyanide cation **5.1**⁺ being favored by about 150 mV compared to phosphite cation **3.1**⁺.

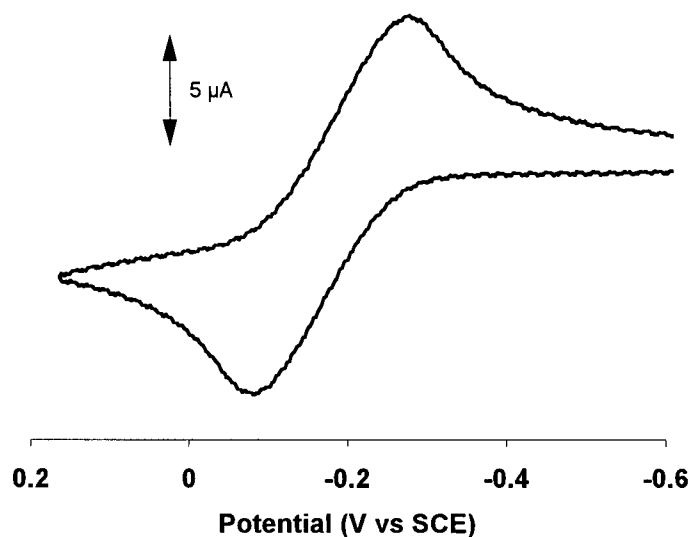
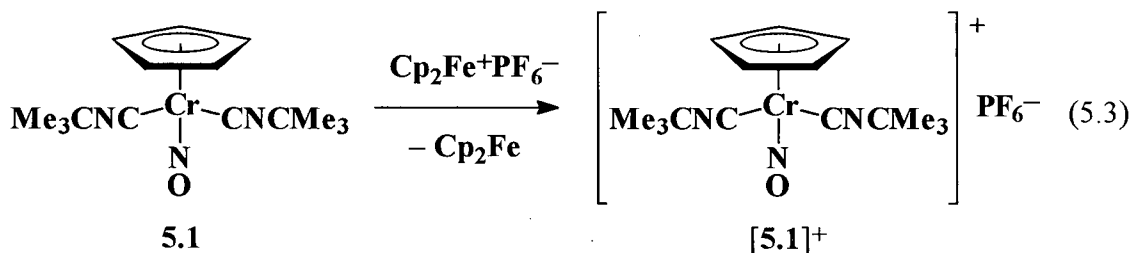


Figure 5.1. Cyclic voltammogram of **5.1** at 0.4 V/s

The peak-to-peak separation of these cyclic voltammograms is approximately equal to that observed for the highly reversible $\text{Cp}_2\text{Fe}/\text{Cp}_2\text{Fe}^+$ couple under identical conditions. This indicates that there is little reorganizational energy required to effect the redox process and, therefore, that there is little or no structural difference between **5.1** and $[\mathbf{5.1}]^+$.

The oxidative generation of $[\text{CpCr}(\text{NO})(\text{CNCMe}_3)_2]^+$ can easily be performed on a chemical scale. Reaction of equimolar amounts of $\text{CpCr}(\text{NO})(\text{CNCMe}_3)_2$ and $[\text{Cp}_2\text{Fe}]^+[\text{PF}_6]^-$ results in a rapid electron transfer and the formation of $[\text{CpCr}(\text{NO})(\text{CNCMe}_3)_2]^+[\text{PF}_6]^-$ ($[\mathbf{5.1}]^+[\text{PF}_6]^-$) as a bright yellow material (eq 5.3). As expected, the properties of this salt differ markedly from those of the 18e precursor. The yellow isocyanide salt is soluble only in solvents such as CH_2Cl_2 or THF, but is insoluble in Et_2O or hydrocarbon solvents. The complex $[\mathbf{5.1}]^+[\text{PF}_6]^-$ is more air-sensitive than the 18e analogue, as it transforms to a viscous brown tar within minutes of exposure to the atmosphere. Under inert atmosphere it appears to be indefinitely stable at room temperature.



As with the comparison of phosphite complexes **3.1** and $[\mathbf{3.1}]^+$, the one-electron oxidation causes a dramatic change in the nitrosyl-stretching frequency of the isocyanide species, with the Nujol mull spectrum of 17e $[\mathbf{5.1}]^+[\text{PF}_6]^-$ exhibiting a band nearly 100 cm^{-1} greater in energy than that of 18e **5.1** (1698 cm^{-1} vs. 1602 cm^{-1} , Figure 5.2). As well, the same effect is manifested in the IR bands due to the isocyanide ligands, which are affected by the change in electron density to an even greater extent than the nitrosyl. The C-N functional group, like N-O, exhibits an intense band in the IR spectrum, and the same orbital interactions between metal and ligand apply to both nitrosyl and isocyanide, since both are π -acidic, $(1\sigma, 2\pi)$ ligands. Thus, the decrease of electron density caused by oxidation of **5.1** to $[\mathbf{5.1}]^+$ results in less π -backbonding to both the nitrosyl and

the isocyanide ligands, so both the nitrosyl N-O and isocyanide C-N bonds are strengthened, and the stretching frequencies of both these groups move to higher energy.

Interestingly, the IR spectrum of $[5.1]^+$ exhibits only one apparent C-N band in both solution and the solid state, whereas two would be expected. Indeed, two C-N bands are evident in the spectrum of **5.1**, though they are broad and ill-defined in this case. This "loss" of an isocyanide band upon the oxidation of an 18e $\{\text{Cr}(\text{NO})\}_6$ complex to the 17e derivative has been observed previously.^{5a,c}

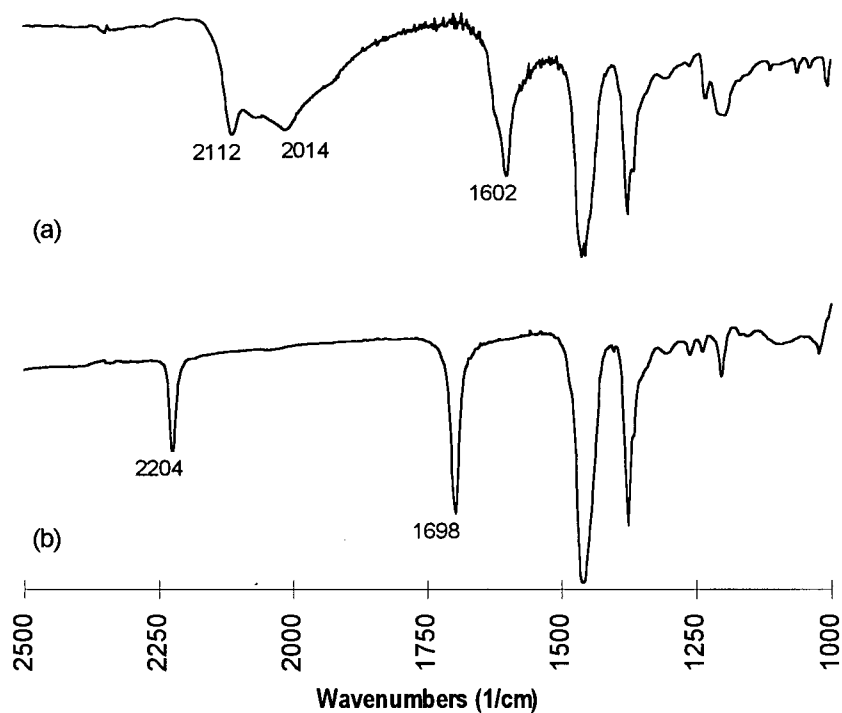


Figure 5.2. Nujol mull IR spectra of bis(isocyanide) complexes (a) **5.1** and (b) $[5.1]^+[\text{PF}_6]^-$

The other spectroscopic properties of $[5.1]^+[\text{PF}_6]^-$ are as expected. FAB-MS exhibits the parent peaks for both the cation and the anion, and the ESR spectrum of the complex in CH_2Cl_2 displays coupling of the unpaired electron to both the ^{14}N of the nitrosyl ligand and the 9.55 % abundant ^{53}Cr nucleus, as well as exhibiting fine structure due to coupling to the six equivalent protons of the Cp ligand.

5.4.3 Structural Analysis of $[\text{CpCr}(\text{NO})(\text{CNCMe}_3)_2]^+$ ($[\mathbf{5.1}]^+$)

As with other cationic species structurally characterized in this Thesis, X-ray quality crystals of cation $[\mathbf{5.1}]^+$ could only be formed using BPh_4^- as the counterion, the resulting salt crystallizing as orange needles. The solid-state structure of $[\mathbf{5.1}]^+$ is depicted in Figure 5.3. Although other nitrosyl isocyanide complexes are known, in both $\{\text{Cr}(\text{NO})\}^6$ and $\{\text{Cr}(\text{NO})\}^5$ configurations,⁵ this is the first such $\{\text{Cr}(\text{NO})\}^5$ complex to be structurally characterized.

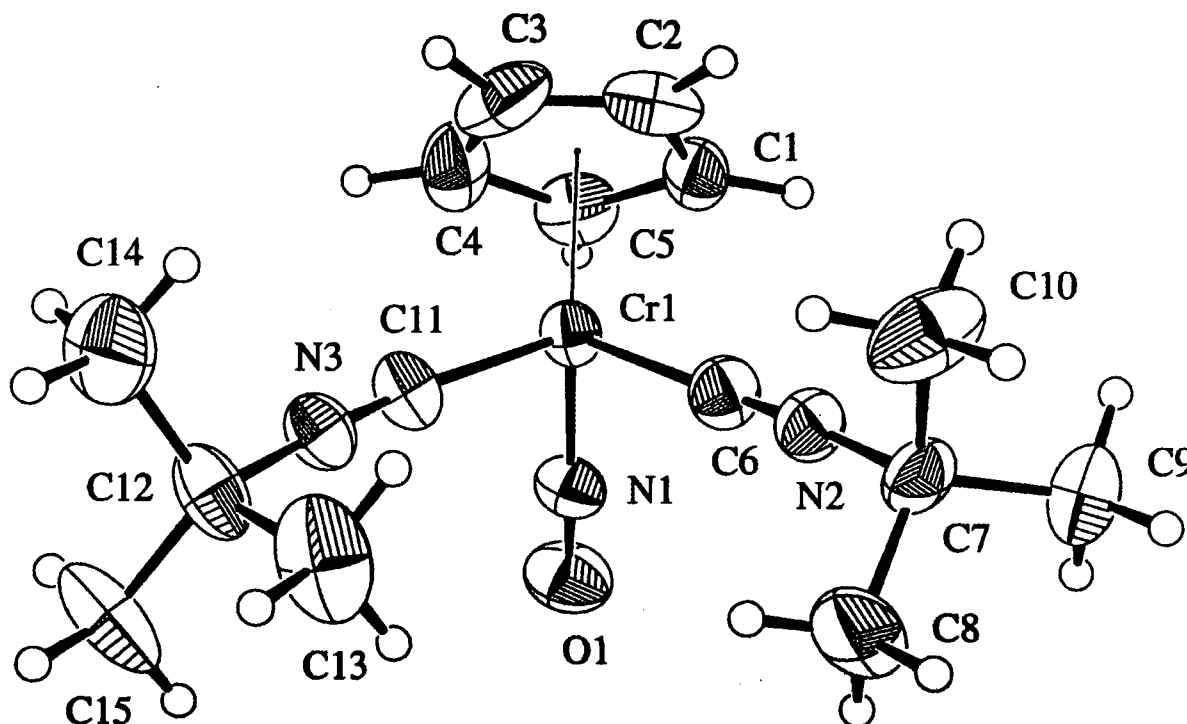


Figure 5.3. Molecular structure of $[\mathbf{5.1}]^+$. 50% probability ellipsoids are shown for non-hydrogen atoms. Hydrogen atoms are depicted as spheres of arbitrary radius.

The cation exhibits the expected three-legged piano-stool arrangement of ligands. Both the nitrosyl and the isocyanide ligands are essentially linear, with a Cr-N-O angle of $170.5(4)^\circ$ and Cr-C-N angles of $174.3(5)^\circ$ and $173.7(4)^\circ$. The angle between the two isocyanide ligands ($87.2(2)^\circ$) is somewhat more acute than the angle between the isocyanides and the nitrosyl ($98.2(2)^\circ$ and $99.5(2)^\circ$). The structure of $[\mathbf{5.1}]^+$ may be compared to that of other $\{\text{Cr}(\text{NO})\}^5$ $[\text{CpCr}(\text{NO})(\text{L})_2]^+$ cations, namely $[\text{CpCr}(\text{NO})(\text{NCMe}_2)]^+$ ⁶ and $[\text{CpCr}(\text{NO})(\text{NH}_3)_2]^+$ ($[\mathbf{2.1}]^+$).⁷ The M-L bond lengths to the isocyanide carbon atoms in $[\mathbf{5.1}]^+$ of $2.006(5)$ and $2.002(5)$ Å are

similar to those to the nitrile nitrogen atoms in $[\text{CpCr}(\text{NO})(\text{NCMe})_2]^+$ at 1.993 (12) and 2.025 (16) Å, and somewhat less than the Cr-N distances to the ammonia ligands of 2.082 (3) and 2.077 (3) Å in $[\mathbf{2.1}]^+$. The bis(ammonia) complex also differs from the other two species in the Cr-N-O bond lengths. The nitrosyl Cr-N distance of 1.665 (3) Å in $[\mathbf{2.1}]^+$ is somewhat shorter than those of $[\mathbf{5.1}]^+$ or $[\text{CpCr}(\text{NO})(\text{NCMe})_2]^+$, being 1.683 (4) and 1.685 Å, respectively. As well, the N-O distance of 1.203 (4) Å in $[\mathbf{2.1}]^+$ is somewhat longer, the corresponding distances in $[\mathbf{5.1}]^+$ and $[\text{CpCr}(\text{NO})(\text{NCMe})_2]^+$ being 1.178 (4) and 1.168 (8) Å.

These data are consistent with a more electron-rich metal center in the bis(ammonia) cation $[\mathbf{2.1}]^+$, which results in greater back-donation of electron density to the nitrosyl in the ammonia complex as compared to the nitrile or isocyanide species. This conclusion is in accord with the IR spectra of the same compounds. The nitrosyl-stretching frequencies observed in the Nujol mull and THF solution IR spectra of $[\text{CpCr}(\text{NO})(\text{NCMe})_2]^+$ (1709 and 1710 cm^{-1}) and $[\mathbf{5.1}]^+$ (1698 and 1712 cm^{-1}) are similar and are greater in energy than the corresponding bands for ammonia complex $[\mathbf{2.1}]^+$ (1667 and 1676 cm^{-1}).

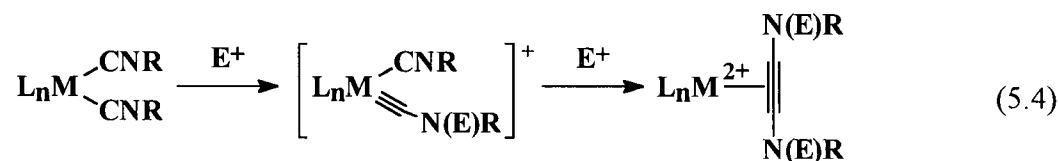
The conclusion that can be drawn from these data is that CNCMe_3 is a much poorer electron-donor ligand than NH_3 in the $[\text{CpCr}(\text{NO})(\text{L})_2]^+$ system, but it is comparable to NCMe. Given the π -acceptor properties of isocyanide ligands, CNCMe_3 must in fact be a better σ -base than NCMe, but this greater donation is offset by its π -acid ability, resulting in an approximately equal net donation of electron density to the metal.

The structure of the 18e derivative **5.1** has not been determined, but is expected to be similar to that of $[\mathbf{5.1}]^+$. Given that the electrochemical interconversion of **5.1** and $[\mathbf{5.1}]^+$ is highly reversible (*vide supra*), there cannot be any great structural distinction between the two complexes. The bis(phosphite) species **3.1** and $[\mathbf{3.1}]^+$ interconvert with the same degree of electrochemical reversibility, and the greatest structural difference between the two species is a 0.1 Å change in the chromium-phosphorus bond lengths.⁸ The largest expected structural difference between the two bis(isocyanide) compounds would similarly be a manifestation of the π -bonding in the complexes. Reduction of the 17e species leads to a greater backdonation of electron density to the isocyanide ligands, thus strengthening the Cr-C bonds and weakening the

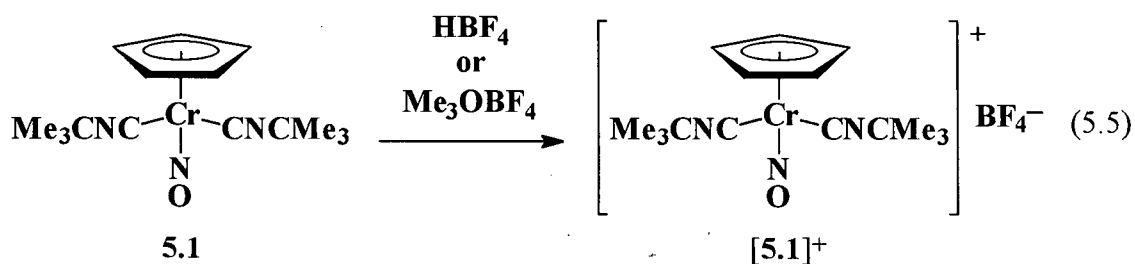
C-N bonds, the latter effect being observed in the IR spectra of the two compounds. Thus, 18e **5.1** is expected to have slightly shorter Cr-C bonds and slightly longer C-N bonds than those of 17e [**5.1**]⁺. Such a structural effect is exhibited by Cr(CNPh)₆⁺ and Cr(CNPh)₆.⁹

5.4.4 Reaction of Bis(isocyanide) **5.1** with Electrophiles

Isocyanide ligands are known to be susceptible to attack by electrophiles such as protons and alkyl cations, particularly in the case of zero-valent metal complexes.¹⁰ The end result of these reactions is often the coupling of two isocyanide ligands to yield a metal-bound diamidoacetylene. These reactions proceed via the formation of an intermediate amidocarbene ligand, which is the expected initial product of electrophilic attack on an isocyanide ligand (eq 5.4). Thus, it was of interest to investigate the reaction of bis(isocyanide) **5.1** with sources of both H⁺ and R⁺.



Instead of producing either a carbyne or an isocyanide-coupled product, reaction of CpCr(NO)(CNCMe₃)₂ with either HBF₄·Et₂O or [Me₃O]⁺[BF₄]⁻ results in the oxidation of the 18e isocyanide complex to its 17e cationic derivative (eq 5.5), which can be isolated as the tetrafluoroborate salt. The reaction with a solution of HBF₄·Et₂O is essentially instantaneous in Et₂O, and is noticeably endothermic. The corresponding reaction with [Me₃O]⁺[BF₄]⁻ leads to the same product, but is considerably slower, though it is probable that this is due primarily to the insolubility of the ionic oxonium salt in Et₂O.



The reduction byproduct of reaction 5.5 is presumably H₂ in the case of HBF₄ and ethane in the case of trimethyloxonium, though no efforts were made to detect these products. However, given the ease of oxidation of 18e **5.1** ($E_{1/2} = -0.18$ V), the oxidation of this compound by H⁺ to generate H₂ and [**5.1**]⁺ is clearly a thermodynamically favored redox reaction. Thus, instead of electrophilic attack at the isocyanide nitrogen, H⁺ simply effects a one-electron oxidation.

5.4.5 Treatment of Bis(isocyanide) **5.1** with Nucleophiles and other Small Molecules

Like carbonyl ligands, isocyanide ligands are known to be prone to attack by nucleophiles at the metal-bound carbon, generating amidocarbene complexes.¹¹ However, prolonged treatment of bis(isocyanide) **5.1** at ambient temperature in Et₂O with MeLi, PhLi, and Superhydride (LiEt₃BH) results in no apparent reaction as discerned by IR spectroscopy. Similarly, treatment of **5.1** in C₆D₆ with an excess of nucleophilic reagents such as H₂O or MeOH results in no change observable by ¹H NMR spectroscopy, and a similar lack of reaction was observed toward each of H₂, CO, and *p*-tolNCO, even when these solutions were heated to 60 °C.

5.4.6 Thermolysis of Bis(isocyanide) **5.1**

As noted above, C₆D₆ solutions of **5.1** are unchanged by exposure to H₂O, MeOH, H₂, CO, or *p*-tolNCO when heated to 60 °C. However, increasing the temperature of the solutions to 100 °C does effect a change in the ¹H NMR spectrum in that the signals due to **5.1** (δ 4.89, 1.05 ppm) are gradually lost and replaced by two new signals (δ 4.72, 1.59 ppm). The same signals are observed regardless of the added reagent, and are also observed in the absence of added reagent. This indicates that the generation of the newly-formed species does not involve a reaction with any of the added reagents, but is rather the result of a thermal transformation of **5.1** alone. The observed ¹H NMR spectra of the reaction in the presence of H₂ are depicted in Figure 5.4.

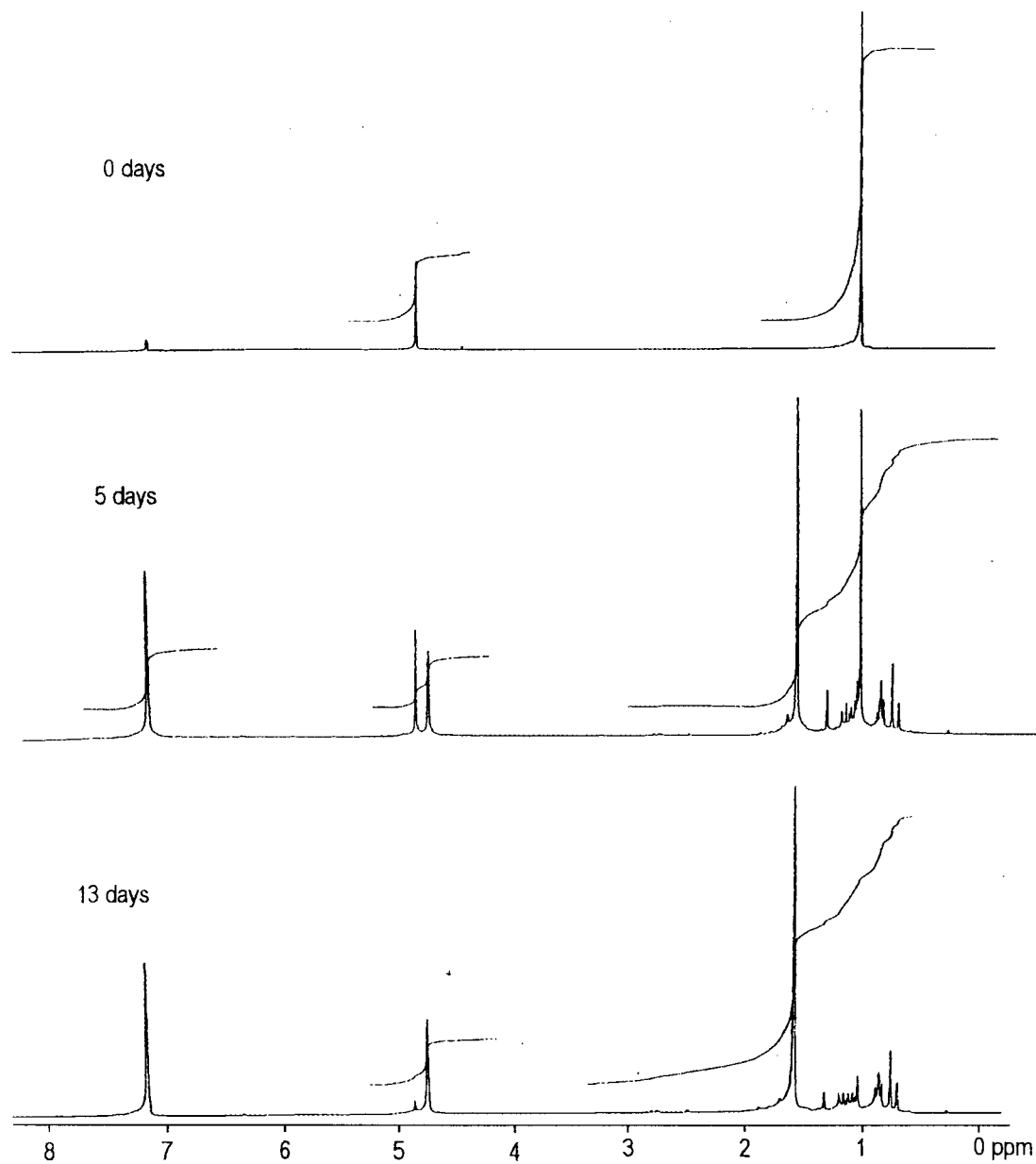


Figure 5.4. ^1H NMR spectra of $\text{CpCr}(\text{NO})(\text{CNCMe}_3)_2$ (5.1) in C_6D_6 in the presence of H_2 after heating at 100 °C for 0, 5, and 13 d.

An attempt was made to prepare this complex on a preparative scale. Heating of a THF solution of bis(isocyanide) **5.1** to 100 °C for 7 days results in the loss of the nitrosyl and isocyanide bands of the starting material from the solution IR spectrum, and the appearance of two new bands at 1690 and 2143 cm^{-1} . Unfortunately, attempts to isolate this new nitrosyl complex have not yet succeeded. Workup of the reaction mixture does afford an insoluble tan powder exhibiting a nitrosyl band at 1686 cm^{-1} as a Nujol mull, but the material is contaminated with paramagnetic byproducts.

5.4.7 Attempted Preparation of other CpCr(NO)(L)_2 Complexes

Attempts to extend eq 5.1 to ligands other than P(OMe)_3 and *t*-BuNC, i.e. the reduction of a 17e complex to form a new 18e species, did not meet with success. Attempts at zinc reduction of the 17e cation $[\text{CpCr(NO)(THF)}_2]^+$ in the presence of $\text{MeO}_2\text{CC}\equiv\text{CCO}_2\text{Me}$ or $\text{PhC}\equiv\text{CPh}$ resulted in no tractable products. Similar treatment of $[\text{CpCr(NO)(THF)}_2]^+$ with $\text{HC}\equiv\text{CH}$ appears to be hampered by acetylene polymerization. Treatment with pyridine affords only a small amount of the unreduced 17e species, $[\text{CpCr(NO)(py)}_2]^+$. Similarly, treatment of $[\text{CpCr(NO)I}]_2$ with zinc in the presence of 2,3-dimethylbutadiene and ethylene yielded no tractable materials.

Some reactions bore indications of the formation of the desired $\{\text{Cr(NO)}\}^6$ CpCr(NO)(L)_2 species; either in the form of the red-to-yellow colors distinctive of such complexes, observed nitrosyl frequencies in the solution IR spectra, or both. However, no new complexes could be isolated from these reaction mixtures. Treatment of $[\text{CpCr(NO)(THF)}_2]^+$ with zinc and 2,3-dimethylbutadiene afforded an orange solution exhibiting an IR band at 1685 cm^{-1} , while 1,10-phenanthroline afforded a red-orange solution. Reaction of $[\text{CpCr(NO)I}]_2$ with zinc in the presence of 1,5-cyclooctadiene afforded a yellow oil, while $\text{PhC}\equiv\text{CH}$ and $\text{PhC}\equiv\text{CPh}$ yielded orange and red solutions, the latter exhibiting a strong IR band at 1637 cm^{-1} , when $[\text{CpCr(NO)I}]_2$ was reduced by cobaltocene. Reduction in the presence of $\text{HC}\equiv\text{CH}$ afforded a small amount of a red material, the partial characterization of which suggests the formation of a

nitrosyl-acetylene complex. Although it seems probable that these latter reactions did in fact produce 18e products, the products were clearly not generated in a high enough yield to allow their isolation and characterization.

These reactions may suffer in part from the variable nature of the 17e complex that undergoes reduction. Although $[\text{CpCr}(\text{NO})(\text{THF})_2]^+$ itself is easily reduced,¹² this complex may well not remain intact in the presence of an excess of Lewis base, so that it will be a ligand-substituted derivative that must undergo reduction. Similarly, $[\text{CpCr}(\text{NO})\text{I}]_2$ exists as the solvated monomer in THF, and this species too will be prone to substitution. In the reductive formations of bis(phosphite) **3.1** and bis(isocyanide) **5.1**, it is likely the complexes $\text{CpCr}(\text{NO})(\text{P}\{\text{OMe}\}_3)\text{I}$ and $\text{CpCr}(\text{NO})(\text{CNCMe}_3)\text{I}$ and not the starting reagent that are reduced by zinc. Thus, these reactions may require the added Lewis base to perform two roles: not only must it serve as a suitable trapping agent that will stabilize the desired 18e product, but it may also need to serve as a ligand to a 17e precursor and render that precursor more prone to reduction. Thus, the generally poor nucleophilicity of olefins and alkynes may account for the lack of isolable products in these reactions.

5.5 Epilogue and Future Work

The synthesis of both $\text{CpCr(NO)(CNCMe}_3)_2$ and $[\text{CpCr(NO)(CNCMe}_3)_2]^+[\text{PF}_6]^-$ affords the second pair of CpCr(NO) complexes that differ by one electron and so are stable in both the 17 and 18e configurations. The reversible redox behavior is consistent with the known electronic properties of the CNCMe_3 ligand, which can function as both a σ -donor and a π -acceptor. Although this work has defined the extreme limits of redox behavior, i.e. $[\text{CpCr(NO)(NH}_3)_2]^+$ is irreversibly reduced at a large negative potential, CpCr(NO)(CO)_2 is irreversibly oxidized at high positive potential, and $[\text{CpCr(NO)(L)}_2]^{o/+}$ ($\text{L} = \text{P(OMe)}_3, \text{CNCMe}_3$) are reversibly interchanged at near-zero potential, these merely represent three points indicative of an underlying continuum. The limits of how electron-rich or -poor a system will exhibit reversible reduction or oxidation remain to be defined, and a series of aryl-substituted $\text{CpCr(NO)(CNaryl)}_2$ complexes would be well-suited to this task.

As in the case of bis(phosphite) species **3.1** and $[\mathbf{3.1}]^+$, the pair of bis(isocyanide) complexes provide an opportunity to compare reactivities of compounds in the two configurations, though in the case of the bis(isocyanide) species the differences in reactivity could be manifested in both ligand-based as well as metal-based chemistry. Although some effort has been made to examine the chemistry of the neutral $\{\text{Cr(NO)}\}^6$ species, that of the cationic $\{\text{Cr(NO)}\}^5$ form remains unexplored. For instance, it is apparent that 18e $\text{CpCr(NO)(CNCMe}_3)_2$ is resistant toward attack by nucleophiles. It is likely that the lesser electron density of the 17e derivative will render the CNR ligand more susceptible to nucleophilic attack, such a trend in isocyanide reactivity having been previously observed.¹³ Nucleophilic attack at the metal-bound carbon of an isocyanide ligand would yield an amidocarbene complex, and the carbene ligand is one that has seen little investigation in the CpM(NO) system. As other ligands capable of both σ - and π -bonding, carbene and derivative carbyne ligands would be worthy of study with respect to the various electronic configurations of the CpCr(NO) complexes.

5.6 References and Notes

- (1) Legzdins, P.; Nurse, C. R. *Inorg. Chem.* **1985**, *24*, 327.
- (2) The hexafluorophosphate salt was prepared by addition of NaPF_6 to an aqueous $[\text{Cp}_2\text{Fe}]_2\text{SO}_4$ solution. Jolly, W. L. *The Synthesis and Characterization of Inorganic Compounds*; Prentice-Hall: Englewood Cliffs, NJ, 1970; p 487.
- (3) Collman, J. P.; Hegedus, L. S.; Norton, J. R.; Finke, R. G. *Principles and Applications of Organotransition Metal Chemistry*; University Science Books: Mill Valley, CA, 1987; p 148.
- (4) Geiger, W. E.; Rieger, P. H.; Tulyathan, B.; Rausch, M. D. *J. Am. Chem. Soc.* **1984**, *106*, 7000. The reduction results in a bending of the nitrosyl ligand so as to avoid the unfavorable $19e$ configuration. Such a bending is consistent with the $\{\text{M}(\text{NO})\}^7$ configuration of the $[\text{CpCr}(\text{NO})(\text{CO})_2]^-$ anion.
- (5) (a) Robinson, W. R.; Wigley, D. E.; Walton, R. A. *Inorg. Chem.* **1985**, *24*, 918. (b) Wigley, D. E.; Walton, R. A. *Inorg. Chem.* **1983**, *22*, 3138. (c) Wigley, D. E.; Walton, R. A. *Organometallics* **1982**, *1*, 1322.
- (6) Chin, T. T.; Legzdins, P.; Trotter, J.; Yee, V. C. *Organometallics* **1992**, *11*, 913.
- (7) Chapter 2, and also see: Legzdins, P.; McNeil, W. S.; Batchelor, R. J.; Einstein, F. W. B. *J. Am. Chem. Soc.* **1995**, *117*, 10521.
- (8) Chapter 3, and also see reference 7.
- (9) Bohling, D. A.; Mann, K. R. *Inorg. Chem.* **1984**, *23*, 1426.
- (10) (a) Filippou, A. C.; Grünleitner, W. *Z. Naturforsch., B* **1991**, *46*, 216. (b) Acho, J. A.; Lippard, S. J. *Organometallics* **1994**, *13*, 1294. For a recent review of coupling reactions of isocyanides and other two-faced π ligands, see: Mayr, A.; Bastos, C. M. In *Progress in Inorganic Chemistry, Vol. 40*, Lippard, S. J., Ed.; John Wiley & Sons, New York: 1992.
- (11) Reference 3, p 404.

- (12) $[\text{CpCr}(\text{NO})(\text{THF})_2]^+[\text{PF}_6]^-$ exhibits an irreversible reduction at $E_{p,c} \sim -0.08$ V in THF at a scan rate of 0.4 V/s. Legzdins, P.; Shaw, M. J., unpublished observations.
- (13) Chatt, J; Richards, R. L.; Royston, G. H. D. *J. Chem. Soc., Dalton Trans.* **1973**, 1433.

Appendix

Table A1. Crystallographic Data for Complexes [2.1]⁺[BPh₄]⁻·NCMe, 2.7, 3.1, [3.1]⁺[BPh₄]⁻, and [5.1]⁺[BPh₄]⁻.

	[2.1] ⁺ BPh ₄ ⁻ ·NCMe	2.7	3.1	[3.1] ⁺ BPh ₄ ⁻	[5.1] ⁺ BPh ₄ ⁻
formula	C ₃₁ H ₃₄ N ₄ OBCr	C ₈ H ₁₂ N ₂ OCl	C ₁₁ H ₂₃ NO ₇ P ₂ Cr	C ₃₅ H ₄₃ NO ₇ BP ₂ Cr	C ₃₉ H ₄₃ N ₃ OBCr
formula weight	541.44	331.09	395.25	714.48	632.59
crystal color	green	green	orange	yellow	orange
cryst. size (mm)	0.11x0.18x0.19	0.11x0.20x0.22	0.22x0.33x0.39	0.17x0.31x0.36 0.28x0.34x0.40	0.20x0.25x0.50
crystal system	monoclinic	triclinic	monoclinic	monoclinic	monoclinic
space group	P2 ₁ /n	P2 ₁ /n	P $\bar{1}$	P2 ₁ /a	P2 ₁ /n
a (Å)	9.478 (3)	8.0497 (8)	18.080 (4)	10.086 (2)	13.197 (1)
b (Å)	19.288 (7)	8.3273 (17)	9.320 (4)	22.253 (3)	17.658 (3)
c (Å)	15.427 (6)	9.3284 (9)	21.068 (3)	16.150 (4)	16.758 (1)
α (degrees)		108.182 (12)			
β (degrees)	91.99 (3)	92.370 (8)	93.02 (2)	90.42 (2)	112.554 (7)
γ (degrees)		94.759 (2)			
V (Å ³)	2818.5	590.54	3545.1	3624.7	3606.7
Z	4	2	8	4	4
D _{calc} (g/cm ³)	1.276	1.862	1.481	1.309	1.165
λ (Mo Kα ₁) (Å)	0.70930	0.70930	0.70930	0.70930	0.71069
μ (Mo Kα)	4.2 cm ⁻¹	35.0 cm ⁻¹	8.3 cm ⁻¹	4.4 cm ⁻¹	3.5 cm ⁻¹
T (K)	200	295	205	195	294
trans	0.934-0.955	0.560-0.707	0.715-0.802	-	0.971-1.000
2θ _{max}	45	50	45	45	50
no. observations	2185	1756	3356	3334	2554
no. variables	310	123	411	449	430
goodness of fit	1.60	1.63	1.86	2.23	1.74
R	0.038	0.024	0.040	0.044	0.041
R _w	0.036	0.033	0.050	0.052	0.033
max shift/error	0.01	0.01	0.04	0.02	0.01

Table A2. Fractional Coordinates and Equivalent Isotropic Displacement Parameters (\AA^2) for the Non-hydrogen Atoms of $[\text{CpCr}(\text{NO})(\text{NH}_3)_2][\text{BPh}_4]\cdot\text{NCMe}$

Atom	x	y	z	U_{eq}^a
Cr	0.86980(7)	0.26549(3)	0.21633(4)	0.0283
O	0.9917(4)	0.19297(15)	0.07582(21)	0.0474
N(1)	0.9510(4)	0.22237(16)	0.13900(22)	0.0310
N(2)	0.9297(4)	0.20307(15)	0.32135(20)	0.0362
N(3)	1.0345(3)	0.33286(15)	0.24842(20)	0.0349
N(4)	0.3530(5)	0.18396(21)	0.9708(3)	0.0627
C(1)	0.6423(5)	0.2404(3)	0.2144(4)	0.0457
C(2)	0.6657(5)	0.2918(3)	0.2774(4)	0.0458
C(3)	0.7132(5)	0.35060(24)	0.2376(4)	0.0440
C(4)	0.7207(5)	0.3360(3)	0.1490(4)	0.0432
C(5)	0.6731(5)	0.2685(3)	0.1347(4)	0.0471
C(6)	0.1859(5)	0.07932(20)	0.9857(3)	0.0424
C(7)	0.2796(5)	0.13794(22)	0.9785(3)	0.0391
C(11)	1.00769(17)	0.01959(12)	0.28695(15)	0.0215
C(12)	0.92481(24)	0.03870(12)	0.21344(12)	0.0255
C(13)	0.78268(23)	0.05336(13)	0.21749(14)	0.0279
C(14)	0.71517(18)	0.05028(13)	0.29579(18)	0.0337
C(15)	0.7930(3)	0.03224(13)	0.36907(14)	0.0326
C(16)	0.93510(24)	0.01720(12)	0.36452(12)	0.0273
C(21)	1.23766(24)	-0.02009(11)	0.19489(13)	0.0205
C(22)	1.37343(23)	-0.00634(11)	0.16818(15)	0.0267
C(23)	1.43087(19)	-0.03735(13)	0.09624(16)	0.0291
C(24)	1.3522(3)	-0.08509(12)	0.04790(13)	0.0312
C(25)	1.21715(24)	-0.10004(11)	0.07177(14)	0.0330
C(26)	1.16245(18)	-0.06862(12)	0.14481(15)	0.0265
C(31)	1.2371(3)	0.09044(9)	0.30230(15)	0.0205
C(32)	1.2590(3)	0.11856(11)	0.38542(13)	0.0305
C(33)	1.2999(3)	0.18640(12)	0.39934(14)	0.0352
C(34)	1.3196(3)	0.23049(9)	0.33018(19)	0.0342
C(35)	1.2951(3)	0.20476(11)	0.24761(15)	0.0325
C(36)	1.2548(3)	0.13713(12)	0.23482(12)	0.0269
C(41)	1.23972(24)	-0.04399(10)	0.35863(14)	0.0197
C(42)	1.37470(22)	-0.03852(10)	0.39844(15)	0.0250
C(43)	1.43097(20)	-0.08985(13)	0.45291(15)	0.0316
C(44)	1.3544(3)	-0.14814(11)	0.47059(14)	0.0317
C(45)	1.2206(3)	-0.15564(10)	0.43317(16)	0.0307
C(46)	1.16583(19)	-0.10477(12)	0.37839(15)	0.0285
B	1.1792(5)	0.01103(21)	0.2862(3)	0.0212

^a U_{eq} is the cube root of the product of the principal axes of the displacement ellipsoid.

Table A3. Fractional Coordinates and Isotropic Displacement Parameters (\AA^2) for the Hydrogen Atoms of $[\text{CpCr}(\text{NO})(\text{NH}_3)_2][\text{BPh}_4]\cdot\text{NCMe}$.

Atom	x	y	z	U_{iso}
H(1)	0.61103(41)	0.19442(26)	0.22466(35)	0.0534(63)
H(2)	0.65103(44)	0.28679(26)	0.33773(34)	0.0539(63)
H(3)	0.73668(44)	0.39330(24)	0.26524(36)	0.0557(63)
H(4)	0.75289(45)	0.36688(25)	0.10598(35)	0.0579(63)
H(5)	0.66321(42)	0.24581(27)	0.08014(33)	0.0555(63)
H(6)	0.87557(219)	0.16273(71)	0.31990(120)	0.0795(94)
H(7)	1.02488(84)	0.19164(127)	0.31790(116)	0.0795(94)
H(8)	0.91546(287)	0.22678(71)	0.37296(39)	0.0795(94)
H(9)	1.04601(207)	0.36423(93)	0.20269(83)	0.0728(91)
H(10)	1.11756(86)	0.30716(49)	0.25765(175)	0.0728(91)
H(11)	1.01380(163)	0.35726(106)	0.29905(101)	0.0728(91)
H(12)	0.96825(33)	0.04162(18)	0.15898(14)	0.0231(23)
H(13)	0.73048(32)	0.06570(19)	0.16611(17)	0.0302(23)
H(14)	0.61735(19)	0.06042(19)	0.29862(25)	0.0330(23)
H(15)	0.74878(34)	0.03008(19)	0.42334(16)	0.0342(23)
H(16)	0.98591(33)	0.00467(18)	0.41633(14)	0.0262(23)
H(22)	1.42962(31)	0.02584(15)	0.20073(21)	0.0254(23)
H(23)	1.52388(22)	-0.02587(18)	0.08019(23)	0.0298(23)
H(24)	1.39103(36)	-0.10712(17)	-0.00093(16)	0.0315(23)
H(25)	1.16103(33)	-0.13179(16)	0.03850(20)	0.0326(23)
H(26)	1.06995(21)	-0.08082(17)	0.16111(22)	0.0247(23)
H(32)	1.24498(37)	0.08968(15)	0.43426(15)	0.0295(23)
H(33)	1.31468(40)	0.20295(17)	0.45694(15)	0.0345(23)
H(34)	1.34919(38)	0.27708(10)	0.33923(25)	0.0356(23)
H(35)	1.30620(38)	0.23424(15)	0.19900(19)	0.0344(23)
H(36)	1.23811(39)	0.12139(17)	0.17702(12)	0.0249(23)
H(42)	1.42960(30)	0.00162(13)	0.38786(23)	0.0233(23)
H(43)	1.52324(23)	-0.08442(19)	0.47803(22)	0.0323(23)
H(44)	1.39276(38)	-0.18294(15)	0.50808(20)	0.0343(23)
H(45)	1.16625(35)	-0.19570(12)	0.44505(24)	0.0308(23)
H(46)	1.07403(22)	-0.11126(17)	0.35300(22)	0.0273(23)
H(61)	0.22302(204)	0.04778(92)	1.02790(156)	0.1048(115)
H(62)	0.09576(116)	0.09482(65)	1.00263(207)	0.1048(115)
H(63)	0.17651(284)	0.05633(110)	0.93129(70)	0.1048(115)

Table A4. Fractional Coordinates and Equivalent Isotropic Displacement Parameters (\AA^2) for the Non-Hydrogen Atoms of CpCrI(NO) ($\text{NH}_2\text{CH}_2\text{CHCH}_2$)

Atom	x	y	z	U_{eq}^a
I	0.29225 (3)	0.21692 (3)	0.13749 (3)	0.0518
Cr	0.61443 (7)	0.33267 (7)	0.21080 (6)	0.0378
O	0.5945 (4)	0.6838 (4)	0.2475 (3)	0.0592
N(1)	0.5959 (4)	0.5365 (4)	0.2222 (3)	0.0435
N(2)	0.6696 (4)	0.2503 (4)	-0.0155 (3)	0.0428
C(1)	0.7329 (8)	0.4047 (7)	0.4412 (5)	0.0632
C(2)	0.6178 (6)	0.2618 (9)	0.4219 (5)	0.0646
C(3)	0.6751 (7)	0.1268 (6)	0.3089 (6)	0.0610
C(4)	0.8197 (5)	0.1875 (6)	0.2622 (5)	0.0543
C(5)	0.8542 (6)	0.3585 (7)	0.3405 (5)	0.0626
C(6)	0.8219 (5)	0.3313 (6)	-0.0572 (5)	0.0580
C(7)	0.8467 (6)	0.2711 (7)	-0.2212 (5)	0.0644
C(8)	0.9744 (8)	0.2087 (8)	-0.2827 (7)	0.0918

^a U_{eq} is the cube root of the product of the principal axes of the displacement ellipsoid.

Table A5. Fractional Coordinates and Isotropic Displacement Parameters (\AA^2) for the hydrogen atoms of CpCrI(NO) ($\text{NH}_2\text{CH}_2\text{CHCH}_2$).

Atom	x	y	z	U_{iso}
H(1)	0.7279	0.5145	0.5117	0.088 (8)
H(2)	0.5202	0.2574	0.4750	0.102 (8)
H(3)	0.6230	0.0137	0.2716	0.090 (8)
H(4)	0.8857	0.1223	0.1877	0.078 (8)
H(5)	0.9454	0.4314	0.3273	0.088 (8)
H(61)	0.9157	0.3079	-0.0045	0.105 (14)
H(62)	0.8153	0.4505	-0.0269	0.105 (14)
H(7)	0.7575	0.2805	-0.2872	0.162 (22)
H(81)	1.0670	0.1966	-0.2218	0.193 (22)
H(82)	0.9775	0.1740	-0.3896	0.193 (22)
H(21)	0.6797	0.1382	-0.0410	0.079 (12)
H(22)	0.5825	0.2678	-0.0706	0.079 (12)

Table A6. Fractional Coordinates and Equivalent Isotropic Displacement Parameters (\AA^2) for the Non-hydrogen Atoms of $\text{CpCr}(\text{NO})\{\text{P}(\text{OMe})_3\}_2$.

Atom	x	y	z	U_{eq}^a
Cr(1)	0.80465(4)	0.35311(8)	0.12347(3)	0.0225
Cr(2)	0.65483(4)	-0.08167(8)	0.38287(4)	0.0234
P(1)	0.88762(7)	0.30400(15)	0.20322(6)	0.0318
P(2)	0.86472(7)	0.23219(14)	0.05039(6)	0.0270
P(3)	0.60119(7)	-0.20407(16)	0.45928(6)	0.0336
P(4)	0.62228(8)	-0.23438(14)	0.30504(6)	0.0322
O(1)	0.86830(23)	0.6269(4)	0.09388(22)	0.0501
O(2)	0.79268(19)	-0.2327(5)	0.40458(23)	0.0499
O(11)	0.97267(18)	0.2655(4)	0.19211(18)	0.0466
O(12)	0.86824(20)	0.1654(4)	0.24400(16)	0.0411
O(13)	0.90378(22)	0.4242(4)	0.25645(19)	0.0488
O(21)	0.87008(20)	0.0596(4)	0.05045(16)	0.0377
O(22)	0.94710(18)	0.2873(4)	0.04318(17)	0.0410
O(23)	0.83106(20)	0.2310(4)	-0.02208(16)	0.0385
O(31)	0.63560(21)	-0.3588(4)	0.46932(17)	0.0449
O(32)	0.6026(3)	-0.1370(5)	0.53003(20)	0.0635
O(33)	0.51437(22)	-0.2269(6)	0.46145(23)	0.0650
O(41)	0.55333(21)	-0.1859(4)	0.26027(18)	0.0462
O(42)	0.59431(23)	-0.3970(4)	0.31753(20)	0.0514
O(43)	0.68389(23)	-0.2770(4)	0.25695(19)	0.0577
N(1)	0.84346(21)	0.5104(5)	0.10682(19)	0.0335
N(2)	0.73433(22)	-0.1686(4)	0.39611(20)	0.0325
C(1)	0.6884(3)	0.3957(6)	0.0920(3)	0.0330
C(2)	0.70413(24)	0.2505(6)	0.08191(24)	0.0323
C(3)	0.7233(3)	0.1875(6)	0.1415(3)	0.0326
C(4)	0.71863(24)	0.2963(6)	0.18766(24)	0.0315
C(5)	0.6969(3)	0.4231(6)	0.1576(3)	0.0358
C(6)	0.6981(3)	0.1303(5)	0.3617(3)	0.0334
C(7)	0.6703(3)	0.1373(5)	0.4223(3)	0.0361
C(8)	0.5942(3)	0.1106(5)	0.4157(3)	0.0376
C(9)	0.5751(3)	0.0882(5)	0.3516(3)	0.0317
C(10)	0.6396(3)	0.0984(5)	0.3181(3)	0.0330
C(11)	1.0210(3)	0.3755(8)	0.1691(3)	0.0563
C(12)	0.9157(4)	0.1182(8)	0.2971(3)	0.0599
C(13)	0.8565(3)	0.5416(7)	0.2670(3)	0.0550
C(21)	0.9010(3)	-0.0149(6)	0.1048(3)	0.0423
C(22)	0.9937(3)	0.2301(8)	-0.0052(3)	0.0582
C(23)	0.8094(4)	0.3638(7)	-0.0504(3)	0.0578
C(31)	0.6115(4)	-0.4600(7)	0.5159(3)	0.0562
C(32)	0.6710(5)	-0.0913(8)	0.5596(3)	0.0710
C(33)	0.4667(3)	-0.2346(9)	0.4088(4)	0.0616
C(41)	0.5283(4)	-0.2707(8)	0.2054(3)	0.0702
C(42)	0.6429(4)	-0.5083(6)	0.3376(3)	0.0521
C(43)	0.7349(4)	-0.1688(7)	0.2370(3)	0.0578

^a U_{eq} is the cube root of the product of the principal axes of the displacement ellipsoid.

Table A7. Fractional Coordinates and Isotropic Displacement Parameters (\AA^2) for the Hydrogen Atoms of $\text{CpCr(NO)}\{\text{P(OMe)}_3\}_2$.

Atom	x	y	z	U_{iso}
H(1)	0.6745	0.4638	0.0600	0.041(7)
H(2)	0.7022	0.2027	0.0420	0.041(7)
H(3)	0.7368	0.0902	0.1491	0.041(7)
H(4)	0.7287	0.2846	0.2321	0.041(7)
H(5)	0.6891	0.5126	0.1778	0.041(7)
H(6)	0.7482	0.1452	0.3519	0.043(7)
H(7)	0.6981	0.1564	0.4609	0.043(7)
H(8)	0.5611	0.1082	0.4492	0.043(7)
H(9)	0.5267	0.0694	0.3336	0.043(7)
H(10)	0.6432	0.0856	0.2737	0.043(7)
H(111)	1.0691	0.3368	0.1649	0.13(2)
H(112)	1.0237	0.4531	0.1983	0.13(2)
H(113)	1.0019	0.4088	0.1289	0.13(2)
H(121)	0.8953	0.0347	0.3153	0.10(1)
H(122)	0.9635	0.0968	0.2830	0.10(1)
H(123)	0.9195	0.1921	0.3282	0.10(1)
H(131)	0.8772	0.5986	0.3008	0.17(2)
H(132)	0.8513	0.5981	0.2294	0.17(2)
H(133)	0.8093	0.5072	0.2777	0.17(2)
H(211)	0.8999	-0.1152	0.0967	0.05(1)
H(212)	0.9508	0.0151	0.1133	0.05(1)
H(213)	0.8729	0.0058	0.1405	0.05(1)
H(221)	1.0406	0.2760	-0.0021	0.19(3)
H(222)	0.9999	0.1298	0.0009	0.19(3)
H(223)	0.9708	0.2473	-0.0461	0.19(3)
H(231)	0.7908	0.3474	-0.0928	0.14(2)
H(232)	0.8510	0.4260	-0.0507	0.14(2)
H(233)	0.7720	0.4065	-0.0267	0.14(2)
H(311)	0.6396	-0.5457	0.5136	0.16(2)
H(312)	0.6185	-0.4196	0.5571	0.16(2)
H(313)	0.5605	-0.4811	0.5075	0.16(2)
H(321)	0.6626	-0.0548	0.6007	0.31(5)
H(322)	0.7042	-0.1703	0.5632	0.31(5)
H(323)	0.6918	-0.0182	0.5346	0.31(5)
H(331)	0.4177	-0.2488	0.4217	0.13(2)
H(332)	0.4803	-0.3125	0.3828	0.13(2)
H(333)	0.4690	-0.1477	0.3854	0.13(2)
H(411)	0.4868	-0.2255	0.1845	0.18(3)
H(412)	0.5673	-0.2782	0.1770	0.18(3)
H(413)	0.5147	-0.3638	0.2189	0.18(3)
H(421)	0.6156	-0.5945	0.3421	0.14(2)
H(422)	0.6669	-0.4834	0.3773	0.14(2)
H(423)	0.6789	-0.5219	0.3069	0.14(2)
H(431)	0.7680	-0.2102	0.2086	0.10(1)
H(432)	0.7623	-0.1320	0.2731	0.10(1)
H(433)	0.7081	-0.0932	0.2162	0.10(1)

Table A8. Fractional Coordinates and Isotropic or Equivalent Isotropic Displacement Parameters (\AA^2) for the Non-hydrogen Atoms of $[\text{CpCr}(\text{NO})\{\text{P}(\text{OMe})_3\}_2][\text{BPh}_4]$.

Atom	x	y	z	$U_{iso/eq}^a$
Cr	0.63726(7)	0.41498(3)	0.13163(4)	0.0344
P(1) ^b	0.85838(22)	0.39189(11)	0.10085(14)	0.0365
P(101) ^c	0.8475(20)	0.3825(11)	0.0874(14)	0.0365
P(2)	0.68660(12)	0.44992(6)	0.26522(7)	0.0357
O(1)	0.6452(5)	0.53216(19)	0.0587(3)	0.0832
O(11) ^b	0.9697(3)	0.43147(17)	0.14095(22)	0.0470
O(111) ^c	0.944(3)	0.4417(10)	0.0682(19)	0.046(8)
O(12) ^b	0.8932(3)	0.32734(17)	0.13518(21)	0.0408
O(112) ^c	0.934(4)	0.3517(14)	0.1591(16)	0.046(8)
O(13) ^b	0.9003(4)	0.39502(19)	0.00720(20)	0.0509
O(113) ^c	0.861(3)	0.3475(13)	-0.0013(15)	0.046(8)
O(21)	0.8045(3)	0.49546(14)	0.26445(19)	0.0468
O(22)	0.7173(3)	0.40455(14)	0.33688(18)	0.0423
O(23)	0.5610(3)	0.48229(16)	0.30050(20)	0.0512
N	0.6449(4)	0.48302(20)	0.0901(3)	0.0522
C(1)	0.5570(5)	0.32700(24)	0.1722(4)	0.0477
C(2)	0.5791(5)	0.32494(24)	0.0880(4)	0.0505
C(3)	0.4994(5)	0.36726(24)	0.0489(3)	0.0476
C(4)	0.4261(5)	0.39666(23)	0.1107(3)	0.0485
C(5)	0.4624(5)	0.3711(3)	0.1862(4)	0.0522
C(11) ^b	0.9900(6)	0.4937(3)	0.1157(4)	0.0604
C(111) ^c	1.090(6)	0.447(3)	0.060(4)	0.076(8)
C(12)	1.0247(5)	0.3022(3)	0.1354(3)	0.0627
C(13) ^b	0.8267(9)	0.3662(3)	-0.0585(4)	0.0671
C(113) ^c	0.855(12)	0.3768(23)	-0.0808(17)	0.0671
C(21)	0.8704(5)	0.5192(3)	0.3370(3)	0.0535
C(22)	0.8296(5)	0.36363(22)	0.3358(3)	0.0466
C(23)	0.5439(5)	0.5011(3)	0.3848(3)	0.0563
C(31)	0.2322(4)	0.18014(19)	0.05965(23)	0.0238
C(32)	0.2739(4)	0.23437(19)	0.0264(3)	0.0320
C(33)	0.2088(5)	0.26264(22)	-0.0389(3)	0.0409
C(34)	0.0952(5)	0.23671(24)	-0.0724(3)	0.0417
C(35)	0.0489(4)	0.18408(23)	-0.0396(3)	0.0382
C(36)	0.1162(4)	0.15644(20)	0.0240(3)	0.0305
C(41)	0.2282(4)	0.17890(19)	0.22061(24)	0.0264
C(42)	0.2703(4)	0.23154(20)	0.2598(3)	0.0348
C(43)	0.2002(5)	0.25885(22)	0.3236(3)	0.0385
C(44)	0.0840(5)	0.23448(24)	0.3506(3)	0.0411
C(45)	0.0367(4)	0.18333(24)	0.3136(3)	0.0361
C(46)	0.1071(4)	0.15599(21)	0.2502(3)	0.0340
C(51)	0.4656(4)	0.16209(18)	0.14232(24)	0.0240
C(52)	0.5417(4)	0.16361(18)	0.0706(3)	0.0308
C(53)	0.6778(4)	0.16979(20)	0.0705(3)	0.0361
C(54)	0.7455(4)	0.17473(21)	0.1440(3)	0.0398
C(55)	0.6761(4)	0.17271(22)	0.2165(3)	0.0393
C(56)	0.5399(4)	0.16651(20)	0.2152(3)	0.0335
C(61)	0.2948(4)	0.07543(19)	0.1389(3)	0.0251
C(62)	0.3133(4)	0.04275(19)	0.0663(3)	0.0326
C(63)	0.3193(5)	-0.01951(21)	0.0652(3)	0.0421
C(64)	0.3065(5)	-0.05213(22)	0.1367(3)	0.0405
C(65)	0.2879(5)	-0.02197(22)	0.2096(3)	0.0416
C(66)	0.2821(4)	0.04034(21)	0.2103(3)	0.0338
B	0.3051(4)	0.14934(22)	0.1405(3)	0.0250

^a U_{eq} is the cube root of the product of the principal axes of the displacement ellipsoid.

^b Site occupancy = 0.907(5).

^c Site occupancy = 1 - 0.907(5) = .093.

Table A9. Fractional Coordinates and Isotropic Displacement Parameters (\AA^2) for the Hydrogen Atoms of $[\text{CpCr}(\text{NO})\{\text{P}(\text{OMe})_3\}_2][\text{BPh}_4]$.

Atom	x	y	z	U_{iso}
H(1)	0.5992	0.3026	0.2128	0.079(8)
H(2)	0.6396	0.29897	0.0609	0.075(8)
H(3)	0.4947	0.37511	-0.0089	0.073(8)
H(4)	0.3629	0.42779	0.1024	0.070(8)
H(5)	0.4285	0.3820	0.2388	0.078(8)
H(111)	^a 1.0615	0.5104	0.1466	0.21(3)
H(112)	^a 1.0101	0.4950	0.0583	0.21(3)
H(113)	^a 0.9116	0.5161	0.1256	0.21(3)
H(114)	^b 1.122	0.486	0.049	0.21(3)
H(115)	^b 1.129	0.432	0.109	0.21(3)
H(116)	^b 1.112	0.421	0.015	0.21(3)
H(121)	^a 1.0228	0.2631	0.1589	0.15(2)
H(122)	^a 1.0822	0.3271	0.1671	0.15(2)
H(123)	^a 1.0561	0.2998	0.0801	0.15(2)
H(124)	^b 1.0711	0.2879	0.1828	0.15(2)
H(125)	^b 1.0865	0.3164	0.0958	0.15(2)
H(126)	^b 0.9741	0.2704	0.1119	0.15(2)
H(131)	^a 0.8706	0.3742	-0.1092	0.14(2)
H(132)	^a 0.7392	0.3819	-0.0611	0.14(2)
H(133)	^a 0.8231	0.3241	-0.0497	0.14(2)
H(134)	^b 0.873	0.3491	-0.1239	0.14(2)
H(135)	^b 0.901	0.4133	-0.0908	0.14(2)
H(136)	^b 0.763	0.3845	-0.0790	0.14(2)
H(211)	0.9386	0.5460	0.3207	0.18(2)
H(212)	0.8080	0.5399	0.3702	0.18(2)
H(213)	0.9079	0.4869	0.3678	0.18(2)
H(221)	0.8299	0.34011	0.3849	0.07(1)
H(222)	0.9095	0.38608	0.3328	0.07(1)
H(223)	0.8227	0.33797	0.2889	0.07(1)
H(231)	0.4597	0.5196	0.3907	0.12(1)
H(232)	0.6116	0.5289	0.3995	0.12(1)
H(233)	0.5492	0.4669	0.4200	0.12(1)
H(32)	0.3505	0.25300	0.0494	0.024(5)
H(33)	0.2421	0.29932	-0.0606	0.035(5)
H(34)	0.0498	0.25558	-0.1171	0.036(5)
H(35)	-0.0295	0.16635	-0.0614	0.031(5)
H(36)	0.0821	0.11971	0.0450	0.022(5)
H(42)	0.3507	0.24960	0.2421	0.038(6)
H(43)	0.2333	0.29457	0.3485	0.048(6)
H(44)	0.0364	0.25282	0.3944	0.052(6)
H(45)	-0.0446	0.16628	0.3314	0.044(6)
H(46)	0.0721	0.12047	0.2258	0.039(6)
H(52)	0.4973	0.15984	0.0188	0.031(5)
H(53)	0.7244	0.17048	0.0196	0.038(5)
H(54)	0.8391	0.17955	0.1447	0.042(5)
H(55)	0.7221	0.17600	0.2678	0.044(5)
H(56)	0.4948	0.16462	0.2666	0.033(5)
H(62)	0.3215	0.06390	0.0155	0.032(6)
H(63)	0.3327	-0.03987	0.0143	0.042(6)
H(64)	0.3107	-0.09478	0.1358	0.043(6)
H(65)	0.2794	-0.04378	0.2599	0.046(6)
H(66)	0.2683	0.06011	0.2617	0.033(6)

^a Site occupancy = 0.907(5).

^b Site occupancy = 1 - 0.907(5) = .093.

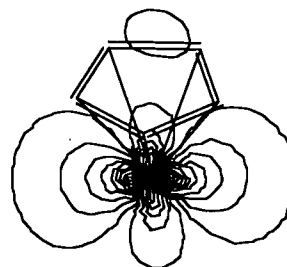
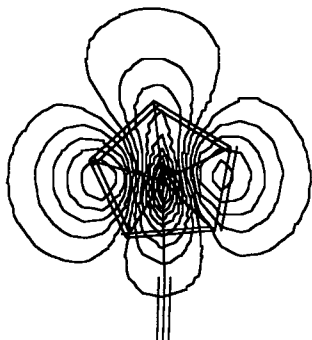
Table A10. Fractional Coordinates and B(eq) for the Non-Hydrogen Atoms of [CpCr(NO)(CNCMe₃)₂][BPh₄]

atom	x	y	z	B(eq)
Cr(1)	0.39254(06)	0.43290(04)	0.12554(05)	4.00(3)
O(1)	0.4880(03)	0.4082(02)	0.0012(02)	6.9(2)
N(1)	0.4565(03)	0.4215(02)	0.0567(02)	4.7(2)
N(2)	0.4734(03)	0.5961(02)	0.1969(03)	5.0(2)
N(3)	0.5860(03)	0.3815(02)	0.2965(03)	4.8(2)
C(1)	0.2205(04)	0.4562(03)	0.0498(04)	5.6(3)
C(2)	0.2339(04)	0.4581(04)	0.1352(05)	6.8(4)
C(3)	0.2677(05)	0.3887(05)	0.1700(04)	7.6(4)
C(4)	0.2759(04)	0.3413(03)	0.1058(06)	7.3(3)
C(5)	0.2439(04)	0.3838(04)	0.0304(03)	5.8(3)
C(6)	0.4419(04)	0.5382(03)	0.1666(03)	4.9(3)
C(7)	0.5194(04)	0.6691(03)	0.2375(04)	5.1(3)
C(8)	0.6407(05)	0.6645(04)	0.2694(06)	9.3(4)
C(8a)	0.586(06)	0.700(03)	0.192(04)	10(1)
C(9)	0.4745(06)	0.7293(03)	0.1689(04)	7.6(4)
C(9a)	0.422(05)	0.721(03)	0.225(04)	10(1)
C(10)	0.4751(06)	0.6827(04)	0.3083(05)	8.3(4)
C(10a)	0.592(04)	0.648(03)	0.337(03)	7(1)
C(11)	0.5136(04)	0.3959(03)	0.2332(03)	4.7(2)
C(12)	0.6820(05)	0.3695(04)	0.3775(03)	5.9(3)
C(13)	0.7280(06)	0.4476(04)	0.4079(05)	9.0(4)
C(13a)	0.679(05)	0.405(04)	0.444(04)	8(1)
C(14)	0.6414(06)	0.3328(05)	0.4420(05)	9.6(5)
C(14a)	0.700(05)	0.283(04)	0.392(04)	10(1)
C(15)	0.7617(06)	0.3195(05)	0.3577(05)	9.2(4)
C(15a)	0.786(05)	0.381(03)	0.349(04)	9(1)
C(16)	0.1565(03)	0.5112(02)	0.3268(02)	3.1(2)
C(17)	0.1499(03)	0.4429(03)	0.3673(03)	3.9(2)
C(18)	0.2415(05)	0.4016(03)	0.4182(03)	4.8(2)
C(19)	0.3441(04)	0.4259(03)	0.4306(03)	5.1(3)
C(20)	0.3559(04)	0.4924(03)	0.3923(03)	5.3(3)
C(21)	0.2634(04)	0.5337(02)	0.3415(03)	4.2(2)
C(22)	0.0709(03)	0.6125(02)	0.1964(03)	3.1(2)
C(23)	0.0303(03)	0.5948(02)	0.1094(03)	3.8(2)
C(24)	0.0522(04)	0.6383(03)	0.0489(03)	5.2(3)
C(25)	0.1158(04)	0.7017(03)	0.0737(03)	5.6(3)
C(26)	0.1588(04)	0.7216(03)	0.1591(04)	5.4(3)
C(27)	0.1367(04)	0.6777(02)	0.2188(03)	4.4(2)
C(28)	0.0089(03)	0.6135(02)	0.3334(03)	3.1(2)
C(29)	-0.0267(04)	0.6882(03)	0.3161(03)	5.0(2)
C(30)	-0.0684(04)	0.7284(03)	0.3673(04)	5.8(3)
C(31)	-0.0762(04)	0.6968(03)	0.4387(03)	5.1(3)
C(32)	-0.0421(04)	0.6242(03)	0.4585(03)	5.8(3)
C(33)	-0.0005(04)	0.5838(02)	0.4065(03)	4.6(2)
C(34)	-0.0575(03)	0.5032(02)	0.2181(02)	3.1(2)
C(35)	-0.1651(04)	0.5231(03)	0.2026(03)	4.3(2)
C(36)	-0.2551(04)	0.4779(03)	0.1562(03)	5.7(3)
C(37)	-0.2387(04)	0.4093(03)	0.1235(03)	5.2(3)
C(38)	-0.1342(04)	0.3875(02)	0.1368(03)	4.7(2)
C(39)	-0.0459(03)	0.4337(03)	0.1830(03)	3.8(2)
B(1)	0.0466(04)	0.5603(03)	0.2690(03)	3.0(2)

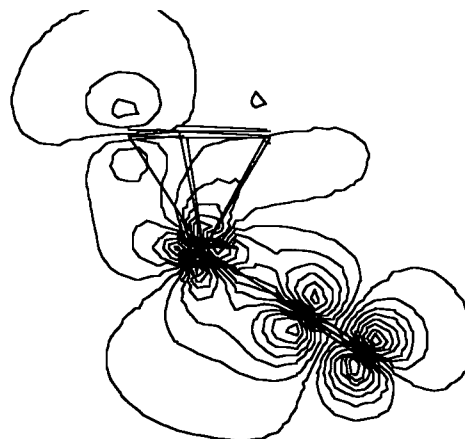
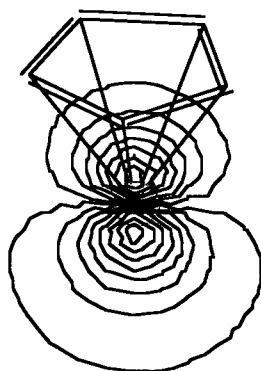
Table A11. Fractional Coordinates and B(eq) for the Hydrogen Atoms of
 $[\text{CpCr}(\text{NO})(\text{CNCMe}_3)_2][\text{BPh}_4]$

atom	x	y	z	B(eq)
H(1)	0.1982	0.4990	0.0095	6.8
H(2)	0.2211	0.5020	0.1658	8.1
H(3)	0.2838	0.3742	0.2301	9.1
H(4)	0.2996	0.2883	0.1128	8.8
H(5)	0.2389	0.3658	-0.0263	7.0
H(6)	0.6668	0.6234	0.3117	11.2
H(7)	0.6627	0.6546	0.2208	11.2
H(8)	0.6727	0.7125	0.2969	11.2
H(9)	0.5027	0.7789	0.1937	9.2
H(10)	0.4973	0.7186	0.1209	9.2
H(11)	0.3942	0.7295	0.1478	9.2
H(12)	0.5029	0.7311	0.3369	9.9
H(13)	0.3947	0.6841	0.2825	9.9
H(14)	0.4992	0.6416	0.3508	9.9
H(15)	0.7932	0.4431	0.4615	10.8
H(16)	0.7480	0.4719	0.3634	10.8
H(17)	0.6725	0.4783	0.4184	10.8
H(18)	0.5884	0.3664	0.4521	11.5
H(19)	0.6062	0.2844	0.4189	11.5
H(20)	0.7037	0.3241	0.4966	11.5
H(21)	0.7267	0.2709	0.3351	11.0
H(22)	0.7838	0.3442	0.3145	11.0
H(23)	0.8266	0.3109	0.4107	11.0
H(24)	0.0772	0.4235	0.3594	4.7
H(25)	0.2320	0.3544	0.4454	5.8
H(26)	0.4086	0.3966	0.4662	6.2
H(27)	0.4293	0.5108	0.4006	6.4
H(28)	0.2742	0.5809	0.3150	5.1
H(29)	-0.0159	0.5497	0.0896	4.5
H(30)	0.0218	0.6233	-0.0121	6.2
H(31)	0.1305	0.7326	0.0308	6.7
H(32)	0.2051	0.7667	0.1779	6.5
H(33)	0.1685	0.6928	0.2797	5.2
H(34)	-0.0220	0.7132	0.2655	6.0
H(35)	-0.0930	0.7807	0.3519	6.9
H(36)	-0.1056	0.7257	0.4749	6.2
H(37)	-0.0468	0.6001	0.5096	7.0
H(38)	0.0235	0.5315	0.4226	5.5
H(39)	-0.1786	0.5715	0.2255	5.2
H(40)	-0.3296	0.4947	0.1468	6.8
H(41)	-0.3011	0.3767	0.0912	6.2
H(42)	-0.1214	0.3391	0.1136	5.6
H(43)	0.0281	0.4166	0.1913	4.5

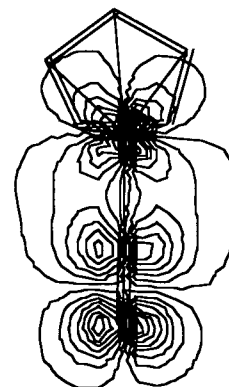
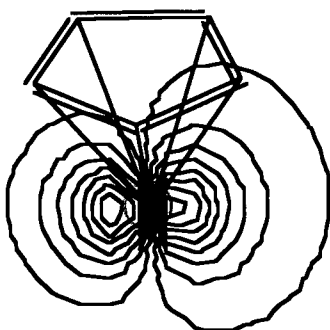
Figure A1. Frontier Molecular Orbitals of the CpCr(NO) Fragment



HOMO viewed along the CP-Cr axis and the Cr-N axis, centered on the Cr atom



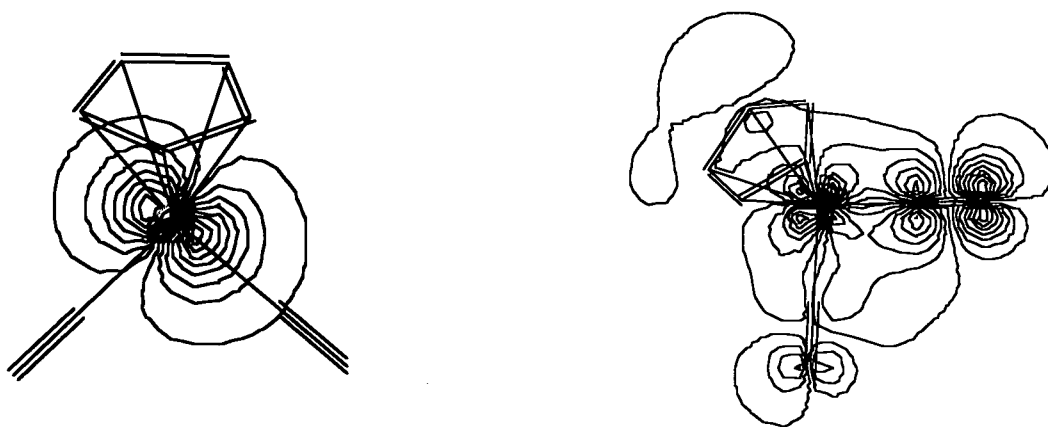
HOMO-1 as viewed along the Cr-N axis centered on N, and in the CP-Cr-N plane



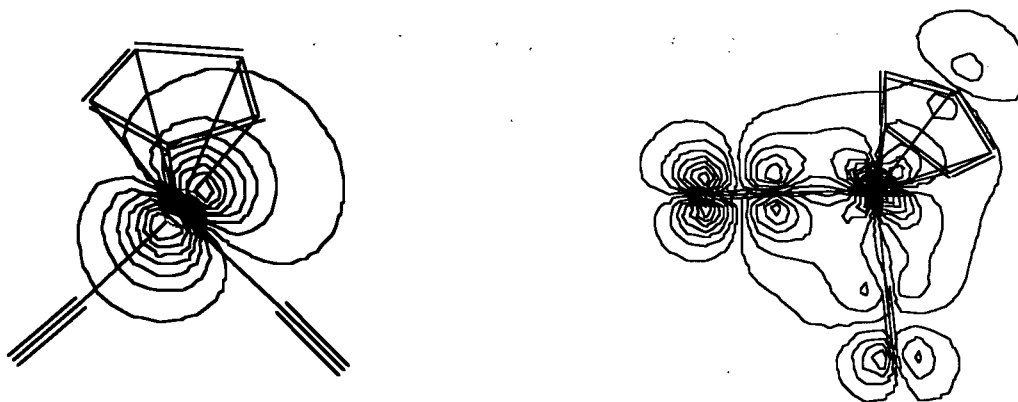
HOMO-2 as viewed along the Cr-N axis centered on N and in the Cr-N-O plane

Figure A2. Frontier Molecular Orbitals of CpCr(NO)(CO)_2 

HOMO as viewed along the CP-Cr axis centered on Cr, and in the OC-Cr-CO plane

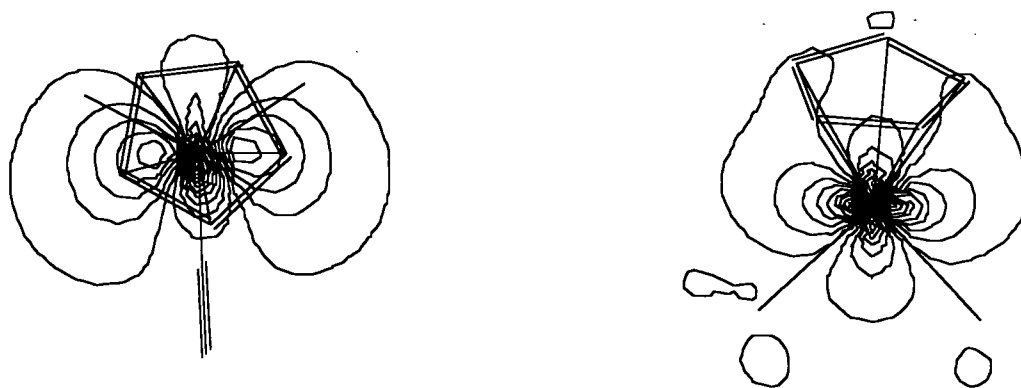


HOMO-1 as viewed along the Cr-N axis centered on N, and in one OC-Cr-NO plane

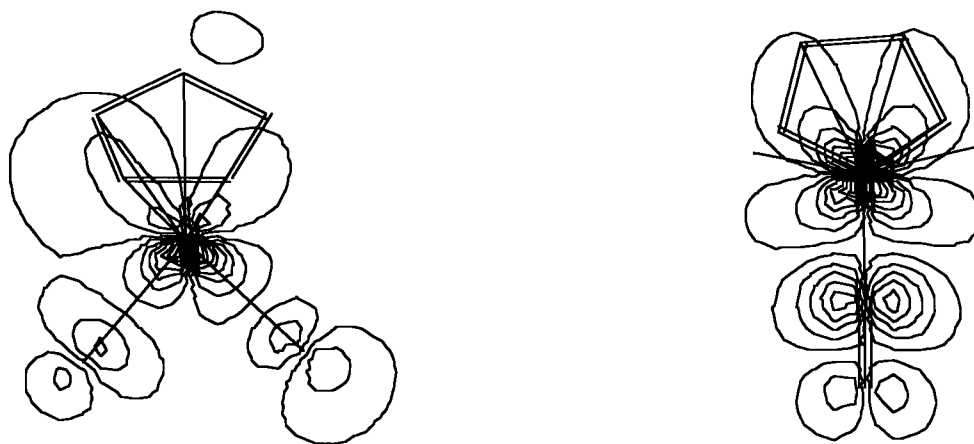


HOMO-2 as viewed along the Cr-N axis centered on N, and in the other OC-Cr-NO plane

Figure A3. Frontier Molecular Orbitals of $[\text{CpCr}(\text{NO})(\text{NH}_3)_2]^+$



SOMO as viewed along the Cp-Cr and Cr-NO axes, centered on Cr



LUMO as viewed in the $\text{H}_3\text{N-Cr-NH}_3$ and Cr-N-O planes